

More than what meets the eye: cryptic speciation and hidden diversity in land snails

Inauguraldissertation
der Philosophisch-naturwissenschaftlichen Fakultät
der Universität Bern

vorgelegt von

Jeannette Kneubühler

von Ettiswil LU

Leiter der Arbeit:
Prof. Dr. Christian Kropf
Naturhistorisches Museum Bern



This work is licensed under a Attribution-NonCommercial-NoDerivatives 4.0 International (CC BY-NC-ND 4.0) license with the exception of Chapters 1 and 2 (CC BY 4.0).

You are free to:



- **Share** — copy and redistribute the material in any medium or format

The licensor cannot revoke these freedoms as long as you follow the license terms.

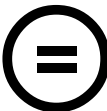
Under the following terms:



- **Attribution** — You must give [appropriate credit](#), provide a link to the license, and [indicate if changes were made](#). You may do so in any reasonable manner, but not in any way that suggests the licensor endorses you or your use.



- **NonCommercial** — You may not use the material for [commercial purposes](#).



- **NoDerivatives** — If you [remix, transform, or build upon](#) the material, you may not distribute the modified material.

No additional restrictions — You may not apply legal terms or [technological measures](#) that legally restrict others from doing anything the license permits.

Notices:

You do not have to comply with the license for elements of the material in the public domain or where your use is permitted by an applicable [exception or limitation](#).

No warranties are given. The license may not give you all of the permissions necessary for your intended use. For example, other rights such as [publicity, privacy, or moral rights](#) may limit how you use the material.

**More than what meets the eye: cryptic speciation and hidden
diversity in land snails**

Inauguraldissertation
der Philosophisch-naturwissenschaftlichen Fakultät
der Universität Bern

vorgelegt von

Jeannette Kneubühler

von Ettiswil LU

Leiter der Arbeit:
Prof. Dr. Christian Kropf
Naturhistorisches Museum Bern

Von der Philosophisch-naturwissenschaftlichen Fakultät angenommen.

Bern, 18.08.2022

Der Dekan
Prof. Dr. Zoltan Balogh

Table of contents

Introduction.....	1
Chapter 1	6
Kneubühler, J., Jochum, A., Prieto, C.E., Neubert, E. (2022). Molecular investigation and description of <i>Iberozospeum</i> n. gen., including the description of one new species (Eupulmonata, Ellobioidea, Carychiidae). <i>Organisms Diversity & Evolution</i> (22) 61–92. https://doi.org/10.1007/s13127-021-00517-9	
Chapter 2.....	38
Kneubühler, J., Baggenstos, M., Neubert, E. (2022). On the verge of extinction – revision of a highly endangered Swiss alpine snail with description of a new genus, <i>Raeticella</i> gen. n. (Gastropoda, Eupulmonata, Hygromiidae). <i>ZooKeys</i> 1104: 69–91. https://doi.org/10.3897/zookeys.1104.82866	
Chapter 3.....	61
Kneubühler, J., Proćków, M., Bischof, E., Neiber, M.T., Bober, S., Gargominy, O., Proschwitz, von, T., Neubert, E. (manuscript to be submitted to the European Journal of Taxonomy). How many species? Limits of morphological species concepts in the genus <i>Trochulus</i> (Gastropoda, Eupulmonata, Hygromiidae)	
Chapter 4.....	171
Jochum, A., Machalik, P., Inäbnit, T., Kneubühler, J., Slapnik, R., Vrabec, M., Schilthuizen, M., Ruthensteiner, B. (manuscript to be submitted to the European Journal of Taxonomy). Uncovering a taxonomic ghost: an integrative study reveals <i>Zospeum troglobalcanicum</i> along with X new and allied species from proximal caves of its southernmost Dinaride distribution (Gastropoda: Eupulmonata: Carychiidae)	
Favre, A., Kneubühler, J., Jochum, A. (ongoing research, working title) Revision of the genus <i>Carychium</i> using an integrative study yields X new species (Gastropoda: Eupulmonata: Carychiidae)	
Discussion	171
Outlook	173
Acknowledgements	174
References	175
Erklärung	181
Curriculum vitae.....	182

Introduction

Following arthropods, molluscs are the second largest phylum of invertebrate animals with about 110,000 accepted living species (MolluscaBase, July 2022). They inhabit almost every habitat on earth, ranging from geothermal vents of the deep sea to shallow lagoons, freshwater lakes and rivers, tropical forests, deserts, high mountain peaks (e.g., Purchon 1977) and caves as deep as 980 m (Weigand *et al.* 2013). Due to their calcareous shells, they show a rich fossil record, dating to the late Cambrium (ca. 534 mya) (Maloof *et al.* 2010). Although 25,000 accepted fossil-only species are known (MolluscaBase, July 2022), another 100,000 yet undiscovered species are expected (Schneider, pers. comm. 2022). Molluscs have always been important ecosystem engineers, helping to structure aquatic bottom environments while providing protection, food and habitat to a wide range of other species (Fortunato 2015). Throughout human history, they have played an important role as food source (e.g., Khan & Liu 2019), tools, currency, decoration and in palliative care (i.e., *Conus* toxins); they are used in biomonitoring programs and in biomedical research (e.g., Bingham *et al.* 2010). Despite their many benefits, certain molluscs can also be pests or invasive species, or act as intermediate hosts of dangerous parasites (Lindberg 2001). The diversity in size, shape and colour of molluscs have always fascinated people. Especially the class Gastropoda displays an enormous variability in shell morphology. Shells of molluscs are mainly made of calcium carbonate and protect the animals against predation, dehydration and mechanical damage (Vermeij 1993). On the one hand, shell size is genetically inherited, but on the other hand, it is influenced by environmental factors. For example, humidity, substrate or population density can have an influence on the effective size of a land snail shell (Goodfriend 1986). Living in certain habitats favours different shell shapes. For example, flat species are more likely to be found on low-angle or horizontal surfaces and high-spired species are more likely to be found on high-angle or vertical surfaces and intermediate species are found on a wide variety of surfaces (Goodfriend 1986). Close relationship and/or similarly colonized habitats with similar environmental conditions can lead to species having similar shells (e.g., Goodfriend 1986, Gemmell *et al.* 2018).

The shell is a hard, resistant component and persists well beyond the death of the animal (Pearce *et al.* 2008). This is one of the main reasons, why historic taxonomic descriptions of most snail species are based on morphological characteristics of the shell, omitting others such as chemical, anatomical or genetic characteristics. By considering only morphological features, the diversity of cryptic species remains unrevealed (Bickford *et al.* 2007). A species is called cryptic, when two or more distinct species are classified as one species based on morphological similarity (e.g., Bickford *et al.* 2007; Pfenninger & Schwenk 2007). A literature survey by Struck *et al.* (2018) showed, that cryptic species have been defined based on

taxonomic history and molecular data, without quantifying morphological disparity, which wrongly leads to lumping of species. It is not clear from the definitions of numerous studies how many characters are needed to speak of cryptic species (see Struck *et al.* 2018). The prevalence of cryptic species skews biodiversity estimation and depends on how species are defined (Bickford *et al.* 2007; Adams *et al.* 2014; Struck *et al.* 2018). The unified species concept of de Queiroz (2007) contains two elements: the general concept of species as separately evolving metapopulation lineages and second, it treats this property as the only necessary property of species. Under a unified species concept, there should no longer be any disagreement about the numbers and boundaries of species that merely result from disagreements about the definition of the species category. Disagreements about species delimitation should result only from differences in e.g., the reliability of certain methods or the relevance of certain data (de Queiroz 2007). Therefore, taxonomists must discriminate characters according to their suitability and quality for species delineation (Jörger & Schrödl 2013). In order to distinguish and quantify cryptic species, information on morphological disparity has to be related with levels of gene flow, reproductive isolation and genetic divergence. For young species with a short divergence time, it could be, that the time was too short to accumulate considerable morphological differences (Struck *et al.* 2018). Another hypothesis is, that cryptic species appear to differ either by non-visual mating signals and/or are under selection that causes morphological stasis (Bickford *et al.* 2007). Cryptic diversity can also be a consequence of parallel or convergent morphological evolution under similar selection pressure (Trontelj & Fišer 2009). These themes elude our visual perception in the morphological description of species and require consideration of the evolutionary history of the taxa (e.g., Sites & Marshall 2003; Bickford *et al.* 2007, Struck *et al.* 2018). Accurate species identifications are crucial for the identification of invasive and pest species, diagnosis and prevention of disease and for the implementation of biological control (e.g., Bickford *et al.* 2007; Pfenninger & Schwenk 2007). Also, for conservation and natural resource management and protection, the correct identification and description of species is essential (e.g., Bickford *et al.* 2007; Fišer *et al.* 2018; Horsáková *et al.* 2019).

Today, many integrative taxonomic studies are carried out, which involve more than just morphological characteristics to improve species discovery and description (Padial *et al.* 2010). In integrative taxonomy, different data sets are investigated, such as for example morphology, genetic data, mating signals, behavioural traits, bioacoustics data, and biogeography (e.g., Bickford *et al.* 2007; Jörger & Schrödl 2013). Numerous population genetic studies, phylogenetic studies or biogeographic studies in any organism groups (e.g., Hebert *et al.* 2004; Funk *et al.* 2011; Cruse *et al.* 2022) have discovered cryptic species in recent years. Especially within snails, there are frequently discrepancies when animals are sequenced and

compared to species that are based only on the description of an empty shell (e.g., Johnson *et al.* 2014; Horsáková *et al.* 2019; Hofman *et al.* 2022).

In my doctoral work, I used integrative taxonomy to unravel cryptic species in different terrestrial snail groups. With the inclusion of mitochondrial and nuclear DNA, shell morphological features, histological sections, and the investigation of the morphology of the radula, it was possible to describe the new genus *Iberozospeum* Jochum, Kneubühler, Prieto & Neubert, 2022 and a new species from Spain (Chapter 1). The focus of my doctoral work was on the resolution of the species complex within the hairy snail genus *Trochulus* Chemnitz, 1786. A rich sampling from the entire distribution area of the genus made it possible to clarify the complicated taxonomy of *Trochulus* (Chapters 2 and 3). In addition, I resolved phylogenetic problems within the ellobiid micro snail genera *Zospeum* Bourguignat, 1856 and *Carychium* O.F. Müller, 1773 (Chapter 4).

Chapter 1

The micro snails of the ellobiid genus *Zospeum* are known to inhabit a wide network of caves underlying the Pyrenean-Cantabrian region of northern Spain. Due to their tiny size (< 2 mm) and their transparent shell, it is difficult to find them alive. Recent studies of northern Spanish *Zospeum* shells (Jochum *et al.* 2015) have provided valuable but limited insights towards understanding the evolutionary processes in this genus. The species within *Zospeum* are difficult to distinguish based on their shells, as they show great intraspecific variability with smooth transitions to other species. Recent collection efforts have provided significant finds and enabled the investigation of 57 populations in an integrative study. Two mitochondrial (COI and 16S) and two nuclear (H3 and 5.8S rRNA+ITS2) markers were examined, which revealed that the northern Spanish species form a radiation separate from the Dinaric *Zospeum* clades, for which the new genus *Iberozospeum* was proposed. In this work, several species were confirmed by genetic data, and one new species was described based on morphological and genetic evidence. However, the widespread species, *I. vasconicum* (Prieto, de Winter, Weigand, Gómez & Jochum, 2015), was found to consist of three cryptic clades. In this study, morphological evidence acquired via histological analysis of *I. vasconicum* (collected at the type locality Cueva de la Ermita de Sandaili, Spain) and scanning electron microscope (SEM) analyses of radulae of eastern Alpine, Dinaric and Iberian congeners, underscored the separation of these members to the new genus. This study revealed that the columellar muscle in *Iberozospeum* shows prominent humps containing vasculature extending to the tips of these humps, matching up perfectly to corresponding microstructure on the abutting lamellae. Additionally, radula ribbons harbour more and smaller teeth per transverse row and are longer and broader in *Iberozospeum* compared to those of Dinaric taxa.

Chapter 2

Trochulus biconicus (Eder, 1917) is an endemic land snail known from only a few localities in the Central Swiss Alps. This species is classified as “vulnerable” by Swiss law (Federal Office of Environment) and is protected. It is also considered “endangered” (EN) by the International Union for Conservation of Nature (IUCN). Although some studies (e.g., Kruckenhauser *et al.* 2014; Proćków *et al.* 2021) in the past examined specimens of *T. biconicus*, the phylogenetic affiliation remained unclear. In my work here, living specimens from large populations were collected at 11 sites of the known distribution area, enabling a contemporary integrative study, incorporating molecular, anatomical and morphological shell data. Phylogenetic analyses revealed that *T. biconicus* forms a monophyletic clade, clearly separated from all known genera within the tribe of Trochulini. These findings are supported by morphological investigations of the genital organs, which revealed only four instead of six or eight mucous glands and a very long flagellum when compared to *Trochulus*. Therefore, the new monotypic genus *Raeticella* was introduced. *Raeticella biconica* lives on mountain peaks on the right and left side of the Engelberger valley between 1890 and 2575 m a.s.l. With its flat shell, it is perfectly adapted to live under or between stones. Low genetic diversity within the analysed populations indicates, that this species underwent a bottleneck event during the Pleistocene and the Last Glacial Maximum, whereby, some isolated populations survived this icy period on neighbouring nunataks (glacial islands). This stenoeious species is prone to extinction because of climate change. It already reached the summits of the mountains and there is no more alternative to avoid disagreeable climate conditions. If climate change proceeds at its current rapid pace, this species could become extinct in a few years.

Chapter 3

Most of the species’ descriptions of the hairy snail genus *Trochulus* are based on morphological and anatomical characters. Unfortunately, they fail to address the diversity of *Trochulus* by leaving cryptic species unrevealed. Previous phylogenetic studies have included various specimens, but only from a small part of the distribution range and therefore, could not resolve the actual phylogenetic relationships within the genus. The enormous number of available names for an unknown number of biological entities led to a chaotic taxonomic situation. Until today, weak conception and widespread contradiction in the application of these names precluded a well-grounded species identification. Recent, intense collecting efforts and the examination of collection specimens from various museum collections, provided a remarkably rich sampling from the entire distribution range of the genus (ca. 570 specimens). Additional sequences from genetic data bases were included. Maximum Likelihood and Bayesian Inference based phylogenetic analyses, comprising two mitochondrial (COI and 16S) and one nuclear (5.8S rRNA+ITS2) marker, revealed 21 stable clades within *Trochulus*.

Additionally, the shell morphology was analysed using landmarks- and semi landmarks-based geometric morphometric methods (GMM). In contrast to traditional linear measurement methods, the shape variations of morphologies are covered in GMM. Considering the GMM data with the occurrence of hairs and the shell size, some clades could be morphologically well separated, while some cryptic species could not.



Molecular investigation and description of *Iberozospeum* n. gen., including the description of one new species (Eupulmonata, Ellobioidea, Carychiidae)

Jeannette Kneubühler^{1,2} · Adrienne Jochum^{1,2,3} · Carlos E. Prieto⁴ · Eike Neubert^{1,2}

Received: 30 April 2021 / Accepted: 30 August 2021 / Published online: 5 November 2021
© The Author(s) 2021

Abstract

The subterranean realm of the Cantabrian-Pyrenean region of northern Spain harbours a rich diversity of *Zospeum*. Due to their tiny size and the difficulty of finding them alive, scarce animal material has been available for scientific investigation. Recent investigations of *Zospeum* shells have provided valuable, but limited insights towards our understanding of the evolutionary processes occurring within this taxon in northern Spain. In an integrative study, we investigate 57 populations of *Zospeum* from northern Spanish caves using two mitochondrial (COI and 16S) and two nuclear markers (H3 and 5.8 S rRNA + ITS2). Revealed is a separate radiation of the northern Spanish species for which the new genus, *Iberozospeum*, is proposed. The independent radiation of Dinaric *Zospeum* from that of northern Spain justifies the designation of *Iberozospeum* n. gen. Morphological evidence is provided via histological analysis of *Iberozospeum vasconicum* and SEM analyses of radulae of eastern Alpine, Dinaric and Iberian species. Important differences in morphological structure and character states are presented, including the first view of the sexually mature female and the presence of the giant albumen gland in an individual of the subterranean, troglobitic Carychiidae. Significant differences are revealed in superficial crystallographic structure of the columellar lamellae, the morphology of the columellar muscle and in the radula. Radular ribbon length, ribbon broadness, straightness of the ribbon base and cusp configuration are distinctive in the Iberian species. One new species is described corroborated by genetic and morphological characters.

Keywords Cave-dwelling species · Cryptic diversity · Histology · Intraspecific variability · Microgastropods · Subterranean land snail

Introduction

Tiny subterranean snails of the genus *Zospeum* (Bourguignat, 1856), are known to inhabit the broad network of caves underlying the Pyrenean-Cantabrian region of northern Spain (Fig. 1). Although recent collection efforts have provided significant

finds, many new discoveries have remained parked in the lab due to doubts and complications regarding the taxonomic status of the oldest-described species from Spain, *Iberozospeum schaufussi* (von Frauenfeld, 1862; Jochum et al., 2019). Only until recently were these taxonomic issues clarified such that the description of new species could proceed unhindered in a region known to harbour rich “*Zospeum*” diversity (Jochum et al., 2019). We emphasise that northern Spanish material molecularly assessed by Weigand et al. (2013) as cf. *Z. suarezi* (Gittenberger, 1980) and deposited in the BOLD data base under this name was revised (Jochum et al., 2019) and is now in sync with this investigation, *I. schaufussi* (von Frauenfeld, 1862). Caves harbouring two to three different morphotypes are considered not unusual (Alonso et al., 2018). Despite this suggested richness, only eight species have been formally described, including *I. schaufussi* (von Frauenfeld, 1862), *I. bellesi* (Gittenberger, 1973), *I. biscaiense* (Gómez & Prieto, 1983), *I. vasconicum* (Prieto et al., 2015 in Jochum et al., 2015a), *I. zaldivarae* (Prieto et al.,

✉ Jeannette Kneubühler
jeannette.kneuebuehler@nmbe.ch

¹ Natural History Museum Bern, 3005 Bern, Switzerland

² Institute of Ecology and Evolution, University of Bern, 3012 Bern, Switzerland

³ Senckenberg Research Institute and Natural History Museum, 60325 Frankfurt am Main, Germany

⁴ Departamento de Zoología Y Biología Celular Animal, Facultad de Ciencia Y Tecnología, Universidad del País Vasco (UPV/EHU), Apdo.644, 48080 Bilbao, Spain

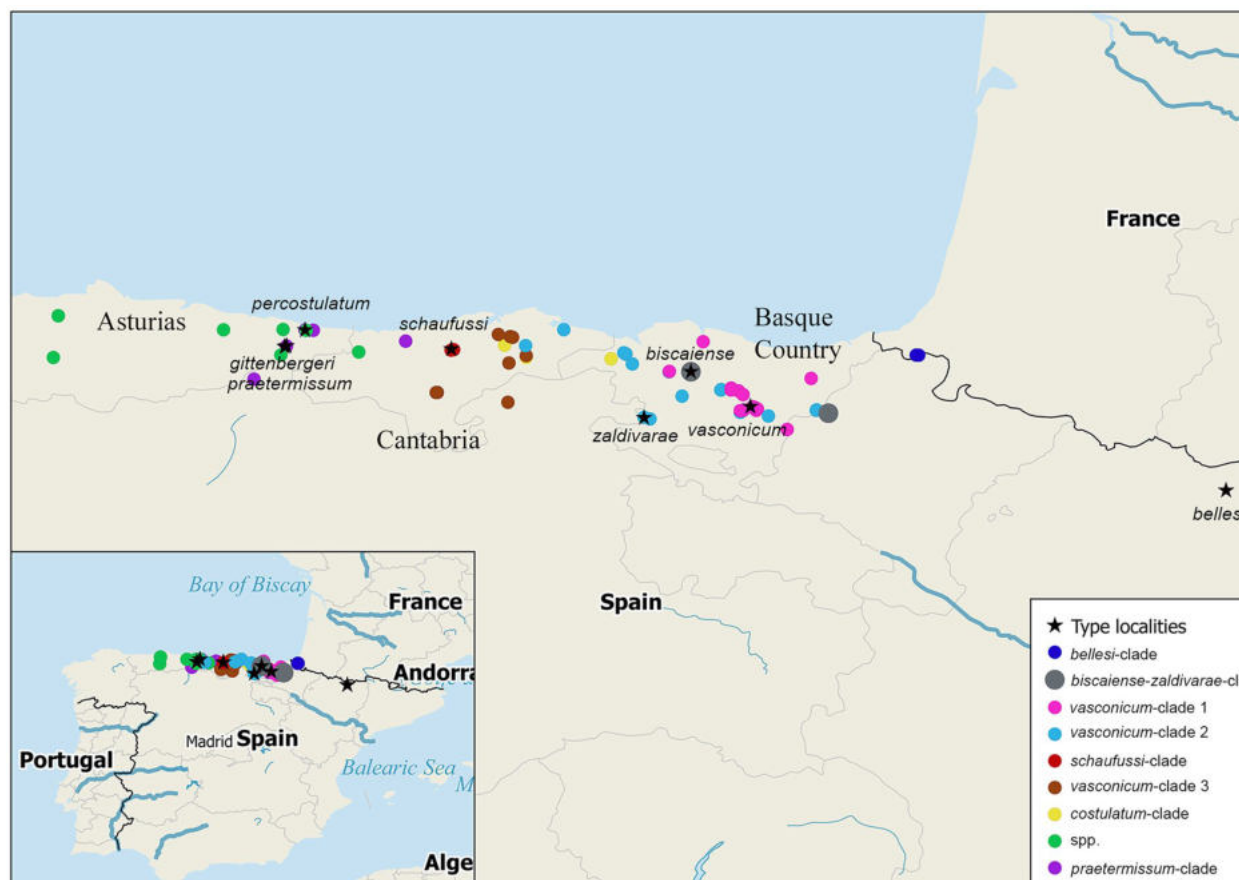


Fig.1 Sampling locations of *Iberozospeum* specimens from northern Spanish caves grouped into clades named by province of origin and designated by coloured circles; stars represent the type localities of the hitherto known species

2015 in Jochum et al., 2015a), *I. percostulatum* (Alonso et al., 2018) and recently, *I. gittenbergeri* (Jochum et al., 2019) and *I. praetermissum* (Jochum et al., 2019).

Weigand et al. (2013) presented the first phylogenetic study incorporating Iberian “*Zospeum*” species, whereby nine populations of “*Zospeum*” are clustered into six evolutionary lineages (EL), with those from the Cantabrian Mountains being monophyletic. This study and additional phylogenetic investigations have since demonstrated the high incidence of intraspecific variability and cryptic diversity in Iberian, Eastern Alpine (Kruckenhauser et al., 2019; Weigand et al., 2011) and Dinaride (Inäbnit et al., 2019) *Zospeum* species.

In order to further understand zospeid evolutionary history in caves of northern Spain, we molecularly assess recent finds encompassing 57 populations. Anatomical perspectives of zospeid radulae and organ systems remain rare and few in number. Seven studies are known so far (see Jochum, 2011; Jochum et al., 2015b; Inäbnit et al., 2019). By studying histological sections of topotypic *I. vasconicum*, topotypic *Z. isselianum* (Pollonera, 1887) and *Z. amoenum* (von

Frauenfeld, 1856) (see Jochum et al. 2015b) and *Z. spelaeum* (Rossmässler, 1839), we compare the presence of specific structures and character states in the visceral mass of one northern Spanish and three Dinaride taxa. We additionally describe significant differences in radular morphology and crystallographic structure on the columellar lamellae using scanning electron microscopy (SEM). Together, these investigations support the erection of the new genus, *Iberozospeum*.

Material and methods

Material is housed in the following collections:

AJC: Adrienne Jochum Collection, Kelkheim, Germany.
 CAA: Collection of Alvaro Alonso, Spain.
 CSQS: Collection of Sergio Quiñonero-Salgado, Spain.
 MHNG: Muséum histoire naturelle Genève, Geneva, Switzerland.

MNCN: Museo Nacional de Ciencias Naturales, Madrid, Spain.

MZB: Museu de Ciències Naturals (Zoologia) de Barcelona, Barcelona, Spain.

NHMW: Naturhistorisches Museum, Wien, Vienna, Austria.

NMBE: Naturhistorisches Museum der Burgergemeinde Bern, Bern, Switzerland.

RMNH: Naturalis Biodiversity Center (formerly Rijksmuseum van Natuurlijke Historie), Leiden, The Netherlands.

ZUPV/FC: Colección de Fauna Cavernícola (Departamento de Zoología) de la Universidad del País Vasco-Euskal Herriko Unibertsitatea, Bilbao, Spain.

Individuals investigated in the molecular study

Individuals used for DNA sequence analyses were collected primarily by Carlos Prieto, Alvaro Alonso Suárez and Sergio Quiñonero-Salgado and additional collectors in caves from Asturias province to as far east as Navarra during the years 1987–2018. A total of 67 individuals were included. Sampling locations and the GenBank accession numbers for the obtained mtDNA (COI, 16S) and nDNA (H3, 5.8 S rRNA + ITS2) sequences are given in Table 1. Molecular analyses include the outgroup species *Zospeum spelaenum* (Rossmässler, 1839), *Zospeum exiguum* (Kušcer, 1932), *Zospeum manitaense* (Inäbnit et al., 2019), *Zospeum robustum* (Inäbnit et al., 2019), *Zospeum frauenfeldii* (Freyer, 1855), *Zospeum obesum* (von Frauenfeld, 1854) and *Zospeum pretneri* (Bole, 1960) from the Dinaric Alps (Inäbnit et al., 2019; Weigand et al., 2013). Additionally, sequences of *I. vasconicum* (No. 151 in Weigand et al., 2013), *I. schaufussi* (as *I. suarezi*, No. 140 in Weigand et al., 2013) and *I. zaldivarae* (No. 162 and 163 in Weigand et al., 2013) from their type localities were included. All images and DNA extracts of the specimens investigated in this study are housed in the Natural History Museum Bern (NMBE), Bern, Switzerland.

DNA extraction, PCR amplification, and sequence determination

Live specimens were preserved in 80% ethanol. Before DNA extraction, every specimen was imaged under sterile conditions from frontal and apical view with a Leica DFC425 microscope camera using the image-processing program (IMS Client V15Q4, Imagic, Switzerland). For total DNA extraction, the Qiagen Blood and Tissue Kit (Qiagen; Hilden, Germany) was used. Each specimen was placed in a mix of 180 µl ATL buffer and 20 µl Proteinase K. It was then incubated for ca. 2 h at 56 °C in a heater (Labnet, Vortemp 56, witec AG, Littau, Switzerland). For subsequent

DNA extraction, 200 µl Buffer AL was added. The mixture was vortexed and incubated at 56 °C for 10 min. Ethanol of 200 µl (100%) was added and vortexed again. The mixture was pipetted in a DNeasy Mini spin column placed in a 2 ml collection tube and centrifuged at 8000 rpm (Centrifuge 5424, Eppendorf) for 1 min. The spin column was placed in a new 2 ml collection tube and 500 µl Buffer AW1 was added. It was centrifuged for 1 min at 8000 rpm. The spin column was placed in a new 2 ml collection tube, and 500 µl Buffer AW2 was added. It was centrifuged for 3 min at 14,000 rpm. Afterwards, the spin column was transferred to a new 1.5 ml Eppendorf tube. The DNA was then eluted by adding 200 µl Buffer AE. It was incubated for 1 min at room temperature (ca. 23 °C) and centrifuged for 1 min at 8000 rpm.

In this study, two mitochondrial (mtDNA) markers (COI and 16S) and two nuclear (nDNA) markers (H3 and 5.8 S rRNA + ITS2) were investigated. PCR mixtures consisted of 12.5 µl GoTaq G2 HotStart Green Master Mix (Promega M7423), 4.5 µl ddH₂O, 2 µl forward and reverse primer each and 4 µl DNA template. In Table 2 the respective primer pairs for the PCR are listed. The following PCR cycles were used as follows: for COI the admixture was heated 2 min at 94 °C, followed by 35 cycles of 1 min at 95 °C, 1 min at 40 °C and 1 min at 72 °C and, finally, 5 min at 72 °C; for 16S the admixture was heated 5 min at 95 °C, followed by 45 cycles of 30 s at 95 °C, 30 s at 48 °C and 45 s at 72 °C and, finally, 5 min at 72 °C; for H3 the admixture was heated 3 min at 95 °C, followed 40 cycles of 1 min at 95 °C, 1 min at 42 °C and 1 min at 72 °C and, finally, 10 min at 72 °C; and for 5.8 S rRNA + ITS2 the admixture was heated 1 min at 96 °C, followed by 45 cycles of 30 s at 94 °C, 30 s at 50 °C and 1 min at 72 °C and, finally, 10 min at 72 °C (SensoQuest Tabcyclet and Techne TC-512, witec AG, Littau, Switzerland). The purification and sequencing of the PCR products were performed by LGC (LGC Genomics Berlin, Germany).

Specimens collected in 2011 or later could be successfully sequenced. Since the DNA content in older specimens was too low for any analyses, sequences of those specimens could not be included in our study. Long-term storage in ethanol proved to be problematic for the successful sequencing of such tiny snails (< 1.5 mm).

Phylogenetic analyses

The software package Geneious v9.1.8 (Biomatters Ltd) was used for sequence processing and editing. Maximum likelihood (ML) topology was estimated with the Geneious RAxML plug-in (Stamatakis, 2006) using rapid bootstrapping setting to compute the best scoring ML tree and 1500 bootstrapping replicates. The protein-coding gene fragments of COI was defined in two data blocks. The first and third codon positions were defined as one block and the second

Table 1 Sampled northern Spanish caves with their geographic location and the GenBank accession numbers for the analysed mtDNA (COI, 16S) and nDNA (H3, 5.8 S rRNA + ITS2) sequences

NMBE-No	ZUPV-No	Cave and Province	Latitude	Longitude	Altitude [m]	GenBank accession number COI	GenBank accession number 16S	GenBank accession number H3	GenBank accession number ITS2
540551_1	1847	Akaitz Txiki (Gipuzkoa)	42.9818	-2.0925	824	MW626838	MW621911	MW622169	MW621272
540552_1	2039	Azkillar (Bizkaia)	43.0882	-2.5912	1030	MW626839	MW621915	MW622173	MW621275
540552_3	2039	Azkillar (Bizkaia)	43.0882	-2.5912	1030	MW626841	MW621917	MW622175	MW621277
540553_1	1066	Elorrea (Bizkaia)	43.0538	-2.7956	1059	-	MW621919	MW622177	-
540554_4	1309	Arrikruz (Gipuzkoa)	42.9988	-2.4265	495	-	MW621920	MW622181	MW621282
540555_2	937	Basotxo (Navarra)	42.8798	-2.246	705	-	-	MW622183	-
540556_1	874	Hatxondo (Bizkaia)	43.1835	-2.862	300	-	-	MW622184	-
557136	4885	Herreria (Asturias)	43.39784	-4.75967	50	-	MW621921	MW622188	MW621284
557138	4702	Baja (Cantabria)	43.40163	-3.41371	51	MW626842	MW621922	MW622189	MW621285
557140	4862	Collubina (Asturias)	43.39841	-4.72264	45	MW626843	MW621923	MW622190	MW621286
557142	3671	Cumbre (Asturias)	43.26893	-4.89248	1761	-	MW621924	MW622191	-
557144	4136	Udias (Cantabria)	43.34163	-4.23989	109	MZ620729	MW621925	MW622192	MW621287
557146	3820	Montosas (Cantabria)	43.22731	-3.70042	725	MW626844	MW621926	MW622193	MW621288
557150	3405	Txomenkoba (Gipuzkoa)	42.98131	-2.47352	810	MW626845	MW621927	MW622194	MW621289
557152	3758	San Valerio (Gipuzkoa)	43.08203	-2.50105	444	MW626846	MW621928	MW622195	MW621290
557154	3849	Penpelin (Gipuzkoa)	43.062	-2.47655	690	MW626847	MW621929	MW622196	MW621291
557156	3856	Artegi (Bizkaia)	43.09628	-2.53847	540	MW626848	MW621930	MW622197	MW621292
557158	4601	Saiturri-2 (Gipuzkoa)	42.96902	-2.49111	1063	MW626849	MW621931	MW622198	MW621293
557160	4757	Urkoba (Gipuzkoa)	42.97802	-2.49103	1020	-	-	MW622199	MW621294
557162	4821	Perusaroi-1 (Gipuzkoa)	42.95026	-2.34416	1156	-	MW621932	-	MW621295
557166	4990	Aizkirri (Gipuzkoa)	42.99568	-2.41728	600	MW626850	MW621933	MW622200	MW621296
557168	5005	Arlaban (Gipuzkoa)	43.08629	-2.53928	382	MW626851	MW621934	MW622201	MW621297
557174	1008	Eskatxabel-2 (Bizkaia)	43.27509	-3.0888	565	-	-	MW622202	MW621298
557178	1607	Paules (Burgos)	42.94287	-2.99363	830	MW626852	MW621935	MW622203	MW621299
557180	1740	Leजार (Araba)	42.93484	-2.96285	836	-	MW621936	MW622204	MW621300
557182	874	Hatxondo (Bizkaia)	43.18162	-2.86335	300	-	MW621937	-	-

Table 1 (continued)

NMBE-No	ZUPV-No	Cave and Province	Latitude	Longitude	Altitude [m]	GenBank accession number COI	GenBank accession number 16S	GenBank accession number H3	GenBank accession number ITS2
557187	1847	Akaitz Txiki (Gipuzkoa)	42.97995	-2.09384	824	MW626853	MW621938	MW622205	MW621301
557188	1847	Akaitz Txiki (Gipuzkoa)	42.97995	-2.09384	824	MW626854	MW621939	MW622206	MW621302
557189	2039	Azkillar (Bizkaia)	43.08632	-2.59251	1030	MW626855	MW621940	MW622207	MW621303
557198	no number	Fuente de Estragueña (Cantabria)	43.2997	-4.6066	-	-	-	MW622208	MW621304
557200	854	San Juan-9 (Bizkaia)	43.28078	-3.1001	637	MW626856	MW621941	MW622209	-
557207	3861	Azkonar Zulueta (Gipuzkoa)	42.98749	-2.40171	790	-	MW621942	-	MW621305
557209	3904	Iritegi (Gipuzkoa)	42.9798	-2.40768	527	MW626857	MW621943	MW622210	MW621306
557211	4864	Grazal (Bizkaia)	43.22227	-3.05541	148	MW626858	MW621944	MW622211	MW621307
557213	5006	Garcia (Burgos)	43.022	-3.7057	935	MW626859	MW621945	MW622212	MW621308
557215	5091	Arrigueras (Cantabria)	43.07316	-4.07478	660	-	-	MW622213	MW621309
557217	4930	Mendikute (Gipuzkoa)	43.14687	-2.12069	710	MW626860	MW621946	MW622214	MW621310
557219	5087	Munarri Arrola (Bizkaia)	43.33892	-2.68541	63	MW626861	MW621947	MW622215	MW621311
557221	2874	Irutxin (Navarra)	42.966	-2.02518	1095	-	-	MW622216	MW621312
557223	3728	Otxas (Bizkaia)	43.18599	-2.74773	488	MW626862	MW621948	MW622217	MW621313
557225	4102	Toyo (Cantabria)	43.28468	-4.48524	190	MW626863	MW621949	MW622218	MW621314
557226	4102	Toyo (Cantabria)	43.28468	-4.48524	190	MW626864	MW621950	MW622219	MW621315
557227	4714	Cuvias Negras (Cantabria)	43.25668	-3.60984	250	-	-	MW622220	-
557229	4723	San Juan de Socueva (Cantabria)	43.26569	-3.60993	430	-	-	MW622221	MW621316
557231	3078	Valdebeci (Bizkaia)	43.24918	-3.1663	188	-	-	MW622222	MW621317
557232	4017	Princesa (Bizkaia)	43.2738	-3.08898	620	MW626865	MW621951	MW622223	MW621318
557234	3371	Lexotoa-2 (Navarra)	43.26819	-1.55843	215	MW626866	MW621952	MW622224	MW621319
557236	3323	Lezea (Navarra)	43.26853	-1.57164	210	MW626867	MW621953	MW622225	MW621320
557238	2875	Irutxin (Navarra)	42.96476	-2.03077	1095	MW626868	MW621954	MW622226	MW621321
557240	3727	Otxas (Bizkaia)	43.18165	-2.74923	488	-	MW621955	MW622227	MW621322
557242	4057	Cubija (Cantabria)	43.31812	-3.61307	269	MW626869	MW621956	MW622228	MW621323

Table 1 (continued)

NMBE-No	ZUPV-No	Cave and Province	Latitude	Longitude	Altitude [m]	GenBank accession number COI	GenBank accession number 16S	GenBank accession number H3	GenBank accession number ITS2
557244	559	Paules (Burgos)	42.94287	-2.99363	840	-	-	MW622229	MW621324
557246	5210	Valdemora (Asturias)	43.47417	-6.0556	310	MW626870	MW621957	MW622230	MW621325
557247	5302	Valdemora (Asturias)	43.47417	-6.0556	310	-	-	MW622231	MW621326
557249	4915	Llagar (Asturias)	43.25613	-6.08141	990	MW626871	MW621958	MW622232	-
557251	5211	Caleru (Asturias)	43.40077	-5.1919	80	MW626872	MW621959	MW622233	MW621327
557253	5209	Herreria (Asturias)	43.39987	-4.76584	45	MW626873	MW621960	MW622234	MW621328
557255	5208	Busecu (Leon)	43.14277	-5.03276	770	MW626874	MW621961	MW622235	-
559620	5257	Puente Inguanzo (Asturias)	43.31626	-4.86252	225	MW626875	MW621962	MW622236	MW621329
559622	5258	Zurra (Asturias)	43.40259	-4.88078	-	MW626876	MW621963	MW622237	MW621330
559624	5203	Iglesia (Cantabria)	43.36562	-3.69331	65	MW626877	MW621964	MW622238	MW621331
559626	3807	Cesareo (Cantabria)	43.32034	-3.72279	258	MW626878	MW621965	MW622239	MW621332
559628	5175	Soldados (Cantabria)	43.29725	-3.9894	370	MW626879	MW621966	MW622240	MW621333
559630	5171	Buho (Cantabria)	43.29427	-4.0028	420	MW626880	MW621967	MW622241	MW621334
559632	5213	Arrigueras (Cantabria)	43.07284	-4.0806	660	MW626881	MW621968	MW622242	MW621335
559634	5200	Murcielagos (Cantabria)	43.36159	-3.68115	70	MW626882	MW621969	MW622243	MW621336
559636	5196	Prementera (Cantabria)	43.37676	-3.75574	125	-	MW621970	MW622244	MW621337

codon position as a second block. The non-coding regions from 16S and 5.8 S rRNA + ITS2 were defined as a single data block. The nucleotide model Gamma GTR I was used.

Partitionfinder-2.1.1 (Lanfear et al., 2016) was applied for searching optimal evolutionary models for the partitions using the corrected Akaike Information Criterion (cAIC).

Table 2 Primer designs used for PCR reactions

Gene	Primer	Sequence	Sequence length (bp)	Reference
COI	LCO1490	5'-GGTCAACAAATCATAAAGATATTGG-3'	680	Folmer et al. (1994)
	HCO2198	5'-TAAACTTCAGGGTGACCAAAAAATCA-3'		
16S	16S ar	5'-CGC CTG TTT ATC AAA AAC AT-3'	440	Simon et al. (1994)
	16S br	5'- CCG GTC TGA ACT CTG ATC AT -3'		
H3	H3AD	5'-ATGGCTCGTACCAAGCAGACVGC-3'	380	Colgan et al. (1998)
	H3BD	5'-ATATCCTTRGGCATRATRG TGAC-3'		
ITS2	ITS2ModA	5'-GCTTGCGGAGAATTAATGTGAA-3'	900	Bouaziz-Yahiatene et al. (2017)
	ITS2ModB	5'-GGTACCTTGTCGCTATCGGA-3'		

Bayesian Inference (BI) was performed using Mr. Bayes v3.2.6×64 (Altekar et al., 2004; Huelsenbeck & Ronquist, 2001; Ronquist & Huelsenbeck, 2003) through the HPC cluster from the University of Bern (<http://www.id.unibe.ch/hpc>). For the concatenated data set, Partitionfinder-2.1.1 was used for finding the optimal evolutionary models for each subset with the model = all function. The Monte Carlo Markov Chain (MCMC) parameter was set as follows: starting with four chains and four separate runs for 20 million generations with a tree sampling frequency of 1000 and a burn in of 25%.

Species delimitation

The species delimitation method, Automatic Barcoding Gap Discovery (ABGD) was applied via the web browser (<https://bioinfo.mnhn.fr/abi/public/abgd/abgdweb.html>). The ABGD method (Puillandre et al., 2012) sorts the sequences into hypothetical species based on the barcode gap. ABGD was conducted using the COI alignment of the investigated *Iberozospeum* specimens. The input variables were chosen according to Weigand et al. (2013) and Inäbnit et al. (2019). The parameters were set as follows: Pmin = 0.001; Pmax = 0.1; Steps = 10; X = 1; Nb bins = 20; and distance: Jukes-Cantor.

Morphological analyses using scanning electron microscopy (SEM)

Radulae of the eastern Alpine and Dinaride *Zospeum* used in the comparative analyses are presented in Inäbnit et al. (2019). For reasons of space, only images of the radular ribbons of *Z. exiguum* and *Z. pretneri* are presented here (Fig. 14). Topotypic *I. vasconicum* and *I. zaldivarae* were collected by AJ for radular investigation. Individuals from the westernmost sampled caves (Asturias Province), derived from the collection of Jos Notenboom, housed at the Naturalis Biodiversity Center, Leiden, NL: RMNH.MOL.234108 Cueva de Torcona (exception from Burgos); RMNH.MOL.234147 Cueva de la Huertas; RMNH.MOL.234109 Cueva de la Foz; RMNH.MOL.234116 Cueva a Sul; RMNH.MOL.234144 Cueva de Rales.

Radulae were prepared according to Holznagel (1998), preserved in 96% ethanol and mounted onto prepared SEM aluminium stubs. The radulae were sputtered with gold (1–2× for 60 s) in the Agar Sputter Coater (Agar Scientific, Stanstead, UK) and viewed in the high vacuum mode of the Hitachi S-4500 scanning electron microscope (15 kV, probe current 20–100 pA) using the secondary electron detector. Photographs were taken with DISS—Digital Image Scanning System 5 (Point Electronic, Halle, Germany). All

processing of radulae was conducted at the Goethe University (Frankfurt, Germany).

SEM images of all Spanish shells showing crystallographic structure were made at the Naturalis Biodiversity Center (Leiden, NL) using the JEOL JSM-6480LV scanning electron microscope. Aluminium stubs were coated with gold–palladium using the Polaron Equipment LTD-E5100 SEM auto-coating sputter system. Shells of three potential new species, awaiting further investigation beyond our purposes here, derive from the J. Notenboom Collection: RMNH.MOL.234104 Cueva del Comediante; RMNH.MOL.234141 Cueva a Sul; and RMNH.MOL.234120, Cueva Refugio, Basinagre, Trucios. The former two shells were preserved in 75% ethanol by the collector (Notenboom & Meijers, 1985), and, thus, finer morphological structure is consequently eroded in these shells.

Histological sectioning and light microscopy follow Jochum et al. (2015b). Three individuals used in the comparative morphology include *Z. isselianum* (AJC 2287), Turjeva jama, Slovenia (46.2435, 13.5046); *Z. spelaeum* (AJC 848), Betalov Spodmol cave, Slovenia (45.7922, 14.1877); and *I. vasconicum* (AJC 1848), Cueva de la Ermita de Sandaili (42.9994, 2.4381).

Results

The maximum likelihood and Bayesian inference tree (Fig. 2) shows the concatenated data set (COI, 16S, H3 and 5.8 S rRNA + ITS2) of 67 specimens of species from the west European radiation from 55 caves and seven Dinaride outgroup taxa. The dataset was supplemented with genetic data from Weigand et al. (2013) of topotypic specimens of *I. vasconicum* (No. 151 in Weigand et al., 2013), *I. zaldivarae* (No. 162 and 163 in Weigand et al., 2013) and *I. schaufussi* (designated as *I. suarezi*, No. 140 in Weigand et al., 2013). The tree was rooted by two species of *Carychium* from the collection of AJ (in the NMBE). The topology reveals nine larger clades, which follow a geographic pattern (cf. Fig. 1).

The basic node separates Dinaride *Zospeum* taxa from taxa inhabiting northern Spanish caves. This node has a full ML and BI support and justifies the designation of the western *Zospeum* radiation to a separate new genus, *Iberozospeum* n. gen. The p-distances which show the numbers of base differences per site between sequences were calculated (Kumar et al., 2018). The mean p-distance from *Iberozospeum* n. gen. and *Zospeum* is 0.0767 (Table S1 in the supplementary material). The mean p-distance from *Zospeum* and *Carychium* is 0.1285. The mean p-distance of *Iberozospeum* n. gen. and *Carychium* is 0.1177.

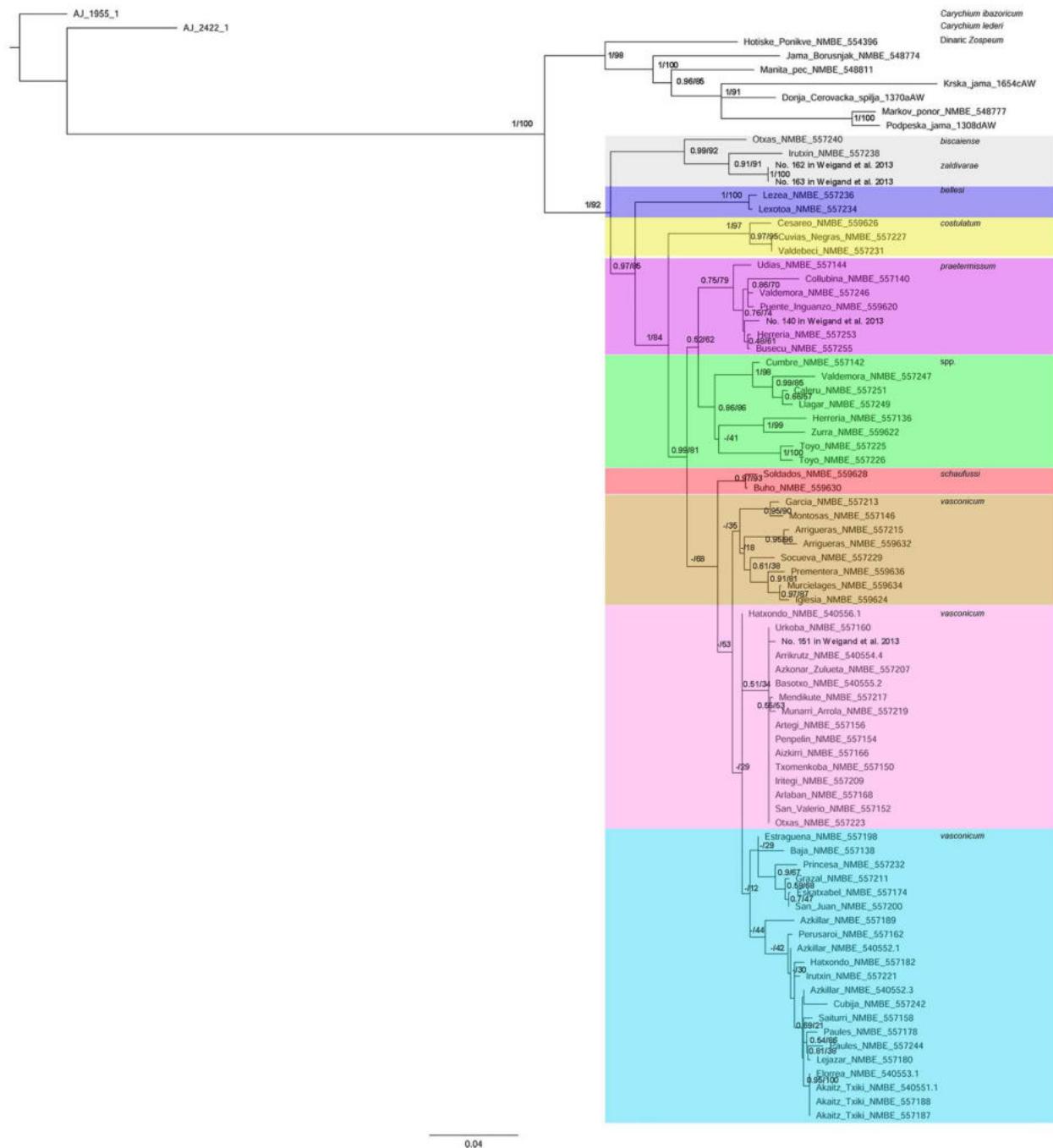


Fig. 2 Combined maximum likelihood (RAxML) and Bayesian inference (BI) tree based on concatenated data set of COI, 16S, H3 and 5.8 S rRNA + ITS2. The analysis comprises 67 individuals of northern Spanish *Iberozeugospeum* from 55 caves and seven Dinaride outgroup taxa. The tree was rooted by two species of *Carychium* from

the collection of AJ (in the NMBE). Additionally, sequences of *I. schaufussi*, *I. vasconicum* and *I. zaldivarae* from their type localities are included. The numbers at the nodes represent the Bayesian posterior probabilities (left) and the bootstrap support values (right). The dash (-) means that the node is not supported

In order to study the effect of incomplete genetic data, a reduced set comprising 42 individuals was computed (Fig. 3). Here, only specimens were used with a complete record of all four markers. The bootstrap support values and

the Bayesian posterior probabilities are over all higher in the tree with complete marker sets (Fig. 3).

The *biscaiense-zaldivarae*-clade (grey clade in Figs. 2 and 3) harbours congeners from two different caves (Otxas

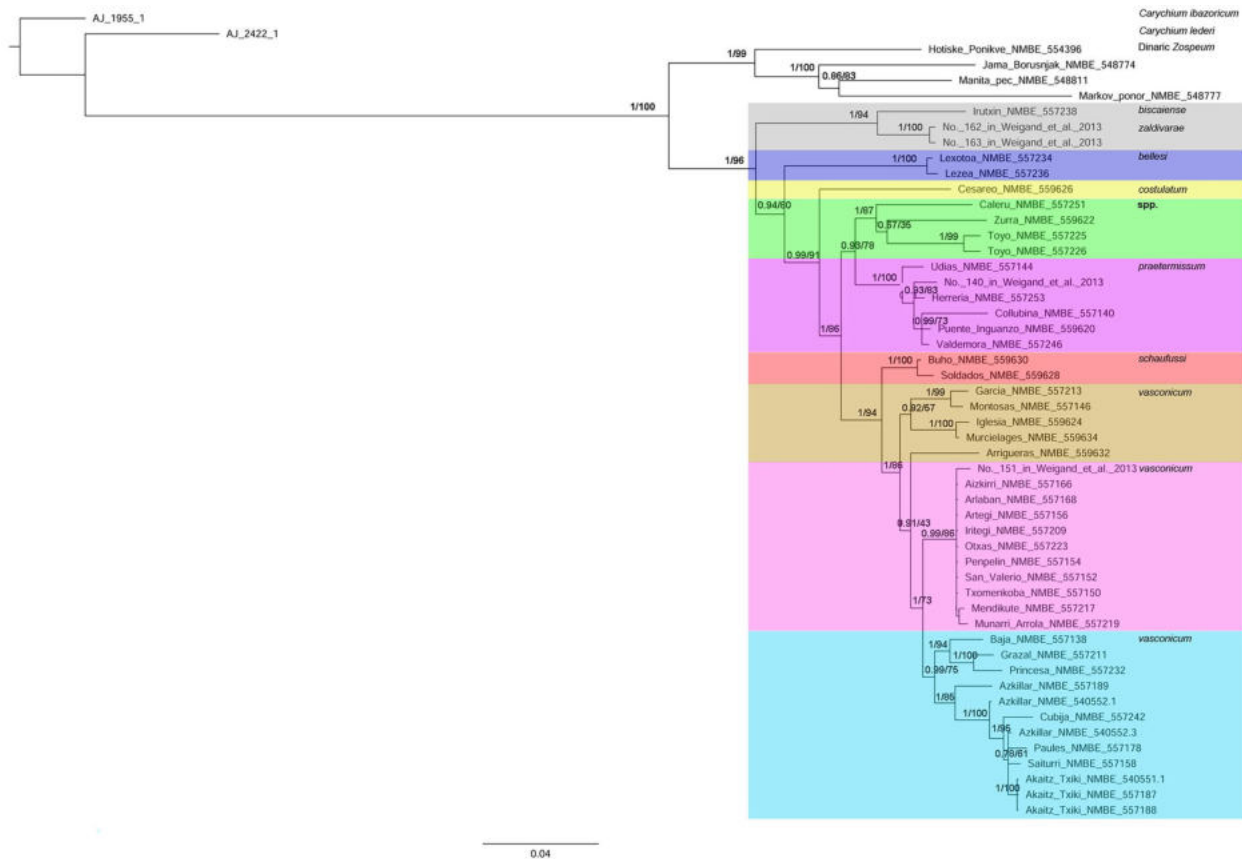


Fig. 3 Combined maximum likelihood (RAxML) and Bayesian inference (BI) tree based on concatenated data set of COI, 16S, H3 and 5.8 S rRNA + ITS2. The analysis consists of 42 individuals of northern Spanish *Iberozospeum* from 37 caves and four Dinaride outgroup taxa. Only specimens with complete marker sets are included. The

tree was rooted by two species of *Carychium* from the collection of AJ (in the NMBE). Additionally, sequences of *I. schauffussi*, *I. vasconicum* and *I. zaldivarae* from their type localities are included. The numbers at the nodes represent the Bayesian posterior probabilities (left) and the bootstrap support values (right)

and Irutxin) which cluster with specimens of *zaldivarae* from the type locality (No. 162 and 163 in Weigand et al., 2013). The caves, Otxas and Irutxin, are about 100 km apart from each other and are non-contiguous. Congeners from these two caves are also found in the low-resolution *vasconicum*-clade 1 (pink clade in Figs. 2 and 3) and *vasconicum*-clade 2 (light blue clade in Figs. 2 and 3). From the external perspective, the investigated specimen (NMBE 557240) in the grey clade shows a typical *biscaiense* morph (Figs. 4a). It is found in the cave Otxas, which is the type locality of *I. biscaiense*. The specimen from the cave Irutxin (NMBE 557238) displays typical character states of *zaldivarae*.

The specimens from the *bellesi*-clade (dark blue clade in Figs. 2 and 3) were collected in the caves Lezea and Lexotoa at the border of Spain and France. The caves are 1 km apart from each other and probably contiguous. This node is supported in our investigation (posterior probability of 0.97 and bootstrap value of 85 in Fig. 2, respectively, 0.94 and

80 in Fig. 3). In both phylogenetic trees (Fig. 2 and 3), the two investigated specimens have a bootstrap value of 100. The p-distance is 0.0039. From a morphological perspective, they have a similarly high-spined, conical shell form, but the aperture is clearly different. The aperture of the specimen from Lexotoa (NMBE 557234) (Fig. 5b) is oblique and has a moderately angular parietal shield. On the other hand, the parietal shield of the specimen from Lezea (NMBE 557236) (Fig. 5a) is compact and consists of thick callus, which is seemingly fused onto the body whorl. The peristome of the Lezea specimen is thick and roundish in form.

The Basque clade (Figs. 6 and 7) splits into two: a narrow, more centrally distributed *vasconicum*-clade 1 (pink clade in Figs. 2 and 3; Fig. 6) and a broader, western-reaching distribution comprising the *vasconicum*-clade 2 (light blue clade in Figs. 2 and 3; Fig. 7). The node of the split of these two clades has a low support (bootstrap value of 29 in Fig. 2, respectively 73 in Fig. 3). The split of these two clades is

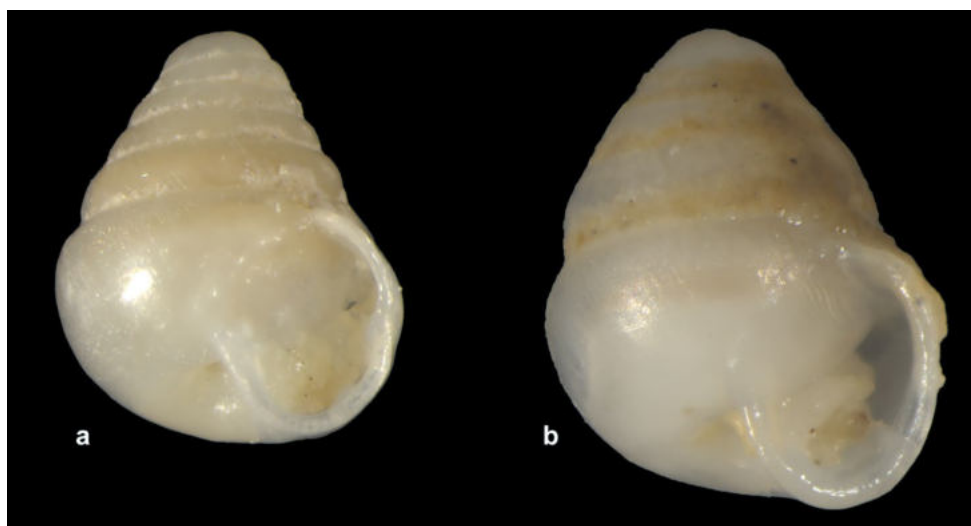


Fig. 4 Grey clade; (a) *Iberozospeum biscaiense* NMBE 557240, Durang, Igorre, Cueva Otxas, 23.3.2016, sh: 1.37 mm; (b) *Iberozospeum zaldivarae* NMBE 557238, Aralar, Arbizu, Cueva Irutxin, 20.6.2015, sh: 1.59 mm. — All phot. $\times 40$

not supported by the Bayesian posterior probability. The topotypic specimen of *I. vasconicum* (No. 151 in Weigand et al., 2013) clusters within the pink clade. Morphologically, shells from caves clustering in the pink *vasconicum*-clade 1 (Fig. 6) showed a commensurate similarity in shell shape and apertural configuration with noticeable differences in spire height in shells from Basotxo cave (Ton de Winter, unpubl. data 2015). The two westernmost specimens NMBE 557138 and NMBE 557242 (cf. Fig. 1 and Fig. 7b, j) in the light blue *vasconicum*-clade 2 differ morphologically from the remaining *vasconicum*-like specimens in the clade.

The *vasconicum*-clade 3 (brown clade in Figs. 2 and 3) has high posterior probability and bootstrap support only in the terminal nodes. The deep nodes in the brown clade are

not supported in the ML analysis (bootstrap support of 53, respectively, 57 in Fig. 3). Morphologically, they resemble typical *I. vasconicum* due to shell shape and the apertural configuration. The specimen in Fig. 8a is about 1.5 times bigger than the smallest specimen from the brown clade, but the shell shape is very similar to the other specimens in this clade. Figure 8g is remarkable due to its broad conical form, the deeply pronounced suture and the obvious, broadly deepened umbilicus. We consider it a new species.

Support values in the *schaufussi*-clade (red clade in Figs. 2 and 3) are high. In Fig. 9a, a specimen from the cave Búho, Puente Viesgo, is illustrated, which is the type locality of *I. suarezi* (Gittenberger, 1980). However, comparing our specimen with the holotype of *I.*

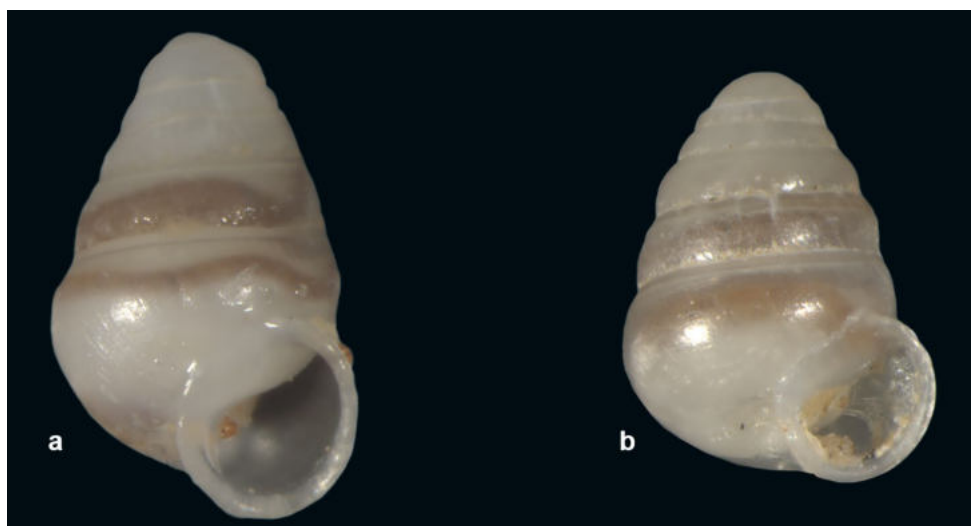
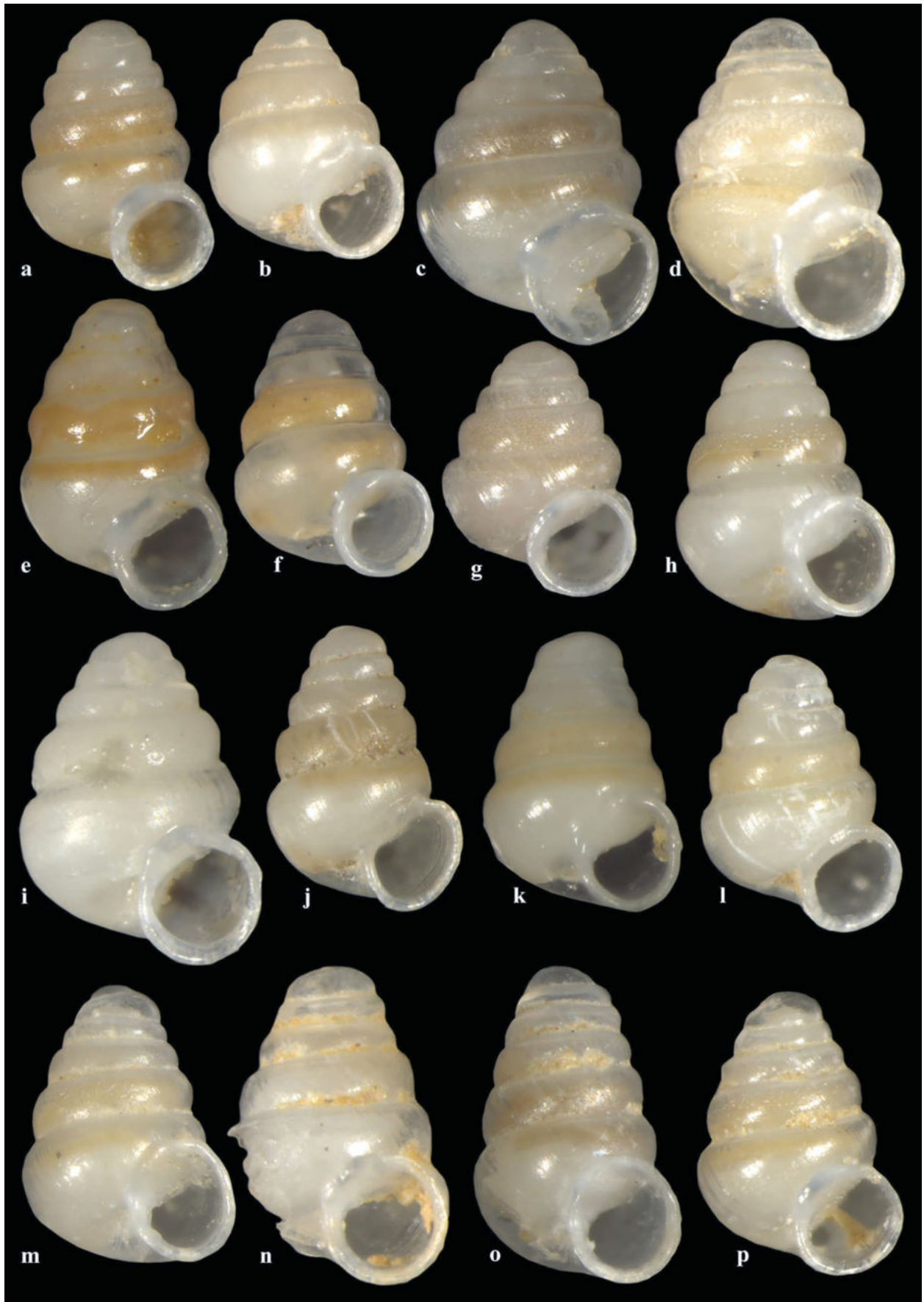


Fig. 5 *Iberozospeum bellesi*. Dark blue clade; (a) NMBE 557236, Zugarram, Sare, Lezea, 13.12.2015, sh: 1.67 mm. (b) NMBE 557234, Zugarram, Zugarramurdi, Lexotoa-2, 20.12.2015, sh: 1.38 mm. — All phot. $\times 40$



Fig. 6 *Iberozospeum vasconicum*. Pink clade; (a) NMBE 557207, Aizkorri, Onati, Azkonar Zulueta, 28.5.2016, sh: 1.31 mm; (b) NMBE 557160, Aizkorri, Eskortatza, Urkoba, 8.3.2017, sh: 1.18 mm; (c) NMBE 557217, Ernio, Tolosa, Mendikute, 23.9.2017, sh: 1.5 mm; (d) NMBE 557219, Bust-Lea, Forua, Munarri Arrola, 9.12.2017, sh: 1.56 mm; (e) NMBE 557209, Aizkorri, Onati, Cueva Iritegi, 28.5.2016, sh: 1.43 mm; (f) NMBE 557150, Aizkorri, Onati, Txomenkoba Goikoa, 16.12.2015, sh: 1.27 mm; (g) NMBE 557156,

Udalaitz, Elorrio, Cueva Artegi, 17.5.2016, sh: 1.48 mm; (h) NMBE 557168, Aizkorri, Onati, Arlaban, 11.2017, sh: 1.27 mm; (i) NMBE 557154, Udalaitz, Aretxabaleta, Cueva Penpelin, 26.4.2016, sh: 1.34 mm; (j) NMBE 557166, Aizkorri, Onati, Aizkirri, 11.2017, sh: 1.59 mm; (k) NMBE 557223, Durang, Igorre, Otxas, 23.3.2016, sh: 1.24 mm; (l) NMBE 557152, Udalaitz, Arrasate, San Valerio (Galarra), 23.3.2016, sh: 1.25 mm. No picture of NMBE 540554.4, 540555.2, 540556.1 (shell destroyed). — All phot. $\times 40$



◀**Fig. 7** *Iberozospeum vasconicum*. Light blue clade; (a) NMBE 557198, Cueva de la Fuente de Estragueña, 16.6.2011, sh: 1.26 mm; (b) NMBE 557138, Castro, Laredo, La Baja, 12.4.2017, sh: 1.11 mm; (c) NMBE 557232, Triano, Galdames, Mina Princesa (superior), 3.7.2016, sh: 1.51 mm; (d) NMBE 557211, Triano, Güenes, Grazal, 2.10.2016, sh: 1.49 mm; (e) NMBE 557174, Triano, Galdames, Escachabel-2 (Uralaga), 1.4.2013, sh: 1.44 mm; (f) NMBE 557200, Triano, Galdames, Bitzkaia, Cueva de la San Juan, 10.6.2012, sh: 1.23 mm; (g) NMBE 557189, Durang, Atxondo, Azkillar (=Galtaikoba), 16.3.2014, sh: 1.19 mm; (h) NMBE 557182, Durang, Zeberio, Cueva Hatxondo, 30.12.2012, sh: 1.28 mm; (i) NMBE 557221, Aralar, Arbizu, Cueva Irutxin, 20.6.2015, sh: 1.54 mm; (j) NMBE 557242, Ason, Matienzo, Cueva Cubija (=Marcos), 19.7.2016, sh: 1.34 mm; (k) NMBE 557178, Salvada, Berberana, Las Paules, 21.6.2011, sh: 1.3 mm; (l) NMBE 557180, Salvada, Izarra, Torca Lejazar, 28.12.2013, sh: 1.29 mm; (m) NMBE 557244, Salvada, Berberana, Las Paules, 9.11.2013, sh: 1.28 mm; (n) NMBE 557158, Aizkorri, Eskoriatza, Saiturri-2, 22.2.2017, sh: 1.47 mm; (o) NMBE 557187, Aralar, Ataun, Cueva Akaitz Txiki, 14.1.2014, sh: 1.47 mm; (p) NMBE 557188, Aralar, Ataun, Cueva Akaitz Txiki, 14.1.2014, sh: 1.32 mm. NMBE 557162, Aizkorri, Parzoneria, Perusaroi-1, 15.5.2017 (subadult shell, not shown on plate). No pictures of NMBE 540551.1, 540552.1, 540552.3, 540553.1 (shells destroyed). — All phot. ×40

suarezi (RMNH.MOL.55383) (Jochum et al., 2019: 72, Fig. 4a–c), it is evident that this is the same species. The specimens from the two Cantabrian clades have a more elliptical aperture compared with the *vasconicum*-clade specimens (pink, light blue and brown clades in Figs. 2, 3, 6, 7, and 8).

The Asturian clade splits into two subclades (purple and green clades in Figs. 2 and 3). Support values within these clades are moderate to high. Weigand et al. (2013: Fig. 5) sequenced two specimens from the Cueva del Bosque/Cueva Inguanzo, which cluster within the purple clade (Figs. 2 and 3). Moreover, Weigand et al. (2013) identified these two specimens as *I. suarezi* and considered them “evolutionary lineage Z14” (No. 140 in Weigand et al., 2013 in our trees). Jochum et al. (2019: 83–84, Fig. 15) explained that this cave is situated 1 km opposite of the cave, Cueva del Puente de Inguanzo, which is the cave Gittenberger (1980) considered to be inhabited by *I. schaufussi* sensu Gittenberger (1980: Fig. 1) and *I. suarezi* Gittenberger (1980: Fig. 2). These two taxa were recognised by Jochum et al. (2019) to be misidentifications and were subsequently described as new species, viz., *I. gittenbergeri* Jochum (Jochum, Prieto & De Winter, 2019 in Jochum et al., 2019) and *I. praetermissum* Jochum (Jochum, Prieto & De Winter, 2019 in Jochum et al., 2019). Since *I. gittenbergeri* is known only from a single shell and no clearly definable, live adult snail was found, it could not be included in this study. In Figs. 2 and 3, a specimen from the “evolutionary lineage Z14” (Weigand et al., 2013) and another species (Fig. 10f) from Cueva del Puente Inguanzo are included. The specimen in Fig. 10f was found at the type locality of *I. praetermissum*. This specimen is a juvenile and the identification is not clear since the aperture is not

fully grown. The specimens in Figs. 10a–e have a high, conical spire and a barely developed lamella on the columella (Fig. 10d) and are considered to be *I. praetermissum*. The p-distance from the specimen in Fig. 10f and the topotypic specimen No. 140 from Weigand et al. (2013) is 0.0086. The mean p-distance from the investigated specimens in the purple clade (Figs. 2 and 3, Fig. 10a–f) and the specimen, No. 140 from Weigand et al. (2013), is 0.006.

The green clade contains various morphs. The topotype specimen of *I. percostulatum* (Fig. 10h) from the cave Herreña is a juvenile. In this cave, another species, here considered to be *I. praetermissum*, (Fig. 10b) lives in syntopy or at least in sympatry with *I. percostulatum*. Another well-supported lineage is visible in Fig. 10i and j, with both specimens originating from the same population in El Toyo in Cantabria; the two shells are morphologically quite different, illustrating shell variability within the lineage. The shell of the specimen from the Picos (Fig. 10k) is broadly conical, with a remarkably narrow-stepped coiling pattern of the teleoconch whorls and a large elliptical aperture. The group comprising Fig. 10l–n, forms another lineage in the green clade, which is characterised by broad conical shells resembling the specimen from the Picos, but with high and well-rounded teleoconch whorls.

The yellow clade (Figs. 2, 3, and 11) contains ribbed specimens with varying degrees of superficial striation. Although the specimen in Fig. 11a has less-pronounced ribs, they are clearly visible in apical view. This shell bears a deep suture and its aperture is elliptical and reverted. The specimen in Fig. 11b is a juvenile but the ribs are clearly visible. Although the shell morphology is different, it clusters together with specimen 11c, with a bootstrap support of 95 (Fig. 2). The p-distance of these individuals is 0 since only the nuclear marker H3 could be sequenced for both specimens and this sequence is identical. On the other hand, the strongly ribbed specimen in Fig. 10c constitutes the new species, *Iberozospeum costulatum* n. sp.

The ABGD assigned the 45 *Iberozospeum* COI sequences into 22 groups. The Barcode gap distance is 0.012. In Table 3 are the groupings of the ABGD analysis. Since we do not have the COI sequences of all investigated animals, not all specimens could be assigned to a group. The two animals from the same population from Toyo Cave (NMBE 557225 and 557226) were divided into different groups. Using ABGD, all animals from the pink *vasconicum*-clade were classified into group 1. Group 2 consists exclusively of animals from the light blue *vasconicum*-clade. Some animals from the light blue *vasconicum*-clade were classified into other groups (Table 3). The two animals from the *schaufussi*-clade (NMBE 559628 and 559630) were placed in group 6. The specimens from the *praetermissum*-clade were placed in group 7. The two specimens from the *bellesi*-clade (NMBE 557234 and 557236) were assigned in group 15. The remaining groups each contain only one animal.

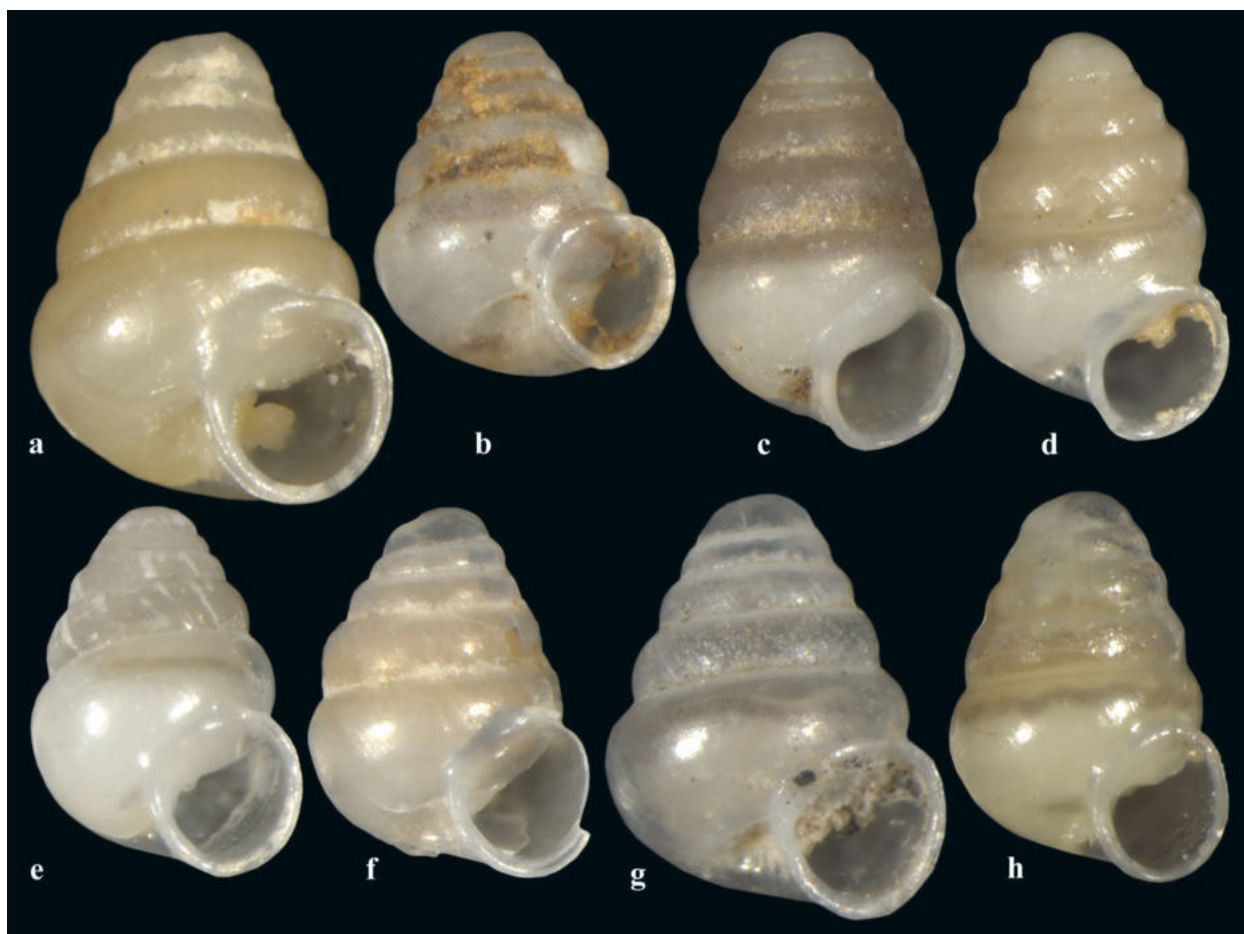


Fig. 8 *Iberozospeum vasconicum*. Brown clade; (a) NMBE 559634, Cantabria, Entrambasaguas, Murcielagos, 28.3.2018, sh: 1.56 mm; (b) NMBE 559624, Cantabria, Entrambasaguas, Iglesia, 28.3.2018, sh: 1.14 mm; (c) NMBE 557215, Cantabria, Santiurde de Reinosa, Las Arrigueras, 20.1.2018, sh: 1.39 mm; (d) NMBE 559632, ditto, 29.3.2018, sh: 1.36 mm; (e) NMBE 557213, Guareña, Merindad de

Sotoscueva, Garcia, 26.11.2017, sh: 1.23 mm; (f) NMBE 557146, Miera, Soba, Las Montosas, 20.2.2016, sh: 1.23 mm; (g) NMBE 557229, Ason, Arredondo, San Juan de Socueva, 12.4.2017, sh: 1.41 mm; (h) NMBE 559636, Cantabria, Entrambasaguas, Prementera, 28.3.2018, sh: 1.3 mm. — All phot. $\times 40$

Morphology

Although only one member of *Iberozospeum* is histologically sectioned here, sections of the upper visceral complex of topotypic *I. vasconicum* (AJC 1848) show that the anatomy follows the general carychiid design (Morton, 1955; Harry, 1997–1998) and that described for *Zospeum* in Maier (1982), Dörge (2010), and Jochum et al. (2015b) as well as in Barker (2001) for aspects of the Ellobiidae (Fig. 12). The cross-sections reveal no phylogenetic differences but rather, seasonal differences in the specific individuals. The *I. vasconicum* individual, collected in June 2011, is aphallate. Euphally was detected by Jochum et al. (2015b) in *Z. amoenum* (von Frauenfeld, 1856) (species revised from “*Zospeum* sp.” in Inäbnit et al., 2019), collected in August 2008 from Konečka zijalka, Slovenia. The histological sections of the upper visceral complex of individuals of topotypic *Z. isselianum* (Pollonera, 1887) (AJC 2287) and *Z.*

spelaeum (Rossmässler, 1839) (AJC 848) from the Dinarides (Fig. 12a–b) in this work also show that these snails were aphallate during time of collection in June and October, respectively. The same upper visceral region of the snail (cuts 14–22) in our histological sections (Fig. 12) shows different perspectives due to the generally larger size of the two Dinaride individuals in this study. Visible in clockwise rotation from the outside in, *Z. isselianum* shows the mantle gland (mag), the cerebral ganglion (cg), the mantle cavity (mc), the pleural ganglion (pg), the foot (f), the pharynx (ph), the oesophagus (oe), the statocyst containing otoliths and the columellar muscle (cm) (Fig. 12a). For *Z. spelaeum*, the same clockwise perspective shows the mantle gland (mag), the foot (f), some haemolymph (hl), the pharynx (ph), the oesophagus (oe), a hump shaped upper, non-vascularized columellar muscle (cm) and a moderately long genital opening (go) (Fig. 12b). For *I. vasconicum*, a remarkably huge, glandular albumen gland (ag) is clearly

visible (Fig. 12c). This is a compound, sac-like enlargement of the oviduct and is responsible for producing albumen for the formation of the eggs (Luchtel et al., 1997). The albumen gland is a female accessory sex gland, which enlarges with sexual maturation of the animal. The size of this gland is considered to determine the maximum number of eggs that can be produced at any one time (Barker, 2001). Due to the presence and large size of the albumen gland (indicative of the female phase) here, modification in existing structures and superposition of others on the fundamental carychiid pattern is clearly the case. Also, strikingly apparent is the large, well-developed, mucous gland (stained reddish violet) (mg). Additionally, visible in the clockwise perspective of the upper visceral complex of *I. vasconicum* is the kidney (k) with a prominent renopericardial passage and the heart (h) located at the base of the kidney, haemolymph (hl) at the foot section (f), the contractile pneumostome (p), the mantle gland (mag), the pharynx (ph) and oesophagus (oe), the vascularized, 2-humped columellar muscle (cm) and the long genital opening (go) (Fig. 12c). We remark that deeper analysis of anatomical aspects and individual structural analyses of *Iberozospeum* is beyond the scope of this paper and will be presented in a future work.

Significant however, for *Iberozospeum* n. gen., is that the columellar muscle shows prominent humps, which contain vasculature extending to the tips of these humps (Fig. 12c). In our investigation of the columellar lamellae of *Iberozospeum*, the dense, scaly crystallographic structure on localised zones of the lamellae correlates perfectly with the corresponding points of contact of these two hump-like elevations of the columellar muscle (Fig. 13). In sync with this observation, Barker (2001) emphasized there is a trend amongst the Ellobiidae that the columellar muscle becomes detached from the body wall from its origin on the columella and has become largely free in the haemocoel. The columellar muscle, thus, runs forward to attach on the cephalic organs and anterior body wall (Barker, 2001). In this case, rather than just simply retracting, the cephalopodal mass becomes inverted when the animal retracts into the shell (Barker, 2001). In *Iberozospeum*, the columellar muscle is indeed detached except at these two points of contact. In the Alpine and Dinaride species of *Zospeum*, crystallographic structure is not overlapping and not restricted to specific points. Moreover, it is comprised of low shoals of crystallographic structure (seen also in fossil Carychiidae in Jochum et al., 2015c, Fig. 5), randomly interspersed over the columellar lamellae deep in the shells of *Z. spelaeum* from two separate caves in Slovenia (MCBI CSR SASA 37049a, Velika Pasica and AJC 847, Betalov Spodmol Grotte) (Fig. 13a–b) here. Remarkable are the dense, localised, overlapping wedges of crystallographic structure on the complementary points of the columellar lamellae in the empty shells of the Iberian taxa: *Iberozospeum* sp. RMNH.MOL.234120 (Cueva

Refugio, Trucios) (Fig. 13c–d), on the upper part of the lamella of *Iberozospeum* sp. RMNH.MOL.234104 (Cueva del Comediante) and on the lamella of *Iberozospeum* sp. RMNH.MOL.234141 (Cueva a Sul, Oviedo) (Fig. 13e–f) as well as on that of *I. vasconicum* (AJC 1849, Cueva Arrikruz) (Fig. 13g–h). The lower lamella of *I.* sp. RMNH.MOL.234120 (Cueva Refugio, Trucios) clearly shows the specific locality of the contact point of the columellar muscle (Fig. 13c–d). Shells of RMNH.MOL.234104 (Cueva del Comediante) and RMNH.MOL.234141 (Cueva a Sul, Oviedo) (Fig. 13e–f), which were initially preserved in 75% ethanol, still show the characteristic, rough crystallographic structure despite deterioration by the ethyl-alcohol treatment subjected to them by the collector (Notenboom & Meijers, 1985).

Our morphological investigations also included the radulae of four Dinaride and eastern Alpine taxa described and imaged in Inäbnit et al. (2019, Supplementary Figs. S17–21) including *Z. exiguum* (Kuščer, 1932) (NMBE 553384) (Inäbnit et al., 2019, Fig. S17a–d); *Z. obesum* (von Frauenfeld, 1854) (NMBE 553409) (Inäbnit et al., 2019, Fig. S18f–h); *Z. pretneri* (Bole, 1960) (NMBE 553290) (Inäbnit et al., 2019, Fig. S19a–d); and *Z. spelaeum* (Rossmässler, 1839) (NMBE 553311) (Inäbnit et al., 2019, Fig. S20e–f). These were compared with radulae extracted from individuals collected from the westernmost-sampled caves by Oviedo (Asturias) and radulae from topotypic material of *Z. vasconicum* (Prieto et al., 2015 in Jochum et al., 2015a) (AJC 1847) and *Z. zaldivarae* (Prieto et al., 2015 in Jochum et al., 2015a) (AJC 1876).

In this comparative study, the narrow radular ribbons of Dinaride *Zospeum* are tapered to an obtuse or to a straight base as in *Z. exiguum* (Fig. 14a) or a straight base as in *Z. pretneri* (Fig. 14b). The Iberian radulae have a tapered

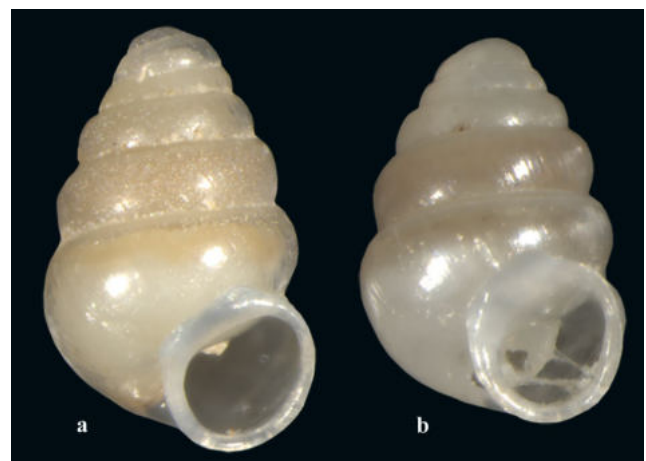


Fig. 9 *Iberozospeum schaufussi*. Red clade: (a) NMBE 559630, Cantabria, Puente Viesgo, Búho, 27.3.2018, sh: 1.41 mm; (b) NMBE 559628, Cantabria, Puente Viesgo, Soldados, 27.3.2018, sh: 1.28 mm. — All phot. $\times 40$



Fig. 10 *Iberozospeum praetermissum*. Purple clade; a–f. (a) NMBE 557144, Cantabria, Cabezon-MS, Udias, Udias (Cobijon), 28.8.2016, sh: 1.25 mm; (b) NMBE 557253, Asturias, Llanes, Cueva La Herreña, 23.12.2017, sh: 1.34 mm; (c) NMBE 557255, Leon, Soto de Sajambre, Cueva Busecu, 10.3.2018, sh: 1.37 mm; (d) NMBE 557246, Asturias, Candamo, Cueva de la Peñona de Valdemora, 5.3.2018, sh: 1.22 mm; (e) NMBE 557140, Asturias, Llanes, Collubina, 18.7.2017, sh: 1.35 mm; (f) NMBE 559620, Cantabria, Cueva Puente Inguanzo, 6.4.2018, sh: 1.29 mm. — *Iberozospeum* spp. Green clade; g–n. (g) NMBE 559622, Cantabria, Cueva La Zurra, 6.4.2018, sh: 1.31 mm; (h) NMBE 557136, Asturias, Llanes, La Herreña, 18.7.2017, sh: 1.14 mm; (i) NMBE 557226, Cantabria, Lamason, El Toyo, 11.7.2015, sh: 1.7 mm; (j) NMBE 557225, Cantabria, Lamason, El Toyo, 11.7.2015, sh: 1.33 mm; (k) NMBE 557142, Asturias, Picos, Cabrales, Torca Cumbre, .8.2016, sh: 1.45 mm; (l) NMBE 557251, Asturias, Parres, Cueva El Caleru, 10.3.2018, sh: 1.41 mm; (m) NMBE 557249, Asturias, Yernes y Tameza, Cueva Llagar, 2.2.2018, sh: 1.49 mm; (n) NMBE 557247, Asturias, Candamo, Cueva de la Peñona de Valdemora, 5.3.2018, sh: 1.48 mm. — All phot. $\times 40$

anterior end (velum), followed by a well-defined adhesive zone leading to a remarkably straight, carpet-like swath of longitudinal rows of smaller teeth and more of them per transverse row (Figs. 14c–h, 15c). The rachidian and lateral teeth of *I. vasconicum* demonstrate remarkable similarity to those of *Carychium ibazoricum* Bank & Gittenberger,

1985, imaged in Martins (2007, Fig. 138) (Fig. 15e). The rachidian and lateral teeth of the radula of topotypic *I. vasconicum* (AJC 1848) show long endo- and ectocones flanking the mesocone by one half–three fourths the length of the mesocone (Fig. 15e). The radula of topotypic *Z. pretneri* (NMBE 553290), *I. vasconicum*'s externally most similar phenotypic relative from the Dinarides, shows endo- and ectocones that are one third–one half the length of the mesocone (Fig. 15a). Medial grooves are visible on the mesocones of *Z. pretneri* and *Z. isselium* (AJC 874, Turjevka jama, Slovenia) here (Fig. 15a–b) as well as in a number of other eastern Alpine and Dinaride species (see Inäbnit et al., 2019, Supplementary Figs. S17–21). The basal plates are generally more compact and shorter in the radulae of Iberian taxa (Figs. 15c–e, h) versus the longer and thinner versions of those of the eastern Alpine and Dinaride *Zospeum* species (Fig. 15a–b) (see also Inäbnit et al., 2019, Supplementary Figs. S17–21). Basal plates maintain the spacing of teeth and support them in the feeding process (Luchtel et al., 1997). The radular ribbon of topotypic *I. zaldivarae* (AJC 1876) shows a rachidian tooth with a long pointed mesocone and very short endo- and ectocones that are about one fourth the length of the mesocone (Fig. 15g). The lateral teeth bear very short mesocones flanked by long, fang-like endo- and

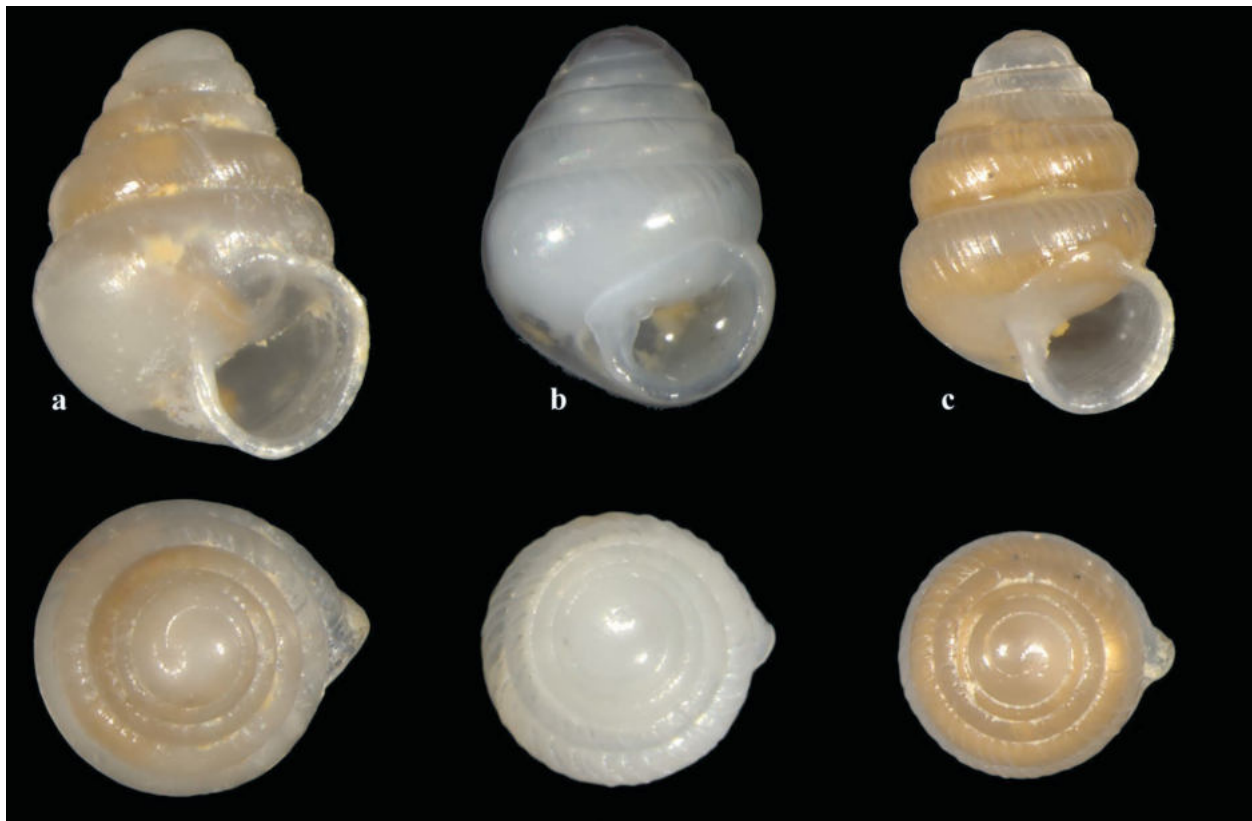


Fig. 11 *Iberozospeum costulatum*. Yellow clade; (a) NMBE 559626, Cantabria, Lierganes, Cesareo, 21.3.2016, sh: 1.42 mm; (b) NMBE 557227, Cantabria, Ason, Soba, Cuvias Negras, 12.4.2017, sh:

1.27 mm; (c) NMBE 557231, Alen, Sopena, Valdebeci, 20.10.2015, sh: 1.27 mm. — All phot. $\times 40$

Table 3 Results of the species delimitation method ABGD

NMBE-No	ZUPV-No	Cave and Province	ABGD group	clade
557150	3405	Txomenkoba (Gipuzkoa)	1	<i>vasconicum</i> (pink)
557152	3758	San Valerio (Gipuzkoa)	1	<i>vasconicum</i> (pink)
557154	3849	Penpelin (Gipuzkoa)	1	<i>vasconicum</i> (pink)
557156	3856	Artegi (Bizkaia)	1	<i>vasconicum</i> (pink)
557166	4990	Aizkirri (Gipuzkoa)	1	<i>vasconicum</i> (pink)
557168	5005	Arlaban (Gipuzkoa)	1	<i>vasconicum</i> (pink)
557209	3904	Iritegi (Gipuzkoa)	1	<i>vasconicum</i> (pink)
557217	4930	Mendikute (Gipuzkoa)	1	<i>vasconicum</i> (pink)
557219	5087	Munarri Arrola (Bizkaia)	1	<i>vasconicum</i> (pink)
557223	3728	Otxas (Bizkaia)	1	<i>vasconicum</i> (pink)
540551_1	1847	Akaitz Txiki (Gipuzkoa)	2	<i>vasconicum</i> (light blue)
540552_1	2039	Azkillar (Bizkaia)	2	<i>vasconicum</i> (light blue)
540552_3	2039	Azkillar (Bizkaia)	2	<i>vasconicum</i> (light blue)
557178	1607	Paules (Burgos)	2	<i>vasconicum</i> (light blue)
557187	1847	Akaitz Txiki (Gipuzkoa)	2	<i>vasconicum</i> (light blue)
557188	1847	Akaitz Txiki (Gipuzkoa)	2	<i>vasconicum</i> (light blue)
559632	5213	Arrigueras (Cantabria)	3	<i>vasconicum</i> (brown)
557189	2039	Azkillar (Bizkaia)	4	<i>vasconicum</i> (light blue)
557138	4702	Baja (Cantabria)	5	<i>vasconicum</i> (light blue)
559628	5175	Soldados (Cantabria)	6	<i>schaufussi</i> (red)
559630	5171	Buho (Cantabria)	6	<i>schaufussi</i> (red)
557140	4862	Collubina (Asturias)	7	<i>praetermissum</i> (purple)
557246	5210	Valdemora (Asturias)	7	<i>praetermissum</i> (purple)
557253	5209	Herreria (Asturias)	7	<i>praetermissum</i> (purple)
557255	5208	Busecu (Leon)	7	<i>praetermissum</i> (purple)
559620	5257	Puente Inguanzo (Asturias)	7	<i>praetermissum</i> (purple)
557249	4915	Llagar (Asturias)	8	spp. (green)
557251	5211	Caleru (Asturias)	8	spp. (green)
559626	3807	Cesareo (Cantabria)	9	<i>costulatum</i> (yellow)
557242	4057	Cubija (Cantabria)	10	<i>vasconicum</i> (light blue)
557213	5006	Garcia (Burgos)	11	<i>vasconicum</i> (brown)
557200	854	San Juan-9 (Bizkaia)	12	<i>vasconicum</i> (light blue)
557211	4864	Grazal (Bizkaia)	12	<i>vasconicum</i> (light blue)
559624	5203	Iglesia (Cantabria)	13	<i>vasconicum</i> (brown)
559634	5200	Murcielagos (Cantabria)	13	<i>vasconicum</i> (brown)
557238	2875	Irutxin (Navarra)	14	<i>biscaiense</i> (grey)
557234	3371	Lexotoa-2 (Navarra)	15	<i>bellesi</i> (dark blue)
557236	3323	Lezea (Navarra)	15	<i>bellesi</i> (dark blue)
557146	3820	Montosas (Cantabria)	16	<i>vasconicum</i> (brown)
557232	4017	Princesa (Bizkaia)	17	<i>vasconicum</i> (light blue)
557158	4601	Saiturri-2 (Gipuzkoa)	18	<i>vasconicum</i> (light blue)
557225	4102	Toyo (Cantabria)	19	spp. (green)
557226	4102	Toyo (Cantabria)	20	spp. (green)
557144	4136	Udias (Cantabria)	21	<i>praetermissum</i> (purple)
559622	5258	Zurra (Asturias)	22	spp. (green)

ectocones on compact basal plates. The size and shape of teeth vary from row to row (Fig. 15h). As it is known for many ellobiids, the transition from the lateral teeth to the pectinate marginal teeth is abrupt (Fig. 15e) or gradual via

a few intermediate, transitional teeth (Fig. 15c, h) (Martins, 1996, 2007). Within the central longitudinal rows of the radulae, the rachidian teeth of the individuals from Asturias (Fig. 15c–d) and Burgos (Fig. 15f) show a long mesocone

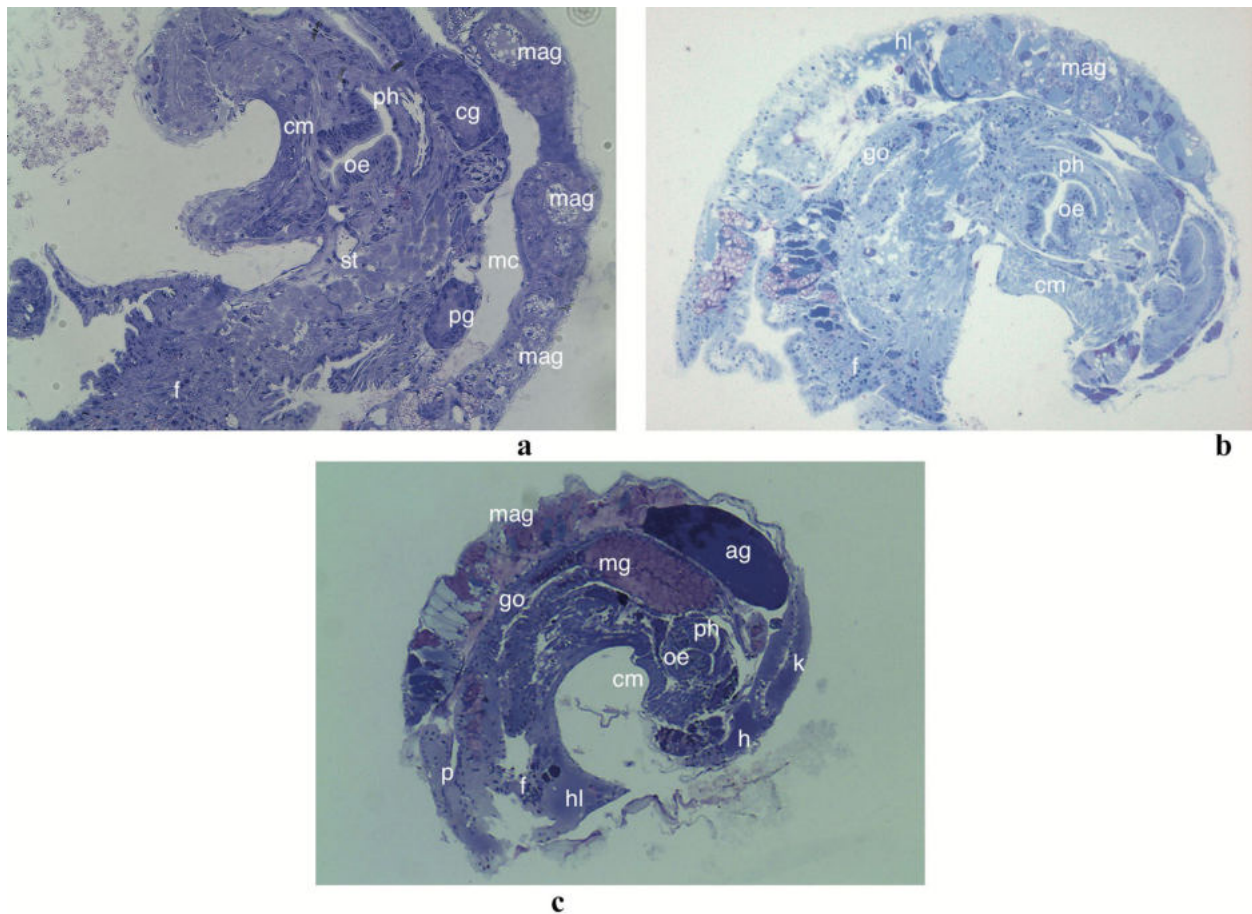


Fig. 12 Light micrograph showing histological overview of the upper visceral mass of *Zospeum* and *Iberozospeum*. Visible structures vary due to the season of collection, degree of sexual maturity of the individual and the presence of certain structures and the superposition of others. Labels proceed clockwise rotating from the outside in; **(a)** topotypic *Z. isselianum* (AJC 2287), Turjeva jama, Slovenia (46.2435, 13.5046): mantle gland (mag), foot (f), mantle cavity (mc), cerebral ganglion (cg), pleural ganglion (pg), pharynx (ph), oesophagus (oe), statocyst (st), pedal ganglion (pg), columellar muscle (cm); **(b)** *Z. spelaenum* (AJC 848), Betalov Spodmol jama, Slove-

nia (45.7922, 14.1877): mantle gland (mag), foot (f), genital opening (go), pharynx (ph), oesophagus (oe), statocyst (st), columellar muscle (cm); **(c)** topotypic *I. vasconicum* (AJC 1848), Cueva de la Ermita de Sandaili, Spain (42.9994, -2.4381): mantle gland (mag), giant albumen gland (ag), kidney with renopericardial passage (k), heart (h), foot with haemolymph (f, hl), long genital opening (go), large mucus gland (mg), pharynx (ph), oesophagus (oe), two humps of vascularised columellar muscle (cm). scale: 500 μ m. — All images taken by Dorian Dörge, Goethe University Frankfurt am Main

flanked by endo- and ectocones of varying lengths from short to long. A hint of a median groove is present on some of the lopsided transitional teeth of *I. zaldivarae* (AJC 1876) (Fig. 15h). In the transverse rows, there is an increased incidence of bi-cuspid, fang-like lateral teeth (i.e. RMNH.MOL. 234,116, Cueva a Sul, Oviedo) flanking both sides of the rachidian tooth (Figs. 15c–d). As is considered for pulmonates (Luchtel et al., 1997), the teeth show constant form in the longitudinal rows but vary considerably in the transverse direction on the radular ribbon.

Individuals of *I. vasconicum* are generally smaller (Jochum et al., 2015a) than the Alpine and Dinaride species of *Zospeum*, except those comprising the *Z. pretneri* clade, which are about the same size and sometimes slightly larger (Inäbnit et al., 2019).

Discussion

In the molecular assessment, the topology generally did not change in the concatenated tree with all investigated specimens (Fig. 2) nor in the concatenated tree with complete marker sets (Fig. 3). In the latter, the support values are slightly higher and corroborate our interpretation of the phylogenetic and morphological findings. In order to understand the morphological traits in *Iberozospeum* n. gen., a figure is added here showing the type specimens of all hitherto described species (Fig. 16).

The *biscaïense-zaldivarae*-clade (grey clade in Figs. 2 and 3) contains sequences of two specimens (No. 162 and 163) from Weigand et al. (2013), who identified these

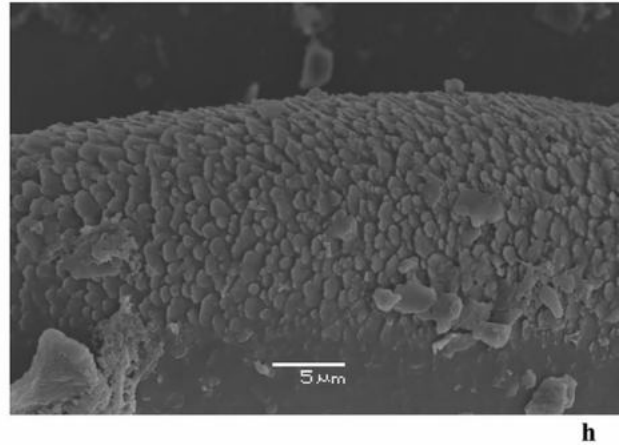
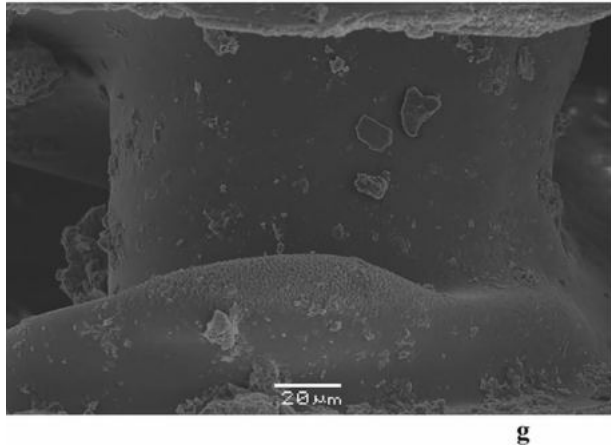
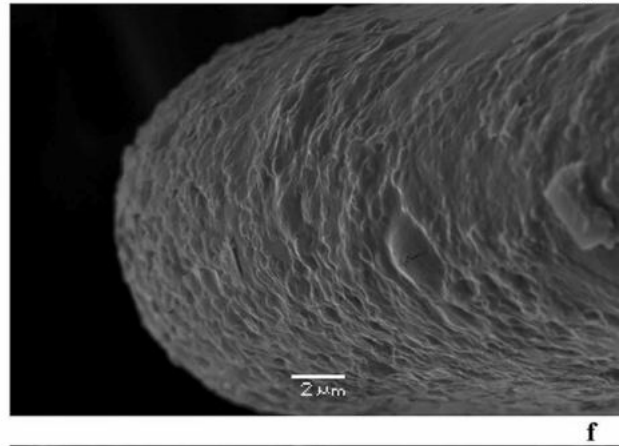
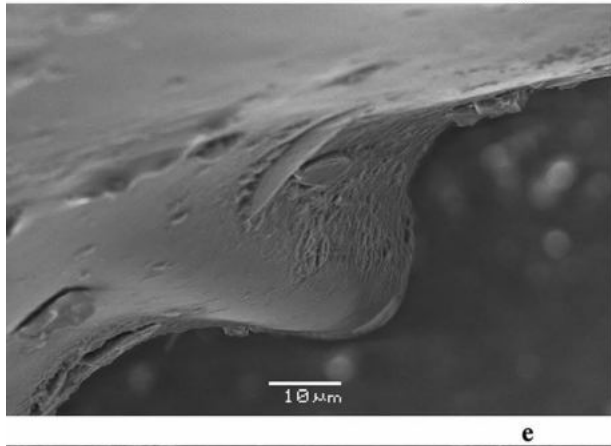
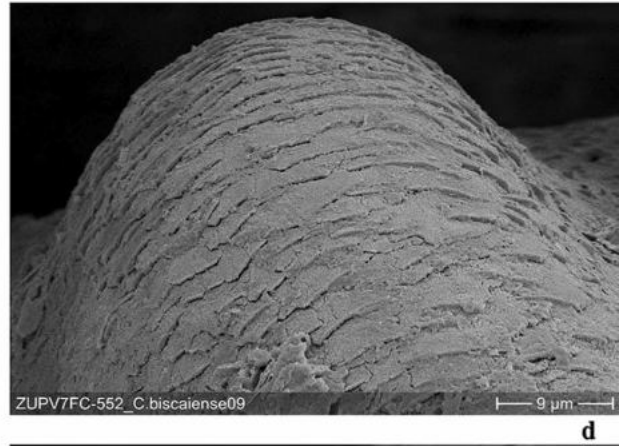
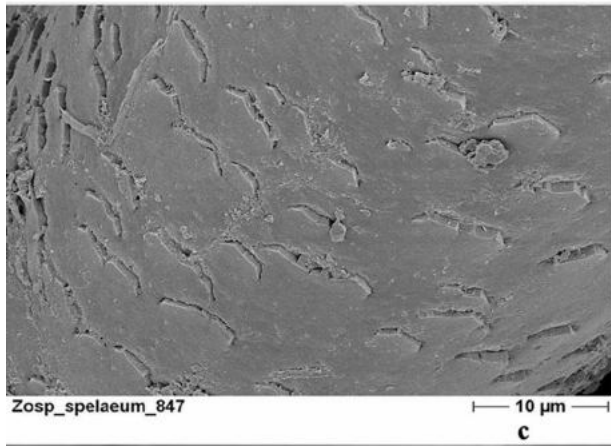
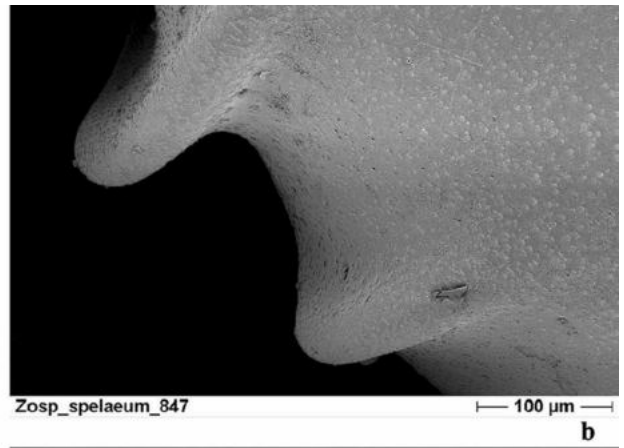
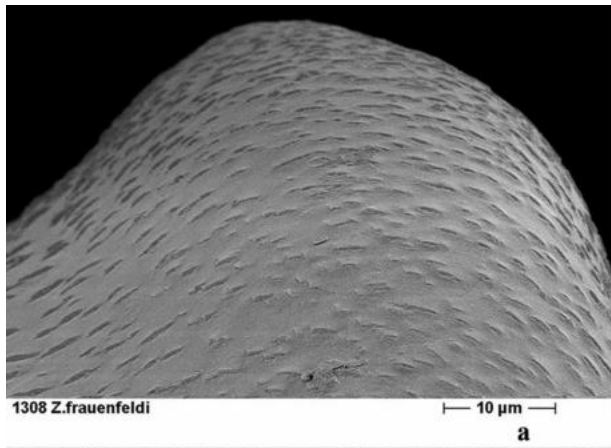


Fig. 13 Crystallographic structure on the columellar lamellae of Dinaride *Zospeum* and *Iberozospeum* shells; (a) *Zospeum spelaum*, (AJC 847), Betalov Spodmol jama, Slovenia (45.7922 14.1877), pattern of low, non-overlapping, wedges of crystallographic structure on the lamella; (b) *Zospeum spelaum*, (MCBI CSR SASA 37049a), Velika Pasica, Slovenia (N45.9189 E14.4934), non-overlapping wedges of crystallographic structure on lamella in old shell; (c) *Iberozospeum* sp., (RMNH.MOL. 234,120), Cueva Refugio, Trucios, overview of dense, overlapping, scale-like wedges of localized, crystallographic structure on upper part of the lower lamella; (d) *ibid.*, closeup view of c; (e) *Iberozospeum* sp., (RMNH.MOL. 234,104), Cueva del Comediate, Santander, upper part of the lamella of chemically treated shell showing dense, overlapping wedges of localized, crystallographic structure; (f) *Iberozospeum* sp., (RMNH.MOL. 234,141), Cueva a Sul, Oviedo, localized, overlapping wedges of crystallographic structure on lamella of chemically treated shell; (g) *Iberozospeum vasconicum*, (AJC 1849), Cueva Arrikutz, overview of dense, localized, crystallographic structure on lower part of the lamella; h, *ibid.*, closeup view of g. — Magnification varies for each perspective, see scale bars; Figs. a–b, g–h) imaged by M. Ruppel, (ret.) Goethe University Frankfurt am Main; Figs. c–f imaged by Dirk Vendermarel, Naturalis Biodiversity Center

specimens as lineage Z18. In 2015, Jochum et al. described the lineage Z18 as *I. zaldivarae*. The sequences of the two specimens of *I. zaldivarae* (Weigand et al., 2013) cluster with one specimen from the cave Irutxin. The cave, Otxas, is the type locality of *I. biscaiense* (Gomez & Prieto, 1983). We consider both species and supported entities; morphologically, the species differ by the mode of shell coiling (tighter in *I. biscaiense* when compared with *I. zaldivarae*) and presence of a small palatal denticle in *I. biscaiense*, which is lacking in *I. zaldivarae*.

The *bellesi*-clade (dark blue clade in Fig. 2) is not supported, although the complete marker set for both investigated specimens could be sequenced (dark blue clade in Fig. 3). A possible explanation for this finding is that *I. bellesi* belongs to a young radiation. The species is morphologically separated from the other known species in the Pyrenees, but our selected genetic markers cannot reveal the genetic differentiation of the species. The known distribution of *I. bellesi* spans the western Pyrenean region, including the French Basque Country and the Navarrese Pyrenees with the Sare-Zugarramurdi massif constituting an isolated enclave (Prieto & Zuazu, 2018). While *I. bellesi* is a unique Pyrenean species, all other known *Iberozospeum* taxa derive from the Basque-Cantabrian Mountains. Genetically, *I. bellesi* is clearly separated from the *biscaiense-zaldivarae*-clade but close to the other known species in Spain. Maybe other genetic markers are needed to reveal the genetic differentiation of *I. bellesi* from the other known species in Spain.

Within the Basque clades (pink and light blue clades in Figs. 2 and 3), the bootstrap support values and Bayesian posterior probabilities are low. This could be due to some missing markers in the concatenated tree (Fig. 2), because in the maximum likelihood tree, with complete marker sets (Fig. 3), the support values in the pink and light blue clades

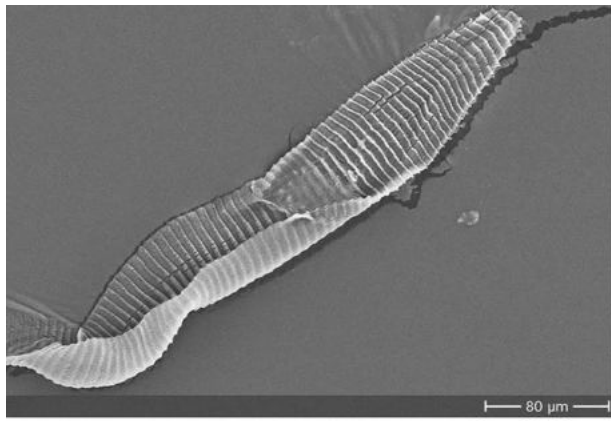
are much higher. The pink clade forms a polytomy with low support values. A possible explanation for this finding could be that these individuals form a young radiation. The selected genetic markers used in this study could not reveal the genetic differentiation of the specimens. The individuals in the light blue clade are genetically more differentiated than in the pink clade, but, bootstrap support values are also low. We included two specimens, NMBE 557178 and NMBE 557244 (Fig. 7k and m), which syntopically inhabit Las Paúles cave with *I. zaldivarae*. Both specimens cluster within the *vasconicum*-clade 2 (light blue clade in Fig. 2 and 3). On the morphological front, they resemble individuals in Fig. 7b and j.

The brown clade is the sister clade to the two *vasconicum*-clades (pink and light blue in Figs. 2 and 3) with high support (posterior probability of 1 and bootstrap value of 86 in Fig. 3). The support values in the deep nodes are low, maybe due to missing mitochondrial markers for some specimens. Due to genetic and morphological similarities to the *vasconicum*-clades 1 and 2 (Figs. 2, 3, 6, and 7), the specimens in the brown clade are considered to be *I. vasconicum*. We remain conservative with this clade because the subclades are not well supported. However, the type population of *I. vasconicum* (Weigand et al., 2013) is included in the pink subclade. For this reason, we consider all three subclades as *I. vasconicum*. Additional molecular methods like Next Generation Sequencing (NGS) are needed to resolve this group properly.

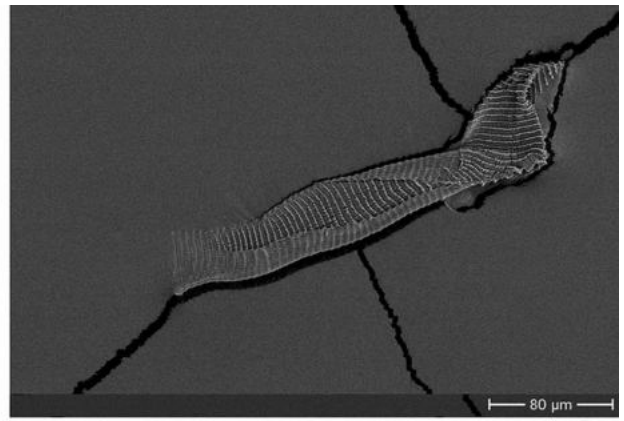
The *schaufussi*-clade (red clade in Figs. 2 and 3) contains a specimen from Cueva del Buho, which is the type locality for *I. suarezi* (Gittenberger, 1980). The investigated specimens from the red clade have an elongate-conical shell, moderately tightly coiled whorls and a roundish-lunate aperture typical for *I. schaufussi* (Jochum et al., 2019).

The purple clade (Figs. 2 and 3) contains the specimen No. 140 from Weigand et al. (2013), which was described by Jochum et al. (2019) as *I. praetermissum*. Morphologically, the individuals in the purple clade (Fig. 10a–f) show a uniform shell shape, except the specimen in Fig. 10f, which is a juvenile. The individual in Fig. 10d contains a clearly visible parietal tooth, which is typical for *I. praetermissum* and differentiates this species from *I. gittenbergeri* (Jochum et al., 2019). The individual in Fig. 10f cannot be clearly assigned to a species since the aperture is not fully grown. We remark, however, that this individual was found at the type locality of *I. praetermissum* (Jochum et al., 2019). The genetic analyses revealed that it clearly belongs to the *praetermissum*-clade even if its morphology is not typical for *I. praetermissum*, leading us to suggest that a certain spectrum of morphological variability within *I. praetermissum* is the case.

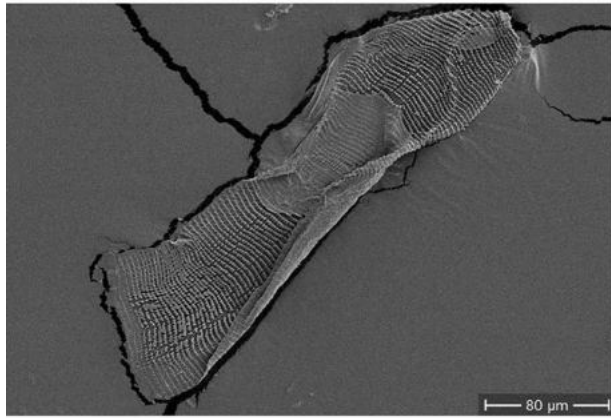
The lineages within the green clade (Figs. 2 and 3) have moderate to high support values but differ morphologically. Each lineage is represented by a different morph. The



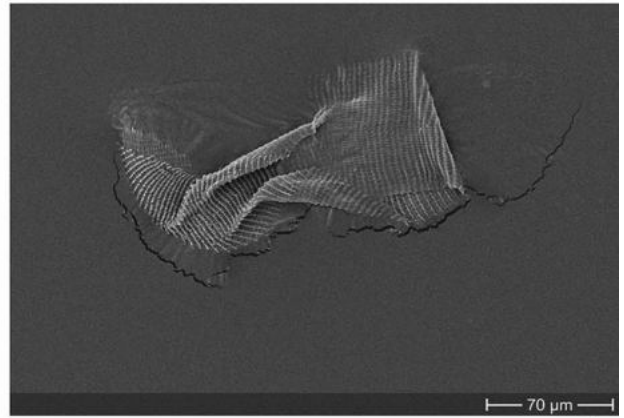
a



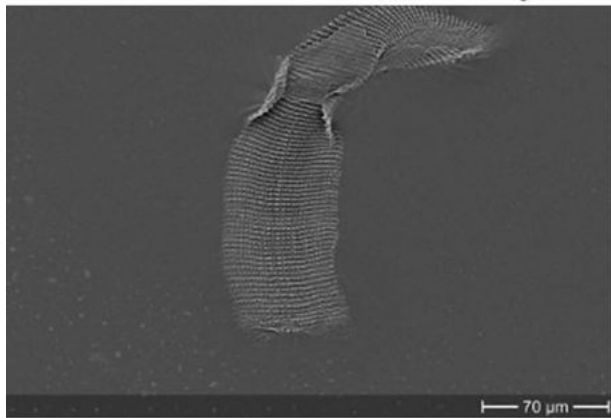
b



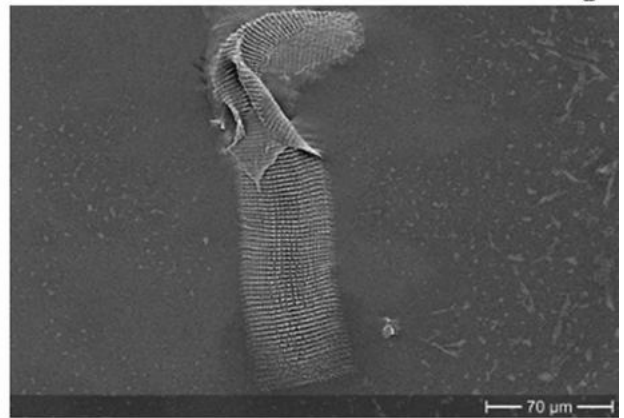
c



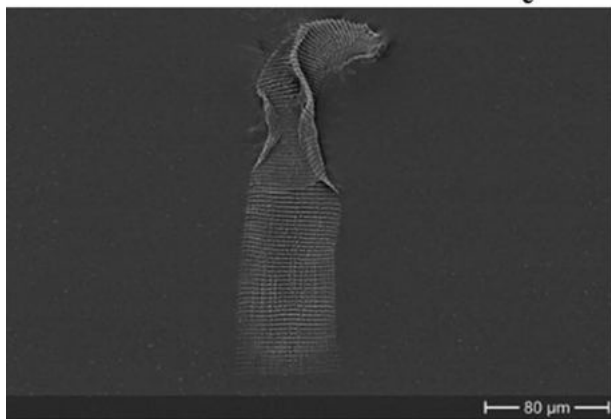
d



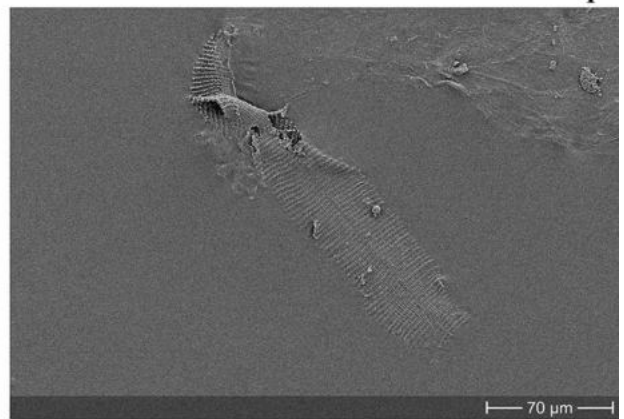
e



f



g



h

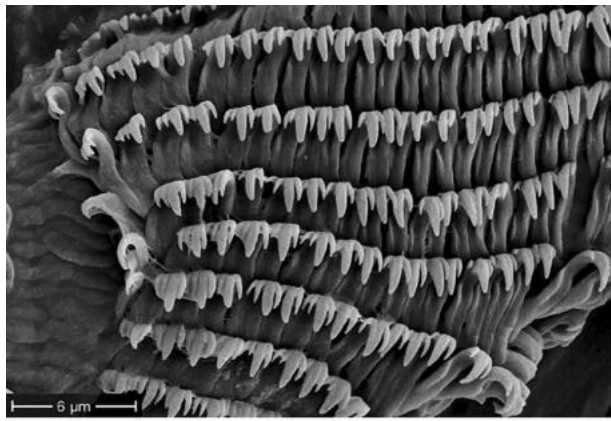
Fig. 14 Scanning electron micrographs (SEM) showing radular ribbon form, middle adhesive zone (az) and rows of dentition (rd) of Dinaride and Iberian individuals (notation denotes aspects on one Dinaride *Zospeum* and one *Iberozospeum* ribbon); **(a)** *Z. exiguum* (NMBE 553384), Križna jama, Slovenia (45.7452, 14.4673), long and narrow, tapered anterior end (tae), short adhesive zone (az), bottom furled with narrow obtuse or straight base (nosb); **(b)** *Z. pretneri*, (NMBE 553290), Gornja Cerovačka pećina, Croatia (44.2701, 15.8855), *ibid.*, with straight base; **(c)** *I. vasconicum*, (AJC 1848), Cueva Ermita de Sandaili (42.9994, -2.4381), moderately long and broad, tapered anterior end (tae), prominent adhesive zone (az), straight base (sb); **(d)** *I. zaldivarae*, (AJC 1876), Cueva de Las Paúles (43.1282, -2.7362), *ibid.*; **(e)** *Iberozospeum* sp. (RMNH.MOL. 234,109), Cueva de la Foz, long and broad, *ibid.*; **(f)** *Iberozospeum* sp., (RMNH.MOL. 234,144), Cueva de Rales, very long and broad, *ibid.*; **(g)** *Iberozospeum* sp., (RMNH.MOL. 234,116), Cueva a Sul, long and broad, *ibid.*; **(h)** *Iberozospeum* sp., (RMNH.MOL. 234,108), Cueva de Torcona, very long and broad, *ibid.* — Magnification varies for each perspective, see scale bars; all Figs imaged by M. Ruppel, (ret.) Goethe University Frankfurt am Main

individual in Fig. 10h is considered to be *I. percostulatum* since it was collected at the type locality in Herrería cave and has strongly developed ribs on the teleoconch whorls, the namesake character typical for *I. percostulatum* (Alonso et al., 2018). Although it clusters together with the individual in Fig. 10g, a specimen from Cueva la Zurra, Cantabria, the specimen in Fig. 10g is considered a new species, i.e. *Iberozospeum* sp.1. It differs from the remaining specimens in the green clade due to the five loosely coiled convex whorls of the spire, an apparent parietal and basal angularity of the thick peristome, the presence of a very low parietal denticle (or thickening) in the lowermost region of the parietal part of the peristome and by the presence of a tiny denticle at the base of the columella. The specimens from El Toyo are considered a new species because they have a characteristically high, narrowly tapering, tightly coiled spire in conjunction with a thickly callused, rounded peristome fused onto the body whorl. It is not possible to recognise any dentition in the aperture in these full-bodied specimens. This combination of characters is not seen in other known Spanish taxa; therefore they are considered as *Iberozospeum* sp.2. The shells of the individuals in Fig. 10k–n resemble that of *I. gittenbergeri* by their relatively large, broad conical shape, their bearing 5.5 regularly coiled whorls and the typical, straight, long angular, thick parietal callus of the peristome (Jochum et al., 2019). The newly discovered species *Iberozospeum* sp.1 and *Iberozospeum* sp.2 are described in separate publications. The species delimitation method (ABGD) (Table 3) yielded four genetically different groups, a finding, which is not fully supported from the shell morphology. Probably, we deal here with a species complex with several cryptic species present.

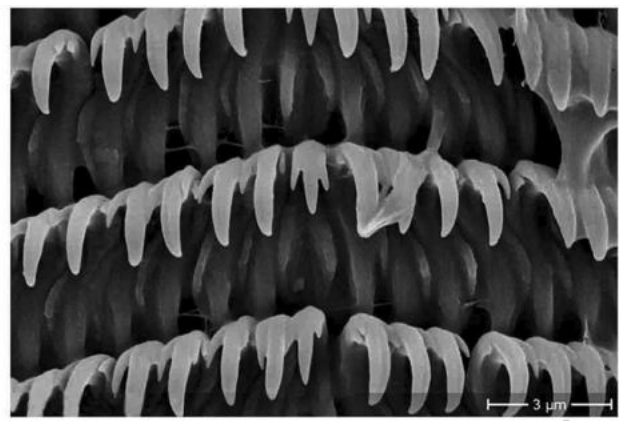
The yellow clade (Figs. 2 and 3) is genetically clearly separated from the remaining clades, albeit that the complete marker set could be sequenced in only one specimen (Table 1 and Fig. 3). Morphologically, the three investigated individuals are completely different compared with the other known taxa in Spain. The specimen in Fig. 11b is a juvenile but resembles the specimen in Fig. 11c. Both specimens contain strong ribs. A new, ribbed species is described from this clade.

The caves of northern Spain show a high incidence of multiple species sympatry in contrast to those reported for the eastern Alpine and Dinaride regions (Inäbnit et al., 2019). In context, we remark here that Inäbnit et al.'s (2019) molecular investigation showed little congruency with Bole's (1974) earlier morphological interpretation of the eastern Alpine and Dinaride taxa, revealing that the incidence of multiple sympatric species is the exception, and not the rule in Dinaride caves. In Table 4, all investigated sympatric *Iberozospeum* species are listed.

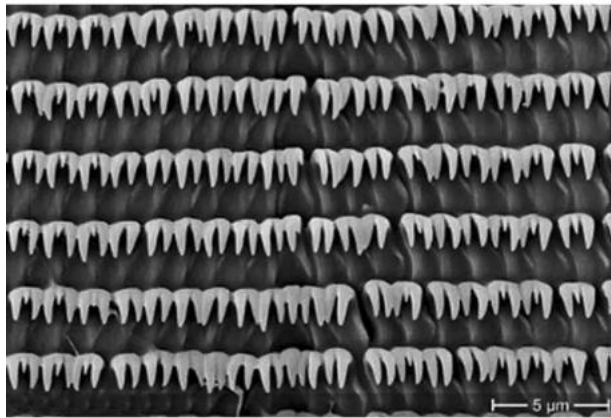
The radulae of Iberian taxa show significant differences in radular ribbon form and dental morphology from those of eastern Alpine and Dinaride *Zospeum*. These differences reflect both odontophore and ribbon constitution in how it flattens out on the dorsal and lateral sections of the muscular odontophore. The ellobiid radula changes with age, with the very young specimens usually showing strongly denticulate crowns (Martins, 2007). Inäbnit et al. (2019) described four ribbon morphologies in eastern Alpine and Dinaride taxa, including those with an attenuated triangular base (*Z. isselianum*, *Z. frauenfeldii*) and those tapered to an obtuse to straight base as in *Z. exiguum* (Fig. 14a) or a straight base as in *Z. pretneri* (Fig. 14b) here. The form and composition of radular teeth vary according to their position on the radular membrane (referred in prepared SEM form here as ribbon) as well as diet, mineral composition of the environment, temperature and other factors (Luchtel et al., 1997). Within the ellobiids, Martins (1996, 2007) considered radular morphology a useful, distinguishing character at the generic level. For *Iberozospeum* here, the radular ribbons are clearly distinguishable from those of the Dinaride taxa. They are long and broad in form and very straight below the zone of the adhesive layer. They also bear more and smaller teeth per transverse row (Fig. 14c–h). Like those in their eastern Alpine and Dinaride relatives, they have a tapered anterior end (velum) above the adhesive layer. However, while the narrower ribbons of the latter taxa are tapered and sometimes straight at the base (i.e. *Z. pretneri*), all those of *Iberozospeum* are so far completely straight at the base, showing a flatter surface area aligned with very straight rows of teeth. We emphasize that this situation is



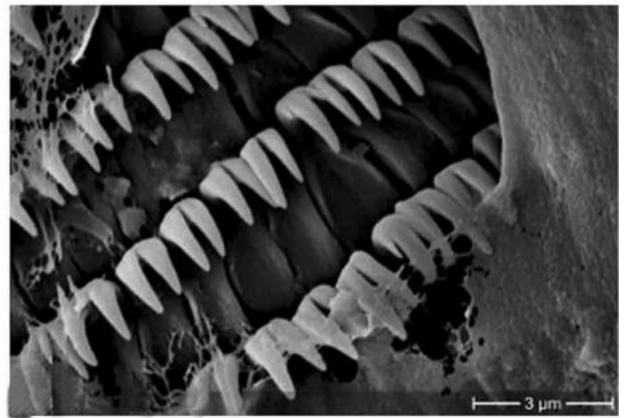
a



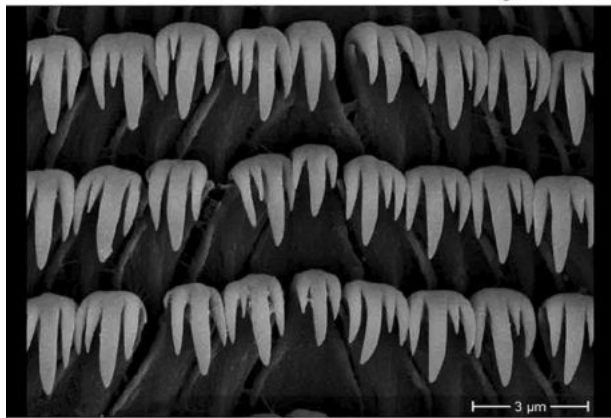
b



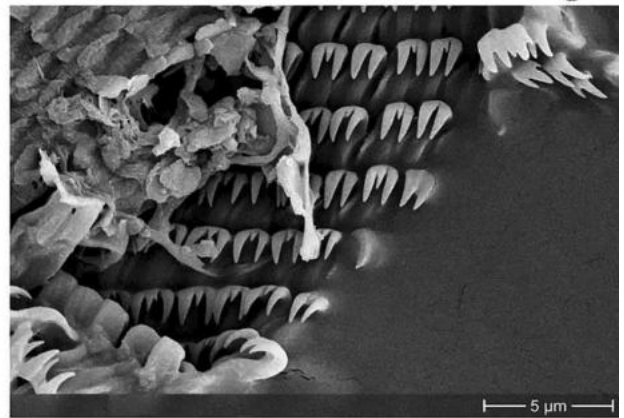
c



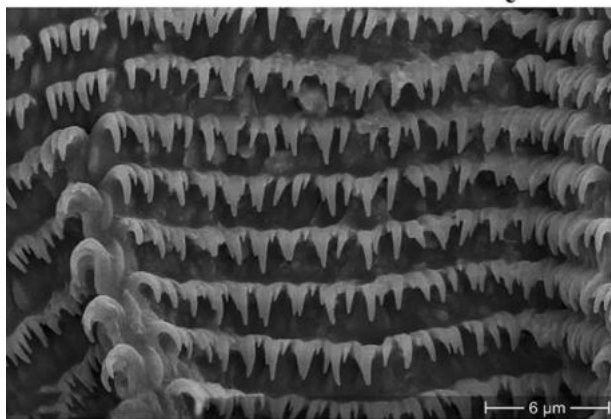
d



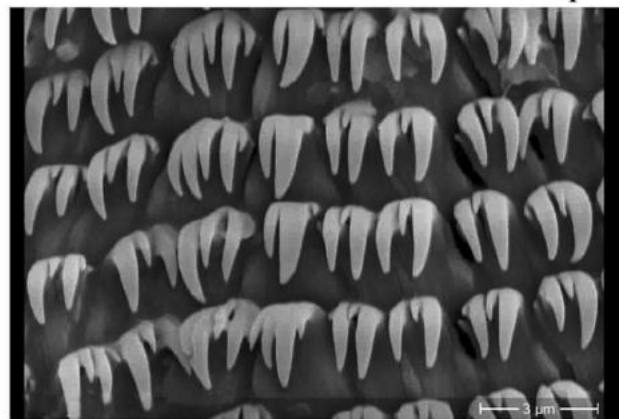
e



f



g



h

◀**Fig. 15** Scanning electron micrographs (SEM) showing transverse rows of dentition on Dinaride *Zospeum* and *Iberozospeum* radulae; (a) *Z. pretneri*, (NMBE 553290), Gornja Cerovačka pećina, Croatia, transverse rows of teeth on long, slender basal plates (bp), rachidian (r) and lateral teeth (l), arrows indicate medial grooves on mesocones of individual teeth; (b) *Z. isselianum*, NMBE 553389, Turjeva jama, Slovenia, *ibid.*; (c) *Iberozospeum* sp. (RMNH.MOL.234.116), Cueva a Sul, straight transverse rows of small, seemingly bi-cuspid lateral teeth (l) with reduced mesocones on compact basal plates; (d) *ibid.*, close up view of rachidian teeth (r), lateral fang-like teeth (l) and transitional teeth (t); (e) *I. vasconicum*, (AJC 1848), Cueva Ermita de Sandaili, rachidian teeth (r) flanked by 4-cuspid lateral teeth (l), *C. ibazoricum*-like in form; (f) *Iberozospeum* sp. (RMNH.MOL.234108), Cueva la Torcona, lateral teeth showing reduced mesocones (me) flanked by long, fang-like endo- and ectocones (e), rachidian tooth (r) (flipped over in upper righthand corner of image); (g) *I. zaldivarae* (AJC 1876a), Cueva de Las Paúles, transverse rows of teeth showing varying cusp lengths; (h) *ibid.*, close up view (left to right) of marginal (m) and transitional teeth (t) on short, compact basal plates (bp). — Magnification varies for each perspective, see scale bars; all Figs taken by M. Ruppel, (ret.) Goethe University Frankfurt am Main

enhanced by the tendency towards increased length (i.e. double the ribbon length below the adhesive zone in those of the Pyrenean-Cantabrian individuals), the further westward (i.e. Asturias) the individuals were found, albeit the exception found in Burgos (RMNH.MOL.234108) (Fig. 14h). The radula of topotypic *I. vasconicum* (Fig. 14c) from the more eastern province of Gipuzkoa, for example, shows a moderately long ribbon in comparison to the exceptionally long ribbons extracted from individuals from Asturias and the one from Burgos. Moreover, since the radula is tensioned and moved over the muscular odontophore by muscles that derive from the buccal mass, radular ribbon form is a reflection of these muscles operating the odontophore and radula in concert. In addition, since the odontophore is moved by muscles extending from the body wall and the columellar muscle (in shelled pulmonates) (Luchtel et al., 1997), it is apparent here that *Iberozospeum* has a different muscle constitution (i.e. muscles and modified muscle cells operating the odontophore, the odontophore itself and the columellar muscle) than *Zospeum*. This situation is revealed here by the presence of crystallographic structure on specific points of muscle adhesion on the columellar lamellae in shells of *Iberozospeum* (Fig. 13). Our observation is in sync with the trend in the Ellobiidae (Barker, 2001) that the columellar muscle becomes detached from the body wall from its origin on the columella and has become largely free in the haemocoel. Moreover, the dense, localized surface structure most probably provides traction for the columellar muscle. On a side note, but worth mentioning in context, is that during the manual preparation for SEM, ribbons from *Iberozospeum* mounted especially easily, like laying a carpet, onto the prepared SEM stub. Those of the eastern Alpine and Dinaride taxa, as well as from some *Carychium* species (AJ unpubl. data), tended to be generally more difficult to mount

due to their flopping over and furling at the sides during the mounting procedure. This difference may be due to mineral composition or quality of the flexible chitin comprising the ribbon or to potential material thinness due to different or enhanced muscular action on the radular membrane in situ. In contrast to the long and broadly straight version of the Iberian taxa, the radular ribbons of the studied Alpine and Dinaride species are long and narrow and tapered on the anterior end and sometimes, on both ends (i.e. *Z. isselianum* and *Z. frauenfeldii*) (Inäbnit et al., 2019). We consider the consistency in shape, length, broadness and the straight-edged base of the radular ribbon systematically significant in *Iberozospeum*.

Ecologically, the westernmost *Iberozospeum* in our radula study were collected from caves characterised by certain aquatic biotopes (Notenboom & Meijers, 1985). These biotopes included influent caves (Cueva de Rales, Prov. Oviedo (now Asturias)) and temporal effluent caves (Cueva de la Foz, Cueva a Sul, Prov. Oviedo (now Asturias)), and caves with pools, puddles or gours (Cueva la Torcona, Prov. Burgos) or a combination of the latter two (Cueva la Torcona). These ecological situations play a role in diet and substrate composition as well as in the density of mud comprising *Iberozospeum* habitats (Jochum et al., 2012). As for the observed differences in *Iberozospeum*'s radular morphology, Jochum et al. (2015b) considered that the cusps of the radular teeth in *Z. isselianum* (Fig. 15b) interacted with substrate composition and structure (i.e. grain), causing adaptive moderations of morphological detail to evolve and correlate with substrate grain. In the case of *Iberozospeum*, it is probable that the longer, seemingly bi-cuspid lateral teeth of the westernmost sampled populations may well reflect environmentally induced adaptive factors in caves of the westernmost part of *Iberozospeum*'s range. We remark that these westernmost populations were not included in the molecular analyses comprising our study, but rather, collected by Jos Notenboom in 1983–1984 during a study of groundwater fauna in caves of northern Spain (Notenboom & Meijers, 1985).

The radiation of *Iberozospeum* aligns into the bigger context of Iberian geological and evolutionary considerations for which the southern peninsulas of Europe served as major refugia during the Pleistocene glaciation (Hewitt, 2004). Moreover, the Iberian Peninsula has been associated with climate stability over geologic time and is considered to be a historically climate-stable region encompassing high species diversity and endemism (Abellán & Svenning, 2014). Specifically, our study underscores the considerations of Abellán and Svenning (2014), in that the repeated range contractions and expansions experienced during the Pleistocene climatic oscillations may have resulted in the generation of multiple isolated lineages of fauna (in this case, *Iberozospeum*) in

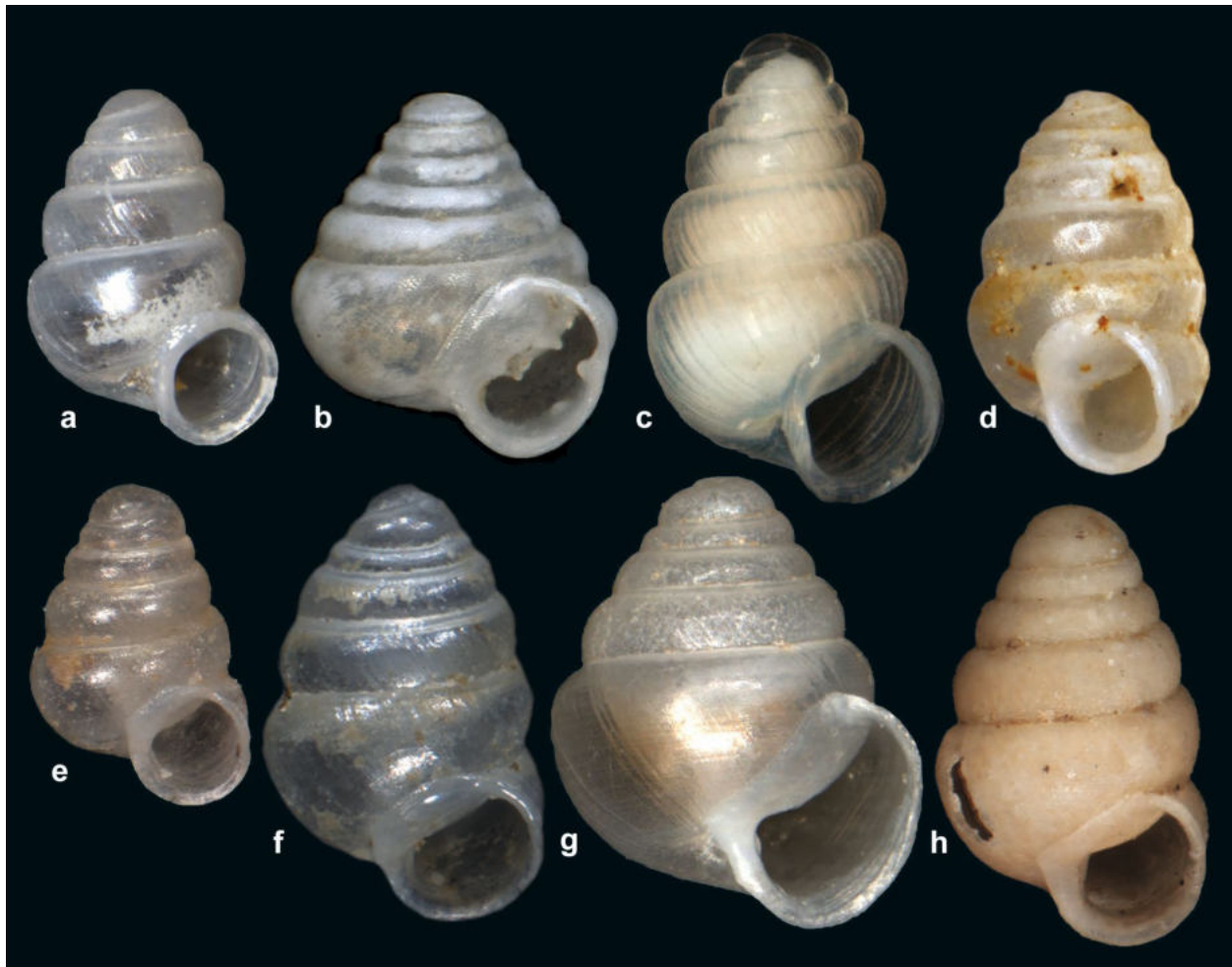


Fig. 16 Type specimens of species of *Iberozospeum*; (a) holotype *I. vasconicum* (Prieto et al., 2015 in Jochum et al., 2015a), Gipuzkoa, Cueva de la Ermita de Sandaili, MNCN15.05/60147H, sh: 1.2 mm; (b) paratype *I. biscaiense* (Gómez & Prieto, 1983), RMNH.MOLL.334913, Urkizu, Yurre, Cueva de Otxas, sh: ca. 1.23 mm (imaged by Ton de Winter); (c) holotype *I. percostulatum* (Alonso et al., 2018), Asturias, Llanes, Cueva de La Herrería, MNCN 15.05/200017H, sh: 1.58 mm; (d) lectotype *I. schaufussi* (von Fraunfeld, 1862), “Spain”, NHMW 71.837, sh: 1.3 mm; (e) holotype *I.*

praetermissum (Jochum et al., 2019), Asturias, Cueva del Puente de Inguanzo, RMNH.MOL.55391, sh: 1.08 mm; (f) paratype *I. bellesi* (Gittenberger, 1973), Huesca, Cueva del Molino de Aso, RMNH.Mol. 234,137, sh: 1.49 mm (imaged by Ton de Winter); (g) holotype *I. zaldivarae* (Prieto et al., 2015 in Jochum et al., 2015a), Burgos, Cueva de Las Paúles, MNCN 15.05/60148H, sh: 1.52 mm; (h) holotype *I. gittenbergeri* (Jochum et al., 2019), Asturias, Cueva del Puente de Inguanzo, RMNH.MOL.234166, sh: 1.49 mm

different refugial areas. The Cantabrian and Pyrenees Mountains, harbouring labyrinthine cave systems, well serve as current refugial areas for *Iberozospeum* species that may have been more widespread during colder periods during the Pleistocene. Moreover, with the Pyrenees-Cantabrian Mountains running east–west together with the main rivers flowing along a north–south axis, the following scenario can be proposed considering climatic, geological and physiographical characteristics of this geologically younger part of Spain (Notenboom & Meijers, 1985): *Iberozospeum* could have survived and spread via altitudinal shifts as cave systems gave way and sank into each other due to geologic processes and groundwater mechanisms, allowing the distribution of species and sympatry of species to occur over time.

Taxonomic implications

We found a well-supported, two-clade system in the genus *Zospeum* (Figs. 2 and 3) and propose here a new genus encompassing the northern Spanish radiation.

Genus *Iberozospeum* Jochum, Kneubühler, Prieto and Neubert, n. gen.

Type species *Zospeum zaldivarae* (Prieto et al., 2015 in Jochum et al., 2015a).

Differential diagnosis *Iberozospeum*, n. gen., differs from *Zospeum* by the generally smaller shell (on the average ca. 1.2 mm). The radula ribbon differs by its greater length,

Table 4 Investigated sympatric *Iberozospeum* species living in Spanish caves

Cave	Species 1	Species 2
Herrería	NMBE 557253 <i>praetermissum</i> (purple clade)	NMBE 557136 <i>percostulatum</i> (green clade)
Irutxin	NMBE 557238 <i>biscaiense</i> (grey clade)	NMBE 557221 <i>vasconicum</i> (light blue clade)
Las Paules	No. 162 and 163 Weigand 2013 <i>zaldivarae</i> (grey clade)	NMBE 557178 and NMBE 557244 <i>vasconicum</i> (light blue clade)
Otxas	NMBE 557240 <i>biscaiense</i> (grey clade)	NMBE 557223 <i>vasconicum</i> (pink clade)
Valdemora	NMBE 557246 <i>praetermissum</i> (purple clade)	NMBE 557247 <i>gittenbergeri</i> (green clade)

regular broadness below the adhesive zone and its perfectly straight base. Radular teeth are smaller and more numerous per transverse row. The basal plates are more compact and shorter than the long, narrow versions in *Zospeum* species. At the microstructural level, it differs by localized, dense, rough, overlapping wedge-like scales of crystallographic structure on the surface of the columellar lamellae. These sites are located only at the points of contact with the columellar muscle. It also appears to differ by the correlating, vascularized humps of columellar muscle to the corresponding zones of microstructural texture on the lamellae.

Etymology The name *Iberozospeum* derives from combining the region of origin of the type species, the Iberian Peninsula, and the generic name of *Zospeum* (Bourguignat, 1856).

Included taxa: all hitherto known species from the Iberian Peninsula:

- Iberozospeum schaufussi* (von Frauentfeld, 1862).
- Iberozospeum bellesi* (Gittenberger, 1973).
- Iberozospeum biscaiense* (Gómez & Prieto, 1983).
- Iberozospeum vasconicum* (Prieto et al., 2015 in Jochum et al., 2015a).
- Iberozospeum zaldivarae* (Prieto et al., 2015 in Jochum et al., 2015a).
- Iberozospeum percostulatum* (Alonso et al., 2018).
- Iberozospeum praetermissum* (Jochum et al., 2019).
- Iberozospeum gittenbergeri* (Jochum et al., 2019).

***Iberozospeum costulatum* Prieto and Jochum, n. sp.**

Type locality Mina del Pedreo (Bizkaia: Arcentales; 43.26800 -3.21402, 440 m).

Holotype A shell of 1.43 mm [MNCN 15.05/200128, ex. ZUPV 1952]; 22.02.2014, C. Prieto, A. Calvo, P. Jiménez leg.

Paratypes Mina del Pedreo [type locality]; 22.02.2014, C. Prieto, A. Calvo, P. Jiménez leg. [ZUPV 1952: 2 shells + 2 juvenile shells] 31.08.2014, C. Prieto, A. Calvo leg. [ZUPV 2578: 15 shells + 3 juvenile shells, ZUPV 2583: 1 shell] [MNCN 15.05/200129: 5 shells]. Cueva de Valdebeci (Bizkaia: Sopuerta: Beci; 43.24516 -3.17316, 188 m); 20.10.2015, A. Calvo leg. [ZUPV 3078: 6 shells] [NMBE 557231: 1 specimen, sequenced; Fig. 11c]. Cueva de Cuvias Negras (Cantabria: Soba: Asón; 43.25132 -3.60688, 250 m); 12.04.2017, C. Prieto, S. Quiñonero, A. Alonso, J. Ruiz-Cobo leg. [ZUPV 4714: 38 shells + 2 specimens] [NMBE 557227: 1 specimen, sequenced; Fig. 11b; NMBE 568196: 5 shells] [SMF 349,424: 5 shells] [MHNG-MOLL-0137391: 5 shells] [MNCN 15.05/200130: 10 shells] [CAA-w/o n°: 19 shells] [CSQS-w/o n°: 25 shells].

Other material Cueva del Cesáreo (Cantabria: Liérganes: Extremera; 43.32034 -3.72279, 258 m); 21.03.2016, S. Quiñonero, J. Ruiz-Cobo, A. Alonso leg. [ZUPV 3807: 3 shells] [CAA-w/o n°: 1 shell] [NMBE 559626: 2 specimens, sequenced; Fig. 11a]. Cueva de Asunción (Cantabria: Ramales de la Victoria: Guardamino; 43.25837 -3.44820, 180 m); 21.03.2016, S. Quiñonero, J. Ruiz-Cobo leg. [ZUPV 3808: 4 shells]. Cueva del Comellante (Cantabria: Ruesga; 43.31111 -3.60806, 170 m); 30.03.2015, S. Quiñonero, J. Ruiz-Cobo leg [ZUPV 3804: 1 shell] [CSQS-w/o n°: 3 shells]. Cueva de Covallarco (Cantabria: San Roque de Riomiera: Merilla; 43.25654 -3.73412, 402 m); 18.06.2016, CP, J. Fernández leg. [ZUPV 3974: 1 shell]. Cueva de Cullalvera (Cantabria: Ramales de la Victoria; 43.25577 -3.45808, 95 m); 19.09.2014, C. Prieto, A. Calvo leg. [ZUPV 2604: 1 shell]. Torca de El Porrón (Cantabria: Ruesga: Porracolina; 43.25111 -3.66356, 920 m); 09.09.2016, M. Gutiérrez leg. [ZUPV 4180: 1 shell]. Cueva de La Puntida (Cantabria: Miera: Ajanedo; 43.25883 -3.71042, 500 m); 12.10.2015, C. Prieto, A. Calvo leg. [ZUPV 3032: 90 shells] [CSQS-w/o n°: 10 shells]. Fuente de La Revilla (Cantabria: Voto: San Miguel de Aras; 43.31972 -3.52036, 55 m); 30.03.2015, S. Quiñonero leg. [ZUPV 3806: 3 shells]. Cueva de Las Cascasojosas (Cantabria: San Roque de Riomiera; 43.25457



◀**Fig. 17** *Iberozospeum costulatum* n. sp. (a–e) holotype, 1.43 mm height [MNCN 15.05/200128, ex. ZUPV 1952], Mina del Pedreo (Bizkaia: Arcentales; 43.26800 -3.21402, 440 m). (f–g) paratype shells from the type locality [ZUPV 1952, F: juvenile shell, G: shell of 1.51 mm height. (h–i) no paratype shell of 1.48 mm height [ZUPV 3807] from Cueva del Cesáreo (Cantabria: Liérganes: Extremera; 43.32034 -3.72279, 258 m). (j–k) paratype shells from Cueva de Cuvias Negras (Cantabria: Soba: Asón; 43.25132 -3.60688, 250 m) [CSQS-w/o n°]. (l) no paratype shell from Cueva del Cesáreo [CSQS-w/o n°]. Photos a–i by Carlos Prieto; j–l by Sergio Quiñonero and Álvaro Alonso

-3.71924, 328 m); 09.03.2018, C. Prieto, J. Ruiz-Cobo leg. [ZUPV 5154: 2 shells]. Cueva del Molino de la Peña (Cantabria: Rasines; 43.29101 -3.36840, 180 m); 04.08.2013, S. Quiñonero, J. Ruiz-Cobo leg. [ZUPV 3802: 2 shells, broken]. Sima PO-153 (Cantabria: San Roque de Riomiera: Porracolina; 43.22984 -3.69050, 585 m); 08.10.2016, M. Gutiérrez leg. [ZUPV 4184: 4 shells]; 12.11.2016, C. Prieto, M. Gutiérrez, J. A. Noriega leg. [ZUPV 4203: 20 shells]. Sima PO-27 (Cantabria: Miera; 43.24695 -3.67023, 910 m); 07.05.2016, M. Gutiérrez leg. [ZUPV 3822: 8 shells]. Cueva de San Juan de Socueva (Cantabria: Arredondo: Socueva; 43.26671 -3.61339, 430 m); 12.04.2017, C. Prieto, S. Quiñonero, A. Alonso, J. Ruiz-Cobo leg. [ZUPV 4722: 12 shells].

Etymology The specific epithet derives from the well-defined ribbing of the last whorls of the shell.

Diagnosis A medium-sized (average, 1.35 mm, $n=52$) and wide (average, 0.76 mm, $n=52$) *Iberozospeum* species with convex whorls bearing well-defined ribs, oblique, reniform aperture with broad straight-edged parietal callus and a strong columellar lamella clearly seen inside the aperture.

Description (Fig. 17). Shell of medium size (1.24–1.55 mm, $n=52$, holotype, 1.43 mm), ovate conical. Spire formed by five (4.6–5.9, $n=52$) rather convex whorls separated by a deep suture. Protoconch (nucleus, 0.175 mm wide) and apical whorls smooth (Fig. 17f) with teleoconch bearing regularly spaced (5–6/0.5 mm; 27 in the body whorl, $n=52$), well-defined ribs, extending from one whorl to the next; ribs of the hind peristome region are more densely aligned and thinner. Body whorl large (holotype, 60% of the shell height), with upper convexity, ascending behind the aperture. Umbilicus closed, with ribs reaching the umbilical cavity. Aperture reniform, obliquely transverse (holotype, 47% of the shell height), attached to the body whorl by a thickly callused, broad, straight-edged parietal callus. Peristome wide and reflexed; lateral and palatal side regularly arched; columellar side almost straight and vertical. Inner

lamella singular, large, oblique, (Fig. 17g) located above the parieto-columellar junction; lamella visible in oblique apertural view (Fig. 17c). Shell surface with micro sculpture of irregular spiral striae.

Geographical distribution *Iberozospeum costulatum* n. sp. inhabits caves throughout western Bizkaia and the eastern part of Cantabria (Fig. 18). In Bizkaia, *I. costulatum* is known from two caves located 4.2 km apart: Mina del Pedreo, where it was first discovered, and Cueva de Valdebeci (holotype, sequenced population). Both caves belong to the same limestone formation (Alén-Lujar) cut by the Barbadun river. The remaining localities are in Cantabria. They are separated from the Bizkaian caves by a distance of 20 km, with Cueva Cullalvera and Cueva de Asunción being the nearest. All Cantabrian localities are located in the limestone massifs belonging to the Miera and Asón river basins with Cueva del Cesáreo (sequenced, Fig. 11a) constituting the most north-western cave separated from this central block. We remark that *I. costulatum* appears to be sympatric with *I. biscaiense* in the Montes de Triano massif west of Bilbao (Prieto & Calvo 2013; unpublished records) and that the east-westward geographic span recorded for *I. costulatum* likely represents the true geographic distribution of this species.

Variability Ribbing is the most conspicuous feature on the shell of *I. costulatum*. Although the shells from the same cave show similar rib strength, spacing and length, a notable spectrum of variability is present in different cave populations. Shells deriving from populations from the Miera upper basin, such as La Puntida, PO-153 or Cuvias Negras (Fig. 17j–k), show poorly developed ribs and a weak columellar lamella, while individuals from Fuente de La Revilla bear strong and irregular ribs. On the other hand, shells from Asunción have well separated ribs (5/0.5 mm). Although obscured by wide intra-population variation, shell size also varies between populations. Shells from Cuvias Negras are the smallest and those from Valdebeci are the largest. The inner columellar lamella also varies somewhat in form in shells from Cueva de Cesáreo, whereby in addition to the columellar lamella, a small basal lamella can be seen from the opening in oblique view (Fig. 17h–i).

Remarks The conspicuous ribbing differentiates *I. costulatum* from all other iberozospeid taxa except *I. percostulatum*. The shell of *I. percostulatum* is higher (1.34–1.80 mm, average 1.55 mm) and narrower (1.32–1.65 mm, average 1.51 mm, $n=42$) and lacks inner lamellae (Alonso et al., 2018). Additionally, their geographic ranges are 80 km apart.

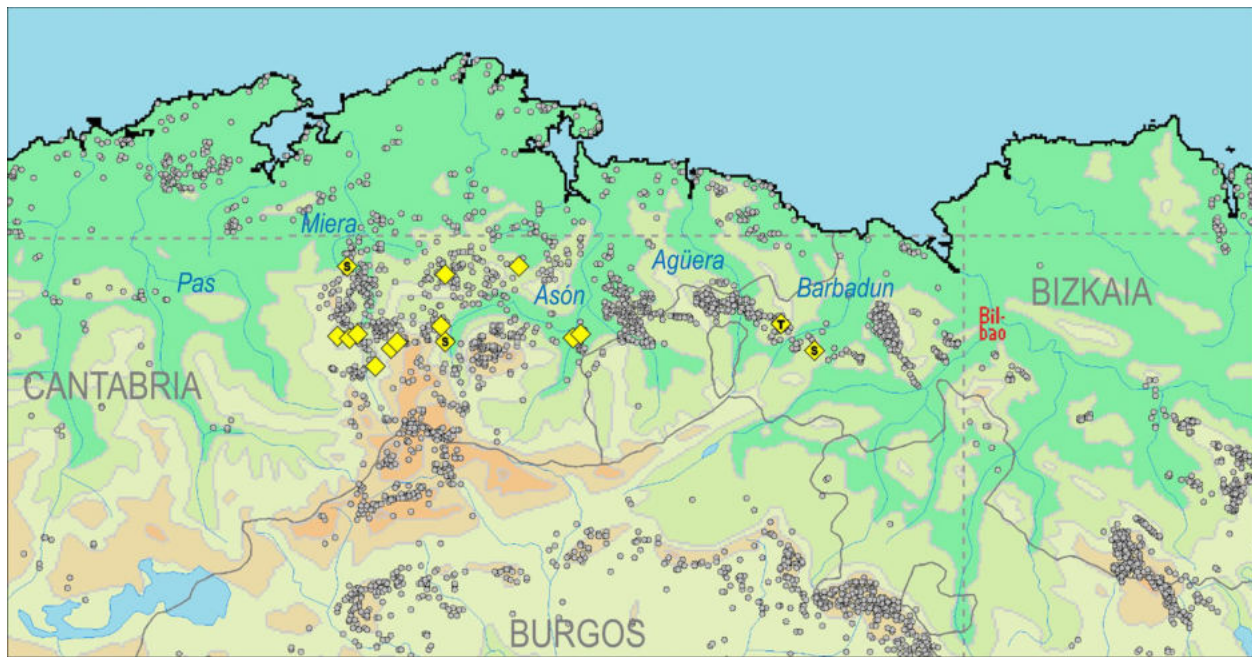


Fig. 18 Geographical distribution of *Iberozospeum costulatum* n. sp. The type locality and sequenced populations are indicated by T and S, respectively

Conclusion

In this integrative study, we investigated 57 populations of cavernicolous zospeid snails using genetic and morphological data. Our study revealed a separate radiation for species inhabiting northern Spanish caves for which the new genus, *Iberozospeum*, has been defined. *Iberozospeum* populations show on-going speciation in situ within isolated cave systems of northern Spain. Our investigations corroborated the proposed ancestral area reconstruction of Weigand et al. (2013) indicating that the “Cantabrian Mountains + Alps” or “Cantabrian Mountains + Dinaric Alps” was the ancestral area of the *Iberozospeum* radiation. Coherent mitochondrial and nuclear sequence patterns as well as common morphological traits were observed in most of the clades. Three new species were molecularly revealed and one, *Iberozospeum costulatum*, is described using additional morphological data.

Our comparative histological investigations revealed the huge size of the albumen gland for the first time in a sexually mature member in the female phase within the subterranean Carychiidae. We found significant morphological and structural differences in both the columellar muscle and the radulae of Dinaride *Zospeum* and *Iberozospeum* species. SEM investigations of the radular ribbon reveal that dentition form, size and alignment, consistency in ribbon shape, length, broadness and the straight-edged base are systematically significant in *Iberozospeum* species and that

it morphologically differentiates these species from those of the Eastern Alpine and Dinaride *Zospeum* taxa.

Our investigations are ongoing. Future collection efforts and phylogeographic investigations will do well to reveal deeper patterns of phylogenetic relatedness and evolutionary processes in *Iberozospeum* populations.

Supplementary Information The online version contains supplementary material available at <https://doi.org/10.1007/s13127-021-00517-9>.

Acknowledgements We gratefully acknowledge Anton J. de Winter for his Einsatz and insights in an earlier project and for kindly allowing AJ access to the Jos Notenboom Collection at the Naturalis Biodiversity Center (Leiden, NL). We are indebted to Alvaro Alonso Suárez, X. Azkoaga, Alfonso Calvo, J. M. Expósito, Jon Fernández, Marta Gutierrez, Jagoba Malumbres, Javi Moreno, Sergio Quiñonero-Salgado, Jesús Ruiz-Cobo and Pantxo Zuazu for their tremendous collecting efforts, encompassing 55 caves. We gratefully acknowledge Claudia Nesselhauf (ret. Goethe University, Frankfurt, Germany) for her extreme patience and skill in extracting radulae from these miniscule snails and to Gabi Elter (Goethe University, Frankfurt, Germany) who prepared the histological sections of *I. vasconicum*. We thank Dirk Vendermarel (Naturalis Biodiversity Center) and Manfred Ruppel (ret.) (Goethe University, Frankfurt, Germany) for their insights and expertise at the SEM. We are grateful to Thomas Inäbnit for his input and technical support and Alexander M. Weigand for earlier discussions. We are indebted to Annette Kolb (former Klussmann-Kolb) for her long-term support of this work as well as to Dorian Dörge (Goethe University, Frankfurt Germany), who imaged the multitude of histological slides. AJ received support via grants from The Malacological Society of London and the SYNTHESYS Project <http://www.synthesys.info/>, which is financed by the European Community Research Infrastructure Action under the FP7 “Capacities” Program.

Funding Open Access funding provided by Universität Bern. Funding for genetic analyses came from the Natural History Museum Bern, Bern, Switzerland.

Data availability All data is published in the manuscript. Sequences are deposited in Genbank.

Code availability Software and programs are cited in the manuscript.

Declarations

Ethics approval Not applicable.

Consent for publication We give permission for the following paper to be published in *Organisms Diversity & Evolution*.

Conflict of interest Not applicable.

Open Access This article is licensed under a Creative Commons Attribution 4.0 International License, which permits use, sharing, adaptation, distribution and reproduction in any medium or format, as long as you give appropriate credit to the original author(s) and the source, provide a link to the Creative Commons licence, and indicate if changes were made. The images or other third party material in this article are included in the article's Creative Commons licence, unless indicated otherwise in a credit line to the material. If material is not included in the article's Creative Commons licence and your intended use is not permitted by statutory regulation or exceeds the permitted use, you will need to obtain permission directly from the copyright holder. To view a copy of this licence, visit <http://creativecommons.org/licenses/by/4.0/>.

References

- Abellán, P., & Svenning, J.-C. (2014). Refugia within refugia – patterns in endemism and genetic divergence are linked to Late Quaternary climate stability in the Iberian Peninsula. *Biological Journal of the Linnean Society*, 113(1), 13–28. <https://doi.org/10.1111/bj.12309>
- Alonso, A., Prieto, C. E., Quiñonero-Salgado, S., & Rolán, E. (2018). A morphological gap for Iberian *Zospeum* filled: *Zospeum percostulatum* sp. n. (Gastropoda, Eupulmonata, Carychiidae) a new species from Asturias (Spain). *Subterranean Biology*, 25, 35–48. <https://doi.org/10.3897/subtbiol.25.23364>
- Altekar, G., Dwarkadas, S., Huelsenbeck, J. P., & Ronquist, F. (2004). Parallel Metropolis-coupled Markov chain Monte Carlo for Bayesian phylogenetic inference. *Bioinformatics*, 20, 407–415.
- Bank, R. A., & Gittenberger, E. (1985). Notes on Azorean and European *Carychium* species (Gastropoda, Basommatophora, Ellobiidae). *Basteria*, 49(4/6), 85–100.
- Barker, G. M. (2001). *The Biology of Terrestrial Mollusks* (p. 558). CABI Publishing.
- Bole, J. (1960). Novi vrsti iz rodu *Zospeum* Bourg. (Gastropoda). *Biološki Vestnik*, 7, 61–64.
- Bole, J. (1974). Rod *Zospeum* Bourguignat 1865 (Gastropoda, Ellobiidae) v Jugoslaviji. *Razprave Slovenska Akademija znanosti in Umetnosti Cl. IV*, 17(5), 249–291.
- Bouaziz-Yahiatene, H., Pfarrer, B., Medjdoub-Bensaad, F., & Neubert, E. (2017). Revision of *Massylaea* Möllendorff, 1898 (Stylommatophora, Helicidae). *ZooKeys* 694, 109–133. <https://doi.org/10.3897/zookeys.694.15001>
- Bourguignat, J. R. (1856). Aménités malacologiques. Du genre *Zospeum*. *Revue et Magasin de Zoologie pure et appliquée* (2)8, 499–516.
- Colgan, D., McLauchlan, A., Wilson, G. D. F., Livingston, S. P., & Edgecombe, G. D. (1998). Histone H3 and U2 snRNA DNA sequences and arthropod molecular evolution. *Australian Journal of Zoology*, 46, 419–437.
- Dörge, D. (2010). Vergleich der Anatomie und Histologie zweier Mikroschneckenarten, *Carychium minimum* Müller, 1774 und *Zospeum isselianum* Pollonera, 1887 (Gastropoda, Pulmonata, Ellobiidae). *Unpublished BSc thesis*, Goethe-University, Frankfurt am Main, Germany.
- Folmer, O., Black, M., Hoe, W., Lutz, R., & Vrijenhoek, R. (1994). DNA primers for amplification of mitochondrial cytochrome c oxidase subunit I from diverse metazoan invertebrates. *Molecular Marine Biology and Biotechnology*, 3(5), 294–299.
- Freyer, H. (1855). Über neu entdeckte Conchylien aus den Geschlechtern *Carychium* und *Pterocera*. *Sitzungsberichte der mathematisch-naturwissenschaftlichen Classe der kaiserlichen Akademie der Wissenschaften* 5, 18–23.
- Gittenberger, E. (1973). Eine *Zospeum*-Art aus den Pyrenäen *Zospeum Bellesi* Spec. Nov. *Basteria*, 37(5–6), 137–140.
- Gittenberger, E. (1980). Three Notes on Iberian Terrestrial Gastropods. *Zoologische Mededelingen*, 55(17), 201–213.
- Gómez, B. J., & Prieto, C. E. (1983). *Zospeum biscaiense* nov. sp. (Gastropoda, Ellobiidae) otro molusco troglobio para la Península Ibérica. *Speleon*, 26–27, 7–10.
- Harry, H. W. (1997–1998). *Carychium exiguum* (Say) of lower Michigan; Morphology, Ecology, Variation and Life History (Gastropoda, Pulmonata). *Walkerana* 9(21), 104
- Hewitt, G. M. (2004). Genetic consequences of climatic oscillations in the Quaternary. *Philosophical Transactions of the Royal Society of London B: Biological Sciences*, 359, 183–195. <https://doi.org/10.1098/rstb.2003.1388>
- Holznagel, W. E. (1998). A nondestructive method for cleaning gastropod radulae from frozen, alcohol-fixed, or dried material. *American Malacological Bulletin*, 14, 181–183.
- Huelsenbeck, J. P., & Ronquist, F. (2001). MRBAYES: Bayesian inference of phylogeny. *Bioinformatics*, 17, 754–755.
- Inäbnit, I., Jochum, A., Kampschulte, M., Martels, G., Ruthensteiner, R., Slapnik, R., Nesselhauf, C., & Neubert, E. (2019). An integrative taxonomic study reveals carychiid microsnails of the troglobitic genus *Zospeum* in the Eastern and Dinaric Alps (Gastropoda, Ellobioidea, Carychiinae). *Organisms Diversity and Evolution*, 19, 135–177. <https://doi.org/10.1007/s13127-019-00400-8>
- Jochum, A. (2011). Evolution and diversity of the troglobitic Carychiidae—A morphological and phylogenetic investigation of the terrestrial ellobioid genera, *Carychium* and *Zospeum*. *The Malacologist*, 57, 16–18.
- Jochum, A., Weigand, A. M., Slapnik, R., Valentinčič, J., & Prieto, C. P. (2012). The microscopic ellobioid, *Zospeum* Bourguignat, 1856 (Pulmonata, Ellobioidea, Carychiidae) makes a big debut in Basque Country and the province of Burgos (Spain). *MalaCo* 8, 400–403. <http://www.journal-malaco.fr>
- Jochum, A., de Winter, A. J., Weigand, A. M., Gómez, B. J., & Prieto, C. E. (2015a). Two new species of *Zospeum* Bourguignat, 1856 from the Basque-Cantabrian Mountains, Northern Spain (Eupulmonata, Ellobioidea, Carychiidae). *ZooKeys*, 483, 81–96. <https://doi.org/10.3897/zookeys.483.9167>
- Jochum, A., Slapnik, R., Klusmann-Kolb, A., Páll-Gergely, B., Kampschulte, M., Martels, G., Vrabec, M., Nesselhauf, N., & Weigand, A. M. (2015b). Groping through the black box of variability: An integrative taxonomic and nomenclatural re-evaluation of *Zospeum isselianum* Pollonera, 1887 and allied species using new imaging technology (Nano-CT, SEM), conchological, histological

- and molecular data (Ellobioidea, Carychiidae). *Subterranean Biology*, 16, 123–165. <https://doi.org/10.3897/subtbiol.16.5758>
- Jochum, A., Neubauer, T. A., & Harzhauser, M. (2015c). Microstructural details in shells of the gastropod genera *Carychiella* and *Carychium* of the Middle Miocene. *Lethaia*, 49, 87–101. <https://doi.org/10.1111/let.12134>
- Jochum, A., Prieto, C. E., Kampschulte, M., Martels, G., Ruthensteiner, B., Vrabec, M., Dörge, D. D., & de Winter, A. J. (2019). Re-evaluation of *Zospeum schaufussi* von Frauenfeld, 1862 and *Z. suarezi* Gittenberger, 1980, including the description of two new Iberian species using Computer Tomography (CT) (Eupulmonata, Ellobioidea, Carychiidae). *ZooKeys*, 835, 65–86. <https://doi.org/10.3897/zookeys.835.33231>
- Kruckenhauser, L., Plan, L., Mixanig, H., & Slapnik, R. (2019). Verwandtschaftsbeziehungen von Kärntner Populationen der Höhlenschnecke *Zospeum isselianum*. *Die Höhle*, 70(1–4), 139–147.
- Kumar, S., Stecher, G., Li, M., Knyaz, C., & Tamura, K. (2018). MEGA X: Molecular Evolutionary Genetics Analysis across computing platforms. *Molecular Biology and Evolution*, 35, 1547–1549. <https://doi.org/10.1093/molbev/msy096>
- Kuščer, L. (1932). Höhlen- und Quellenschnecken aus dem Flussgebiet der Ljubljana. *Archiv Für Molluskenkunde*, 64(2), 60–61.
- Lanfear, R., Frandsen, P. B., Wright, A. M., Senfeld, T. & Calcott, B. (2016) PartitionFinder 2: new methods for selecting partitioned models of evolution for molecular and morphological phylogenetic analyses. *Molecular biology and evolution*. <https://doi.org/10.1093/molbev/msw260>
- Luchtel, D. L., Martin, A. W., Deyrup-Olsen, I., & Boer, H. H. (1997). *Gastropoda: Pulmonata*. In: F. W. Harrison & A. J. Kohn (Eds.) *Microscopic Anatomy of Invertebrates* (vol 6B, pp. 459–718). Mollusca II, Wiley-Liss, Inc., New York.
- Maier H. C. (1982). Zur Systematik, Zoogeographie, Anatomie und Biologie der Gattung *Zospeum* BGT. 1856 (Gastropoda: Basommatophora: Ellobiidae) [DPhil thesis] (p. 175). Vienna, Austria: University of Vienna.
- Martins, A. M. F. (1996). Anatomy and Systematics of the Western Atlantic Ellobiidae (Gastropoda, Pulmonata). *Malacologia*, 37(2), 163–332.
- Martins, A. M. F. (2007). Morphological and anatomical diversity within the Ellobiidae (Gastropoda, Pulmonata, Archaeopulmonata). *Vita Malacologica*, 4, 1–28.
- Morton, J. E. (1955). The functional morphology of the British Ellobiidae (Gastropoda, Pulmonata) with special reference to the digestive and reproductive systems. *Philosophical Transactions of the Royal Society of London* 239(B), 89–160.
- Notenboom, J., & Meijers, I. (1985). Research on the groundwater fauna of Spain: List of stations and first results. *Verslagen En Technische Gegevens, Institute of Taxonomic Zoology, University of Amsterdam*, 42, 5–37.
- Pollonera, C. (1887). Note malacologiche. I. Molluschi della Valle del Natisone (Friuli). *Bullettino della Società Malacologica Italiana*, 12["1886"], 204–208. <http://archive.org/details/bullettino121886soci>
- Prieto, C. E., & Zuazu, F. J. (2018). New records and geographical distribution of *Zospeum bellesi* Gittenberger 1973 (Gastropoda: Ellobiida: Ellobiidae). *Iberus*, 36(2), 73–79.
- Puillandre, N., Lambert, A., Brouillet, S., & Achaz, G. (2012). ABGD, automatic barcode gap discovery for primary species delimitation. *Molecular Ecology*, 21, 1864–1877. <https://doi.org/10.1111/j.1365-294X.2011.05239.x>
- Ronquist, F., & Huelsenbeck, J. P. (2003). MRBAYES 3: Bayesian phylogenetic inference under mixed models. *Bioinformatics*, 19, 1572–1574.
- Rossmässler, E. A. (1839). Iconographie der Land- und Süßwasser-Mollusken, mit vorzüglicher Berücksichtigung der europäischen noch nicht abgebildeten Arten. 1: 2 (3/4). Arnoldische Buchhandlung, Dresden, Leipzig, 46.
- Simon, C., Frati, F., Beckenbach, A., Crespi, B., Liu, H., & Flook, P. (1994). Evolution, weighting, and phylogenetic utility of mitochondrial gene sequences and a compilation of conserved polymerase chain reaction primers. *Annals of the Entomological Society of America*, 87(6), 651–701.
- Stamatakis, A. (2006). RAxML-VI-HPC: Maximum likelihood-based phylogenetic analyses with thousands of taxa and mixed models. *Bioinformatics*, 22(21), 2688–2690. <https://doi.org/10.1093/bioinformatics/btl446>
- von Frauenfeld, G. (1854). Über einen bisher verkannten Laufkäfer beschrieben von L. Miller; und einen neuen augenlosen Rüsselkäfer, beschrieben von F. Schmidt; ferner einige von Schmidt in Schischka neu entdeckte Höhlentiere. *Verhandlungen Des Zoologisch-Botanischen Vereins in Wien*, 4, 23–34.
- von Frauenfeld G. (1856). Die Gattung *Carychium*. *Sitzungsberichte der Mathematisch-naturwissenschaftlichen Classe der Kaiserlichen Akademie der Wissenschaften*, 19(1–2), 70–93, 1 plate. Wien.
- von Frauenfeld, G. (1862). Ueber ein neues Höhlen-Carychium (*Zospeum* Brg.) und zwei neue fossile Paludinen. *Verhandlungen der Zoologisch-Botanischen Gesellschaft in Wien*, 12, 969–972. <http://www.biodiversitylibrary.org/item/95692?page/487/mode/1up>
- Weigand, A. M., Jochum, A., Pfenninger, M., Steinke, D., & Klussmann-Kolb, A. (2011). A new approach to an old conundrum – DNA barcoding sheds new light on phenotypic plasticity and morphological stasis in microsnails (Gastropoda, Pulmonata, Carychiidae). *Molecular Ecology Resources*, 11, 255–265. <https://doi.org/10.1111/j.1755-0998.2010.02937.x>
- Weigand, A. M., Jochum, A., Slapnik, R., Schnitzler, J., Zarza, E., & Klussmann-Kolb, A. (2013). Evolution of microgastropods (Ellobioidea, Carychiidae): Integrating taxonomic, phylogenetic and evolutionary hypotheses. *BMC Evolutionary Biology*, 13(1), 18. <https://doi.org/10.1186/1471-2148-13-18>

Publisher's Note Springer Nature remains neutral with regard to jurisdictional claims in published maps and institutional affiliations.

On the verge of extinction – revision of a highly endangered Swiss alpine snail with description of a new genus, *Raeticella* gen. nov. (Gastropoda, Eupulmonata, Hygromiidae)

Jeannette Kneubühler^{1,2}, Markus Baggenstos³, Eike Neubert^{1,2}

1 Natural History Museum Bern, 3005 Bern, Switzerland **2** Institute of Ecology and Evolution, University of Bern, 3012 Bern, Switzerland **3** Oekologische Beratung Markus Baggenstos, Tottikonstrasse 48, 6370 Stans, Switzerland

Corresponding author: Jeannette Kneubühler (jeannette.kneuebuehler@nmbe.ch)

Academic editor: A. M. de Frias Martins | Received 28 February 2022 | Accepted 12 May 2022 | Published 8 June 2022

<http://zoobank.org/12CD28D8-33FF-44D2-B271-87C11240FA2D>

Citation: Kneubühler J, Baggenstos M, Neubert E (2022) On the verge of extinction – revision of a highly endangered Swiss alpine snail with description of a new genus, *Raeticella* gen. nov. (Gastropoda, Eupulmonata, Hygromiidae). ZooKeys 1104: 69–91. <https://doi.org/10.3897/zookeys.1104.82866>

Abstract

The phylogenetic status of the alpine land snail *Fruticicola biconica* has remained questionable since it was described by Eder in 1917. Considered a microendemic species from mountain tops in Central Switzerland, the shell is specially adapted for life under stones. Herein, we show via molecular and anatomical investigations that *F. biconica* neither belongs to the land snail genus *Trochulus*, nor to any other genus within Trochulini, but rather warrants placement within the newly established genus *Raeticella* Kneubühler, Baggenstos & Neubert, 2022. Phylogenetic analyses reveal that *R. biconica* is clearly separated from *Trochulus*. These findings are supported by morphological investigations of the shell and genitalia.

Keywords

Endemism, integrative taxonomy, LGM, mountains, nunataks, phylogeny, Switzerland, *Trochulus*

Introduction

Discovered in the Bannalp, Nidwalden and known from only a few localities in the Central Swiss Alps, *Fruticicola biconica* was described by the Swiss zoologist Leo Eder in 1917.

Later, *F. biconica*, known as the Nidwaldner hairy snail, was moved to the widely used genus *Trichia* W. Hartmann, 1840 and circulated throughout the European literature under this designation (e.g., Kerney et al. 1983). The generic name, *Trichia*, was subsequently replaced by *Trochulus* Chemnitz, 1786 due to homonymy with *Trichia* De Haan, 1839 (Crustacea, Xanthidae).

Previous studies (Pfenninger et al. 2005; Dépraz et al. 2009; Duda et al. 2014; Kruckenhauser et al. 2014; Proćków et al. 2021) included *T. biconicus* individuals in their genetic analyses of *Trochulus* species. Pfenninger et al. (2005) and Dépraz et al. (2009) used the same sequence of *T. biconicus* collected at the type locality at Bannalp. This sequence clustered within the so far known *Trochulus* species and some newly identified lineages, which were not further described (fig. 2 in Pfenninger et al. 2005; fig. 1 in Dépraz et al. 2009). Most likely, Pfenninger et al. (2005) and Dépraz et al. (2009) used misidentified specimens in their phylogenetic studies, or some samples were mixed. Since these authors did not publish images of the investigated specimens, an unequivocal identification is not possible. Duda et al. (2014) and Kruckenhauser et al. (2014) found that *T. biconicus*, “*T. oreinos oreinos*” (A.J. Wagner, 1915), and “*T. oreinos scheerpeltzi*” (Mikula, 1957) form basal lineages in comparison to specimens of *Trochulus* s. str. The latter two taxa were elevated from subspecies to species level (Bamberger et al. 2020) and are today known to belong to the newly described genus *Noricella* (Neiber et al. 2017). Proćków et al. (2021) found the same phylogenetic pattern as Duda et al. (2014) and Kruckenhauser et al. (2014) and questioned the affiliation of *biconicus* to *Trochulus*. Already Turner et al. (1998) had disputed the phylogenetic position of *T. biconicus*. Until today, the phylogenetic position of *T. biconicus* within the Trochulini remained unclear. Hence, an integrative taxonomic approach is applied in this study to investigate the phylogenetic affiliation of *T. biconicus*.

Materials and methods

Specimens investigated

Living individuals of *T. biconicus* were collected in September 2020 at 11 sites of the known distribution area in Central Switzerland (see Fig. 1 for detailed sampling localities). *Trochulus biconicus* is classified as Vulnerable by Swiss law (Federal Office of Environment) and is protected. It is also considered Endangered by the IUCN (<https://www.iucnredlist.org/species/22107/9360310>). Collecting permits were obtained from the cantonal administrations of Nidwalden, Obwalden, and Uri. At each site, 3–5 snails were collected from large populations (>20 individuals)

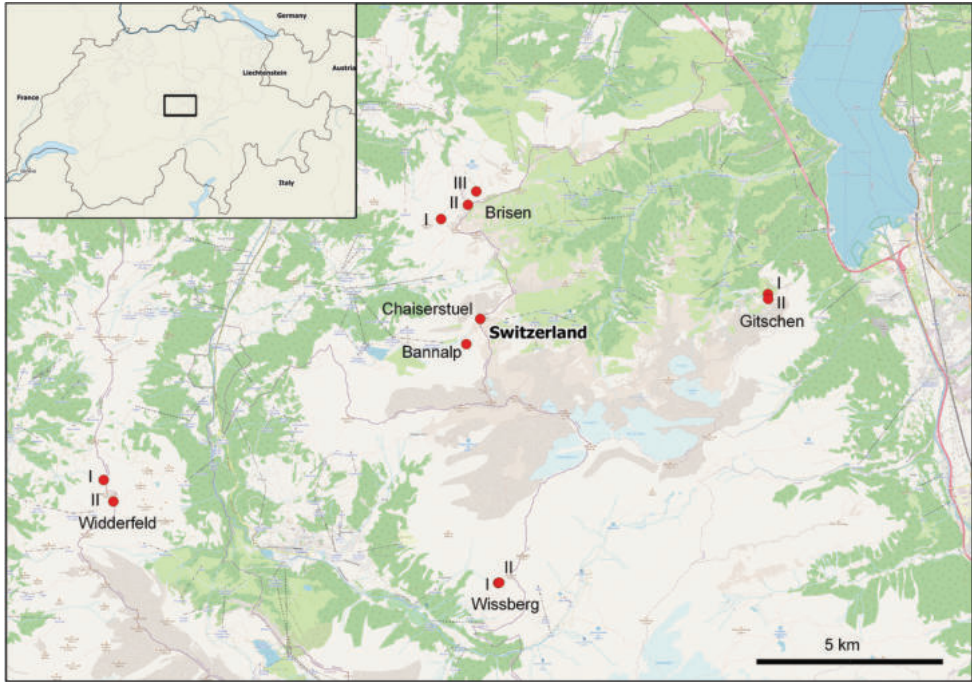


Figure 1. Sampling locations of the investigated individuals of *T. biconicus*.

from under rocks on stony outcrops. The individual snails were preserved in 80% ethanol to keep the body tissue soft for proper anatomical investigations and DNA extraction. In Table 1, sampling localities and GenBank accession numbers are listed for all sequenced specimens of *T. biconicus*, *Trochulus* spp., and *Edentiella edentula*. Usually, two specimens of *T. biconicus* per population were sequenced. Those not destroyed in the extraction process are deposited at the NMBE as voucher material. The map was produced with QGIS (2016, v. 2.18.13) using the Natural Earth data set.

Acronyms of collections

NMBE Natural History Museum Bern, Switzerland;
MNHW Museum of Natural History Wrocław, University of Wrocław, Poland.

Shell morphology and anatomical study of the genitalia

One animal was selected from each population for investigations of the shell morphology and the genital organs. The dissection of the genitalia was performed under a Leica MZ12 stereomicroscope using thin tweezers. The genital organs were removed from the body, spread on a wax-lined bowl and properly pinned with small needles. The

total length of the situs was measured using Mitutoyo callipers. Proportions between different parts of the genitalia were estimated using the total situs length as a reference. Additionally, the inner structures of the penis and the penial papilla were investigated. Pictures of the situs and the shells were taken with a Leica M205 microscope camera using an image-processing program (Leica LAS X v. 3.6.0.20104, Switzerland). The shells were imaged in frontal, lateral, apical, and ventral position. Shell height and shell width were measured using the callipers to assess perpendicularity with the shell axis.

Table 1. Sequenced *T. biconicus* specimens from Central Switzerland. Asterisk (*) marks the type localities of the species studied. Additionally, *Edentiella edentula* (Draparnaud, 1805) and some species of *Trochulus* were sequenced and included for phylogenetic analyses.

Voucher-No.	Species	Locality	Coordinates	Altitude [m]	GenBank accession number COI	GenBank accession number 16S	GenBank accession number ITS2
NMBE 567164	<i>T. biconicus</i>	Bannalp Schonegg*	46.87°N, 8.46°E	2232	MW435154	MW433778	MW433799
NMBE 567165	<i>T. biconicus</i>	Bannalp Schonegg*	46.87°N, 8.46°E	2232	MW435155	MW433779	MW433800
NMBE 567167	<i>T. biconicus</i>	Chaiserstuel	46.87°N, 8.46°E	2263	MW435156	MW433780	MW433801
NMBE 567168	<i>T. biconicus</i>	Chaiserstuel	46.87°N, 8.46°E	2263	MW435157	MW433781	MW433802
NMBE 567149	<i>T. biconicus</i>	Wissberg I	46.81°N, 8.47°E	2335	MW435158	MW433782	MW433803
NMBE 567150	<i>T. biconicus</i>	Wissberg I	46.81°N, 8.47°E	2335	MW435159	MW433783	MW433804
NMBE 567152	<i>T. biconicus</i>	Wissberg II	46.81°N, 8.47°E	2355	MW435160	MW433784	MW433805
NMBE 567153	<i>T. biconicus</i>	Wissberg II	46.81°N, 8.47°E	2355	MW435161	MW433785	MW433806
NMBE 567155	<i>T. biconicus</i>	Widderfeld I	46.83°N, 8.33°E	2120	MW435162	MW433786	MW433807
NMBE 567156	<i>T. biconicus</i>	Widderfeld I	46.83°N, 8.33°E	2120	MW435163	MW433787	MW433808
NMBE 567159	<i>T. biconicus</i>	Widderfeld II	46.83°N, 8.33°E	2290	MW435164	MW433788	MW433809
NMBE 567161	<i>T. biconicus</i>	Brisen I	46.90°N, 8.45°E	2045	MW435165	MW433789	MW433810
NMBE 567137	<i>T. biconicus</i>	Brisen I	46.90°N, 8.45°E	2045	MW435166	MW433790	MW433811
NMBE 567139	<i>T. biconicus</i>	Brisen II	46.90°N, 8.46°E	2130	MW435167	MW433791	MW433812
NMBE 567140	<i>T. biconicus</i>	Brisen II	46.90°N, 8.46°E	2130	MW435168	MW433792	MW433813
NMBE 567142	<i>T. biconicus</i>	Brisen III	46.90°N, 8.46°E	2090	MW435169	MW433793	MW433814
NMBE 567143	<i>T. biconicus</i>	Brisen III	46.90°N, 8.46°E	2090	MW435170	MW433794	MW433815
NMBE 567145	<i>T. biconicus</i>	Gitschen I	46.88°N, 8.57°E	1890	MW435171	MW433795	MW433816
NMBE 567146	<i>T. biconicus</i>	Gitschen I	46.88°N, 8.57°E	1890	MW435172	MW433796	MW433817
NMBE 567148	<i>T. biconicus</i>	Gitschen II	46.88°N, 8.57°E	1970	MW435173	MW433797	MW433818
NMBE 567162	<i>T. biconicus</i>	Gitschen II	46.88°N, 8.57°E	1970	MW435174	MW433798	MW433819
NMBE 568100	<i>T. hispidus</i>	Sweden, prov. Uppland, Uppsala, Linnaeus Garden*	59.8619°N, 17.6342°E		ON477947	–	–
NMBE 568103	<i>T. hispidus</i>	Sweden, Östergötland, Vist	58.3294°N, 15.729°E	70	ON477948	ON479908	ON479901
NMBE 564609	<i>Trochulus</i> sp.	Bullet, Le Chasseron	46.8517°N, 6.5377°E	1606	ON477944	ON479905	ON479898
NMBE 564607	<i>Trochulus</i> sp.	Mervelier, Schelental	47.336°N, 7.5153°E	615	ON477943	ON479904	ON479897
NMBE 543063	<i>Trochulus</i> sp.	St-Cergue, Route de Cuvuloup	46.4487°N, 6.123°E	1208	ON477941	ON479902	ON479895
NMBE 564601	<i>Trochulus</i> sp.	Zernez	46.6998°N, 10.0943°E	1473	ON477942	ON479903	ON479896
NMBE 568094	<i>Trochulus</i> sp.	Lac du Mont d'Orge	46.2321°N, 7.333°E	624	ON477946	ON479907	ON479900
NMBE 565821	<i>T. alpicola</i>	Bannalp Schonegg*	46.8706°N, 8.2491°E	2234	ON477945	ON479906	ON479899
MNHWS_15_29_101	<i>T. villosus</i>	Montagne De Cernier	47.0763°N, 6.8888°E	1385	MW440985	MW447773	MW440678
MNHWS_15_29_02	<i>T. clandestinus</i>	Montagne De Cernier	47.0763°N, 6.8888°E	1385	MW440983	MW447772	MW440676
MNHWS_15_27_12	<i>Trochulus</i> sp.	Gorges de Court	47.2553°N, 7.3439°E	608	MW440984	MW621002	MW440677
MNHWS_15_21_02	<i>T. caelatus</i>	Gorges de Moutier*	47.2856°N, 7.3819°E	477	MW440982	MW621001	MW440675
MNHWS_Er_50	<i>E. edentula</i>	Erschwil	47.3673°N, 7.555°E	459	MW440986	MW621003	MW440679
MNHWS_Er_51	<i>E. edentula</i>	Erschwil	47.3673°N, 7.555°E	459	MW440987	MW621004	MW440680

Abbreviations used in the anatomical descriptions and figures

AG	albumen gland;	Pe	penis;
BC	bursa copulatrix;	PP	penial papilla;
DS	dart sacs;	sh	shell height;
Ep	epiphallus;	sw	shell width;
Fl	flagellum;	Va	vagina;
HD	hermaphroditic duct;	VD	vas deferens.
MG	mucous glands;		

DNA extraction, PCR amplification and sequence determination

For total DNA extraction of the specimens, the Qiagen Blood and Tissue Kit (Qiagen; Hilden, Germany) was used in combination with a QIAcube extraction robot. Circa 0.5 cm³ of tissue was cut and placed in a mixture of 180 µl ATL buffer and 20 µl Proteinase K. It was then incubated for ca. 4 hours at 56 °C in a heater (Labnet, Vortemp 56, witec AG, Littau, Switzerland). For subsequent DNA extraction, the QIAcube extraction robot was used with the Protocol 430 (DNeasy Blood Tissue and Rodent tails Standard). In this study, two mitochondrial markers (COI and 16S) and one nuclear marker (5.8S rRNA+ITS2) were investigated. PCR mixtures consisted of 12.5 µl GoTaq G2 HotStart Green Master Mix (Promega M7423), 4.5 µl ddH₂O, 2 µl forward and reverse primer each, and 4 µl DNA template. The primer pairs implemented for the PCR are listed in Table 2. The following PCR cycles were used: for COI, 2 min at 94 °C, followed by 40 cycles of 1 min at 95 °C, 1 min at 47 °C and 1 min at 72 °C and finally, 5 min at 72 °C; for 16S, 3 min at 96 °C, followed by 40 cycles of 30 s at 94 °C, 30 s at 50 °C and 30 s at 72 °C, and finally, 1 min at 72 °C; and for 5.8S rRNA+ITS2, 3 min at 94 °C, followed by 40 cycles of 30 s at 94 °C, 30 s at 50 °C and 30 s at 72 °C, and finally, 5 min at 72 °C (SensoQuest Tabcyclet and Techne TC-512, witec AG, Littau, Switzerland). The purification and sequencing of the PCR product was performed by LGC (LGC Genomics Berlin, Germany).

Phylogenetic analyses

The phylogenetic analyses were conducted using sequences obtained from GenBank and from this study, which were included as outgroup: *Ichnusotricha berninii* Giusti & Manganeli, 1987, *Plicuteria lubomirskii* (Ślósarski, 1881), *Petasina unidentata* (Draparnaud, 1805), *Noricella oreinos* (A.J. Wagner, 1915), *Noricella scheerpeltzi* (Mikula, 1957) (GenBank numbers and sampling localities published by Neiber et al. 2017), *Edentiella edentula* (Draparnaud, 1805), and several ingroup specimens of *Trochulus* (Table 1). These species were selected to identify the phylogenetic position of *T. biconicus*.

For sequence processing and editing, the software package Geneious v. 9.1.8 (Biomatters Ltd) was used. Topologies were estimated using two different phylogenetic methods: Bayesian Inference (BI) and Maximum Likelihood (ML). Bayesian Inference was performed using Mr. Bayes v. 3.2.6 x64 (Huelsenbeck and Ronquist 2001;

Table 2. Primer pairs used for PCR.

Gene	Primer	Sequence	Sequence length (bp)	Reference
COI	LCO1490	5'-GGTCAACAAATCATAAAGATATTGG-3'	655	Folmer et al. 1994
	HCO2198	5'-TAAACTTCAGGGTGACCAAAAAATCA-3'		
16S	16S cs1	5'-AAACATACCTTTTGCATAATGG-3'	440	Chiba 1999
	16S cs2	5'-AGAAACTGACCTGGCTTACG-3'		
ITS2	ITS2 LSU1	5'-GCTTGGCGAGAATTAATGTGAA-3'	900	Wade and Mordan 2000
	ITS2 LSU3	5'-GGTACCTTGTTCGCTATCGGA-3'		

Ronquist and Huelsenbeck 2003; Altekar et al. 2004) via the HPC cluster from the University of Bern (<http://www.id.unibe.ch/hpc>). Evolutionary models for each subset were set to mixed models. The Monte Carlo Markov Chain (MCMC) parameter was set as follows: starting with four chains and four separate runs for 20 million generations with a tree sampling frequency of 1000 and a burn in of 25%. RAxML plug-in for Geneious (Stamatakis 2014) was implemented for computing ML inference, using Geneious' plug-in with rapid bootstrapping setting, the search for the best scoring ML tree and 1000 bootstrapping replicates. The model, GTR CAT I was implemented.

Results

Phylogenetic analyses

The BI analysis of the concatenated data set (Fig. 2) shows two major clades within the tribe Trochulini. These two clades are separated with full support. One clade contains representative specimens of *Edentiella* and *Noricella* which form a polytomy. The second major clade within Trochulini contains representatives of *Petasina*, *Trochulus*, and the investigated *T. biconicus* specimens. *Trochulus biconicus* is the sister lineage to the selected *Trochulus* specimens. This node has full posterior probability support. *Trochulus hispidus* from the type locality in Sweden clusters together with a second specimen from Sweden and forms the sister group to two Swiss *Trochulus* specimens from Zerneze and Lac du Mont d'Orge. The resolution within the *T. biconicus* clade is moderate because the investigated individuals differ in only few nucleotides in all three investigated markers.

The ML analysis of the concatenated data set (Fig. 3) shows a similar topology as that of the BI analysis. The difference in the ML and the BI tree is the relationship of *Edentiella* and *Noricella*. In the ML tree, *E. edentula* clusters together with *N. scheerpeltzi*. This node has low support value (bootstrap support of 51 in Fig. 3), whereas in the BI analysis (Fig. 2), *Edentiella* and *Noricella* show a polytomy. In both analyses, *T. biconicus* forms the sister lineage to the selected *Trochulus* species. This node has full ML support. The support values within the *Trochulus* clade are moderate to high.

The *p*-distance, which shows the number of base differences per site from between sequences (Kumar et al. 2018) for the COI was calculated using MEGA

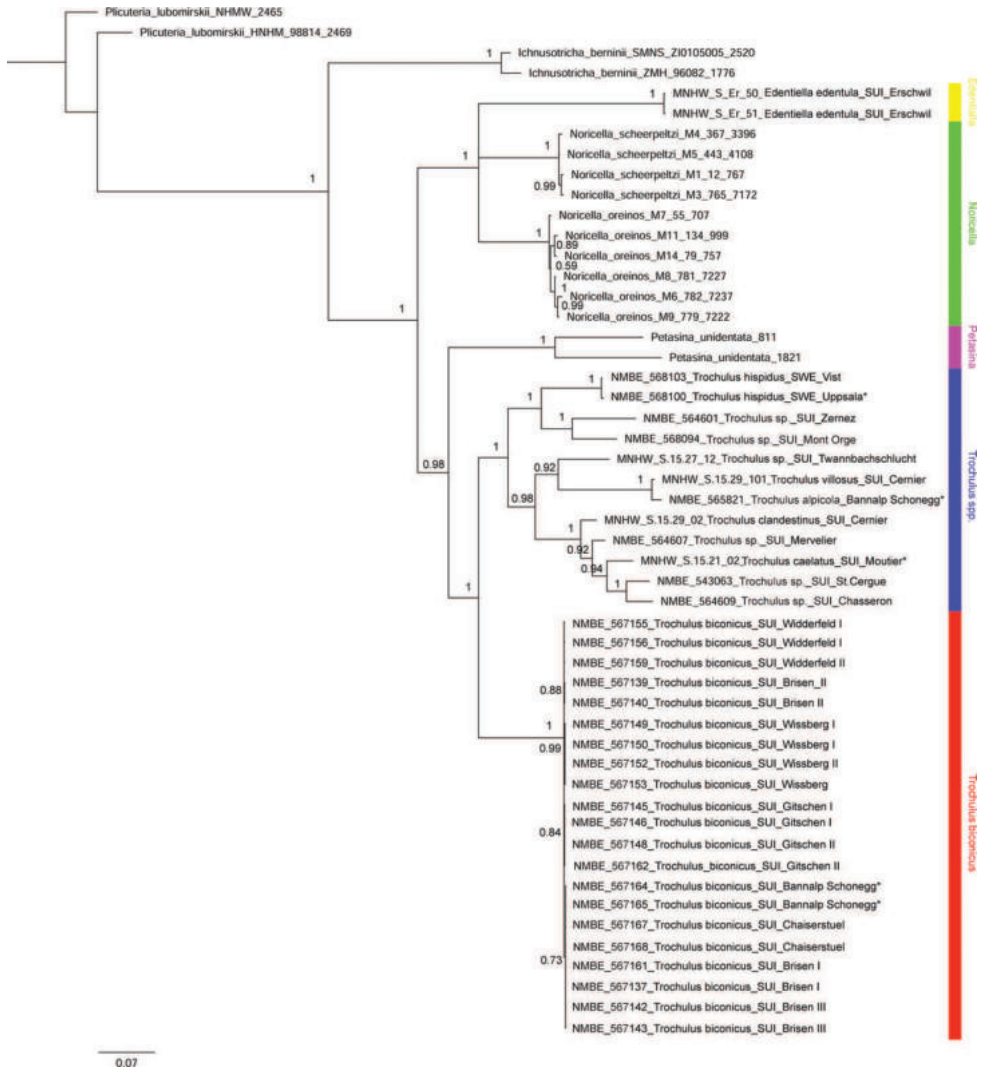


Figure 2. Bayesian Inference (BI) tree based on the concatenated data set of COI, 16S, and 5.8S rRNA+ITS2. Numbers represent Bayesian posterior probabilities.

v. 10.1.8 (<https://www.megasoftware.net/>). The p -distance for *T. biconicus* and the remaining investigated *Trochulus* species ranges from 0.153–0.189, for *T. biconicus* and *E. edentula* from 0.183–0.189, for *T. biconicus* and *Noricella* species from 0.128–0.166, for *T. biconicus* and *P. unidentata* from 0.171–0.176, for *T. biconicus* and *I. berninii* from 0.142–0.147 and for *T. biconicus* and *P. lubomirskii* from 0.177–0.188 (see Suppl. material 1). The genetic investigations in this study clearly show that *T. biconicus* is neither a member of the *Trochulus* clade nor does it belong to another known genus in the Trochulini. It thus, warrants designation in a separate new genus.

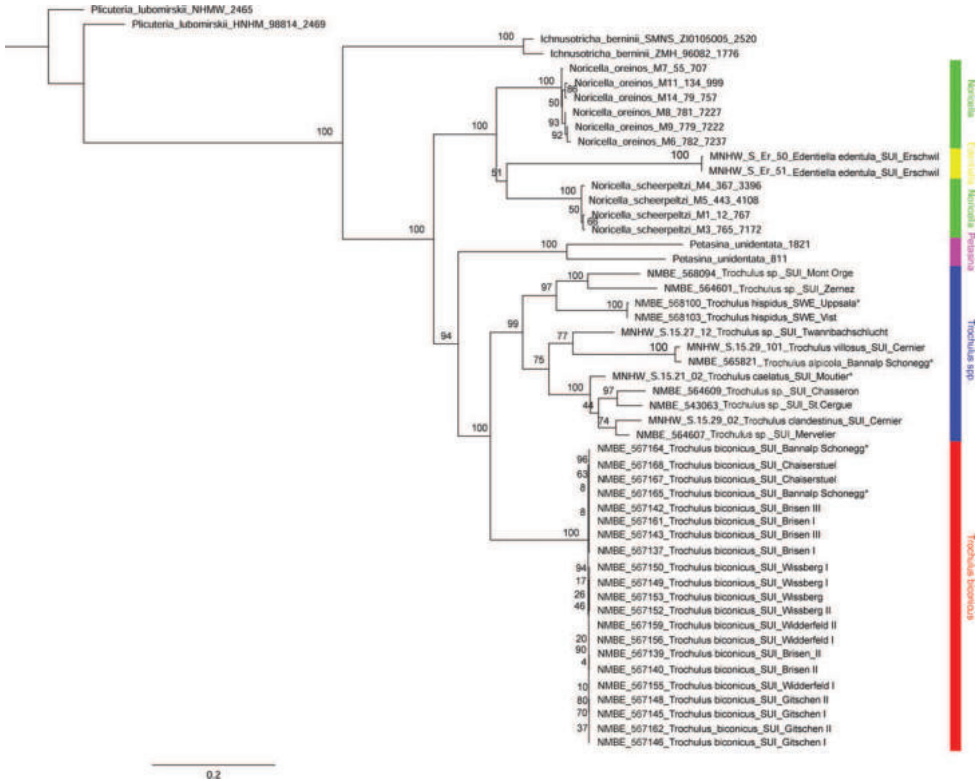


Figure 3. Maximum Likelihood (RAxML) tree based on the concatenated data set of COI, 16S, and 5.8S rRNA+ITS2. Numbers represent bootstrap support values from the ML analysis.

Shell morphology

The shell of *T. biconicus* is flattened, tightly coiled, and beige to brownish. The mean shell width of the investigated individuals ($N = 13$) is 5.63 mm (range: 5.3–6.1 mm; SD = 0.23 mm) with mean shell height reaching 2.67 mm (range: 2.34–2.9 mm; SD = 0.17 mm) (Table 3). The shell bears 5.5–6 whorls which increase only slightly in width towards the perimeter. The umbilicus is entirely open and wide. The crescent-shaped aperture contains a white, poorly developed lip. Neither juveniles nor adults show hairs on the shell (Figs 4–10).

Morphology of the genitalia

The genitalia are characterised by four stylophores, symmetrically placed in two pairs on both sides of the vagina (see fig. 11 in Proćków 2009). The inner dart sacs are somewhat longer and slenderer than the outer sacs. The outer stylophores contain the love darts (see also Proćków 2009). The mucous glands consist of four simple and thin tubes branching off the free oviduct directly above the dart sacs. The vagina is a rather long tube, which is

almost smooth inside or shows some faint elongate tissue folds that connect to the atrium (not shown in the figures). The bursa copulatrix branches off from the free oviduct above the dart sacs and the mucous glands and is terminated by an elongated vesicle.

The penis is fusiform and contains a club-shaped penial papilla which points into the lumen of the penial chamber. The epiphallus is as long as the penis; the penis retractor muscle inserts at the transition zone between epiphallus and penis. The flagellum is about 1.5× the length of the penis and epiphallus each. The epiphallial lumen contains longitudinal tissue ridges (e.g., Fig. 4C). The penial chamber is characterised by smooth walls. The penial papilla contains a lateral subapical pore. The cross section of the penial papilla (Figs 4D, 5D) reveals a central duct surrounded by small folds.

The anatomy of the genitalia of *T. clandestinus* differs from *T. biconicus* by having eight long, thin mucous glands (Fig. 11). The inner dart sacs of the investigated *T. clandestinus* are slightly longer in length than the outer dart sacs. The flagellum has about the same length as the bulbous penis, and the epiphallus is slightly longer than the penis. The cross section of the penial papilla differs in *T. clandestinus* by having several tissue layers around the main tube of the penial papilla (Fig. 11D).

Table 3. Morphological analysis: measurements of the shell and genital organs of *T. biconicus* and *T. clandestinus*. Additionally, some collected dry shells from Bannalp Schonegg (NMBE 567170) and Chaiserstuel (NMBE 567171) were included in the analysis. Asterisk (*) marks the type locality of *T. biconicus*. Umbilicus minor diameter is measured according to Proćków (2009). All measurements are in mm.

Voucher No.	Species	Locality	Coordinates	Altitude [m]	shell width	shell height	umbilicus minor diameter	penis length	epiphallus length	flagellum length	Figure number
NMBE 567151	<i>T. biconicus</i>	Wissberg I	46.81°N, 8.47°E	2335	5.56	2.55	0.8	1.81	2.01	5.98	Fig. 4
NMBE 567160	<i>T. biconicus</i>	Widderfeld II	46.83°N, 8.33°E	2290	5.73	2.59	0.88	2.79	3.42	8.13	Fig. 5
NMBE 567138	<i>T. biconicus</i>	Brisen I	46.90°N, 8.45°E	2045	5.61	2.34	0.73	2.86	3.06	7.25	Fig. 6
NMBE 567163	<i>T. biconicus</i>	Gitschen II	46.88°N, 8.57°E	1970	5.67	2.87	0.84	2.23	3.67	6.38	Fig. 7
NMBE 567166	<i>T. biconicus</i>	Bannalp Schonegg*	46.87°N, 8.46°E	2232	5.75	2.76	0.96	1.84	1.98	4.26	Fig. 8
NMBE 567169	<i>T. biconicus</i>	Chaiserstuel	46.87°N, 8.46°E	2263	5.3	2.46	0.99	2.66	3.21	4.1	Fig. 9
NMBE 567170_1	<i>T. biconicus</i>	Bannalp Schonegg*	46.87°N, 8.46°E	2232	5.7	2.82	1.19	–	–	–	Fig. 10A
NMBE 567170_2	<i>T. biconicus</i>	Bannalp Schonegg*	46.87°N, 8.46°E	2232	6.03	2.73	1.08	–	–	–	Fig. 10B
NMBE 567170_3	<i>T. biconicus</i>	Bannalp Schonegg*	46.87°N, 8.46°E	2232	5.39	2.54	0.99	–	–	–	Fig. 10C
NMBE 567170_4	<i>T. biconicus</i>	Bannalp Schonegg*	46.87°N, 8.46°E	2232	6.1	2.9	1.07	–	–	–	Fig. 10D
NMBE 567171_1	<i>T. biconicus</i>	Chaiserstuel	46.87°N, 8.46°E	2263	5.46	2.76	1.08	–	–	–	Fig. 10E
NMBE 567171_2	<i>T. biconicus</i>	Chaiserstuel	46.87°N, 8.46°E	2263	5.41	2.61	0.79	–	–	–	Fig. 10F
NMBE 567171_3	<i>T. biconicus</i>	Chaiserstuel	46.87°N, 8.46°E	2263	5.46	2.83	0.89	–	–	–	Fig. 10G
NMBE 571318	<i>T. clandestinus</i>	Bern, Bümpliz	46.9435°N, 7.3922°E	540	9.64	5.57	1.29	4.24	5.79	4.69	Fig. 11

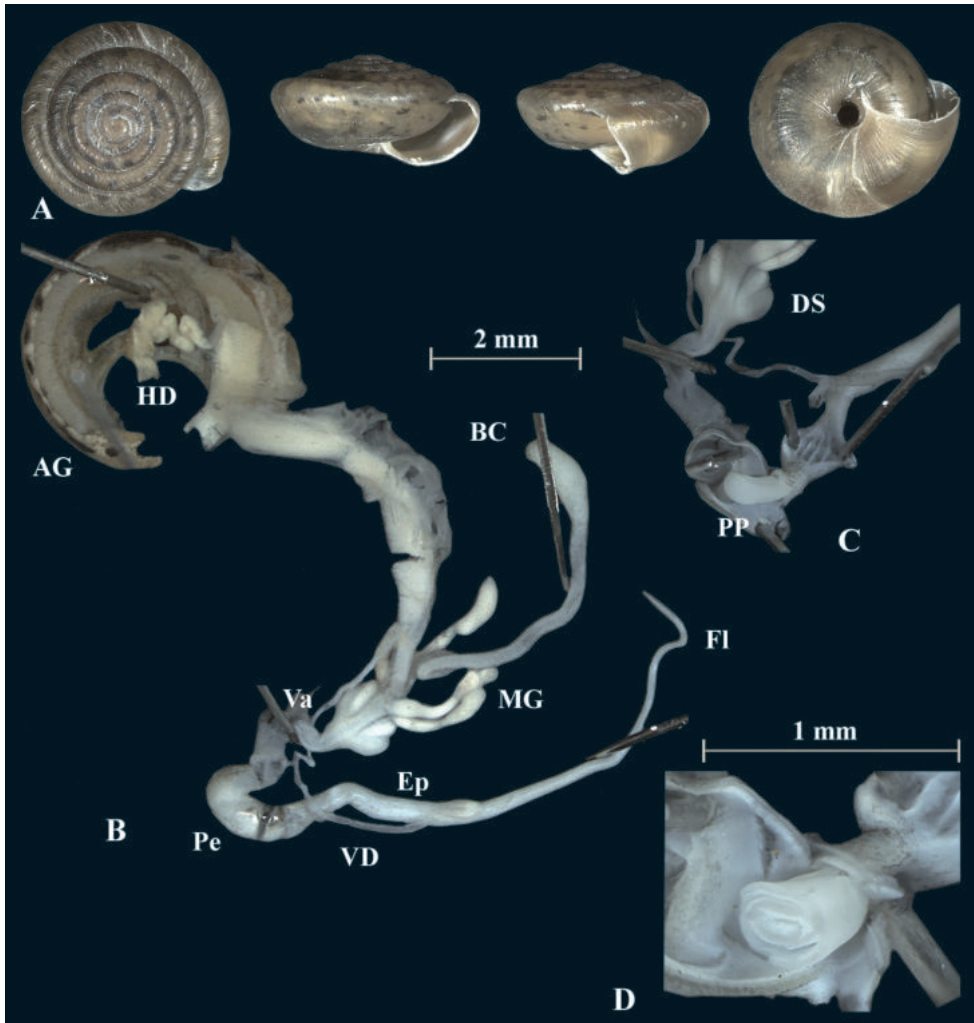


Figure 4. *Trochulus biconicus* (NMBE 567151) collected from Wissberg I **A** shell, sw = 5.56 mm, sh = 2.55 mm **B** situs **C** penis (Pe) with penial papilla (PP) **D** cross section of the penial papilla. Shell \times 5.

Taxonomic and systematic implications

The fully supported split between *T. biconicus* and currently known *Trochulus* species (Figs 2, 3) warrants description of a new genus, *Raeticella* gen. nov., based on *Fruticicola biconica*.

Genus *Raeticella* gen. nov.

<http://zoobank.org/D7620E37-3AA3-45D2-BB3C-B55114AF36F2>

Type species. *Fruticicola biconica* Eder, 1917.

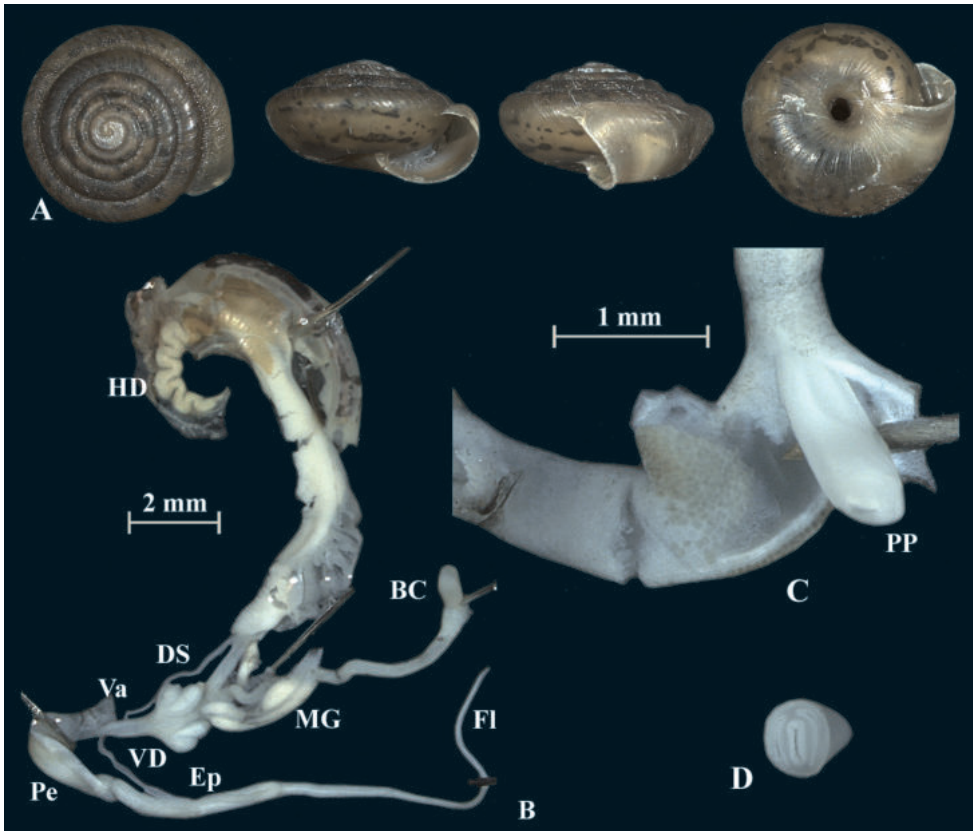


Figure 5. *Trochulus biconicus* (NMBE 567160) collected from Widdersfeld II **A** shell, sw = 5.73 mm, sh = 2.59 mm **B** situs **C** penis (Pe) with penial papilla (PP) **D** cross section of the penial papilla. Shell \times 5.

Genus *Trochulus* Chemnitz, 1786

Trochulus biconicus (Eder, 1917)

Diagnosis. Shell flattened and thin-walled, translucent, compressed in the direction of the axis; no trichome formation; whorls 5.5–6, gradually increasing so that the body whorl is only about twice as wide as the first whorl; the aperture is oblique, narrow, crescent-shaped; lip sharp, whitish and slightly reflexed; the four mucous glands are long, thick and pointed; penis and epiphallus are about the same length; the flagellum is barely separated from the epiphallus.

Differential diagnosis. *Raeticella* gen. nov. differs from *Trochulus* by having a flat, biconical shell, devoid of any periostracal hairs, even in juveniles, and in having only four instead of occasionally six or eight (see Duda et al. 2014) mucous glands. It differs from *Noricella* by lacking a basal tooth, being devoid of any periostracal hairs, the absence of coarse ripples and the absence of an additional fold and bulge in the penial papilla, which occurs in *N. oreinos* (Duda et al. 2014).

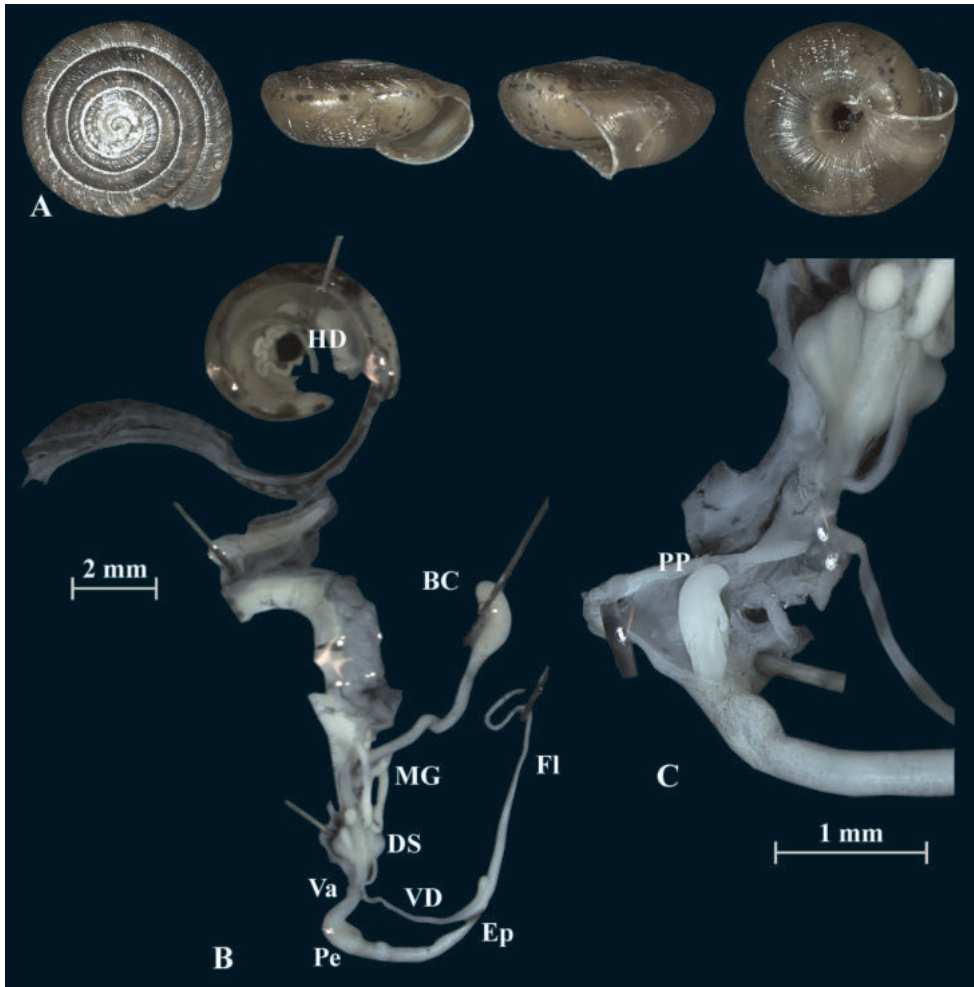


Figure 6. *Trochulus biconicus* (NMBE 567138) collected from Brisen I **A** shell, sw = 5.61 mm, sh = 2.34 mm **B** situs **C** penis (Pe) with penial papilla (PP). Shell $\times 5$.

Etymology. The name is derived from the Roman province of Raetia, which comprised within its larger expansion, the area of what is now known as eastern and central Switzerland. It also refers to the generic name, *Noricella*, which is another recently detected spin-off from *Trochulus* and whose name derives in part from the eastern border province of Raetia (Noricum – now Austria and Slovenia).

Discussion

Neiber et al. (2017) clarified the phylogenetic positions of some species within the Trochulini by establishing the new genus *Noricella* Neiber, Razkin & Hausdorf, 2017. In their study it was proven that *N. oreinos* and *N. scheerpeltzi* differed from the closest

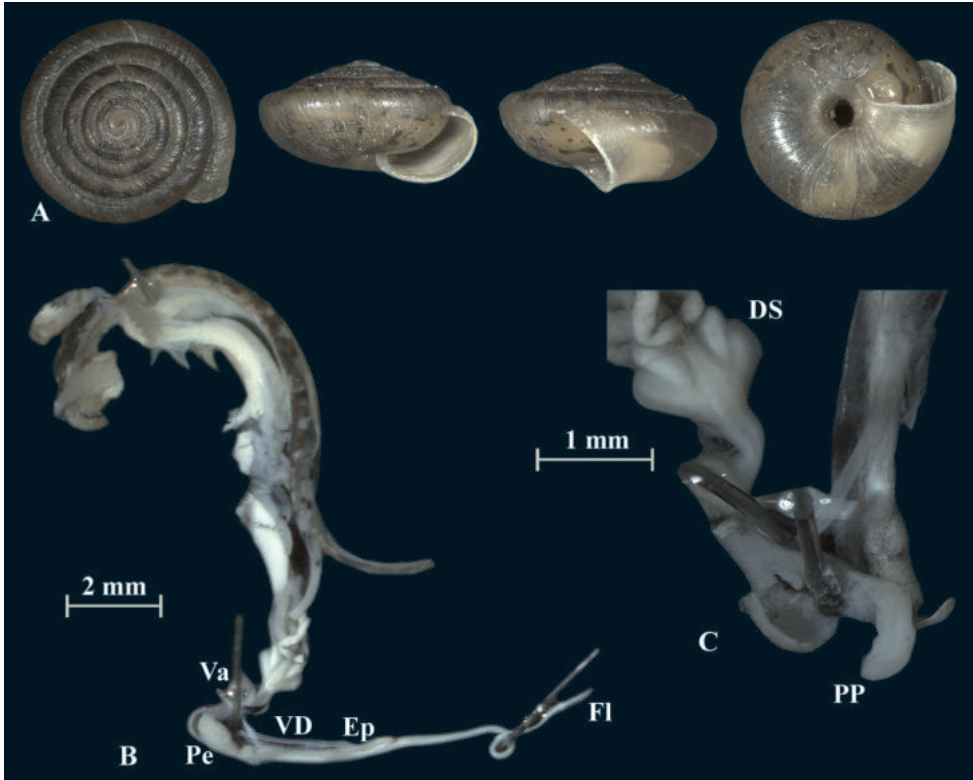


Figure 7. *Trochulus biconicus* (NMBE 567163) collected from Gitschen II **A** shell, sw = 5.67 mm, sh = 2.87 mm **B** situs **C** penis (Pe) with penial papilla (PP). Shell $\times 5$.

related genus *Edentiella* Poliński, 1929 in some apomorphic nucleotide substitutions and by morphological characters. *Edentiella* contains at least one longitudinal septum separating an additional lacuna in the penial papilla which is lacking in *N. oreinos*, in most *Trochulus* species, and in *Petasina* (Neiber et al. 2017). These authors also included some representatives of *Trochulus* but did not have specimens of *R. biconica* available. Turner et al. (1998) had already considered *R. biconica* to be only distantly related to *Trochulus* s. str. because of 1) the lack of periostracal hair even in juveniles, 2) a very long flagellum, and 3) only four instead of six or eight mucous glands. Hence, Turner (1991) suggested to move *R. biconica* into a subgenus of *Trochulus*. The questionable position of *biconicus* in *Trochulus* was recently re-addressed by Proćków et al. (2021). In our analysis, the calculated *p*-distance of *R. biconica* and the investigated *Trochulus* specimens comprises the highest values. The *p*-distance of *R. biconica* and *Noricella* species is lower than for *Trochulus*, which means that *Raeticella* is genetically closer, based on COI, to *Noricella* than to *Trochulus*. Even *Ichmusotricha*, which belongs to the tribe of Ganulini is genetically more similar to *Raeticella* than *Trochulus* is to *Raeticella*.

The shell morphology of *R. biconica* differs from all known *Trochulus* species by having a flat shell with a low spire. The last whorl is bluntly keeled. Adults are always hairless (Proćków 2009). In this regard, it is most like the shells of the two *Noricella*

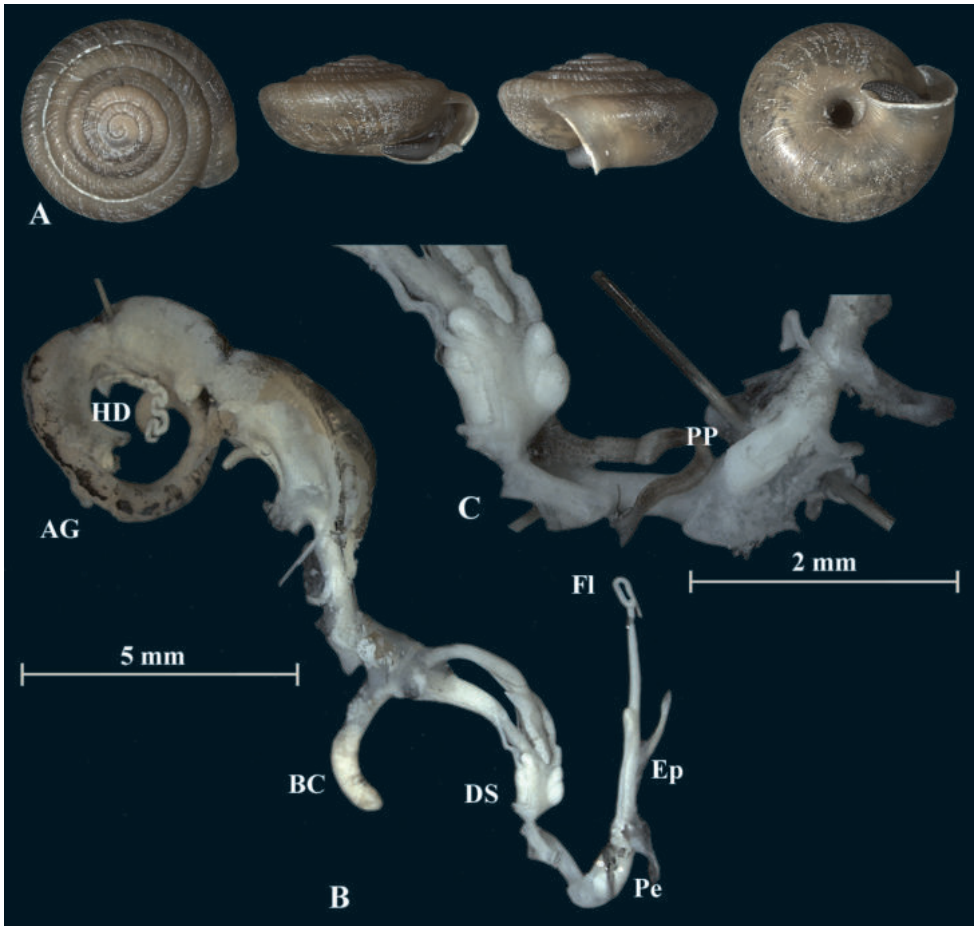


Figure 8. *Trochulus biconicus* (NMBE 567166) collected from Bannalp Schonegg **A** shell, sw = 5.75 mm, sh = 2.76 mm **B** situs **C** penis (Pe) with penial papilla (PP). Shell $\times 5$.

species (Duda et al. 2011, 2014), but the anatomy of the genital organs of these species is different. Both *Noricella* species have four pairs of mucous glands, compared to two pairs in *R. biconica*. *Noricella oreinos* possesses an additional fold and bulge in the penial papilla, which seems to be unique to this species (Duda et al. 2014). The section of the penial papilla in *R. biconica* shows similar internal features as in *T. caelatus* (Proćków 2009), *T. striolatus* (Proćków 2009; Duda et al. 2014; Proćków et al. 2021), and *T. suberectus* (Proćków 2009). *Raeticella biconica* does not possess periostracal hairs, neither as a juvenile nor as an adult. This, however, is considered a typical feature for *Trochulus* species (Proćków 2009).

Hewitt (2004) observed that many taxa in temperate refugial regions in Europe and North America show relatively deep DNA divergence, indicating their presence over several ice ages and suggesting a mode of speciation by repeated allopatry. On the one hand, this possibly explains the deep split between *Raeticella* and *Trochulus* and shifts

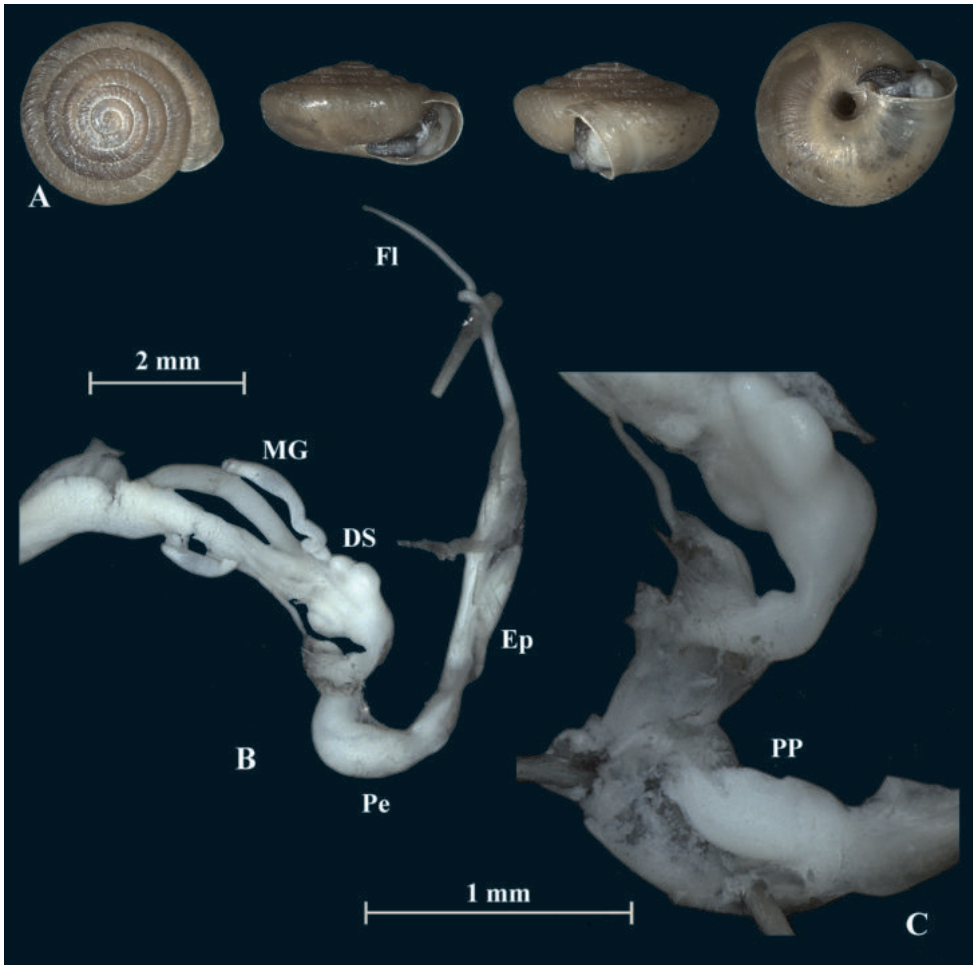


Figure 9. *Trochulus biconicus* (NMBE 567169) collected from Chaiserstuel **A** shell, sw = 5.30 mm, sh = 2.46 mm **B** situs **C** penis (Pe) with penial papilla (PP). Shell $\times 5$.

the splitting event of these groups to the Pliocene. On the other hand, we observed a low genetic diversity within our analysed populations. So, this species probably underwent a bottleneck event during the Pleistocene and the Last Glacial Maximum (LGM). Some isolated populations obviously survived this icy period. The LGM lasted about 30–19 ka in the Alps. During that period, this area was covered by massive ice sheets, and the glaciers reached out to the forelands of both, the northern and southern side of the main alpine chains. However, mountain tops above more than 2000 m were not covered by ice during the LGM. The recession of the glaciers from their maximum extent started around 24 ka (see Ivy-Ochs 2015). We hypothesize that the original distribution area of *R. biconica* was much larger, but only a few individuals survived on neighbouring nunataks (glacial islands) during the LGM. A similar scenario is assumed

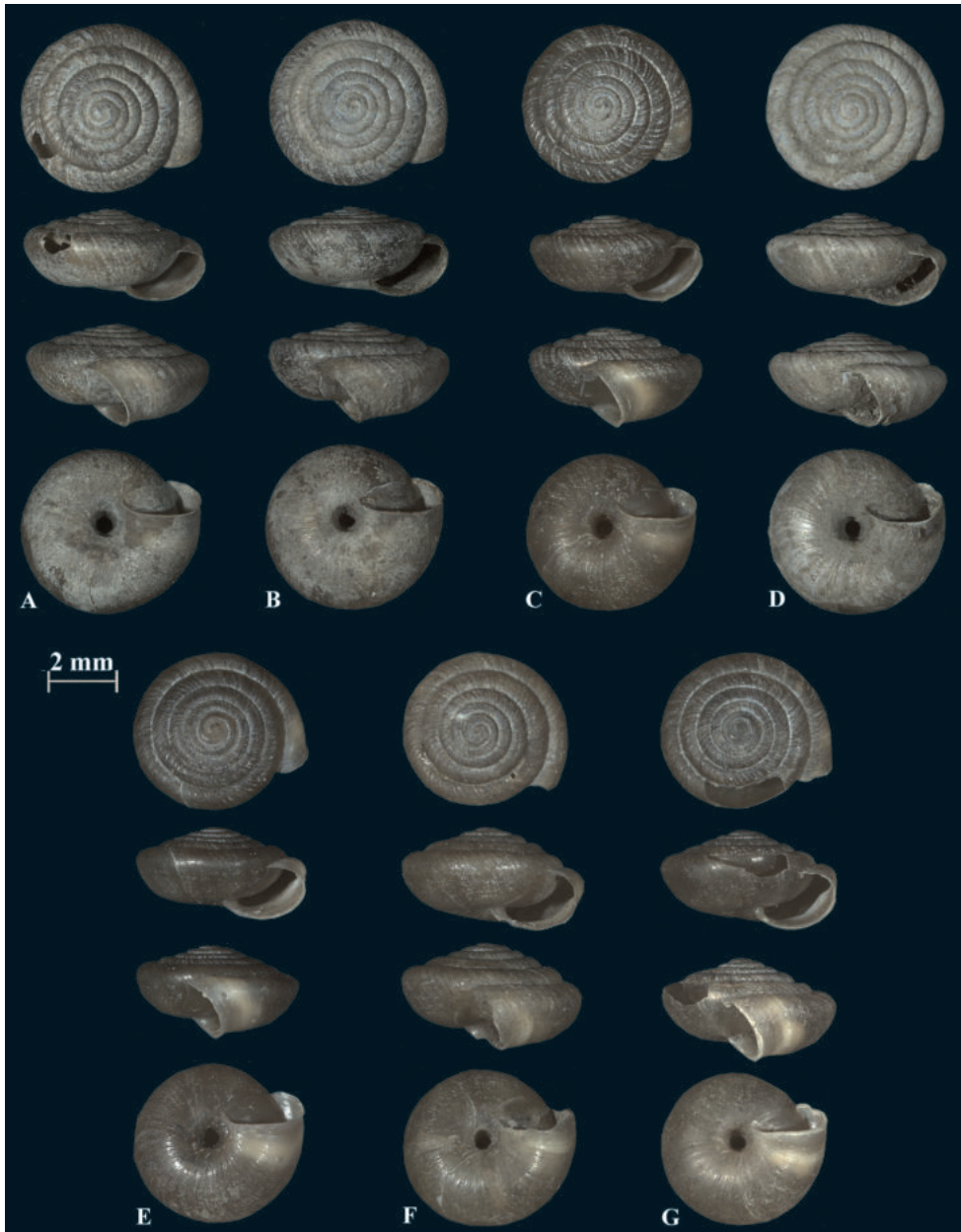


Figure 10. Shells of *Trochulus biconicus* from Bannalp Schonegg (**A–D**) and from Chaiserstuel (**E–G**).

for the evolution of the two *Noricella* species (Duda et al. 2011, 2014; Kruckenhauser et al. 2014). Gittenberger et al. (2004) also hypothesized the survival of *Arianta arbustorum alpicola* (A. Férussac, 1821) on nunataks. A similarly fragmented distribution pattern can be observed in the eastern alpine mollusc species *Cylindrus obtusus* (Draparnaud,

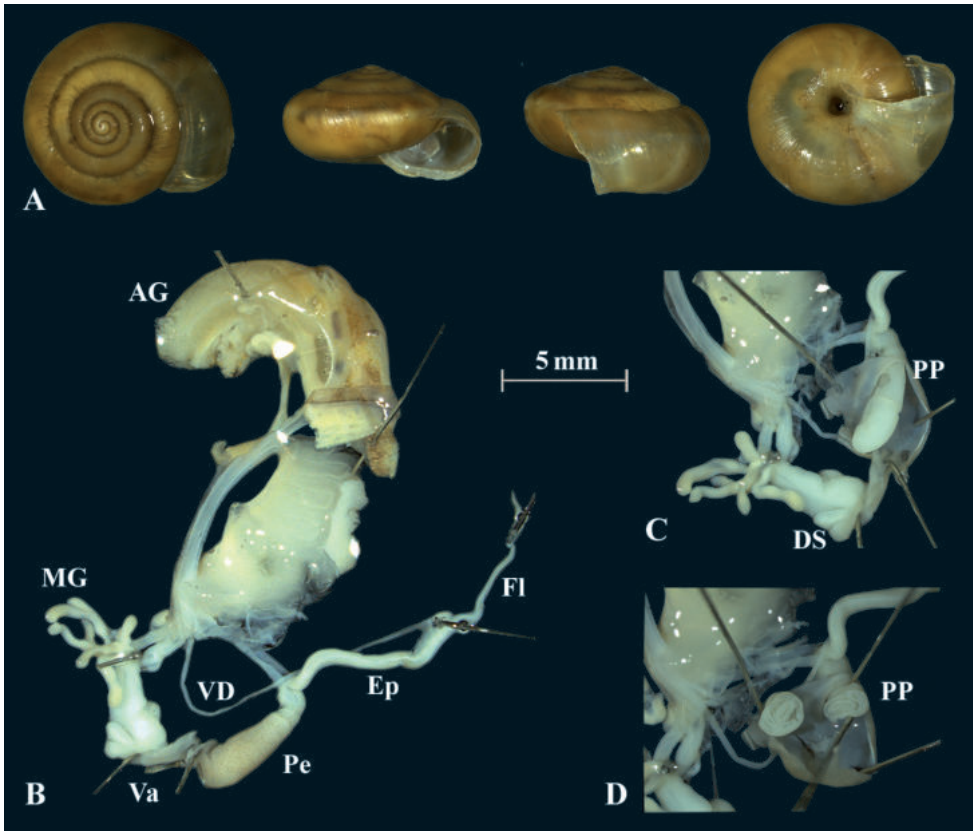


Figure 11. *Trochulus clandestinus* (NMBE 571318) collected from Bümpliz, Bern, Switzerland **A** shell, sw = 9.64 mm, sh = 5.57 mm **B** situs **C** penis (Pe) with penial papilla (PP) **D** cross section of the penial papilla. Shell $\times 3$.

1805) (Schileyko 2012: 95, fig. 2). Schileyko argued that the missing fossil record for this species proves that it was formed at the end of the Würm glaciation approximately 10–12 ka ago. As a species adapted to cold environmental conditions, this species was then assumed to be forced to follow the retreating snow and ice fields, which subsequently lead to habitat fragmentation. This assumption requires an ancestor from interglacials (which is also not found in the fossil record), and has to explain the rapid transformation of an Ariantine species from a globular or even depressed shell to a turritiform shell. This is most unlikely. Based on COI sequences, Cadahía et al. (2014) estimated 1.5–12 mya for the split between *Arianta* and *Cylindrus*. So, we assume that *Raeticella* gen. nov., like the monotypic genus *Cylindrus*, evolved much earlier and survived the Pleistocene by chance on nunatak mountain tops.

The current distribution pattern does not necessarily and strictly reflect the “survivor” populations. ARNAL (2018) found a limited gene flow between the “isolated” populations of *R. biconica*. This shows that dispersal is not completely impossible, but,



Figure 12. Typical habitat of *Raeticella biconica*. This photograph was taken on 25.05.2009 on Chaiserstuel (46.8762°N, 8.4671°E, 2263 m) by Markus Baggenstos.

due to the high-altitude adaptation of the species, it is rather limited to other, hitherto unpopulated high alpine areas. Possible vectors may be large pasturing animals like sheep and goats, but also ibex, chamois, or birds.

In alpine environments, microendemic species with a relict distribution pattern may occur, which were much more widespread in earlier times. They are now restricted to a very small area due to changes in environmental condition (Turner 1991; Cook 2008; Veron et al. 2019). The distribution area of *R. biconica* is currently known to encompass 150 isolated sites on both sides of the Engelberger valley, all situated between 1890 and 2575 m of altitude (Baggenstos 2010).

The habitat of *R. biconica* is very special, and only few other snail species are known to survive in this harsh environment (Eder 1917; Baggenstos 2010). Apart from the occurrence of limestone scree, the snails very much depend on small-scale relief. Slope edges or hilltops, ridges and summits as well as rocky heads and rocky steps are more likely to be colonised by the snail than slope hollows and slope foothills. The highest density of *R. biconica* is reached in areas with more than 50% of rocky scree (Baggenstos 2010). All these sites are covered with snow for a relatively short time in winter. With its flat shell, *R. biconica* is perfectly adapted to live under or between stones (Figs 12, 13). Flatness was interpreted as an adaptation to the cold



Figure 13. Close-up of *Raeticella biconica* crawling on the underside of a stone. This photograph was taken on 09.09.2009 on Chaiserstuel (46.8762°N, 8.4671°E, 2263 m) by Markus Baggenstos.

climate at the top of the mountains and may protect the animals from predators (Baur 1987). When it gets too hot, the snails retreat into the ground. The individuals are mainly active during night (Baggenstos 2010). Almost all known *R. biconica* habitats are blue grass meadows. These are alpine grasslands rich in flowers with a great diversity and a remarkably high proportion of Leguminosae. The prominent structural elements are *Sesleria caerulea* and *Carex sempervirens*. The soil cover is relatively thin, interspersed with gravel and stones and dries out quickly (Delarze et al. 2008). Wigger (2007) observed that *R. biconica* mainly feeds on decaying leaves of blue grass (*Sesleria caerulea*). The landscape of these meadows is strongly influenced by extensive pasturing and hiking tourism. Pasture animals like sheep, goats, and cows can modify the position of large stones and thus create new micro habitats for the snails. However, stronger interventions, such as the removal of stones or a climate-related transfer of the rubble-rich sites into closed meadows or woodland formations would cause the snail to disappear (Turner 1991).

This stenoeccious species is prone to extinction because of climate change. Over the last 100 years temperatures have increased by about 0.12–0.20 °C per decade in the Swiss Alps and the snow seasons have shortened (Kohler et al. 2014). *Raeticella biconica* already reached the summits of the mountains in their vicinity, and there is no more alternative for avoiding unsuitable climate conditions. Considering that global warming is ongoing, *R. biconica* may well become extinct in just a few years.

Conclusion

Long known morphological characteristics in conjunction with our genetic analyses show that *R. biconica* should be assigned to a new genus. Morphologically, the investigated individuals of *R. biconica* strongly resemble *N. oreinos* (Duda et al. 2011). But the genetic analyses of several different species from all genera within Trochulini reveal that *R. biconica* does not belong to any currently known genus. Therefore, a new monotypic genus within Trochulini is introduced.

Acknowledgements

We are indebted to Małgorzata Proćków for providing tissue samples of *E. edentula* and some *Trochulus* specimens, to Ted von Proschwitz for providing *T. hispidus* samples from the Swedish type locality, to Adrienne Jochum for the linguistic revision, to Tom Burri for paleoecological insights, to the Swiss Federal Office of Environment (FOEN) for financial support (contract no. 110010344 / 8T30/00.5147.PZ/0006), and to the cantonal authorities of Nidwalden (Felix Omlin), Obwalden (Andreas Bacher), and Uri (Georges Eich) for providing sampling permits.

References

- Altekar G, Dwarkadas S, Huelsenbeck JP, Ronquist F (2004) Parallel Metropolis-coupled Markov chain Monte Carlo for Bayesian phylogenetic inference. *Bioinformatics* (Oxford, England) 20(3): 407–415. <https://doi.org/10.1093/bioinformatics/btg427>
- ARNAL Büro für Natur und Landschaft AG (2018) Projekt Naturschutzgenetik – Schlussbericht: Methodik und Resultate (Insbeso. «Verbund»). Report, Herisau, 45 pp.
- Baggenstos M (2010) Verbreitung und Biologie der Nidwaldner Haarschnecke (*Trochulus biconicus*). Report, Stans, 45 pp.
- Bamberger S, Duda M, Tribsch A, Haring E, Sattmann H, Macek O, Affenzeller M, Kruckenhauser L (2020) Genome-wide nuclear data confirm two species in the Alpine endemic land snail *Noricella oreinos* s.l. (Gastropoda, Hygromiidae). *Journal of Zoological Systematics and Evolutionary Research* 58(4): 982–1004. <https://doi.org/10.1111/jzs.12362>
- Baur B (1987) Richness of land snail species under isolated stones in a karst area on Öland, Sweden. *Basteria* 51: 129–133.
- Cadahía L, Harl J, Duda M, Sattmann H, Kruckenhauser L, Fehér Z, Zopp L, Haring E (2014) New data on the phylogeny of Ariantinae (Pulmonata, Helicidae) and the systematic position of *Cylindrus obtusus* based on nuclear and mitochondrial DNA marker sequences. *Journal of Zoological Systematics and Evolutionary Research* 52(2): 163–169. <https://doi.org/10.1111/jzs.12044>
- Chemnitz JH (1786) Neues systematisches Conchylien-Cabinet. Neunten Bandes zwote Abtheilung, enthaltend die ausführliche Beschreibung von den Land- und Flußschnecken,

- oder von solchen Conchylien welche nicht im Meer, sondern auf der Erde und in süßen Wassern zu leben pflegen. Mit zwanzig nach der Natur gemalten und durch lebendige Farben erleuchteten. Raspe, Nürnberg, [xxvi +] 194 pp. [pls 117–136] <https://doi.org/10.5962/bhl.title.125416>
- Chiba S (1999) Accelerated evolution of land snails *Mandarina* in the oceanic Bonin Islands: Evidence from mitochondrial DNA sequences. *Evolution; International Journal of Organic Evolution* 53(2): 460–471. <https://doi.org/10.1111/j.1558-5646.1999.tb03781.x>
- Cook LM (2008) Species richness in Madeiran land snails, and its causes. *Journal of Biogeography* 35(4): 647–653. <https://doi.org/10.1111/j.1365-2699.2007.01801.x>
- Delarze R, Gonseth Y, Galland P (2008) Lebensräume der Schweiz: Ökologie, Gefährdung, Kennarten. Ott Verlag, Thun, 424 pp.
- Dépraz A, Hausser J, Pfenninger M (2009) A species delimitation approach in the *Trochulus sericeus/hispidus* complex reveals two cryptic species within a sharp contact zone. *BMC Evolutionary Biology* 9(1): e171. <https://doi.org/10.1186/1471-2148-9-171>
- Duda M, Sattmann H, Haring E, Bartel D, Winkler H, Harl J, Kruckenhauser L (2011) Genetic differentiation and shell morphology of *Trochulus oreinos* (Wagner, 1915) and *T. hispidus* (Linnaeus, 1758) (Pulmonata: Hygromiidae) in the northeastern Alps. *Journal of Molluscan Studies* 77(1): 30–40. <https://doi.org/10.1093/mollus/eyq037>
- Duda M, Kruckenhauser L, Sattmann H, Harl J, Jaksch K, Haring E (2014) Differentiation in the *Trochulus hispidus* complex and related taxa (Pulmonata: Hygromiidae): morphology, ecology and their relation to phylogeography. *Journal of Molluscan Studies* 80(4): 371–387. <https://doi.org/10.1093/mollus/eyu023>
- Eder L (1917) Eine neue Schweizer Helicide. *Revue Suisse de Zoologie* 25(15): 442–452.
- Folmer O, Black M, Hoe W, Lutz R, Vrijenhoek R (1994) DNA primers for amplification of mitochondrial cytochrome c oxidase subunit I from diverse metazoan invertebrates. *Molecular Marine Biology and Biotechnology* 3(5): 294–299.
- Gittenberger E, Piel WH, Groenbergs DSJ (2004) The Pleistocene glaciations and the evolutionary history of the polytypic snail species *Arianta arbustorum* (Gastropoda, Pulmonata, Helicidae). *Molecular Phylogenetics and Evolution* 30(1): 64–73. [https://doi.org/10.1016/S1055-7903\(03\)00182-9](https://doi.org/10.1016/S1055-7903(03)00182-9)
- Hartmann JDW (1840–1844) Erd- und Süßwasser-Gasteropoden der Schweiz. Mit Zugabe einiger merkwürdigen exotischen Arten. Scheitlin und Zollikofer, St. Gallen, [i–xx,] 36 pp. [pls 1, 2 [30-06-1840]; 37–116, pls 13–36 [1841]; 117–156, pls 37–60 [1842]; 157–204, pls 61–72 [1843]; 205–227, pls 73–84 [1844]]
- Hewitt GM (2004) Genetic consequences of climatic oscillations in the Quaternary. *Philosophical Transactions of the Royal Society of London. Series B, Biological Sciences* 359(1442): 183–195. <https://doi.org/10.1098/rstb.2003.1388>
- Huelsenbeck JP, Ronquist F (2001) MRBAYES: Bayesian inference of phylogeny. *Bioinformatics (Oxford, England)* 17(8): 754–755. <https://doi.org/10.1093/bioinformatics/17.8.754>
- Ivy-Ochs S (2015) Glacier variations in the European Alps at the end of the last glaciation. *Cuadernos de Investigación Geográfica* 42(2): 295–315. <https://doi.org/10.18172/cig.2750>
- Kerney MP, Cameron RAD, Jungbluth JH (1983) Die Landschnecken Nord- und Mitteleuropas. Parey-Verlag, Hamburg/Berlin, 384 pp.

- Kohler T, Wehrli A, Jurek M (2014) Mountains and climate change: a global concern. Sustainable Mountain Development Series. Centre for Development and Environment (CDE), Swiss Agency for Development and Cooperation (SDC) and Geographica Bernensia, Bern, 136 pp. <https://doi.org/10.1659/mrd-journal-d-09-00086.1>
- Kruckenhauser L, Duda M, Bartel D, Sattmann H, Harl J, Kirchner S, Haring E (2014) Paraphyly and budding speciation in the hairy snail (Pulmonata, Hygromiidae). *Zoologica Scripta* 43(3): 273–288. <https://doi.org/10.1111/zsc.12046>
- Kumar S, Steche G, Li M, Knyaz C, Tamura K (2018) MEGA X: Molecular Evolutionary Genetics Analysis across computing platforms. *Molecular Biology and Evolution* 35(6): 1547–1549. <https://doi.org/10.1093/molbev/msy096>
- Neiber MT, Razkin O, Hausdorf B (2017) Molecular phylogeny and biogeography of the land snail family Hygromiidae (Gastropoda: Helicoidea). *Molecular Phylogenetics and Evolution* 111: 169–184. <https://doi.org/10.1016/j.ympev.2017.04.002>
- Pfenninger M, Hrabáková M, Steinke D, Dépraz A (2005) Why do snails have hairs? A Bayesian inference of character evolution. *BMC Evolutionary Biology* 5(1): e59. <https://doi.org/10.1186/1471-2148-5-59>
- Pročków M (2009) The genus *Trochulus* Chemnitz, 1786 (Gastropoda: Pulmonata: Hygromiidae) – a taxonomic revision. *Folia Malacologica* 17(3): 101–176. <https://doi.org/10.2478/v10125-009-0013-0>
- Pročków M, Kuznik-Kowalska E, Pienkowska JR, Zeromska A, Mackiewicz P (2021) Speciation in sympatric species of land snails from the genus *Trochulus* (Gastropoda, Hygromiidae). *Zoologica Scripta* 50(1): 16–42. <https://doi.org/10.1111/zsc.12458>
- Ronquist F, Huelsenbeck JP (2003) MRBAYES 3: Bayesian phylogenetic inference under mixed models. *Bioinformatics (Oxford, England)* 19(12): 1572–1574. <https://doi.org/10.1093/bioinformatics/btg180>
- Shileyko AA (2012) On the origin of *Cochlopupa* (= *Cylindrus* auct.) *obtus*a (Gastropoda, Pulmonata, Helicidae). *Ruthenica: Rossiiskii Malakologicheskii Zhurnal = Russian Malacological Journal* 22: 93–100.
- Stamatakis A (2014) RAxML Version 8: A tool for Phylogenetic Analysis and Post-Analysis of Large Phylogenies. *Bioinformatics* 30(9): 1312–1313. <https://doi.org/10.1093/bioinformatics/btu033>
- Turner H (1991) Die Nidwaldner Haarschnecke gibt es sonst nirgends auf der Welt: ein kleines zoologisches Geheimnis lebt auf der Bannalp. *Nidwaldner Volksblatt* 240(17 Oktober): 13.
- Turner H, Kuiper JGJ, Thew N, Bernasconi R, Rüetschi J, Wüthrich M, Gosteli M (1998) Atlas der Mollusken der Schweiz und Lichtensteins. *Fauna Helvetica* 2. Center Suisse de cartographie de la faune, Schweizerische Entomologische Gesellschaft, Eidg. Forschungsanstalt für Wald, Schnee und Landschaft, Neuchâtel, 527 pp.
- Veron S, Haevermans T, Govaerts R, Mouchet M, Pellens R (2019) Distribution and relative age of endemism across islands worldwide. *Scientific Reports* 9(1): e11693. <https://doi.org/10.1038/s41598-019-47951-6>

- Wade CM, Mordan PB (2000) Evolution within the gastropod molluscs; using the ribosomal RNA gene-cluster as an indicator of phylogenetic relationships. *The Journal of Molluscan Studies* 66(4): 565–570. <https://doi.org/10.1093/mollus/66.4.565>
- Wigger F (2007) Der mikroklimatische und zeitabhängige Aktivitätsrhythmus von *Trochulus biconicus*. Eine Feldstudie im Rahmen der Projektarbeit in Biogeographie der Universität Basel in Zusammenarbeit mit der Oekologischen Beratung Markus Baggenstos. Basel, unpublished report Basel, 12 pp.

Supplementary material I

Calculated p-distances of the COI of the investigated specimens.

Authors: Jeannette Kneubühler, Markus Baggenstos, Eike Neubert

Data type: excel file

Explanation note: Calculated p-distances of the COI of the investigated specimens.

Copyright notice: This dataset is made available under the Open Database License (<http://opendatacommons.org/licenses/odbl/1.0/>). The Open Database License (ODbL) is a license agreement intended to allow users to freely share, modify, and use this Dataset while maintaining this same freedom for others, provided that the original source and author(s) are credited.

Link: <https://doi.org/10.3897/zookeys.1104.82866.suppl1>

How many species? Limits of morphological species concepts in the genus *Trochulus* (Gastropoda, Eupulmonata, Hygromiidae)

Jeannette Kneubühler^{1,2}, Małgorzata Proćków³, Eva A. Bischof¹, Marco T. Neiber⁴, Simon Bober⁴, Olivier Gargominy⁵, Ted von Proschwitz^{6,7}, Eike Neubert^{1,2}

¹ Natural History Museum Bern, Bernastrasse 15, 3005 Bern, Switzerland

² Institute of Ecology and Evolution, University of Bern, Baltzerstrasse 6, 3012 Bern, Switzerland

³ Museum of Natural History, University of Wrocław, Sienkiewicza 21, 50–335 Wrocław, Poland

⁴ Center for Natural History (CeNak), Universität Hamburg, Martin-Luther-King-Platz 3, Hamburg, 20146, Germany

⁵ Muséum national d'Histoire naturelle, 57 Rue Cuvier, 75005 Paris, France

⁶ Göteborg Natural History Museum, PO Box 7283, 40235 Göteborg, Sweden

⁷ Gothenburg Global Biodiversity Centre, University of Gothenburg, Box 46, 40530 Göteborg, Sweden

Corresponding authors: Jeannette Kneubühler, jeannette.kneubuehler@nmbe.ch; Eike Neubert, eike.neubert@nmbe.ch

Abstract

In this study, the genus *Trochulus* is revised including specimens from the whole distribution area of the genus, and, if possible, from type localities. Species are redefined based on clades as result of the genetic research. Species boundaries are derived from the genetically recorded clades. This structure is used as a backbone to explore, whether these clades can be described by apomorphic traits in shell morphology and in characters of the genital organs. A total of 551 *Trochulus* specimens covering almost the complete distribution range of the genus are sequenced by using two mitochondrial (COI and 16S) and one nuclear marker (5.8S rRNA+ITS2). GenBank data and outgroup specimens are used to complement the data set, which sums up to 710 specimens treated. The analysis is performed by using Bayesian Inference, Maximum Likelihood and IQ-TREE calculation. These methods and the current taxon sampling yield a stable framework of 21 *Trochulus* clades with differing relationships depending on the method used. A landmark-based geometric morphometric

study is conducted to reveal shell morphological differences. Some lineages could be well separated morphologically, but some cryptic (?) species could not be identified even with shape-based morphometric analyses. Five tentatively new species have been identified. These species are cryptic and cannot be distinguished based on shell morphology only.

For the following taxa, neotypes are selected: *Trochulus circinnatus* (S. Studer, 1820), *Trochulus sericeus* (O. F. Müller, 1774), *Trochulus plebeius* (Draparnaud, 1805).

Lectotypes here designated: *Trochulus montanus* (S. Studer, 1820), *Trochulus clandestinus* (Hartmann, 1821), *Trochulus plebicola* (Locard, 1888), *Trochulus pascali* (Mabille, 1867).

Keywords

Cryptic species, endemism, geometric morphometrics, integrative taxonomy, phylogeny, RAD sequencing

Introduction

The genus *Trochulus* Chemnitz, 1786 and its species has been target of many studies in the past. One of the major research impediments in this genus was the historical burden of opinions, revisions, and descriptions. In polymorphic groups like this, authors tended to oversplit and described too many nominal taxa. The increasing diversification of interpretations about the attribution of names to a biological species finally hampered the development of robust species concepts.

In many cases, the whereabouts of type specimens was (and is) unclear, descriptions were imprecise, figures insignificant, or the species was recorded from vast areas without a designation of type locality by the original author. Thus, the application of names changed several times throughout the centuries, making it impossible to follow a stringent line. Finally, the “clash of cultures” with the ignorance on both sides between the German school and the French Nouvelle École led to an increase of names, which only can be aligned by cumbersome and pertinacious labour.

Usually, these species descriptions were based on shell morphological traits. If the texts of the descriptions were very simple and short at the beginning, they became too complicated with authors like Bourguignat or Locard, and essential features were emphasised far in excess. Draparnaud knew four species of *Trochulus* (*hispidus*, *sericeus*, *plebeius*, and *villosus*) and it was to the credit of Samuel Studer who soon realised that the Swiss species of the genus could not be covered with this concept. This was the starting point for the subsequent authors of the 19th century, who recognised several new taxa within a short time, re-interpreted the species of previous authors without deeper knowledge, and then added some fossil taxa of different ages to this melange. This is not the place for a

comprehensive historical treatise on the course of the research history on this subject, but it should be noted that we have compiled > 180 names so far, with 10 of them based on fossils, which we consider describing a species of *Trochulus*.

It was Forcart (1966) who, based on Kloeti-Hauser (1920), ventured a new beginning not only for the Swiss *Trochulus* species. He rejected the abusive authorship of Draparnaud for *Helix sericeus*, attributed it to O. F. Müller and presented the species as a mere shell variation of *H. hispidus*; recognized *H. striolatus* C. Pfeiffer, 1828 and *H. concinna* Jeffreys 1830 as distinct species, included *H. plebeia* Draparnaud, 1805 as a western European species, and identified *H. montana* S. Studer, 1820 and *H. caelata* S. Studer, 1820 as distinct endemic Swiss species; and finally affiliated the fossil *H. suberecta* Clessin, 1878 with recent snails from the Engadine (Switzerland) based on an anatomical study of a misidentified *H. sericea* (Wagner, 1915: pl. 19, Fig. 165). Another progress was the inclusion of morphological character states of the genital organs. Hence, Forcart's work represented the starting point for all following "modern" workers on the group, who tried to apply Forcart's concept to the respective area they treated. Some corrections were made, such as the recognition of *H. sericea* as a separate species (Klemm 1974: 393), the summary of the main European taxa in Kerney et al. (1983), and the discussion of French taxa by Falkner et al. (2002). Other work led to the exclusion of some taxa from the genus, such as *Edentiella* and *Petasina*, as independent genera (see Nordsieck 1993). A detailed summary and appreciation of many other works can be found in Proćków (2009). However, all morphology-based approaches failed to address the diversity of *Trochulus*, and leaves for example cryptic species unrevealed. A species is called cryptic, when two or more distinct species are classified as one species based on morphological similarity (Bickford et al. 2007; Pfenninger & Schwenk 2007).

More recent studies combined molecular methods with the investigation of the morphological variation of shells and genital organs, which serves as the backbone for taxonomic decisions (Jörger & Schrödl 2013). Dépraz et al. (2009) studied some Swiss *Trochulus* specimens from a very small area in Canton Vaud finding large morphological overlap between the two lineages recorded. In their work on the genus focusing on Austria, Kruckenhauser et al. (2014) assume a widespread species in Europe, viz. *T. hispidus* (Linnaeus, 1758), which splits into nine clades. Duda et al. (2014) tried to define this and several other species morphologically by an intensive study of the shells and the morphology of the genital organs. In this context, the authors regarded *T. hispidus* as a complex of (cryptic?) species in which species delimitation according to the biological species concept of Mayr (1942) was impossible. The authors reported localities where several clades occur together. Kruckenhauser et al. (2014) showed an unresolved paraphyly, which is explained either by

budding speciation and incomplete lineage sorting, introgression into the mtDNA or the presence of cryptic species. Proćków et al. (2017a) extended the taxon sampling to some southern German and French sites. Here, too, the paraphyletic results complicated the interpretation of the results. In two follow-up papers (Proćków et al. 2017c, 2021), this phenomenon was explained by gene flow between taxa or ancestral polymorphism.

Kruckenhauser et al. (2014) point out that the resolution of the species complex is prerequisite for a stable taxonomy. We fully agree with this statement. After a careful analysis of the aforementioned papers, we seek to resolve the problem by eliminating two major problems. One of them is the size of the taxon sampling, the other refers to the species concept used. All studies published so far widely ignore the enormous radiation of the genus in Switzerland and the neighbouring Franche-Comté in France. Furthermore, we did not base our analysis on *a priori* identified specimens but took a different approach, which is fundamentally different if compared to the aforementioned works, and paraphyletic situations cannot occur. Species are redefined based on clades as result of the genetic research. Species boundaries are derived from the genetically recorded clades.

After an extensive analysis of the literature, we have compiled a list of nominal taxa in question in Europe. The taxon sampling contains, as far as possible, animals from the type localities or nearby, so that a rather reliable relation between a clade and a name could be established. This name has then been used for those animals which co-occur in one lineage.

This study includes 551 *Trochulus* specimens using two mitochondrial (COI and 16S) and one nuclear marker (5.8S rRNA+ITS2) for the genetic analysis. To cover the entire distribution range of species affiliated to this genus, additional sequences from databases of 131 specimens were added. Moreover, the variation of shell morphology in *Trochulus* is analysed using landmark and semi landmark-based geometric morphometric methods (GMM) instead of traditional, linear measurements. The advantage of using landmarks and semi landmarks is, that shape variations of morphologies are covered. Something, which is sometimes overseen or not recognized by linear measurements (Neige 1999). Additionally, GMM allow the separate analysis of size and shape (e.g., Zelditch et al. 2012; Polly & Motz 2016) without introducing artefactual patterns of covariance (Gerber 2017). To morphologically define the lineages found, a 2D landmark-based geometric morphometric analysis was carried out on photos of 195 adult *Trochulus* and *Raeticella* Kneubühler, Baggenstos & Neubert, 2022 specimens. For this, we used the frontal and ventral photo view and combined these two data sets in the analyses. Principal Component Analysis (PCA) and Canonical Variate Analysis (CVA) were run to visualize the multivariate data.

To date, there is no coherent concept to resolve the currently unsatisfactory situation. In our study we resolve some of the most urgent questions addressing the taxonomy and the nomenclature of species included in *Trochulus*.

Material and methods

Abbreviations

MNHN Muséum National d'Histoire Naturelle, Paris, France

NMBE Naturhistorisches Museum der Burgergemeinde Bern, Bern, Switzerland

NMSG Naturmuseum St. Gallen, St. Gallen, Switzerland

SMNS Staatliches Museum für Naturkunde Stuttgart, Stuttgart, Germany

SMF Senckenberg Museum Frankfurt, Frankfurt am Main, Germany

Specimens investigated in the molecular study

We examined 551 *Trochulus* specimens. Additionally, 21 *Raeticella biconica* (Eder, 1917) and seven *Edentiella edentula* (Draparnaud, 1805) specimens were included in the genetic analysis (Supplementary material I). From each population, 1–3 specimens were used. The specimens are housed in the collection of the NMBE, MNHN, SMNS and NMSG or have been freshly collected in recent years, mainly by MP and JK. Our data set was supplemented with specimens from the databases GenBank (<https://www.ncbi.nlm.nih.gov/genbank/>) and BOLD (<https://www.boldsystems.org/>) in order to cover the complete distribution range of *Trochulus*. In total, we included 131 specimens from the publications of Kruckenhauser et al. (2014), Duda et al. (2017), and Proćków et al. (2021), of which the specimens of *Noricella oreinos* (A.J. Wagner, 1915) and *N. scheerpeltzi* (Mikula, 1957) served as outgroup (Bamberger et al. 2020). This sums up to a total of 710 specimens for the genetic analysis. The distribution map of the investigated *Trochulus* and *Raeticella* specimens is shown in Figure 1.

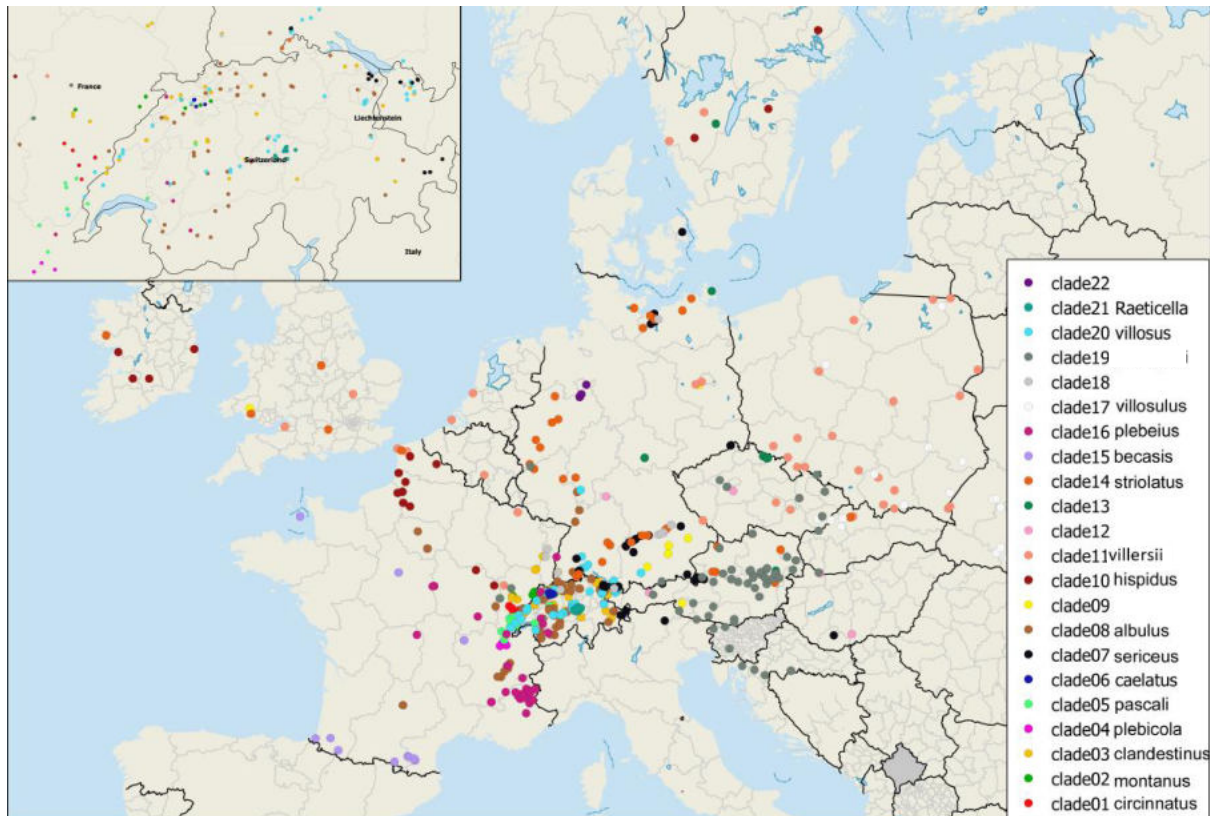


Figure 1: Sampling locations of *Trochulus* and *Raeticella* specimens grouped into clades and designated by coloured circles.

DNA Extraction, PCR Amplification and Sequence Determination

Live specimens were preserved in 80% ethanol. Before DNA extraction, every specimen was imaged under sterile conditions from apical, frontal, lateral and ventral view with a Leica DFC425 microscope camera using the image-processing program (IMS Client V15Q4, Imagic, Switzerland). Three to ten sequential, stacked images were taken from top to bottom of each shell with a single, multistacked image being generated via the Leica software. For total DNA extraction of the specimens the Qiagen Blood and Tissue Kit (Qiagen; Hilden, Germany) was used in combination with a QIAcube extraction robot. Circa 0.5 cm³ of tissue was cut and placed in a mix of 180 µl ATL buffer and 20 µl Proteinase K. It was then incubated for ca. 4 hours at 56 °C in a heater (Labnet, Vortemp 56, witec AG, Littau, Switzerland). For subsequent DNA extraction the QIAcube extraction robot with the Protocol 430 (DNeasy Blood Tissue and Rodent tails Standard) was used. In this study, two mitochondrial markers (COI and 16S) and one nuclear marker (5.8S rRNA+ITS2) were investigated. For some animals only COI was amplified and analysed. PCR mixtures consisted of 12.5 µl GoTaq G2 HotStart Green Master Mix (Promega M7423), 4.5 µl ddH₂O, 2 µl forward and reverse primer each, and 4 µl DNA template. In Table 1, the used primer pairs for the PCR are listed. For some specimens, the primers 16Scs1/cs2 were used instead, which generated a longer sequence. Following PCR cycles were used: for COI

2 min at 94 °C, followed by 40 cycles of 1 min at 95 °C, 1 min at 47 °C and 1 min at 72 °C and finally, 5 min at 72 °C; for 16S 3 min at 96 °C, followed by 40 cycles of 30 s at 94 °C, 30 s at 50 °C and 30 s at 72 °C, and finally, 1 min at 72 °C; and for 5.8S rRNA+ITS2 3 min at 94 °C, followed by 40 cycles of 30 s at 94 °C, 30 s at 50 °C and 30 s at 72 °C, and finally, 5 min at 72 °C (SensoQuest Tabcyclet and Techne TC-512, witec AG, Littau, Switzerland). The purification and sequencing of the PCR product was performed by LGC (LGC Genomics Berlin, Germany).

Table 1: Used primer pairs for the PCR.

Gene	Primer	Sequence	Sequence length (bp)	Reference
COI	LCO1490	5'-GGTCAACAAATCATAAAGATATTGG-3'	655	Folmer et al. (1994)
	HCO2198	5'-TAAACTTCAGGGTGACCAAAAAATCA-3'		
16S	16S ar	5'-CGC CTG TTT ATC AAA AAC AT-3'	440	Simon et al. (1994)
	16S br	5'- CCG GTC TGA ACT CTG ATC AT -3'		
	16Scs1	5'-AAACATACCTTTTGCATAATGG-3'	900	Chiba (1999)
	16Scs2	5'-AGAAACTGACCTGGCTTACG-3'		
ITS2	LSU-1	5'-CTAGCTGCGAGAATTAATGTGA-3'	920	Wade & Mordan (2000)
	LSU-3	5'-ACTTTCCTCACGGTACTTG-3'		

Phylogenetic analyses

The software package Geneious v9.1.8 (Biomatters Ltd) was used for sequence processing and editing. Maximum Likelihood analysis (ML) was performed using RAxML v8.2.12 (Stamatakis 2014) through the HPC cluster from the University of Bern (<http://www.id.unibe.ch/hpc>). The rapid bootstrapping setting to compute the best scoring ML tree and 1000 bootstrapping replicates were chosen. The protein-coding gene fragments of COI was defined in three data blocks. The non-coding regions from 16S and 5.8S rRNA+ITS2 were defined as single data blocks each. Partitionfinder-2.1.1 (Lanfear et al. 2016) was applied for searching optimal evolutionary models for the partitions using the corrected Akaike Information Criterion (cAIC). The nucleotide model GTR CAT I was used. Additional Maximum Likelihood trees were calculated with the command line software IQ-TREE v2.1.3 (Nguyen et al. 2015). The model GTR+G+I was used, the ultrafast bootstrap (UFBoot; Hoang et al. 2018) and the SH-aLRT branch test (Guindon et al. 2010) with 1000 replicates were performed. For speeding up the computation, 4 CPU cores were used. One would typically start to rely on the clade if its SH-aLRT \geq 80% and UFBoot \geq 95%. UFBoot support values are more unbiased than normal bootstrap support. 95% UFBoot support correspond roughly to a probability of 95%, that a clade is true (Minh et al. 2013).

Bayesian Inference (BI) was performed using Mr. Bayes v3.2.6 x64 (Huelsenbeck & Ronquist 2001; Ronquist & Huelsenbeck 2003; Altekar et al. 2004) through the HPC cluster from the University of Bern. For the concatenated data set, Partitionfinder-2.1.1 was used for finding the optimal evolutionary models for each subset with the model = all function. The Monte Carlo Markov Chain (MCMC) parameter was set as follows: starting with four chains and four separate runs for 20 million generations with a tree sampling frequency of 1000 and a burn in of 25%.

Analyses of shell morphology

For the first time, the morphology in *Trochulus* was analysed using landmark and semi landmark-based geometric morphometric methods (GMM) instead of traditional, linear measurements. Of the 572 *Trochulus* and *Raeticella* specimens examined genetically in this study, 195 specimens could be used for morphometric analyses. For the remaining specimens, there were either no photos available, the shell was broken, or the animals were juveniles. Wherever possible, photos of type material were included.

We used the frontal and ventral photo view of the *Trochulus* and *Raeticella* specimens and performed a 2D landmark-based geometric morphometric analysis. The software tpsDig2 v2.31 (Rohlf 2010) was used to obtain the landmarks. On the frontal view, 24 landmarks have been set, of which 16 are fixed landmarks and 8 are sliding semi landmarks. On the ventral view, of the 16 landmarks set, 7 are fixed landmarks and 9 are sliding semi landmarks (Fig. 2). Fixed landmarks are discrete anatomical loci (i.e., transitions of whorls or curvature of the aperture or umbilicus) which are homologous between specimens. The sliding semi landmarks are placed along the surface between two landmarks, in such a way that they best describe the curvature of the outline. Sliding the semi landmarks removes the effect of arbitrary initial spacing (Gunz & Mitteroecker 2013).

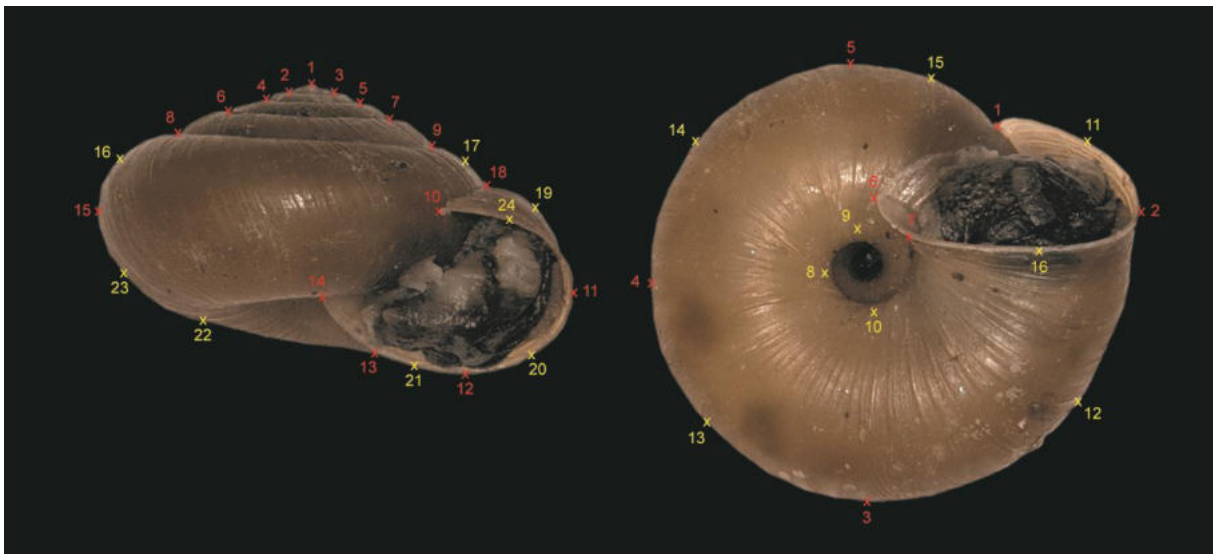


Figure 2: Position of landmarks on the frontal and ventral shell view. Red crosses: fixed landmarks; yellow crosses: sliding landmarks.

Geometric morphometric analysis

For the geometric morphometric analyses, the software R v.4.1.2 (R Core Team, 2021) was used with the packages *geomorph* v4.0.1 (Adams et al. 2020) and *Morpho* v2.9 (Schlager 2017). For subsequent analyses, we used modified scripts from Bischof et al. (2021, 2022). With the R function *Morpho::procSym*, the 2D landmark coordinates underwent a full generalised Procrustes alignment (GPA). The semi landmarks were slid in a way to minimize Procrustes distance. The full Procrustes fit standardizes position, orientation and size while leaving only Procrustes shape coordinates (e.g., Bookstein 1991; Zelditch et al. 2012). The frontal and ventral data was combined with the R function *geomorph::combine.subsets* and set to unit centroid size. The centroid size (CS) is the square root of the sum of the squared distances of the landmarks from the centroid (Zelditch et al. 2012). We then ran a Principal Component Analysis (PCA) for the frontal and ventral data set each and for the combined data set and additionally, a Canonical Variate Analysis (CVA) of the frontal and ventral data set each to visualize the multivariate data.

For modelling shapes at the extreme PC-values, the R function *GeometricMorphometricsMix::reversePCA* (Fruciano 2019) was used. This function recalculates artificial Procrustes shape variables from the extreme PC-values in a morphospace. The thin plate spline (TPS) deformation grid were calculated with the R function *geomorph::plotRefToTarget*. TPS deformation grids visualize shape differences between a reference shape and a target shape based on a set of homologous coordinates (Gunz & Mitteroecker 2013). The frontal and ventral views were analysed separately, as we want to show the extreme values for both views and each clade separately. All plots were created with *ggplot2*.

Results

Phylogeny

The Bayesian Inference, Maximum Likelihood and IQ-TREE trees (Fig. 3, 4 and 5) show the concatenated data set (COI, 16S and 5.8S rRNA+ITS2) of 710 specimens. The data set contains additional sequences of Kruckenhauser et al. (2014), Duda et al. (2017) and Proćków et al. (2021). The trees were rooted by specimens of *N. oreinos* from Bamberger et al. (2020). The topologies of all three methods show the same 21 *Trochulus* clades, but relationships of these clades differ to each other between the methods. These clades follow a geographic pattern (cf. Fig. 1). In all three methods, *R. biconica* (Eder, 1917) forms the

sister clade to the remaining *Trochulus* species. These nodes have high support values in all analyses (Fig. 3, 4 and 5; see also Kneubühler et al. 2022).

In the Bayesian Inference analysis (Fig. 3), we see a large split that divides the *Trochulus* lineages into two large clades. This node has a posterior probability of 0.67. One clade consists of the lineages that lie more in the Jura mountains (referred here as the “Jurassic” clade) and the surrounding countryside, and the other consists of the lineages that are widespread in Europe. The resolution in the “Jurassic” clade is better, as more genes were examined here. The support values for the lineages within the “Jurassic” clade are moderate to high. Within the clades, some of the nodes are not supported. In the clade with the widespread lineages, only the COI was examined for most specimens which results in a polytomy with this large number of individuals.

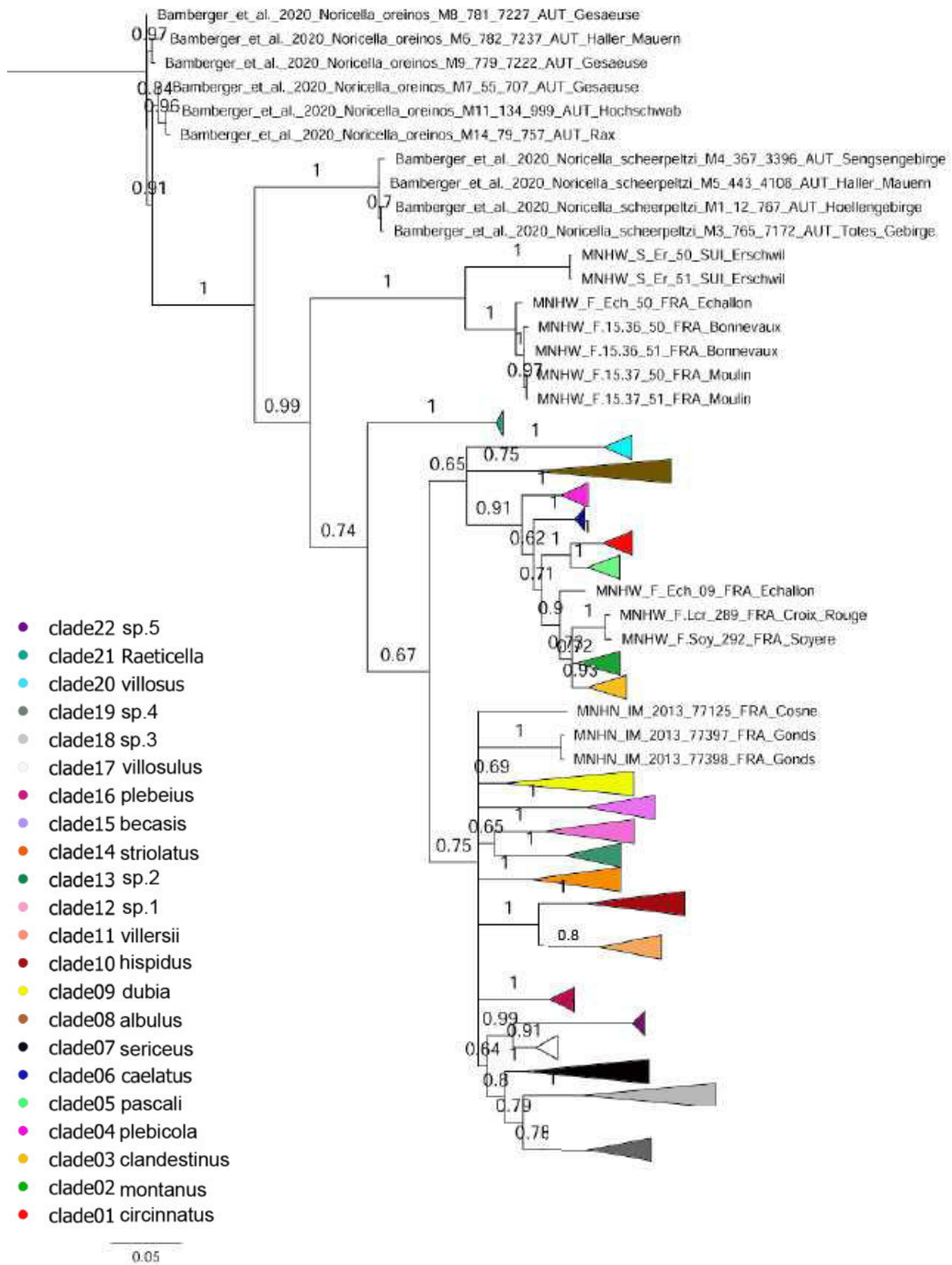


Figure 3: Bayesian Inference (BI) tree based on the concatenated data set of COI, 16S and 5.8S rRNA+ITS2. The analysis comprises 710 individuals of which 10 are outgroup specimens from *N. oreinos* and *N. scheerpeltzi*. Additionally, sequences of Kruckenhauser et al. (2014), Duda et al. (2017) and Proćków et al. (2021) were included. Numbers at the nodes are the posterior probabilities.

In the Maximum Likelihood analysis (Fig. 4), the node of the “Jurassic” clades and the widespread clades has a ML support of 90. In contrast to the BI analysis, where *T. villosus* and *T. albulus* form separate not related clades, they cluster together in the ML analysis. But this node is not supported with a bootstrap support of 57. However, the topology in the rest of the “Jurassic” clade is the same in the BI and ML analysis. The topology of the clades in the widespread clade differs, except for *T. hispidus* and *T. villersii* and *T. sp. 3* and *T. sp. 4*, which form sister groups in the BI and ML analyses respectively. The node of *T. hispidus* and *T. villersii* has a bootstrap support of 94 and a posterior probability of 1 (Fig. 3). The node of *T. sp. 3* and *T. sp. 4* is not supported in the ML and BI analysis respectively. The resolution in the tree is better, as no polytomy occurs with ML analysis.

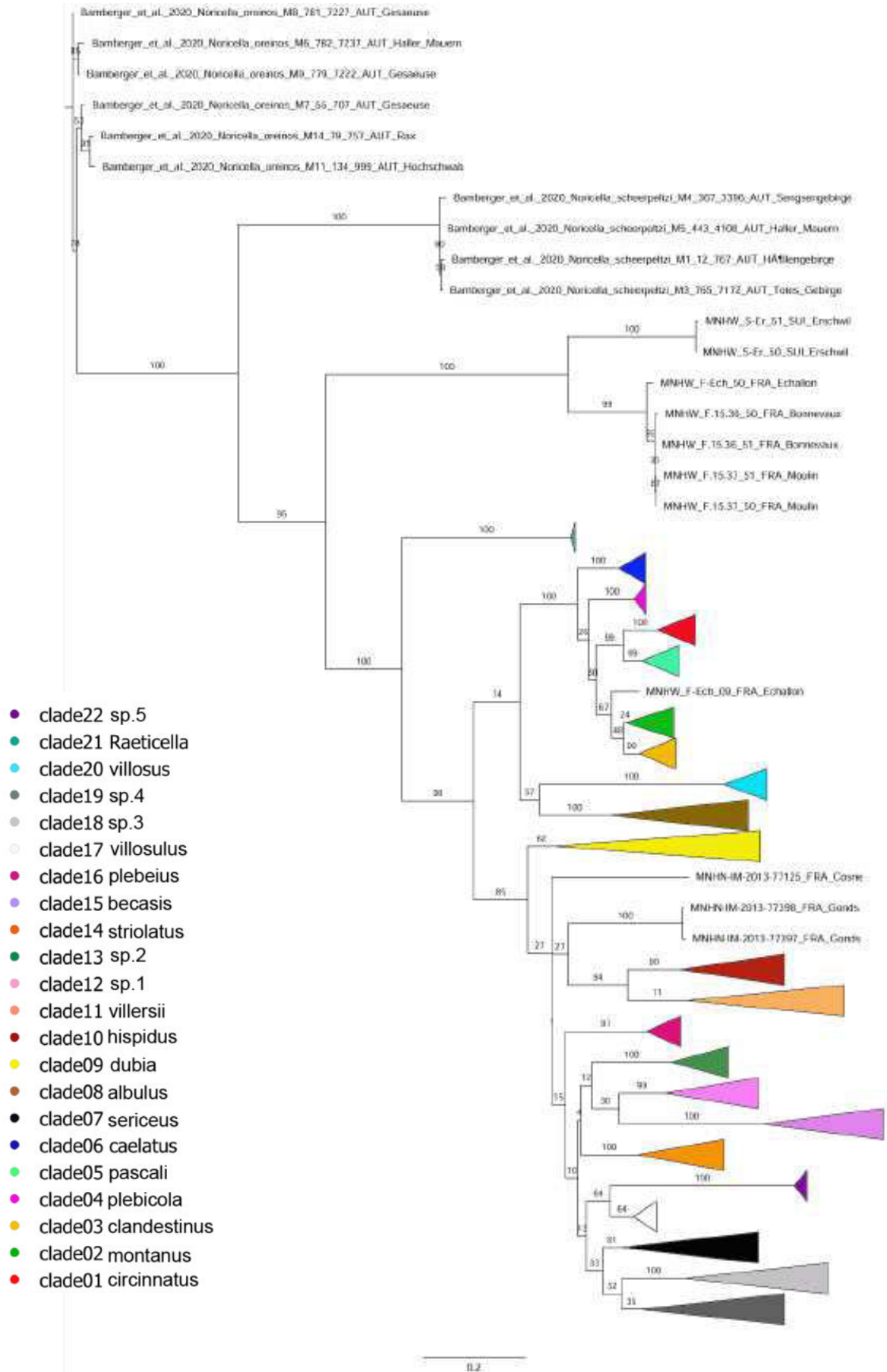


Figure 4: Maximum Likelihood (ML) tree based on the concatenated data set of COI, 16S and 5.8S rRNA+ITS2. The analysis comprises 710 individuals of which 10 are outgroup specimens from *N. oreinos* and *N. scheerpeltzi*. Additionally, sequences of Kruckenhauser et al. (2014), Duda et al. (2017) and Proćków et al. (2021) were included. Numbers at the nodes are the bootstrap support values.

The IQ-TREE analysis (Fig. 5) shows a consensus tree with SH-aLRT (left) and ultrafast bootstrap (right) supports. The IQ-TREE analysis shows a similar topology to RAxML (Fig. 4), as the approach is also based on Maximum Likelihood (ML) trees. We see again the split in “Jurassic” clades and the widespread clades. This node is well supported with SH-aLRT value of 97.2 and UFBoot value of 100. The nodes show overall higher support values as in the BI or RAxML analyses.

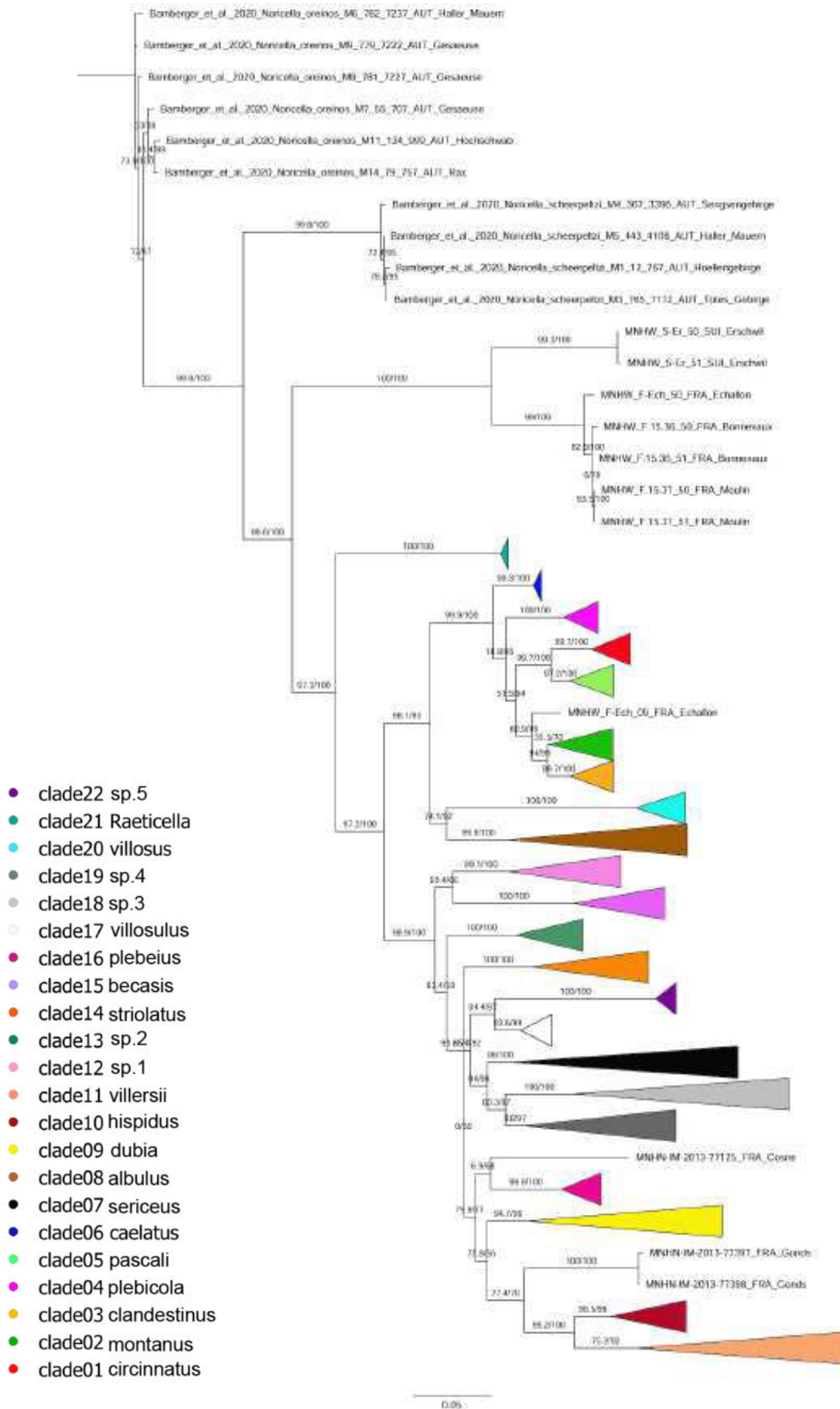


Figure 5: Maximum Likelihood (ML) tree based on the concatenated data set of COI, 16S and 5.8S rRNA+ITS2. The analysis comprises 710 individuals of which 10 are outgroup specimens from *N. oreinos* and *N. scheerpeltzi*. Additionally, sequences of Kruckenhauser et al. (2014), Duda et al. (2017) and Proćków et al. (2021) were included. Numbers at the nodes are the SH-aLRT values (left) and UFBoot support values (right).

Evolutionary distances

For the analysis of the sequence distances of the COI, the software MEGA v10.1.8 (<https://www.megasoftware.net/>) was used. The sequences were assigned to groups according to their affiliation to a clade, following the numbering of the clades. The outgroup genera *Raeticella*, *Edentiella* and *Noricella* were included. In Table 2 the number of base differences per site from averaging over all sequence pairs within each group are shown (Kumar et al. 2018). This analysis involved 665 nucleotide sequences and 655 positions in the final data set. The highest value is found in *T. sp. 3*, which means that within this clade the greatest differences are to be found with regard to the different bases per site. *Trochulus sp. 3* consists of many genetically different animals with a large geographical distribution. *Trochulus caelatus* has the lowest value in this analysis. However, this clade also contains only six sequences with little genetic differences.

In Table 3, the number of base differences per site from averaging over all sequence pairs between groups are shown (Kumar et al. 2018). This analysis involved 665 nucleotide sequences and 655 positions in the final data set. The “Jurassic” clades comprise the lowest values in this analysis. The highest values result from the comparison of *Edentiella* with *Trochulus* species. The second highest values result from the comparison of *T. becasis* and *T. villosus* with the “Jurassic” clades.

Table 2: The number of base differences per site from averaging over all sequence pairs within each species (group).

Species (group)	d
<i>T. circinnatus</i>	0.026
<i>T. montanus</i>	0.0165
<i>T. clandestinus</i>	0.014
<i>T. plebicola</i>	0.0256
<i>T. pascali</i>	0.0104
<i>T. caelatus</i>	0.0018
<i>T. sericeus</i>	0.0851
<i>T. albulus</i>	0.0881
<i>T. dubia</i>	0.0139
<i>T. hispidus</i>	0.0318
<i>T. villersii</i>	0.0112

<i>T. sp. 1</i>	0.0613
<i>T. sp. 2</i>	0.0384
<i>T. striolatus</i>	0.042
<i>T. becasis</i>	0.0495
<i>T. plebeius</i>	0.0047
<i>T. villosulus</i>	0.0242
<i>T. sp. 3</i>	0.1062
<i>T. sp. 4</i>	0.0342
<i>T. villosus</i>	0.0183
<i>T. sp. 5</i>	0.0122
<i>Edentiella</i>	0.0031
<i>Noricella</i>	0.0744
<i>Raeticella</i>	0.0029

Table 3: The number of base differences per site from averaging over all sequence pairs between species. Abbreviations used: cir = *circinnatus*, mon = *montanus*, cla = *clandestinus*, ple = *plebeius*, pas = *pascali*, cae = *caelatus*, ser = *sericeus*, alb = *albus*, dub = *dubia*, his = *hispidus*, vii = *villersii*, str = *striolatus*, bec = *becasis*, viu = *villosulus*, vil = *villosus*, Ede = *Edentiella*, Nor = *Noricella*, Rae = *Raeticella*

	cir	mon	cla	ple	pas	cae	ser	alb	dub	his	vii	T. sp.1	T. sp.2	str	bec	ple	viu	T. sp.3	T. sp.4	vil	T. sp.5	Ede	Nor	Rae
cir																								
mon	0.0915																							
cla	0.0917	0.0364																						
ple	0.0944	0.0834	0.0775																					
pas	0.0700	0.0914	0.0863	0.1023																				
cae	0.0969	0.0837	0.0799	0.0811	0.0946																			
ser	0.1728	0.1714	0.1651	0.1754	0.1766	0.1719																		
alb	0.1526	0.1416	0.1397	0.1523	0.1558	0.1426	0.1713																	
dub	0.1490	0.1462	0.1419	0.1568	0.1513	0.1532	0.1447	0.1544																
his	0.1613	0.1628	0.1604	0.1671	0.1637	0.1546	0.1570	0.1566	0.1283															
vii	0.1565	0.1665	0.1604	0.1440	0.1556	0.1469	0.1715	0.1606	0.1452	0.1395														
T. sp.1	0.1578	0.1619	0.1691	0.1744	0.1650	0.1640	0.1550	0.1718	0.1486	0.1550	0.1600													
T. sp.2	0.1664	0.1642	0.1604	0.1673	0.1686	0.1554	0.1460	0.1730	0.1430	0.1404	0.1560	0.1402												
str	0.1519	0.1561	0.1545	0.1643	0.1583	0.1549	0.1422	0.1639	0.1344	0.1365	0.1419	0.1289	0.1305											
bec	0.1792	0.1866	0.1853	0.1894	0.1834	0.1752	0.1598	0.1719	0.1556	0.1396	0.1615	0.1499	0.1441	0.1466										
ple	0.1601	0.1585	0.1543	0.1669	0.1716	0.1628	0.1405	0.1600	0.1339	0.1307	0.1285	0.1421	0.1275	0.1104	0.1354									
viu	0.1490	0.1471	0.1498	0.1524	0.1548	0.1514	0.1234	0.1524	0.1242	0.1248	0.1441	0.1226	0.1145	0.1016	0.1438	0.1012								
T. sp.3	0.1740	0.1683	0.1680	0.1800	0.1754	0.1691	0.1602	0.1706	0.1629	0.1624	0.1814	0.1725	0.1657	0.1555	0.1740	0.1525	0.1442							
T. sp.4	0.1610	0.1454	0.1453	0.1706	0.1528	0.1561	0.1421	0.1589	0.1502	0.1363	0.1501	0.1504	0.1453	0.1346	0.1552	0.1244	0.1279	0.1478						
vil	0.1742	0.1773	0.1709	0.1821	0.1801	0.1667	0.1731	0.1706	0.1648	0.1556	0.1556	0.1633	0.1427	0.1521	0.1588	0.1579	0.1569	0.1862	0.1669					
T. sp.5	0.1742	0.1674	0.1710	0.1699	0.1777	0.1665	0.1415	0.1702	0.1450	0.1509	0.1712	0.1586	0.1522	0.1463	0.1474	0.1457	0.1030	0.1644	0.1451	0.1783				
Ede	0.1947	0.1931	0.1883	0.1945	0.1834	0.1856	0.1972	0.1816	0.1880	0.1771	0.1672	0.1818	0.1651	0.1920	0.1786	0.1760	0.1710	0.1934	0.1718	0.1790	0.1824			
Nor	0.1545	0.1572	0.1507	0.1560	0.1479	0.1483	0.1665	0.1503	0.1437	0.1469	0.1481	0.1444	0.1544	0.1482	0.1599	0.1414	0.1410	0.1625	0.1508	0.1707	0.1654	0.1730		
Rae	0.1676	0.1556	0.1543	0.1700	0.1687	0.1679	0.1711	0.1674	0.1578	0.1625	0.1629	0.1615	0.1726	0.1726	0.1733	0.1549	0.1487	0.1718	0.1513	0.1768	0.1664	0.1860	0.1479	

Landmark analysis

The shape analysis of the data from the frontal view shows, that the first three Principal Components (PC) account for 65.8% (PC1 = 29.8%, PC2 = 23.4%, PC3 = 12.6%) of the total variation. *Raeticella biconica* is separated from all other clades along PC1. The two investigated specimens of *T. caelatus* are separated from the other clades along PC2 (Fig. 6A) even though the type specimen of *T. caelatus* (blue diamond in Fig. 6) clusters within the main point cloud of the remaining specimens. Even though most of the remaining clades cover a limited area in the morphospace, the overall amount of overlap is too large to make a clear distinction.

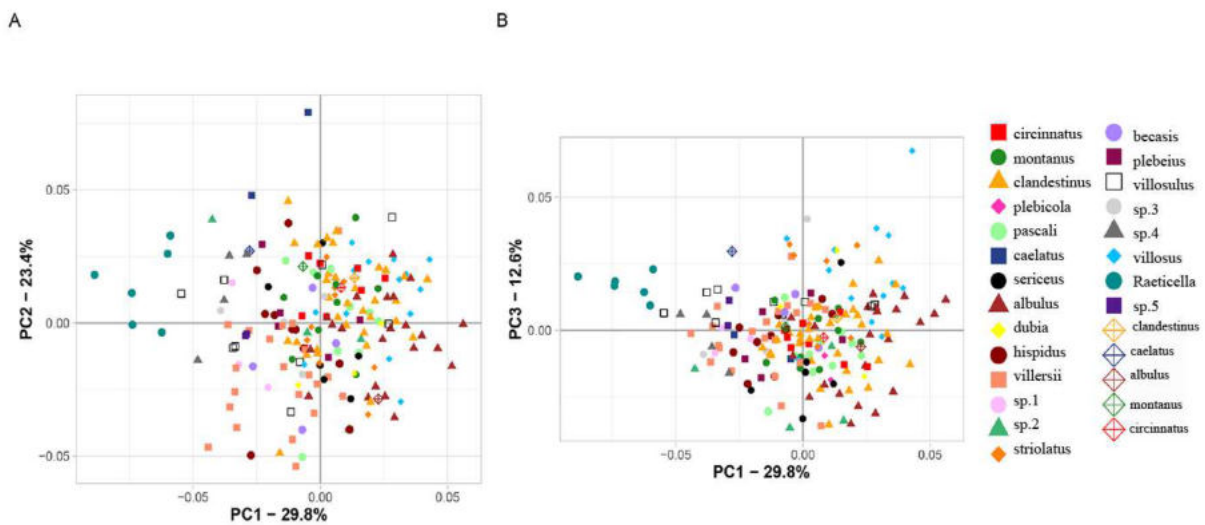


Figure 6: Principal Component Analysis (PCA) of the frontal view data of all investigated specimens ($n = 195$). (A) Principal Component 1 and 2; (B) Principal Component 1 and 3. Values at the axes account for the variation of the data. Diamonds represent type specimens of the respective species.

The shape analysis of the data from the ventral view shows, that the first three Principal Components (PC) account for 70% (PC1 = 35.6%, PC2 = 17.8%, PC3 = 16.6%) of the total variation. The analysis of the ventral data shows a large overlap of the clades (Fig. 7). The species cannot be distinguished based on ventral characteristics alone. Running the analysis with fewer clades does not enhance the separation significantly.

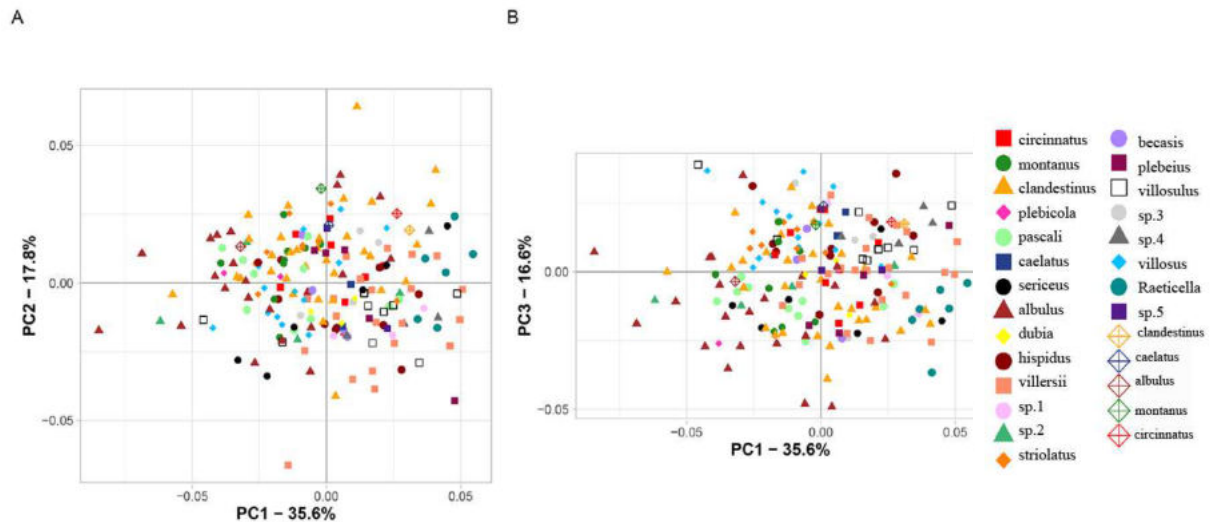


Figure 7: Principal Component Analysis (PCA) of the ventral view data of all investigated specimens ($n = 195$). (A) Principal Component 1 and 2; (B) Principal Component 1 and 3. Values at the axes account for the variation of the data. Diamonds represent type specimens of the respective species.

The shape analysis of the combined data of the frontal and ventral view shows, that the first three Principal Components (PC) account for 52.6% (PC1 = 26.8%, PC2 = 15.4%, PC3 = 10.4%) of the total variation. The PCA of PC1 and PC2 (Fig. 8A) and of PC1 and PC3 (Fig. 8B) reveals a large overlap of the clades, except for *R. biconica*, which is separated from the other clades along PC1. This shape analysis supports our hypothesis that *R. biconica* does not belong to the genus *Trochulus* Chemnitz, 1786, but is placed in a new genus (Kneubühler et al. 2022). The type specimen of *T. albulus* (brown diamond in Fig. 8) clusters well within the point cloud of *T. albulus* (Fig. 8). The type specimen of *T. clandestinus* (orange diamond in Fig. 8), *T. montanus* (green diamond) and *T. circinnatus* (red diamond) cluster close to each other, which means, they are not well distinct based on frontal and ventral shell shape. The point cloud of *T. clandestinus* spans that of *T. montanus* and *T. circinnatus*, which means that the intraspecific variability of *T. clandestinus* is greater than the interspecific variability of those species. Specimens from *T. sericeus*, *T. sp. 1* and *T. villosulus* show great intraspecific variability.

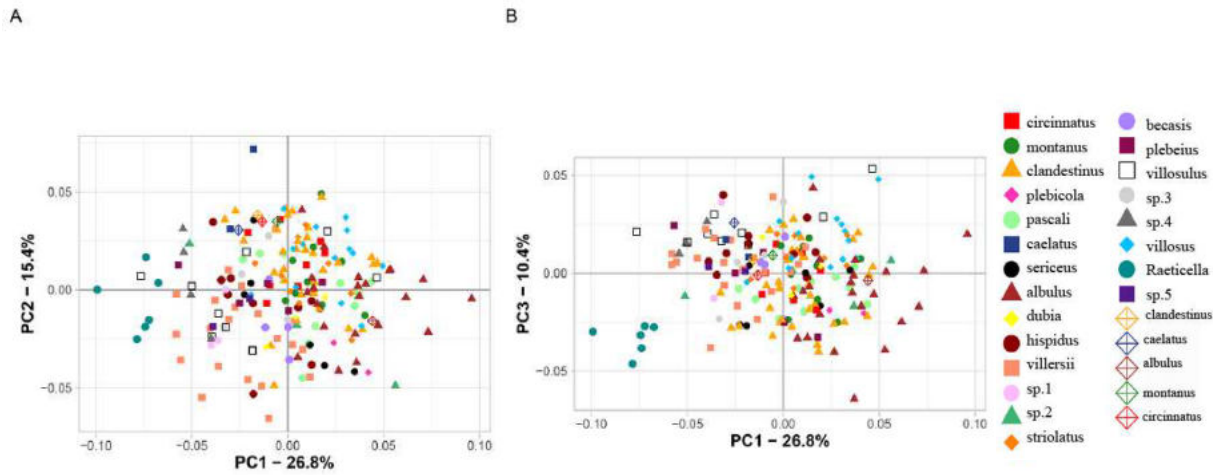


Figure 8: Principal Component Analysis (PCA) of the combined data from frontal and ventral view of all investigated specimens ($n = 195$). (A) Principal Component 1 and 2; (B) Principal Component 1 and 3. Values at the axes account for the variation of the data. Diamonds represent type specimens of the respective species.

In Figure 9, the thin plate spline (TPS) of Procrustes shape of the extreme PC values against the mean shapes of each clade for the frontal view is shown. *Trochulus circinnatus*, *T. montanus*, *T. clandestinus*, and *T. pascali* look very similar. These specimens have a rather flat shell with a large, roundish aperture. *Trochulus caelatus* (Fig. 9) is flat, where the first whorls contribute very little in terms of shell height. Specimens of *T. plebicola* and *T. albulus* have a globular shell with a relatively large aperture. *Trochulus villosus* (Fig. 9) has a flat shell with an elongated aperture. *Raeticella biconcia* (Fig. 9) has a flat, keeled shell with a lunate aperture. *Trochulus hispidus* and *T. villersii* have a rather flat shell with a relatively smaller aperture than clades with a similar shell shape (e.g., *T. circinnatus*, *T. montanus*, and *T. clandestinus*).

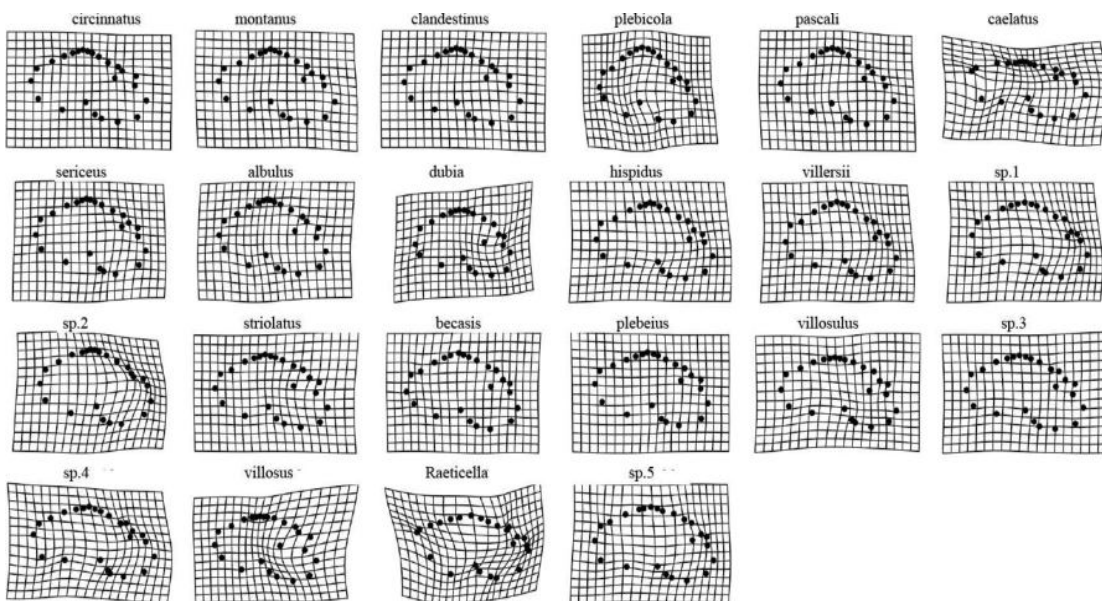


Figure 9: The thin plate spline (TPS) of Procrustes shape of the extreme PC values against the mean shapes of each clade for the frontal view.

Figure 10 shows the thin plate spline (TPS) of Procrustes shape of the extreme PC values against the mean shapes of each clade for the ventral view. *Trochulus plebicola* and *T. albulus* have a narrow umbilicus, slightly hidden by the aperture. The remaining clades have a similar wide, open umbilicus.

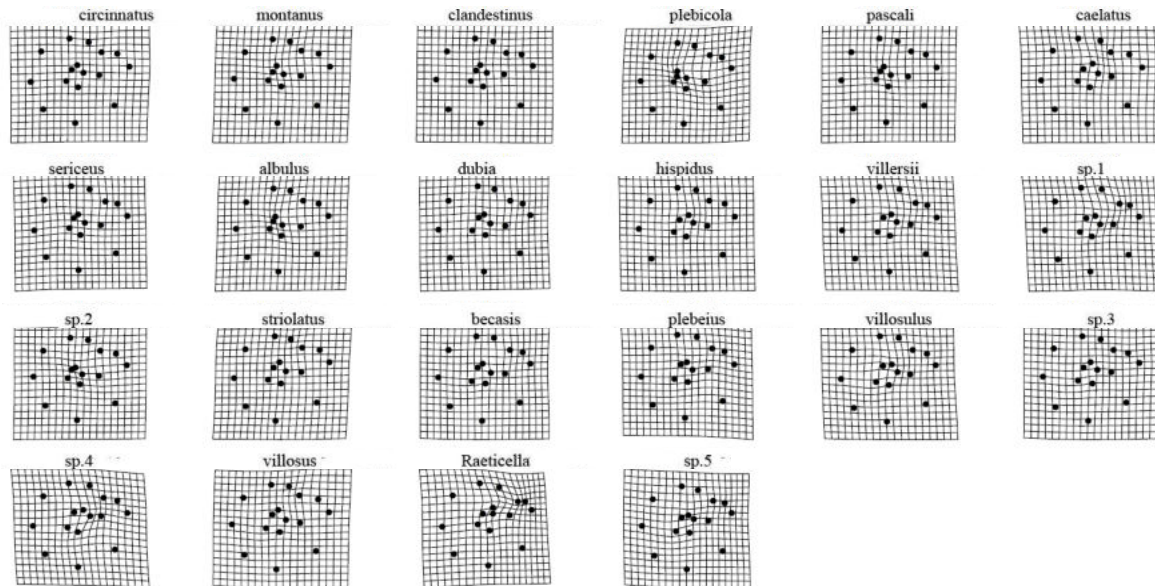


Figure 10: The thin plate spline (TPS) of Procrustes shape of the extreme PC values against the mean shapes of each clade for the ventral view.

Canonical Variate Analysis (CVA) is used to identify and measure the associations among two sets of variables. We calculated a CVA for the frontal (Fig. 11) and the ventral view (Fig. 12) each. *Raeticella biconica* falls out morphologically completely in the analysis. In order to better show the differences between the other species, *R. biconica* was left out of the analyses. In Figure 10, the CVA of the frontal shell view is shown. *Trochulus villosus* is well separated from the remaining species. *Trochulus albulus* and *T. villosulus* show slight tendencies towards delimitation, but nevertheless have an overlap with other species. The scatter within a clade is significantly smaller than with PCA.

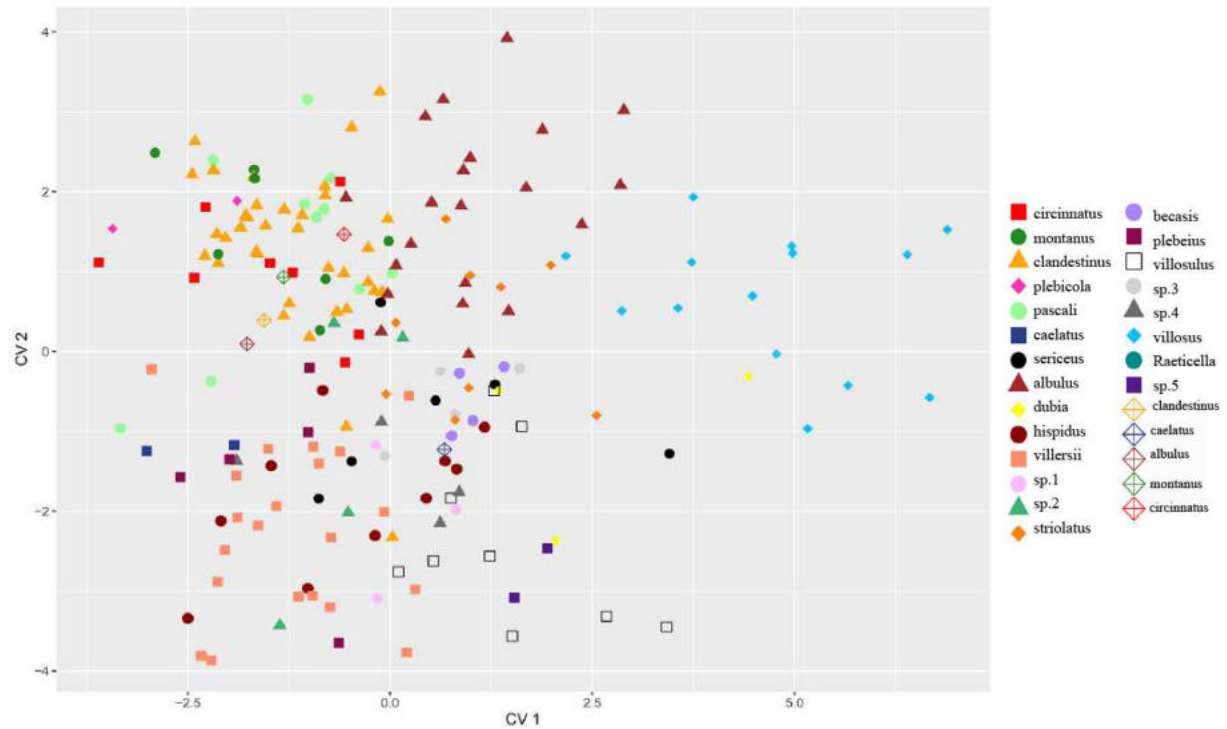


Figure 11: Canonical Variate Analysis (CVA) of the frontal view data of the investigated specimens without *R. biconica* (n = 189). Diamonds represent type specimens of the respective species.

The separation of the specimens based on the ventral view (Fig. 12) is less characteristic than with the frontal data. Only some specimens of *T. albulus* with the very narrow, point-like umbilicus can be separated from the other species in the analysis. The other specimens have a big overlap which indicates that they are morphologically very similar.

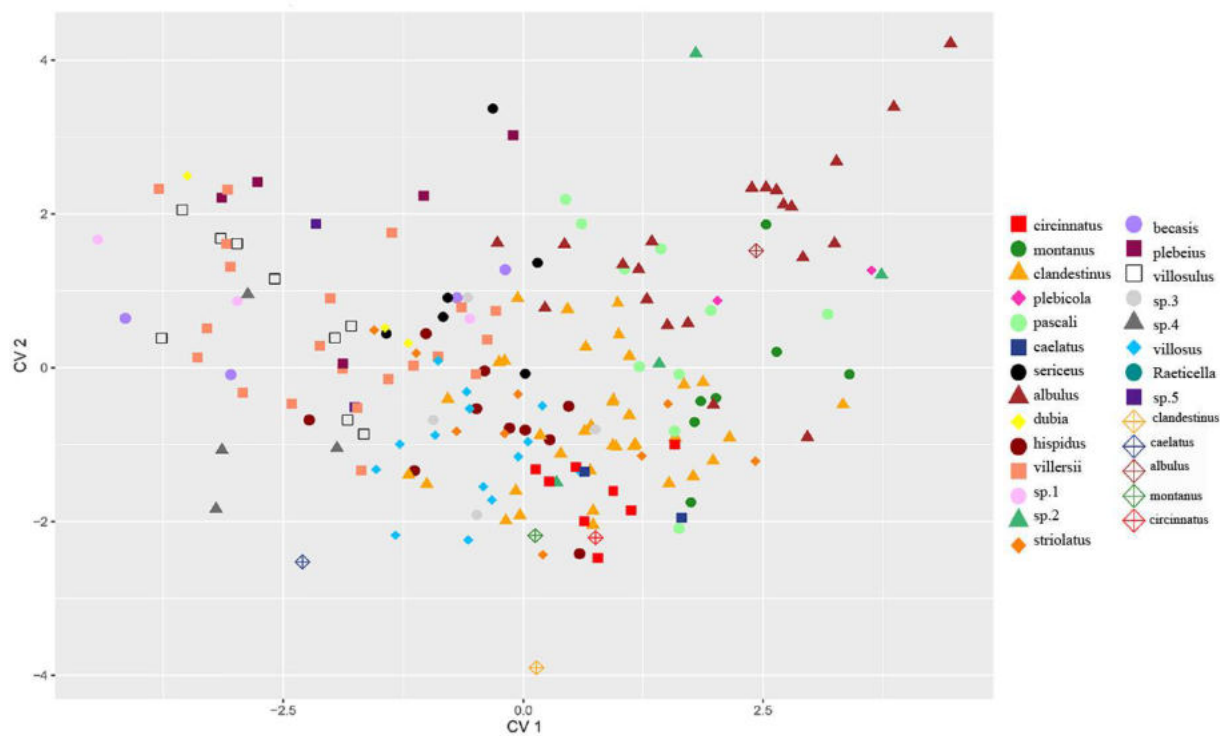


Figure 12: Canonical Variate Analysis (CVA) of the ventral view data of the investigated specimens without *R. biconica* (n = 189). Diamonds represent type specimens of the respective species.

Taxonomic account

The clades are here translated into a taxonomic structure according to the number where they occur in the tree. Variation in shell shape and morphology can be estimated from our plates, which mainly show sequenced specimens (except for some dry type specimens).

Trochulus circinnatus (S. Studer, 1820) [clade01] Figs 13a-f

1820 *Glischrus* (*Helix*) *circinnata* S. Studer, Naturw. Anz. schweiz. Ges. Naturw., 3 (11): 86 [or: Syst. Verz. Schweizer-Conchylien: 12] ["Auf dem Jura"].

1821 *Helix depressa* W. Hartmann, Neue Alpina: 1: 237 ["sie kommt in der Schweiz, aber selten, vor"; Remark: refers to Draparnaud, 1805, Hist. nat. moll. terr. fluv. France: 104, pl. 7 fig. 22 as *Helix hispida* var. γ ; non *Helix depressa* Montagu, 1803].

Type specimens: We consider S. Studer as author of this species based on his indication of the name and differentiation from *Helix* (*Glischrus*) *montana* in the description of the latter species. *Trochulus circinnatus* was mentioned a year later by Hartmann (1821, in: Steinmüller, Neue Alpina, 1: 237, pl. 2 fig. 13) as *Helix hispida* var. *circinnata* with the note: "ich erhielt sie besonders schön aus dem Kanton Waadt und durch Herrn von Charpentier von Mont zwischen Valorbe und Lac de Joux [I received a nice specimen from the Canton Waadt and from Mr. von Charpentier from Mont between Valorbe and Lac de Joux]". Unfortunately, no type specimen could be traced in Studer's collection. The specimens from Hartmann do not originate from Studer, and no other original specimens could be traced in contemporary collections, the designation of a neotype is needed to stabilize the application of the name. We herewith designate NMBE 564609 as lectotype for *T. circinnatus*.

Description: The investigated specimens of *T. circinnatus* have a pale brown shell without any hairs. The shell is roundish-conical with an aperture that is about half of the shell width. The shell is finely striated. Shell width ranges from 9.48–11.98 mm and shell height from 5.48–7.1 mm (N = 9). All measurements can be found in the appendix (supplementary material II). The body whorl height accounts for about 80% of shell height and contains a light band. The specimens have between 5.25–6 whorls. The umbilicus is wide and open. The body is pale brown to greyish.

Distribution (Fig. 14): This species is a small range endemic for the Central Swiss and French Jura. Genetically identified populations inhabit an area roughly between Neuenburg and Lausanne in Switzerland north to Dole and Besançon in France.

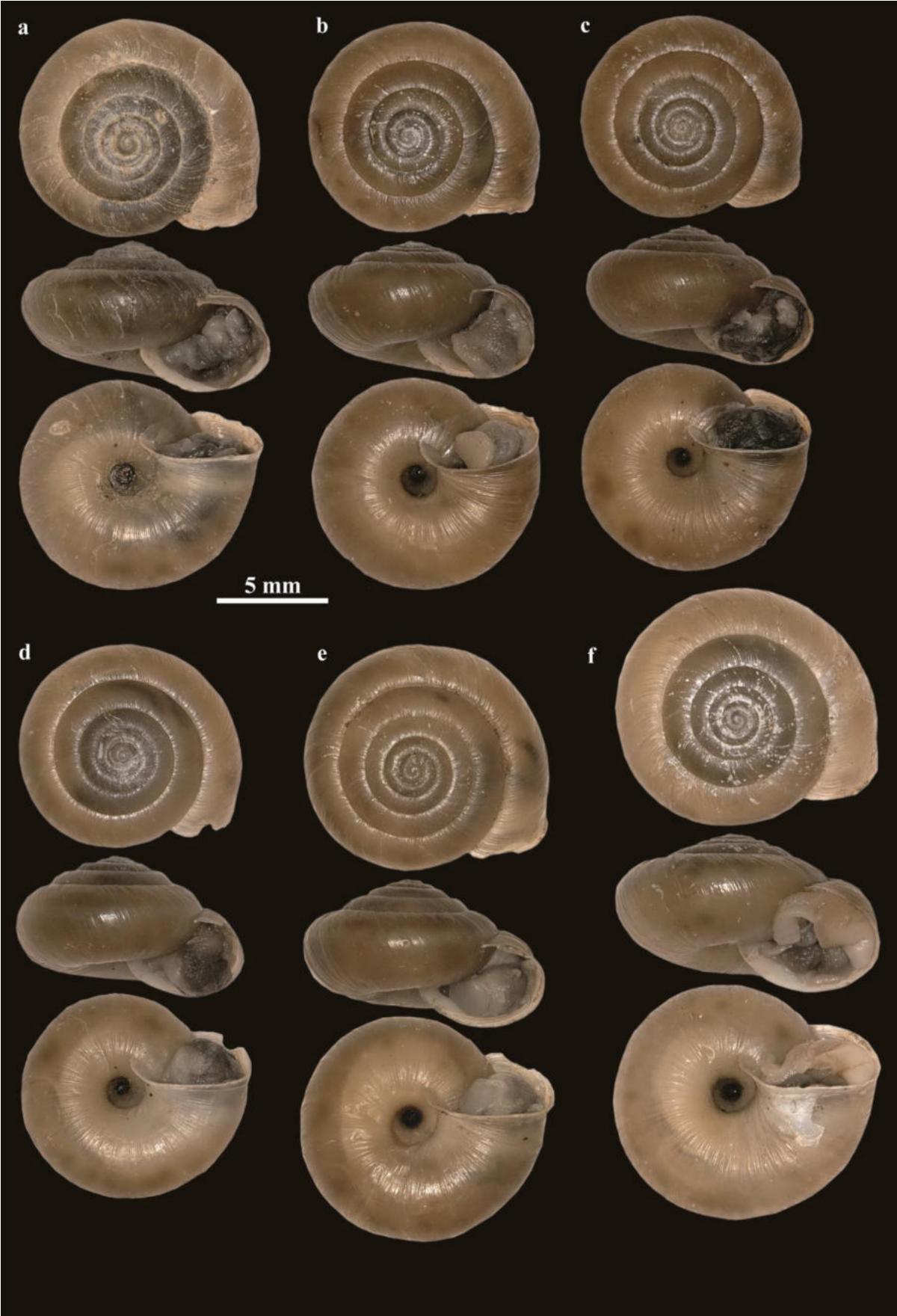


Figure 13: *Trochulus circinnatus*. Clade 01; (a) MNHW_F.15.38_06; France, Chaux-des-Crotenay; (b) MNHW_F.15.35_01; France, Mouthé, Source du Doubs; (c) MNHW_F.15.36_01; France, Bonnevaux; (d) MNHW_F.15.37_06; France, Cascade du Moulin du Saut; (e) MNHW_F.15.37_05; France, Cascade du Moulin du Saut; (f) MNHW_F.15.34_01; France, La Chevy.

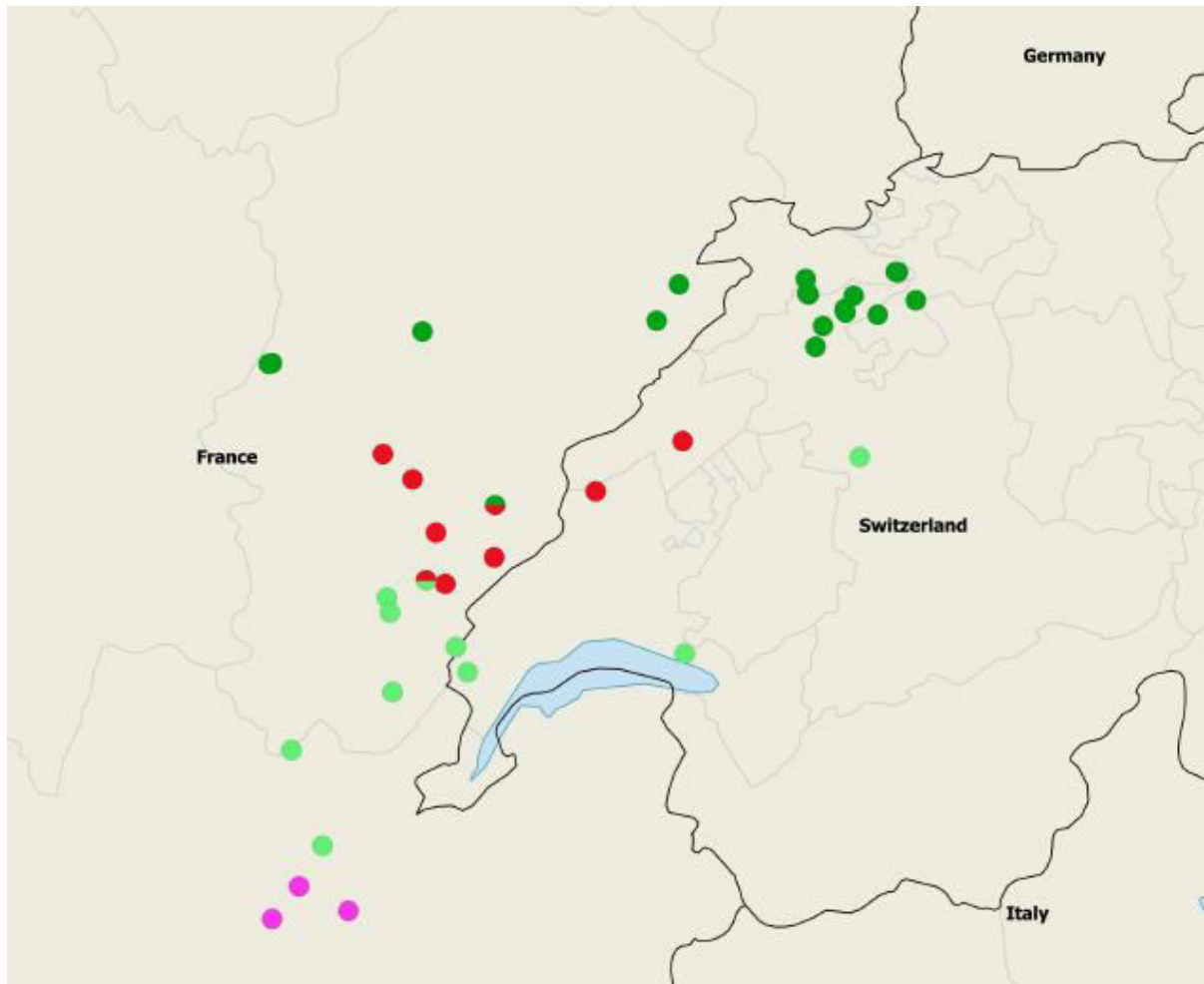


Figure 14: Distribution map of the investigated *T. circinnatus* (red circles), *T. montanus* (dark green circles), *T. plebicola* (pink circles), and *T. pascali* (pale green circles) specimens.

Trochulus montanus (S. Studer, 1820) [clade02] Figs 15a-h

1820 *Glischrus (Helix) montana* S. Studer, Naturw. Anz. schweiz. Ges. Naturw., 3 (11): 86 [or: Syst. Verz. Schweizer-Conchylien: 12] [Auf dem Jura].

1855 *Helix glabra* Dumont, Bull. Inst. natn. genevois: 3: 355 [“du Jura”; junior homonym of *Helix glabra* Gmelin, 1790 In: Linnaeus, Systema Naturae, ed. 13, l: 3658].

Type specimens: The original *Glischrus montana* series of Studer as found by Forcart in 1957 labelled with Studer’s catalogue number “13” contained 12 shells. Without providing a reason, Forcart split the original lot “13” into the following subsets: 13, 13a, 13b, and 13c. So, the original number “13” was selected by him as lectotype for *Glischrus [Helix] montana* STUDER, 1820 containing a single specimen (NMBE 15422). Under “13a”, he separated four specimens, under “13b” three specimens, and finally under “13c” another four specimens. All

these lots constitute paralectotypes of *Glischrus montana*. Later, these lots have been revised by Wüthrich (1977) and Gosteli (1991), both unpublished.

Wüthrich recognized that the lectotype selection by Forcart was erroneous and identified specimen “13” as a juvenile *Urticicola umbrosus* (C. Pfeiffer, 1828). Number “13a” contains *T. montanus* sensu auctores, and Gosteli selected a new lectotype specimen from this series. “13b” contains another three paralectotype specimens of *T. montanus*, while “13c” is a compositum mixtum of two shells of *U. umbrosus*, a single shell of *T. montanus* and a single shell of *T. striolatus*.

We consider Forcart’s lectotype selection as invalid using ICZN 74.2. This article regulates that “If it is demonstrated that a specimen designated as a lectotype was not a syntype, it loses its status of lectotype”. The type locality of *montana* is “Auf dem Jura” – which can be either the Swiss Jura or the French part. However, in both Jura parts, *U. umbrosus* does not occur (in fact, *U. umbrosus* does not occur in the whole of France nor the whole of Switzerland). The shell that has been selected as the lectotype by Forcart can therefore not be a syntype. Hence, Gosteli’s selection is correct, the lectotype is registered under NMBE 15466 (D = 10.9 mm; Fig. 15a).

Description: *Trochulus montanus* has a pale brown, shiny shell without any hairs. The shell is roundish-conical. Shell width of the investigated specimens ranges from 7.84–12.4 mm and shell height from 5.04–6.44 mm (N = 7). All measurements can be found in the appendix (supplementary material II). The body whorl height accounts for about 80% of shell height and contains on some specimens a light band. Specimens contain 5.5–6 whorls. The umbilicus is wide and open. The body is beige to brown.

Distribution (Fig. 14): This species is genetically identified from the Swiss Jura south of Basel and inhabits the mountainous part of the Franche-Comté towards the promontory of Dijon. The southernmost record is from the French Jura between Bourg-en-Bresse and Geneva.

Habitat: We consider this species an endemic of the western Central Jura, where it lives in sympatry with *T. circinnatus*.

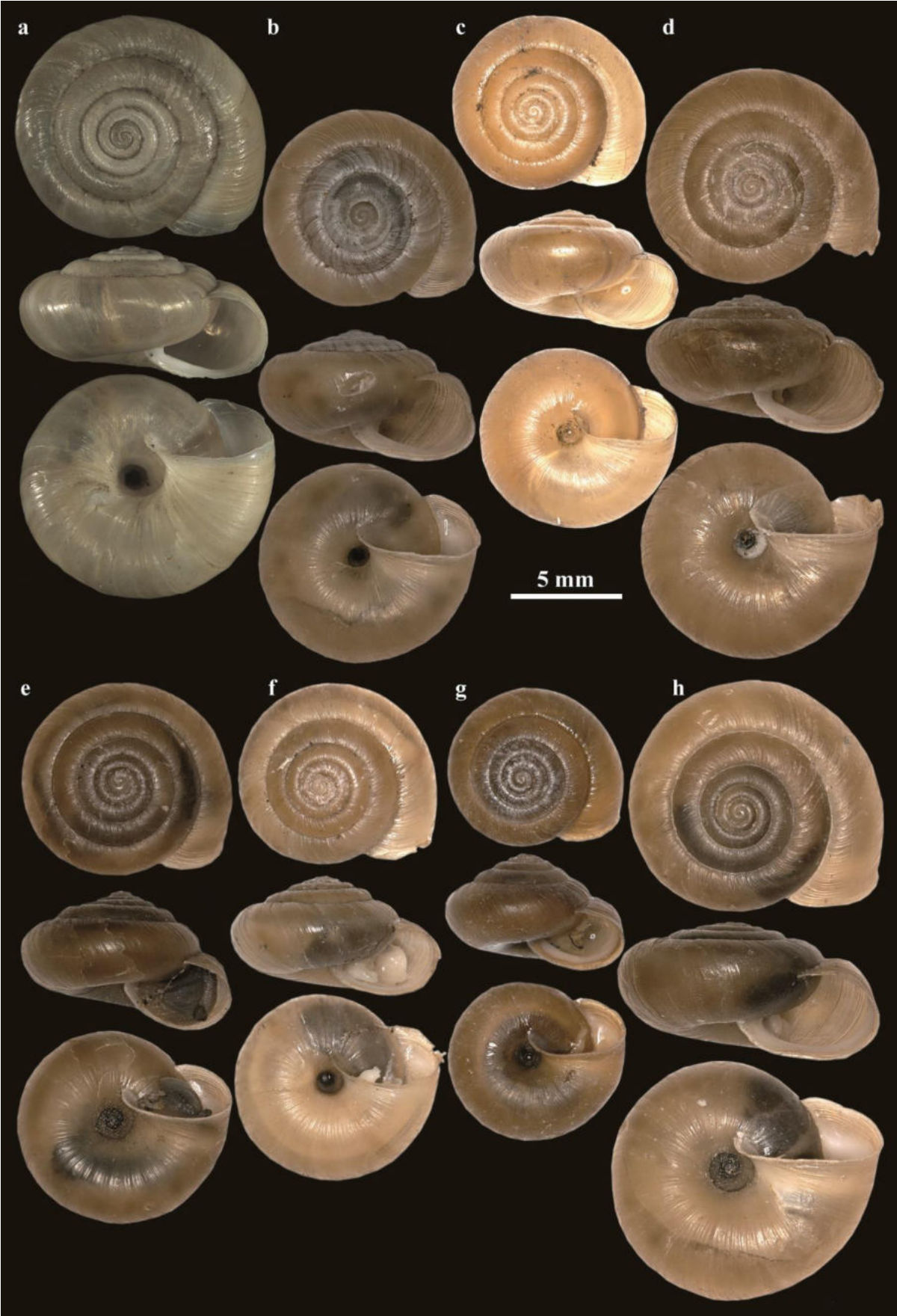


Figure 15: *Trochulus montanus*. Clade02; (a) Lectotype NMBE 15466 «Auf dem Jura»; (b) MNHW_S.15.22a_10 Switzerland, Gorges du Pichoux; (c) MNHW_F.SF_283; France, Source de la Foulotière; (d) MNHW_S.15.17_01; Switzerland, Gorges de Court; (e) MNHW_S.15.20_17; Switzerland, Gorges de Court 4; (f) MNHW_F.Lcr_289; France, La croix rouge; (g) MNHW_F.LR_290; France, La Ruchotte; (h) MNHW_S.15.26_03; Switzerland, Frinvillier 2.

Trochulus clandestinus (Hartmann, 1821) [clade03] Figs 16a-h

1821 *Helix corrugata* var. *clandestina* HARTMANN, in: STEINMÜLLER, Neue Alpina, 1: 236 [ich erhielt sie von Wien und fand sie in der Schweiz bey Zürich [Wien: ex BORN]].

1821 *Helix corrugata* W. Hartmann, Neue Alpina: 1: 236 [Neuwied [identified with Neuweid, Zürich, 47.32701 8.42324]; junior homonym of *Helix corrugata* Gmelin, 1789].

1874 *Helix* [*Fruticiola*] *putonii* Clessin: Jahrb. dtsh. malakozool. Ges., 1 (4): 314 [Belgium and NE France: Bussange, Vogesen].

Type specimen: Lectotype NMSG M942 (D = 10.07 mm), here designated for the specimen from Zurich.

Description: The investigated specimens of *T. clandestinus* have a shiny grey to pale brown shell without any hairs. The shell is roundish-conical. The shell is finely striated. Shell width ranges from 7.18–11.9 mm and shell height ranges from 4.08–6.96 mm (N = 36). All measurements can be found in the appendix (supplementary material II). The last whorl is less wide than in *T. circumnatus* and *T. montanus*. The specimens have 5.25–6 whorls. The umbilicus is wide and open. The body is beige.

Distribution (Fig. 17): This species occurs in France (eastern Franche-Comté and southern Alsace), Germany (southern Black Forest), and Austria (Vorarlberg). In Switzerland, it inhabits the complete northern area, but does not live in the region south of the main alpine chain.

Habitat: *Trochulus clandestinus* is found in the herb layer in damp deciduous forest, below bushes near rivers, but also in cultivated areas like gardens and parks.

Remarks: One of the historical confusions have been started by Hartmann himself, who recorded the species from Vienna and Zurich. However, according to our results, *T. clandestinus*, as used by modern authors, is restricted to the western alpine area. The record from Vienna (specimen not preserved in the Hartmann collection) is a confusion with another *Trochulus* species.

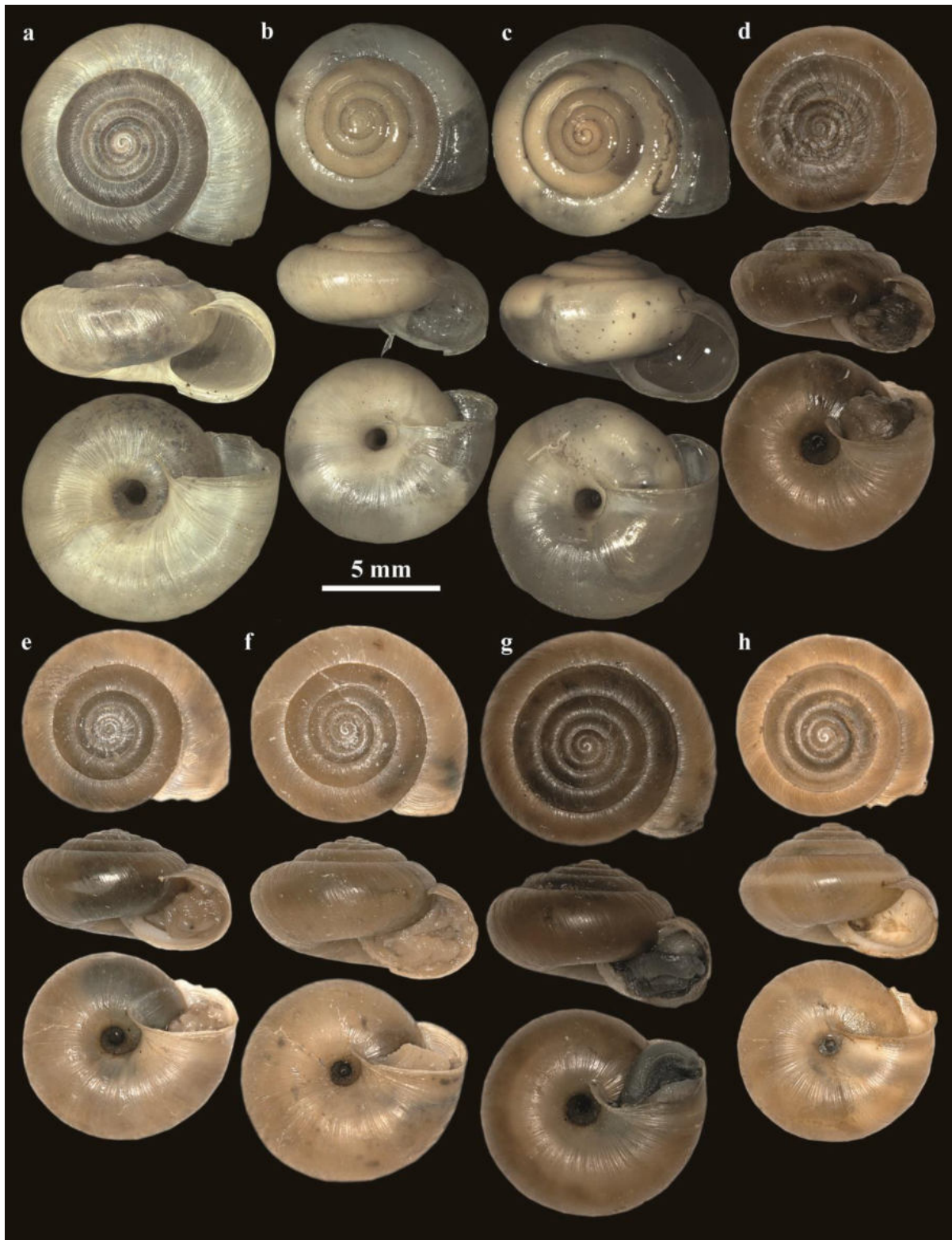


Figure 16: *Trochulus clandestinus*. Clade03; (a) Lectotype NMSG M942; Switzerland, Zürich; (b) NMBE 571142; Switzerland, Bergün; (c) NMBE 571235; Switzerland, Bürglen; (d) MNHW_F.15.31_02; France, Mont d'Or; (e) MNHW_A.Me_05; Austria, Mellau; (f) MNHW_F.15.14_13; France, Source de la Moselle n. Bussang; (g) MNHW_S.15.20_18; Switzerland, Gorges de Court 4; (h) MNHW_F.VM_294; France, Vallon du Moulinot.

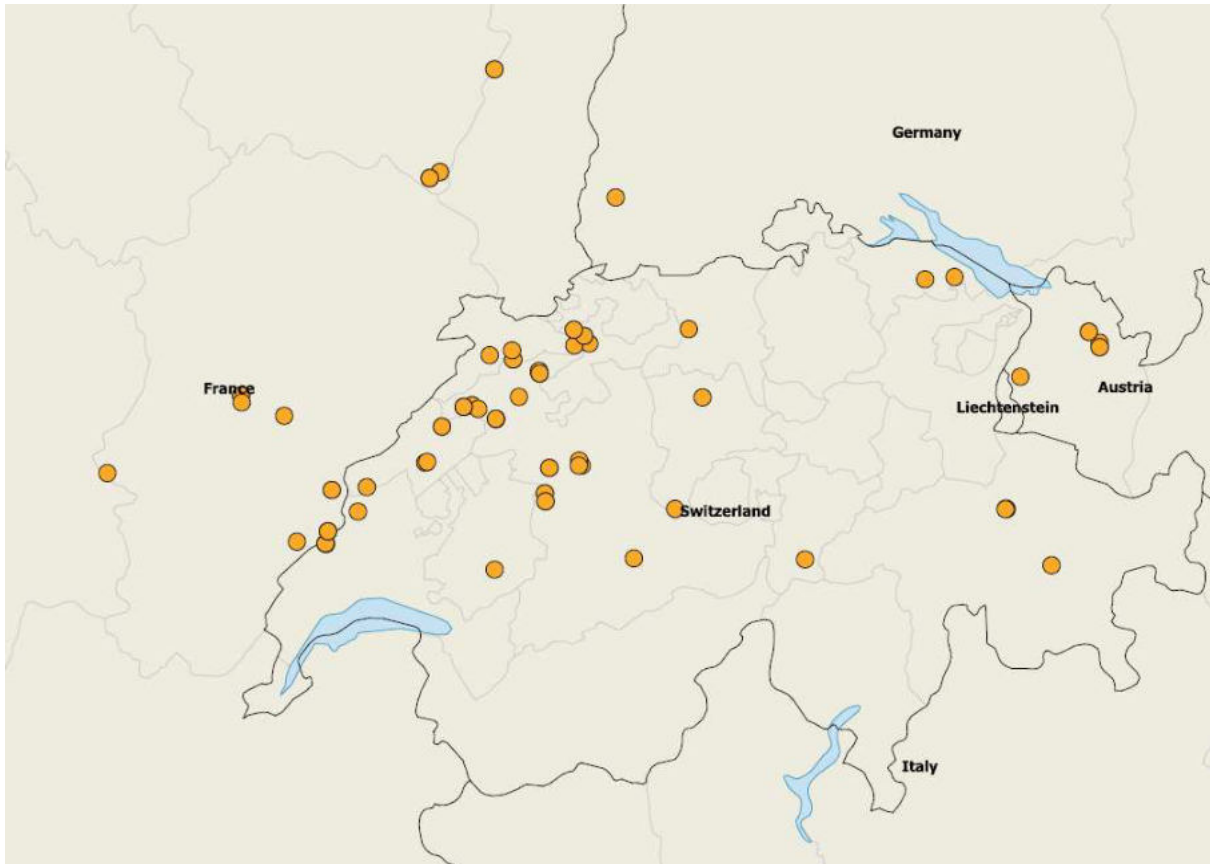


Figure 17: Distribution map of the investigated *T. clandestinus* specimens.

Trochulus plebicola (Locard, 1888) [clade04] Figs 18a-c

1888 *Helix plebicola* Locard, Ann. Soc. Linn. Lyon, (N.S.) 34 ["1887"]: 366-368. Type locality: "Tenay, le Colombier, dans l'Ain; les alluvions du Rhône au nord de Lyon; Évian, dans la Haute-Savoie; Bief-du-Four, dans le Jura; l'Aube."

Type specimens: MNHN XXXXXX (D = 9.35 mm), coll. Locard. We herewith select Tenay (Ain) as type locality for *H. plebicola*. All our specimens originate from localities around Tenay in Dept. Ain and thus are considered to constitute topotypes.

Trochulus plebicola has a pale brown shiny shell without hairs. The shell is globular and finely striated. Shell width of the two investigated specimens are 9.19 mm and 9.89 mm and shell height 6.23 mm respectively 6.75 mm. All measurements can be found in the appendix (supplementary material II). Adult specimens have six whorls. The umbilicus is narrow and open. The body is greyish.

Distribution (Fig. 14): *Trochulus plebicola* has been recorded from three localities in a very small area in the southwestern French Jura. However, this may be a collection bias as we have no records of *Trochulus* specimens between Lyon and Aix-les-Bains.

Remark: We have selected Tenay as type locality of this species. The other places recorded by Locard are unprecise or based on confusion with similar species.

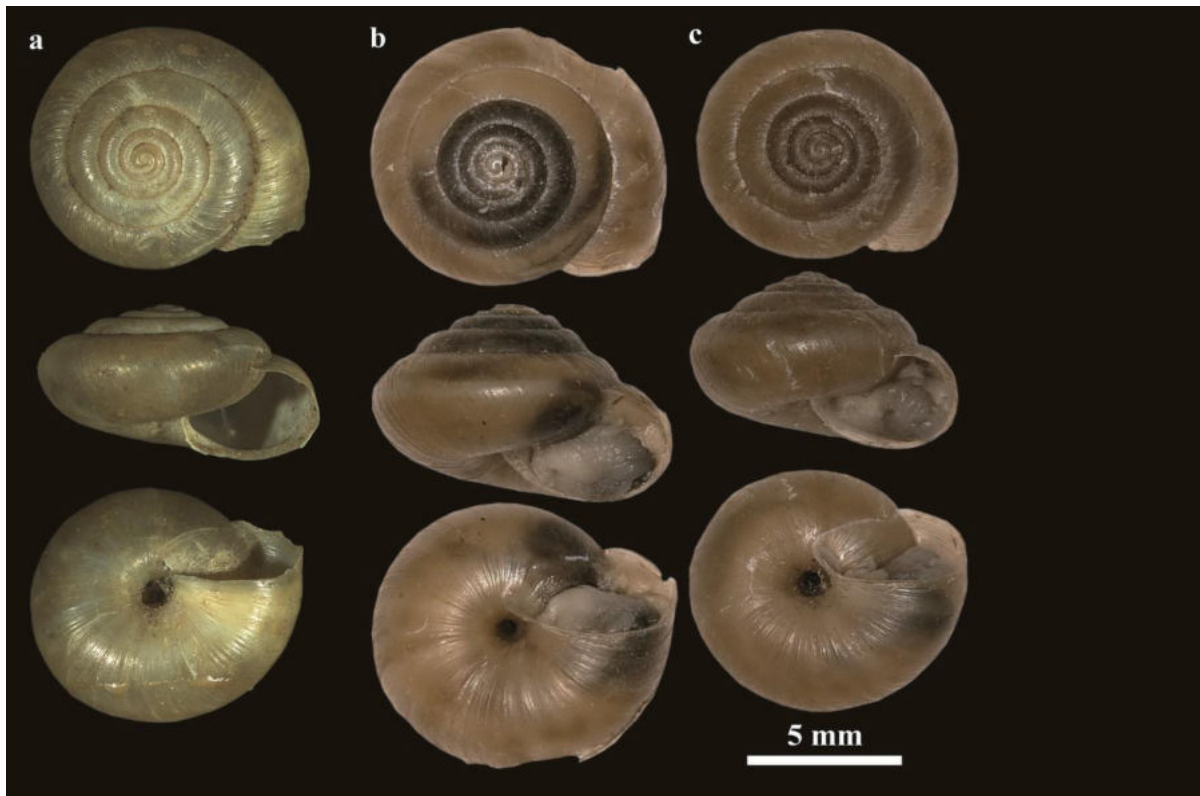


Figure 18: *Trochulus plebicola*. Clade04; (a) MNHN XXXXXX; France, Tenay; (b) MNHW_F.15.42a_03; France, Arandas; (c) MNHW_F.15.42a_04; France, Arandas.

Trochulus pascali (Mabille, 1867) [clade05] Figs 19a-h

1867 *Helix pascali* Mabille, Arch. malac., fasc. 2: 29–30 [Cette espèce habite les lieux frais et montueux de l'est de la France; nous l'avons reçu de Saint-Amour (Jura) et de Bellegarde (Ain)].

1868 *Helix submontana* Mabille, 1868, Rev. Mag. Zool.: (2) 20 (1): 22-23 [Saint-Amour (Jura) et de Bellegarde (Ain); published as *Helix pascali* by Mabille in Arch. malac., fasc. 2: 29–30 (1867)].

1882 *Helix silanica* Bourguignat in Locard, 1882, Prodrome de malacologie française. [I]. Catalogue général des Mollusques vivants de France. Mollusques terrestres, des eaux douces et des eaux saumâtres: 314 [Lac de Silan près de Nantua].

Type specimens: Lectotype MNHN [to be completed].

Description: The specimens of *T. pascali* have a brown shell with fine strips. Some of the specimens have short, straight hairs. The shell is roundish-conical and contains 5–6 whorls. Shell width of the investigated specimens range from 7.49–10.97 mm and shell height from 4.07–7.19 mm (N = 10). All measurements can be found in the appendix (supplementary material II). The umbilicus is narrower compared to the species *T. circinnatus*, *T. montanus* and *T. clandestinus*. The body is pale grey to dark grey.

Distribution (Fig. 14): Most records of this species come from the Haute Jura in France and the neighbouring area in Switzerland. This species is also recorded from the Central Swiss area from Bern to Lausanne but is probably introduced there.

Remark: We herewith select the specimen MNHN XXXXX as lectotype. Our sampling shows that the species lives in partial sympatry with *T. montanus*, *T. circinnatus*, *T. villosus*, and *T. plebeius*.



Figure 19: *Trochulus pascali*. Clade05; (a) TYPE?; (b) MNHW_F.15.33_06; France, Les Rousses-d'Amont; (c) MNHW_F.Col_228; France, Col. De Vac.; (d) MNHW_F.15.38_05; France, Chaux-des-Crotenay; (e) MNHW_F.15.39_01; France, Cascades du Hérisson; (f) MNHW_F.15.47_05; France, Jalinard; (g) MNHW_F.15.39a_01; France, Cascades du Hérisson; (h) MNHW_F.15.47_04; France, Jalinard.

Trochulus caelatus (S. Studer, 1820) [clade06] Figs 20a-c

1820 *Glischrus* (*Helix*) *caelata* S. Studer, 1820, Syst. Verz. Schweizer-Conchylien: 12 ["Auf dem Jura, in Wäldern, an feuchten Felsen"; Lectotype selected by Forcart (1957: 194), who also restricted the type locality based on a manuscript of Studer: "Kt. Bern, Birstal unterhalb Moûtier, an Felsen"]

1821 *Helix coelata* by Hartmann, in: Steinmüller, Neue Alpina, 1: 236, pl. 2 fig. 12 ("in den Gebirgen des Bernerobersandes und auf dem Jura") misspelling, non *Helix coelata* Vallot, 1801].

Type specimen: Lectotype NMBE 15419 (D = 8.2 mm).

Trochulus caelatus is characterised by its strongly flattened, discoidal shell, the wide, open umbilicus and the absence of hairs. The shell is pale brown to greyish with fine strips. Shell width of the two investigated specimens is 7.8 mm and 8.93 mm and shell width 3.67 mm respectively 4.52 mm. The diameter of the type specimen is 8.2 mm. All measurements can be found in the appendix (supplementary material II). The body whorl height accounts for about 90% of the shell height. The last whorl is clearly separated in width from the previous whorls. The body is black.

Distribution (Fig. 21): *Trochulus caelatus* is an endemic species in Switzerland only known around Moutier in the canton Jura and Solothurn.

Habitat: The species lives in shaded limestone habitats (Proćków 2009).

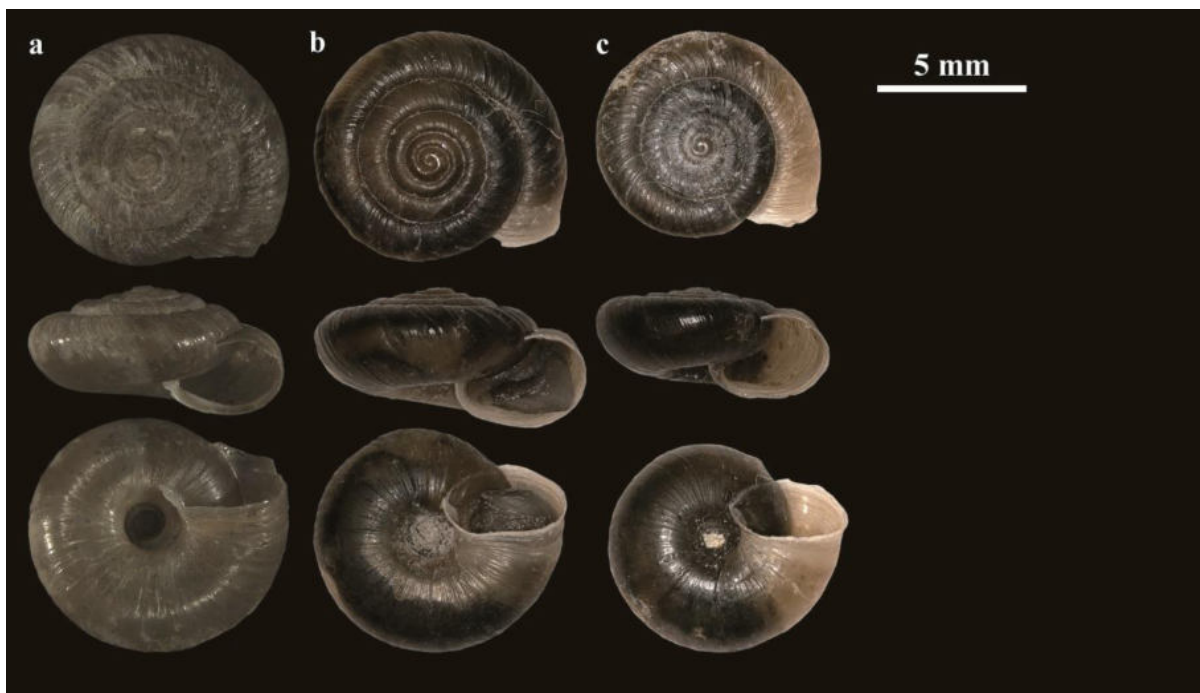


Figure 20: *Trochulus caelatus*. Clade06; (a) Lectotype NMBE 15419; Switzerland, «Auf dem Jura»; (b) MNHW_S.15.21_01; Switzerland, Gorges de Moutier; (c) MNHW_S.15.21_02; Switzerland, Gorges de Moutier.

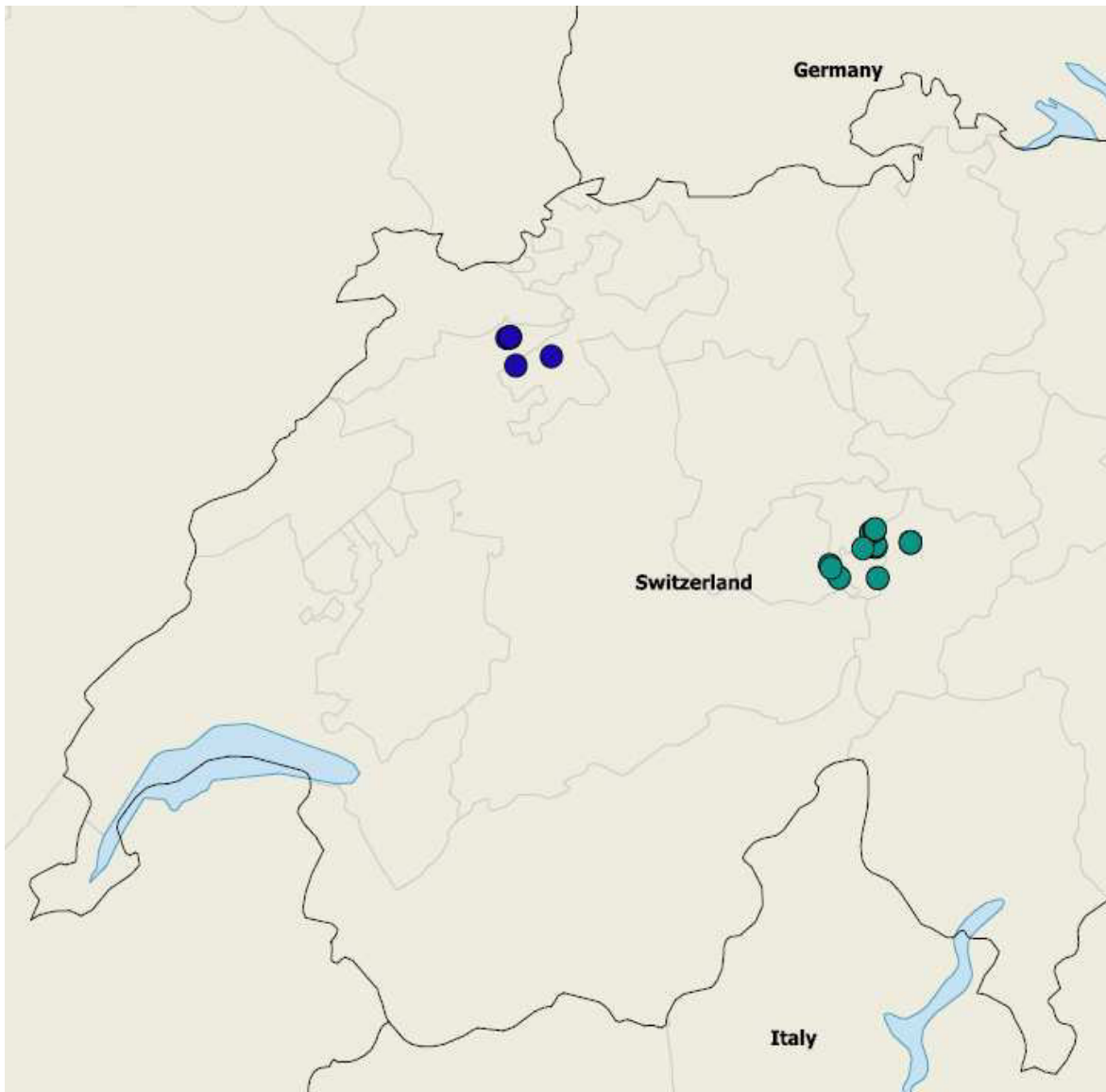


Figure 21: Distribution map of the investigated *T. caelatus* (dark blue circles) and *R. biconica* (turquoise circles).

Trochulus sericeus (O. F. Müller, 1774) [clade07] Figs 22a-f

1774 *Helix sericea* O. F. Müller, 1774, Verm. terr. fluv.: 2: 62–63 [“agri Fridrichsdalensis, sue Daniae”].

1871 *Helix* [*Trichia*] *liberta* Westerlund, Fauna moll. terr. fluv. Sveciae Norvegiae Daniae: 1: 83, 139–140 [prov. Skåne: near Lund].

1874 *Helix* [*Fruticiola*] *septentrionalis* Clessin, Jahrb. dtsh. malakozool. Ges.: 1 (4): 311–312 [Pyrmont, (Norddeutschland), Fredricksdal (Dänemark), Bolteberga, Kinnekulle und Skane (in Schweden), Corbach, Cöln, Breidenstein, Sternberg bei Lemgo (Deutschland); described as having a rather narrow umbilicus].

Type specimens: Syntype *Helix sericea* ZMUC-GAS-670. This type specimen cannot be the original specimen of Müller because it is a juvenile shell of *Monachoides incarnatus* (O. F. Müller, 1774). In his description, Müller talks about the hairs on the shell: “Testa cornei transparentis coloris, aliquantum carinata; pelluciditas carinae major fasciam pallidam mentitur; tota resta tomento minutissimo obtegitur, hoc tamen oculo armato & certo situ, quovis pilo resplendente, tantum conspicitur“ which translates to “Shell of transparent horn colour, somewhat keeled; the transparency of the keel resembles a bright band; the rest of the [shell] is covered with a fine felt, but this is visible only with the armed eye and when the [shell] is in a fixed position, on which each hair shines brightly”. This proves that Müller’s shell was haired, so ZMUC-GAS-670 cannot be the type. Additional research in Müller’s (and Fabricius’ collection, who bought the collection of Müller) surfaced no specimens that could be selected as lectotypes (Tom Schiøtte, pers. comm. Dec. 2021).

For almost a century or longer, the name was attributed to Draparnaud as taxonomic author. However, reading his text it becomes clear that it is an almost verbatim copy of Müller’s text. Certainly, Draparnaud never intended to describe a new taxon; he also does not specify where this species should be living in France.

To stabilize the application of this widely used name, we herewith select the sequenced topotype specimen NMBE 571112 (D = 7.13 mm) as neotype of *Helix sericea* O. F. Müller, 1774.

Description: The sequenced specimens of *T. sericeus* have a brown to greyish, shiny shell. Most of the shells are covered by short, straight hairs. The shell is rather globular with a narrow umbilicus. Shell width ranges from 7.13–8.74 mm and shell height from 4.26–5.51 mm (N = 6). All measurements can be found in the appendix (supplementary material II). The body is pale grey with dark patches.

Distribution (Fig. 23): *Trochulus sericeus* is found in Denmark (Fredriksdal), at the Baltic Sea, in Saxon Switzerland, southern Germany (Black Forest and Bavaria), eastern Switzerland, Tyrol, Austria and Hungary.



Figure 22: *Trochulus sericeus*. Clade07; (a) topotype NMBE 571112; Denmark, Frederiksdal, Furesø; (b) MNHW_A.Gens_201; Austria, Genabend-Sibratsgfäll; (c) MNHW_G.17.05_298; Germany, Pfatter; (d) MNHW_G.17.17_228; Germany, Thannlehen b. Berchtesgaden; (e) MNHW_G.Ott_227; Germany, Ottendorf; (f) MNHW_Re5; Germany, Reichenau.



Figure 23: Distribution map of the investigated *T. sericeus* specimens.

Trochulus albulus (S. Studer, 1820) [clade08] Figs 24a-h

1820 *Glischrus (Helix) albula* Studer, Syst. Verz. Schweizer-Conchylien: 12 ["Ich fand es an schattigen Rainen um Bern"; Lectotype selected by FORCART (1957: 194)].

1821 *Helix charpentieri* W. Hartmann, Neue Alpina: 1: 236 ["bey St. Maurice in Wallis" (ex. Charpentier)].

1821 *Helix glabra* W. Hartmann, Neue Alpina: 1: 238 ["Ich fand sie bey St. Gallen und erhielt sie auch von Bex und aus der Gegend von Joerdon"; junior homonym of *Helix glabra* Gmelin, 1790 In: Linnaeus, Systema Naturae, ed. 13, l: 3658].

1821 *Helix similis* W. Hartmann, Neue Alpina: 1: 237 [in der ganzen Schweiz].

1842 *Trichia erecta* W. Hartmann, Erd- und Süssw.-Gaster. Schweiz: 5: 129 [“Neuwied”; “kommt in dem Jura des Kantons Waadt in der Schweiz, besonders in Val de Joux vor”; “Wien”; “England”].

1855 *Helix pratensis* Dumont, Bull. Inst. natn. genevois: 3: 355 [Sur le sommet des montagnes nues, comme au Méry dans la région des gazons; junior homonym of *Helix pratensis* L. Pfeiffer, Proc. Zool. Soc. London, XIII (153) Feb. 1846, 132].

1864 *Helix phorochaetia* Bourguignat, Malac. Grande-Chartreuse: 52-54, pl. 6 figs 9-14 [le long des sentiers de Saint-Bruno et de Chartreuse].

1882 *Helix vocoutiana* Bourguignat in Locard, Prodr. malac. française: 1: 76, 317 [La Salette près Corps, Isère].

2005 *Trochulus piccardi* Pfenninger & Pfenninger, Archiv für Molluskenkunde: 134 (2): 264-268, figs 2-5 [Chateau d'Oex, Hügel um die Kirche].

Type specimen: Lectotype NMBE 15461 (D = 7.3 mm); Switzerland, “Um Bern”

Description: *Trochulus albulus* is characterized by a globular shell with short, slightly curved hair. The shell of the type specimen lost its hairs, but hair scars are still visible. Shell width ranges from 6.37–8.91 mm and shell height from 3.95–5.92 mm (N = 21). All measurements can be found in the appendix (supplementary material II). The shell contains 4.75–6 whorls and a narrow umbilicus, which is slightly covered by the bent aperture. Some of the specimens have a strong callus. The body is pale grey with dark spots.

Distribution (Fig. 25): *Trochulus albulus* is found everywhere in Switzerland except in Ticino. The species is further found in Austria (Vorarlberg), south-western Germany as far as Frankfurt am Main and western France with its southern most record from the district of Aveyron.



Figure 24: *Trochulus albulus*. Clade08; (a) Lectotype NMBE 15461; Switzerland, “Um Bern”; (b) MNHW_G.15.05_285; Germany, Ketsch; (c) MNHW_S.15.19_11; Switzerland, Gorges de Court 3; (d) MNHW_Sau1; Austria, Sausteig; (e) NMBE 569689; Switzerland, Stansstad; (f) NMBE 569677; Switzerland, Schwarzwasser; (g) NMBE 571095; Switzerland, Grimentz; (h) MNHN-IM-2013-76922; France, Saint-Laurent-du-Pont.

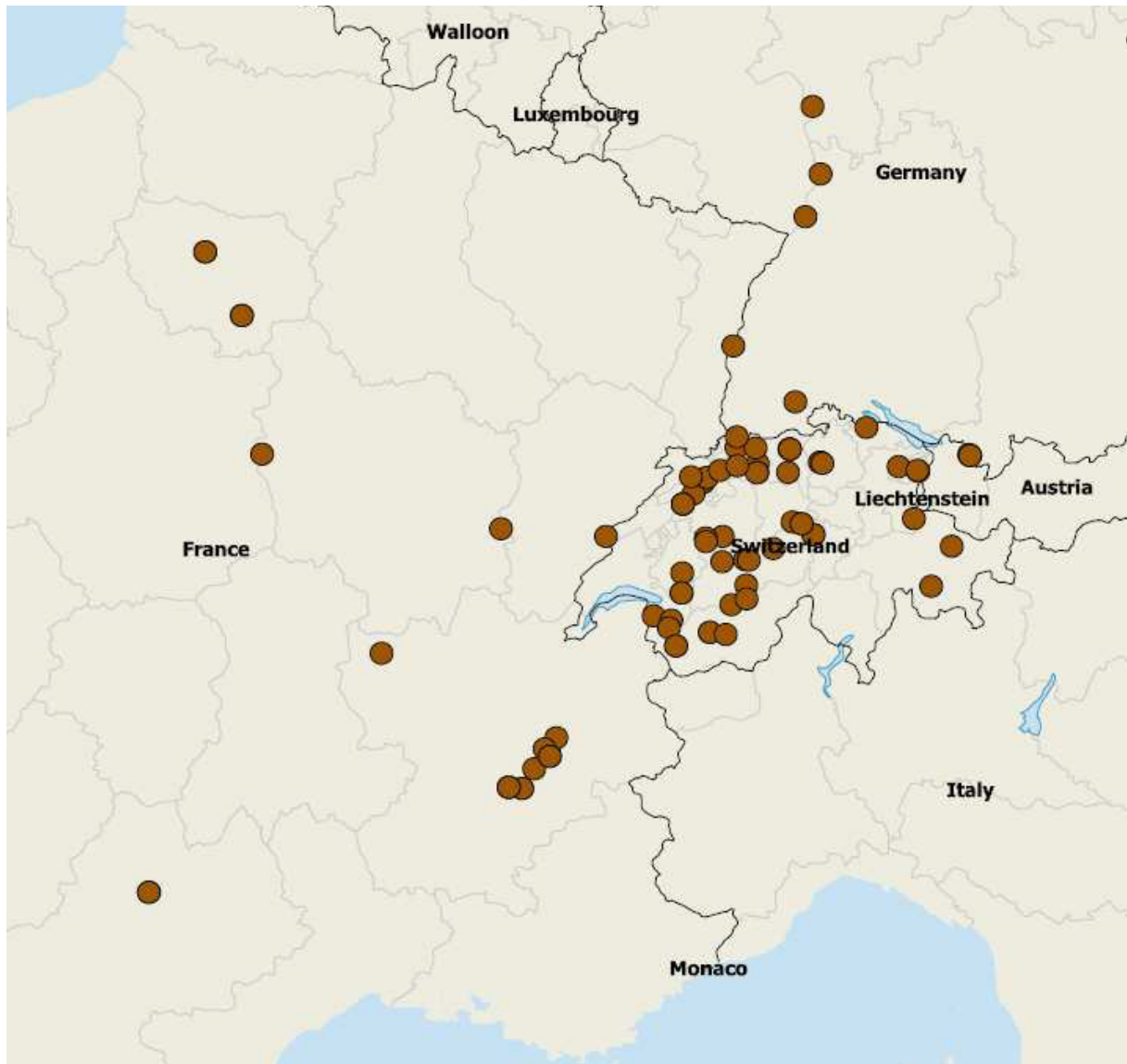


Figure 25: Distribution map of the investigated *T. albulus* specimens.

Trochulus dubia (Clessin, 1874) [clade09] Figs 26a-c

1874 *Helix* [*Fruticiola*] *dubia* Clessin, Jahrb. dtsh. malakozool. Ges.: 1 (4): 327–328, pl. 13 fig. 1 [Sillschlucht bei Innsbruck].

1874 *Helix* [*Fruticiola*] *corneola* Clessin, Jahrb. dtsh. malakozool. Ges.: 1 (4): 326–327, pl. 13 fig. 2 [Eibsee].

1874 *Helix* [*Fruticiola*] *expansa* Clessin, Jahrb. dtsh. malakozool. Ges.: 1 (4): 326, pl. 12 fig. 5 [Dietsamszell].

Type specimen: [not yet investigated].

The investigated specimens of *T. dubia* have a globular shell with short, straight hairs. The umbilicus is wide and open. The inner whorls are not clearly visible. Shell width ranges from

6.92–7.73 mm and shell height from 4.18–4.98 mm (N = 3). All measurements can be found in the appendix (supplementary material II). The body is pale grey with dark spots.

Distribution (Fig. 27): *Trochulus dubia* is found in Bavaria along the river Danube, in western Austria. Single records were made in Potsdam (Germany), Carmel (UK), and Lussat (Central France).

Remark: the denomination of *dubia* Clessin, 1874 is based on a topotypic sequence by Kruckenhauser et al. (2014) from near Innsbruck.

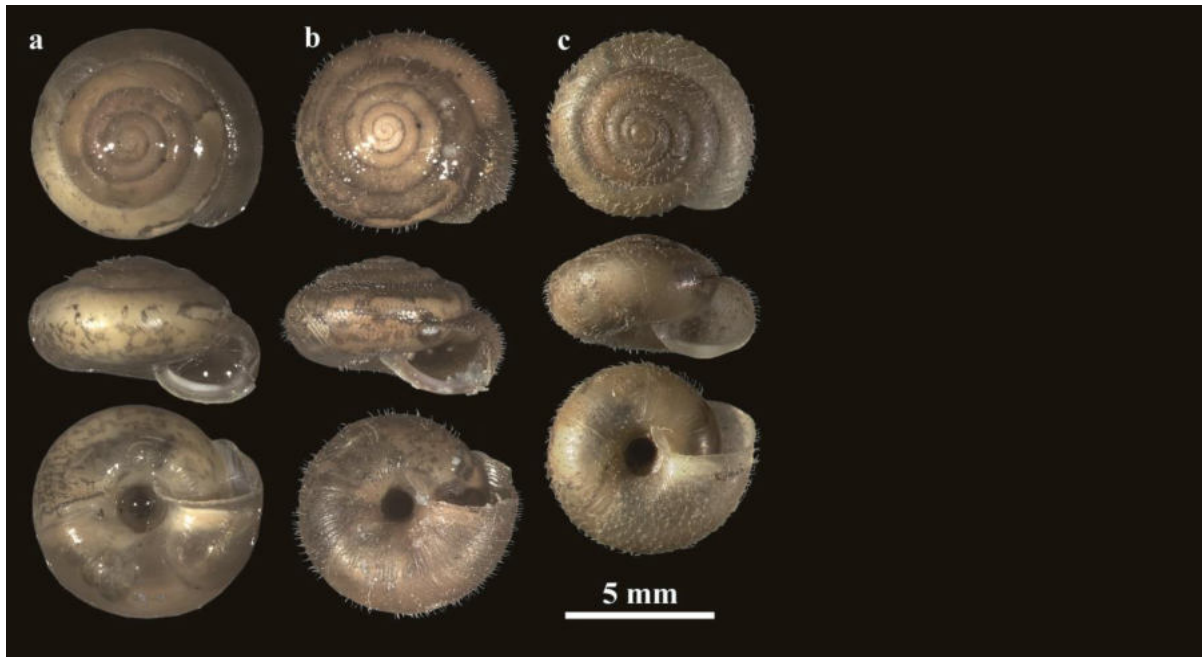


Figure 26: *Trochulus dubia* (Clessin, 1874). Clade09; (a) NMBE 571108; Germany, Diessen am Ammersee; (b) NMBE 571125; United Kingdom, Carmel; (c) MNHW_G-Mo5; Germany, Moosburg.

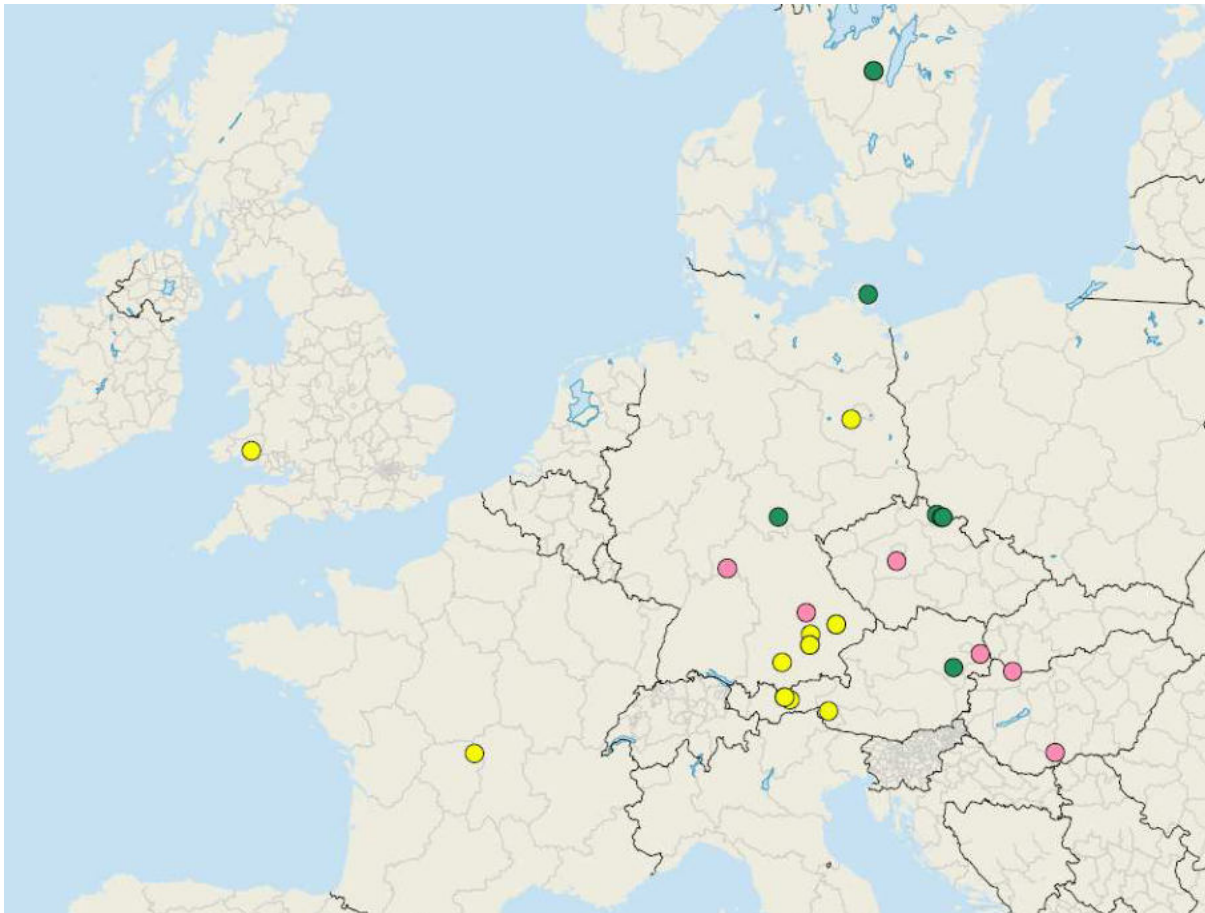


Figure 27: Distribution map of the investigated *T. dubia* (yellow circles), *T. sp. 1* (light pink circles) and *T. sp. 2* (forest green circles) specimens.

Trochulus hispidus (Linnaeus, 1758) [clade10] Figs 28a-h

1758 *Helix hispida* Linnaeus, Systema Naturae: 10: 771 ["Svecia"].

1840 *Helix pallida* Picard, Bull. Soc. linn. Nord France: 1 (3): 228 [type locality not mentioned; junior homonym of *Helix pallida* E. Donovan, 1803].

1841 *Helix conoidea* J. Brown, Ann. Mag. nat. Hist.: (1) 7 (45): 428, 429, pl. 2 fig. 4 ["beds which compose the fluvio-marine deposit at Clacton, on the eastern coast of Essex"; junior homonym of *Helix conoidea* Draparnaud, 1801].

1856 *Helix* [*Zenobia*] *subrufa* Moquin-Tandon, Hist. nat. Moll. terr. fluv. France: 2 (5): 224 [type locality not mentioned; refers to Draparnaud, 1805, Hist. nat. moll. terr. fluv. France: 104 sub *Helix hispida* var. β and Picard, 1840, Bull. Soc. linn. Nord France, 1 (3): 228 sub *Helix hispida* var. *minor*].

1856 *Helix* [*Zenobia*] *rufescens* var. *rubens* Moquin-Tandon, Hist. nat. Moll. terr. fluv. France: 2 (5): 206, 207 [environs de Boulogne].

1862 *Helix conica* Jeffreys, Brit. Conch.: 1: 199 ["At the roots of *Rosa spinosissima* on the sand-hills near Swansea"; junior homonym of *Helix conica* Draparnaud, 1801].

1862 *Helix conica* Baudon, Mém. Soc. acad. Archéol. Sci. Arts Dépt. Oise: 5: 192 ["Prairie d'Hondainville"; junior homonym of *Helix conica* Draparnaud, 1801].

1862 *Helix decora* Baudon, Mém. Soc. acad. Archéol. Sci. Arts Dépt. Oise: 5: 191 [dans la forêt de Hez, près de La Garde; junior homonym of *Helix decora*, Ziegler in E. A. Rossmassler, 1837].

1862 *Helix nana* Jeffreys, Brit. Conch.: 1: 199 [Freshwater, Isle of Wight; junior homonym of *Helix nana* Pennant, 1777].

1862 *Helix nitida* Baudon, Mém. Soc. acad. Archéol. Sci. Arts Dépt. Oise: 5: 191 [Terrain marécageux des bois de Fourneau à Mouy; junior homonym of *Helix nitida* O. F. Müller, 1774].

1862 *Helix pratensis* Baudon, Mém. Soc. acad. Archéol. Sci. Arts Dépt. Oise: 5: 192 [type locality not mentioned; junior homonym of *Helix pratensis* L. Pfeiffer, 1846].

1877 *Helix bellovacina* Mabilie, Bull. Soc. zool. France: 2 (3/4): 305 [in humidis silvisque pagi Compendiaci Galliae].

Type specimens: According to Forcart (1966), the type specimens of *H. hispida* are lost. We consider our specimens from the garden of Linnaeus in Uppsala as topotypes of this taxon. In order to stabilize the application of this name, we herewith designate NMBE 568100 as neotype for *H. hispida*.

Description: *Trochulus hispidus* has a pale brown, shiny shell with short, straight hairs. The shell is roundish-conical with an aperture that is slightly less than half of the shell width. The shell contains fine strips. Shell width of the investigated specimens ranges from 6.72–8.82 mm and shell height from 3.88–5.58 mm (N = 10). All measurements are in the appendix (supplementary material II). The specimens have 5–5.5 whorls. The body pale brown with black spots.

Distribution (Fig. 29): *Trochulus hispidus* is found in southern Sweden with northernmost occurrence at the type locality in Uppsala, in Ireland, at the northern tip of France and in Burgundy near Dijon.

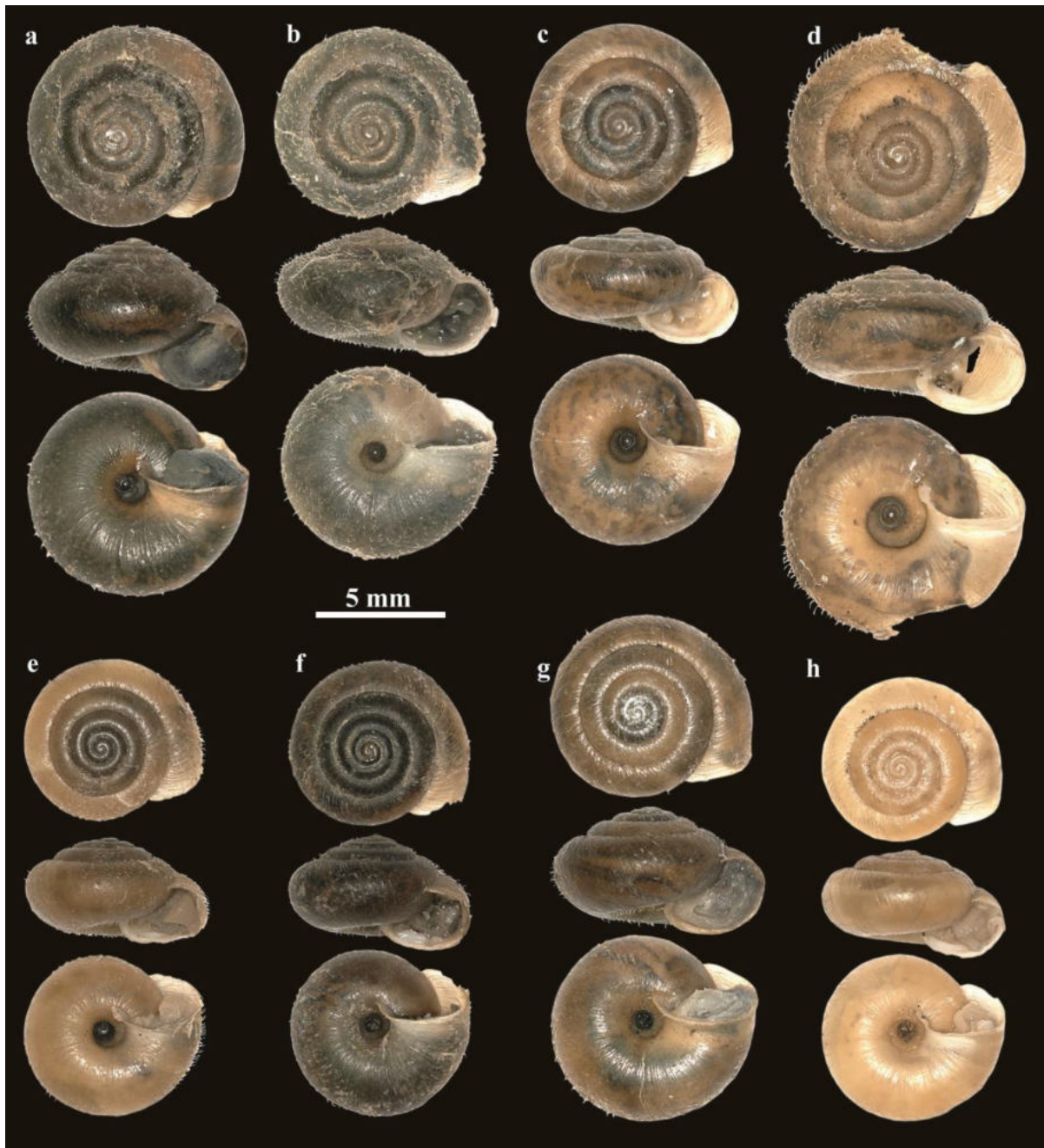


Figure 28: *Trochulus hispidus*. Clade10; (a) MNHW_F.18.05_277; France, Fouquénies; (b) MNHW_F.18.08_221; France, Eaucourt-Sur-Somme; (c) MNHW_I.16.10_232; Ireland, Bealaclogga; (d) MNHW_I.16.3_229; Ireland, Monastery; (e) MNHW_F.18.24_223; France, Le Mont Gournoy 2 (Forêt Indivise d'Eu); (f) MNHW_F.18.14_225; France, Larré; (g) MNHW_F.18.25_279; France, Escames; (h) MNHW_I.16.4_230; Ireland, Rock of Cashel.

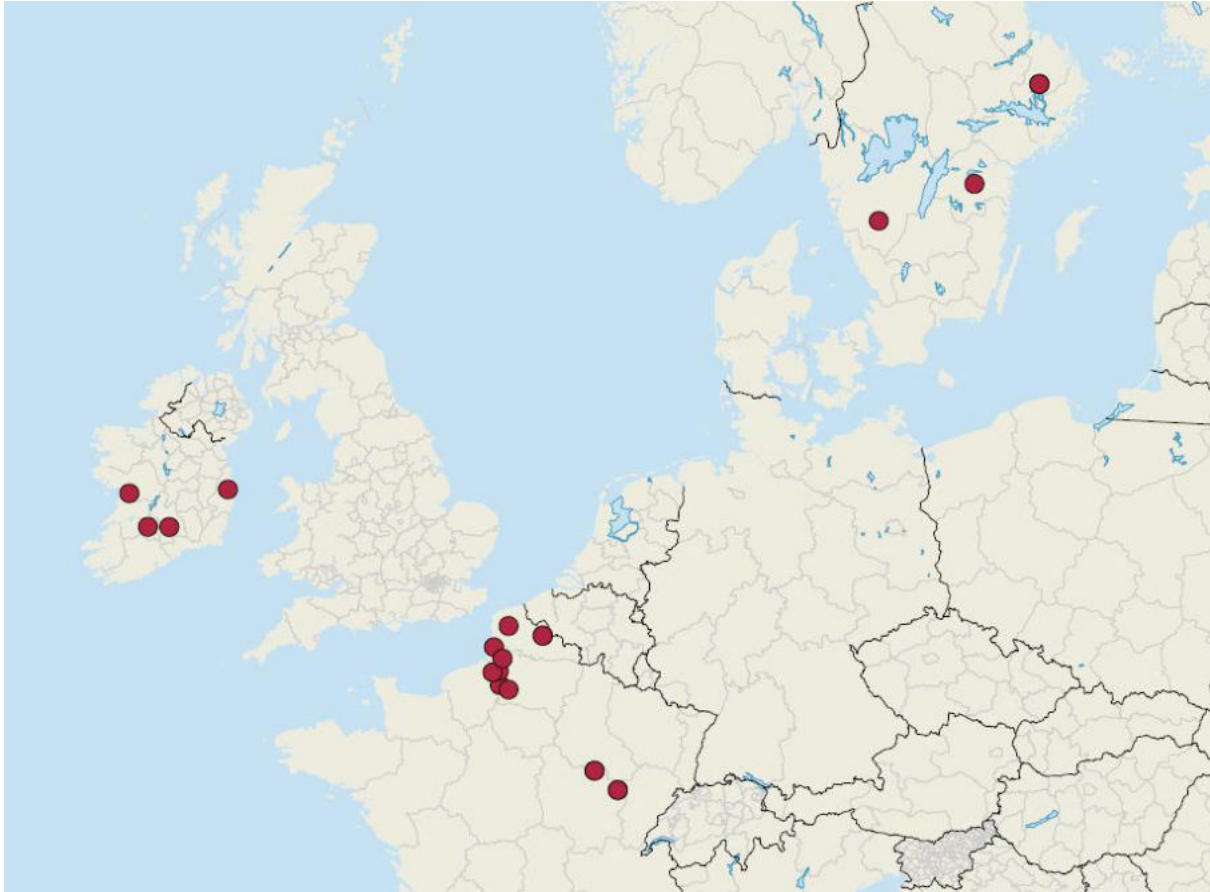


Figure 29: Distribution map of the investigated *T. hispidus* specimens.

Trochulus villersii (De Malzine, 1867) [clade11] Figs 30a-h

1867 *Helix villersii* De Malzine, Essai fauna malac. Belgique: 74 [L'abbaye de Villers].

1868 *Helix fontainei* Colbeau, 1868, Mém. Soc. malac. Belgique: 1: 33, 77 [Papignies, dans les prairies aux bords de la Dendre].

1872 *Helix conoidea* Van den Broeck, Bull. Soc. Malac. Belgique: 6 ["1871"]: XLIV [dans un fossé à Sluys-Kill; junior homonym of *Helix conoidea* Draparnaud, 1801].

1873 *Helix rosea* Van den Broeck, Ann. Soc. Malac. Belgique: 7: LXIII-LXIV [vallée de l'Hermeton].

1888 *Helix abludens* Locard, Ann. Soc. Linn. Lyon, (N.S.): 34 ["1887"]: 334-338 ["en Angleterre de l'île de Jersey; environs de Boulogne-sur-Mer, dans le Pas-de-Calais"; type locality restricted by Proækwó et al. (2021): Boulogne-sur-Mer].

Type specimens: [to be completed].

The investigated specimens of *Trochulus villersii* have a pale brown, finely striated shell. The shell is roundish and contains short, slightly curved hairs. Shell width ranges from 6.83–9.4 mm and shell height from 3.99–5.85 mm (N = 21). All measurements are in the appendix (supplementary material II). The umbilicus is wide and open and the inner whorls are clearly visible. The body is pale brown with dark spots.

Distribution (Fig. 31): *Trochulus villersii* is widely distributed species with occurrence in southern Sweden, southern England, the Netherlands, Belgium, north-eastern France, northern Germany, Czech Republic, Poland, and Slovakia.

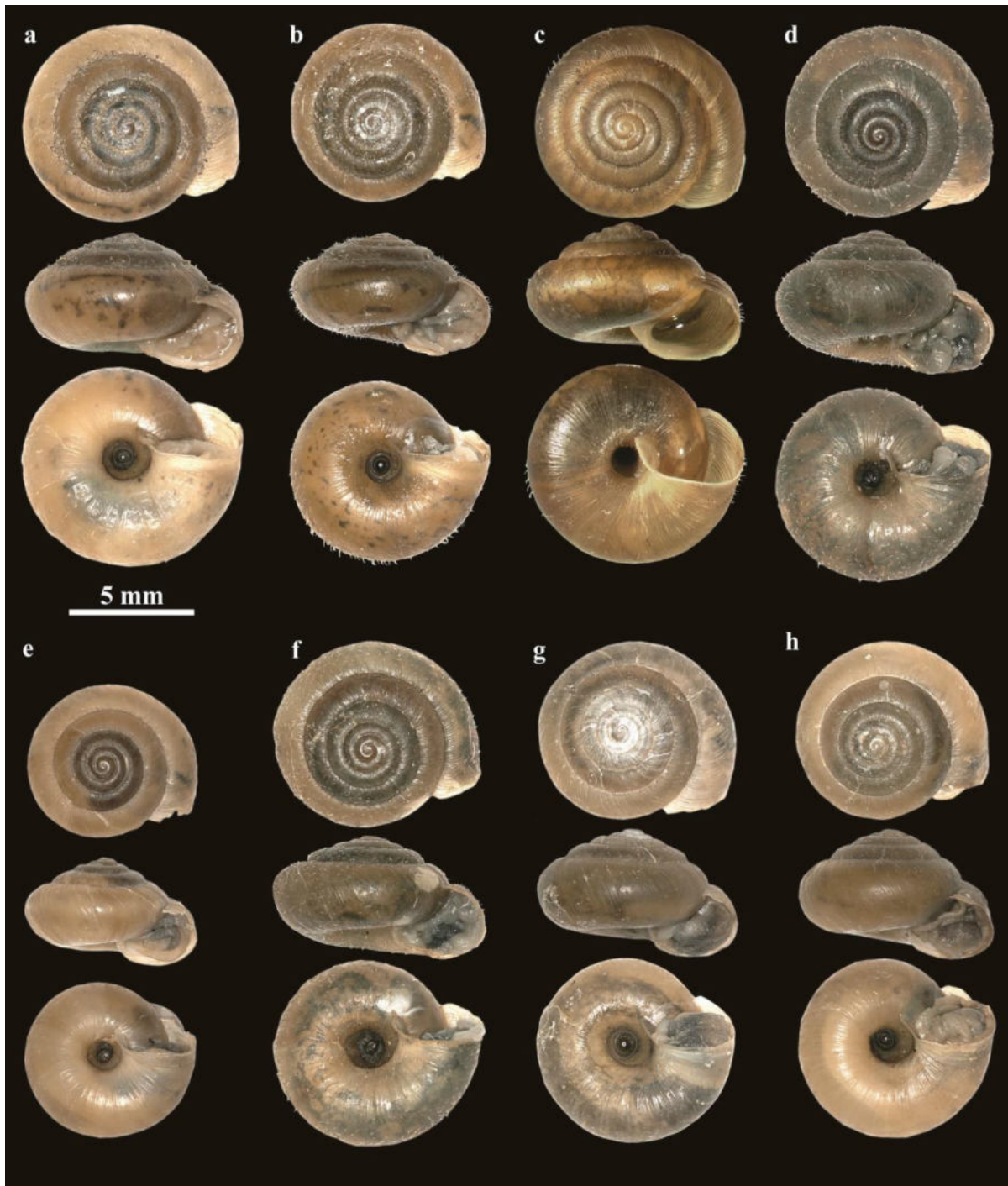


Figure 30: *Trochulus villersii*. Clade11; (a) MNHW_CZ.17.145_212; Czech Republic, Závist; (b) MNHW_CZ.19.43_216; Czech Republic, Debrník; (c) MNHW_UK.En-D_5; United Kingdom, Downside; (d) MNHW_NL.Ost_233; Netherlands, Oestgeest near Leiden; (e) MNHW_F.18.12_224; France, Licques; (f) MNHW_PL.19.10_250; Poland, Małki near Sztum; (g) MNHW_PL.20.22_245; Poland, Stebnik; (h) MNHW_F.15.07_219; France, Bertrange.



Figure 31: Distribution map of the investigated *T. villersii* specimens.

Trochulus sp. 1 (sp. nov.?) [clade12] Figs 32a-c

Type specimen: [to be completed].

Description: The species is characterized by a pale brown, roundish-conical shell. Shell width of the investigated specimens ranges from 7.56–9.27 mm and shell height from 4.6–5.82 mm (N = 3). All measurements are in the appendix (supplementary material II). The umbilicus is wide and open. The body is beige to greyish with small dark dots.

Distribution (Fig. 27): The species is distributed in southern Germany, Czech Republic, eastern Austria, and Hungary.

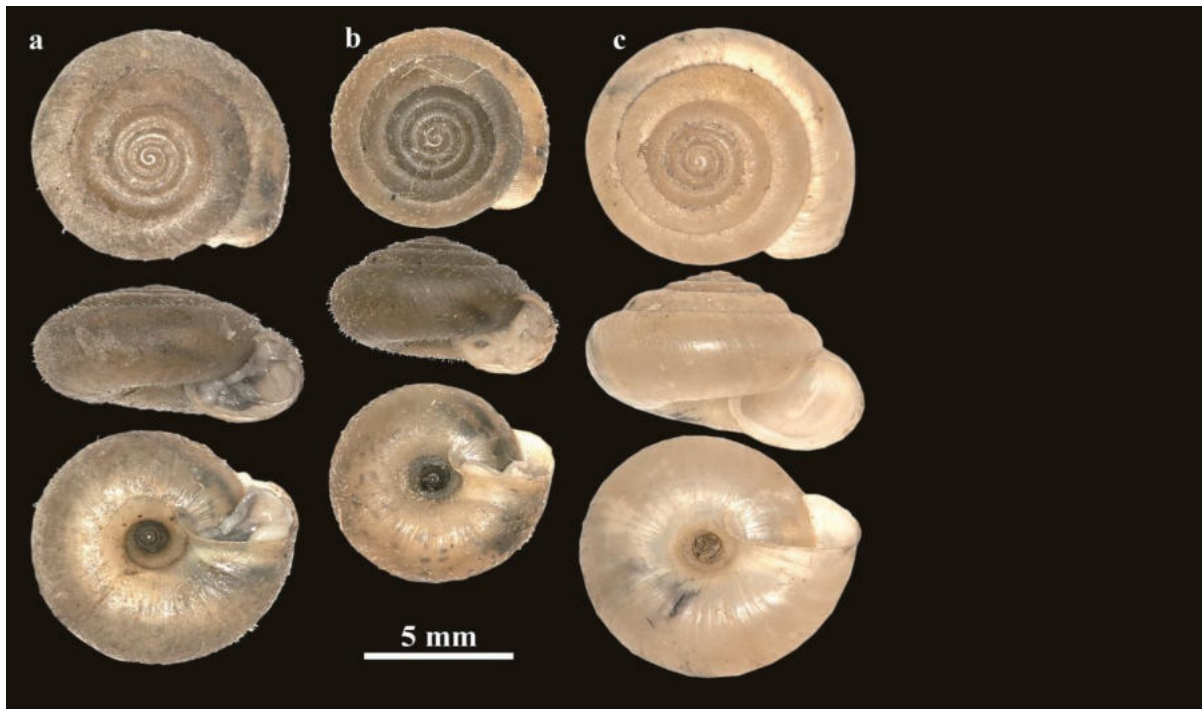


Figure 32: *Trochulus* sp. 1. Clade12; (a) MNHW_SK.19.62_261; Slovakia, Čičov (Čičovský les); (b) MNHW_CZ.19.38_214; Czech Republic, Štěchovice (Maják); (c) MNHW_St-14; Germany, Staubing.

Trochulus sp. 2 (sp. nov.?) [clade13] Figs 33a-d

Type specimen: [to be completed].

Description: The species is characterized by a brown, roundish-conical shell. Shell width of the investigated specimens ranges from 6.87–7.3 mm and shell height from 3.65–4.92 mm (N = 4). All measurements are in the appendix (supplementary material). The umbilicus is narrow and slightly covered by the lip. The body is beige to greyish.

Distribution (Fig. 27): The species is found in southern Sweden, at the Baltic Sea and in Central Germany, in Czech Republic, and eastern Austria.

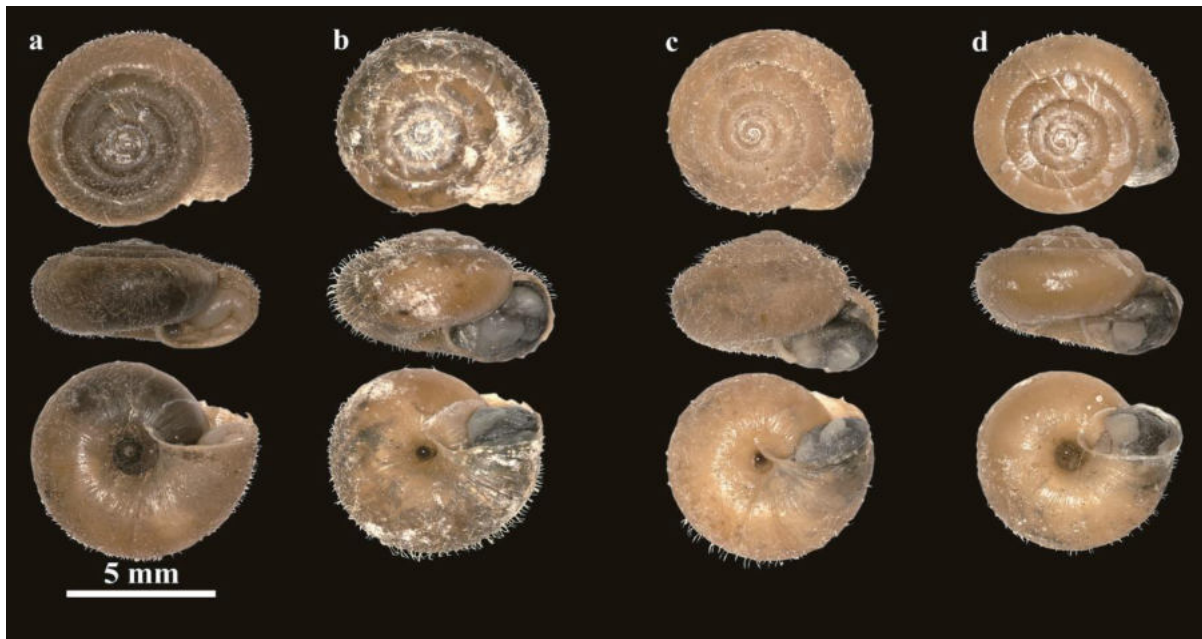


Figure 33: *Trochulus* sp. 2. Clade13; (a) MNHW_A.17.28_203; Austria, Durnbachtal; (b) MNHW_CZ.CD_272; Czech Republic, Černý Důl; (c) MNHW_CZ.Lan_273; Czech Republic, Lánov; (d) MNHW_CZ.Vit_274; Czech Republic, Vitkovice.

Trochulus striolatus (C. Pfeiffer, 1828) [clade14] Figs 34a-f

1828 *Helix striolata* C. Pfeiffer, Naturgesch. dtsch. Land- u. Süßwass.-Moll., 3: 28, pl. VI, fig. 8 ["Bei Heidelberg in ebengelegenen Gärten" (ex Leukart)].

1830 *Helix concinna* Jeffreys, Trans. Linn. Soc. London: (1) 16 (2): 336–337 ["under stones & in dry places in the neighbourhood of Swansea and very plentyfully among the rejectamenta of the Avon river, near Bristol"; "Irish"; homonym of *Helix concinna* Dupuy, 1848]

1841 *Helix rufina* L. Pfeiffer, Symbolae ad historiam Heliceorum: 1: 39 [Germania].

1842 *Trichia imminuata* W. Hartmann, Erd- und Süßw.-Gaster. Schweiz: 5: 130 [Stuttgart].

1842 *Helix complana* W. Hartmann, Erd- und Süßw.-Gaster. Schweiz: 5: 126, 130 ["Stuttgart"; "Neuwied"].

1871 *Helix* [*Trichia*] *gyratus* Westerlund, Fauna moll. terr. fluv. Sveciae Norvegiae Daniae: 1: 138 [prov. Skåne: near Lund].

1874 *Helix* [*Fruticiola*] *subcarinata* Clessin, Jahrb. dtsch. malakozool. Ges.: 1 (3): 181, 189, pl. 8 fig. 6 [Eberbach].

1874 *Helix* [*Fruticiola*] *danubialis* Clessin, Jahrb. dtsch. malakozool. Ges.: 1 (3): 184, pl. VIII, fig. 4 [Bayern, bei Dillingen].

1876 *Helix* [*Fruticiola*] *clessini* Weinland, Jahresh. Ver. Vaterl. Naturk. Württemberg: 32: 285 [Waldtrauf der Vöttelwiese [Wittlingen bei Bad Urach]].

1877 *Helix elaverana* Mabile, Bull. Soc. zool. France: 2 (3/4): 305 [Ivry près Paris].

1877 *Helix goosensis* Mabile, Bull. Soc. zool. France: 2 (3/4): 306 [in locis limpsis ad Firmitatem Adelahidis Galliae" [= La Ferté-Alais]].

1877 *Helix saporosa* Mabile, Bull. Soc. zool. France: 2 (3/4): 305–306 [In silvis pagi Suessoniensis Galliae].

1882 *Helix altenana* Locard, Prodr. malac. française: 79 [dep. Nord: vicinity of Lille; dep. Pas-de-Calais: Boulogne-sur-Mer; dep. Aube: Bar-sur-Seine; Replacement name for *Helix rufescens* sensu Drouët, 1855 (non Pennant); nomen nudum in Locard, 1882; nomen museorum in coll. Bourguignat Geneve].

1888 *Helix coelomphala* Locard, Ann. Soc. Linn. Lyon, (N.S.): 34 ["1887"]: 352–355 [Mt. Righi, Zurich, Lucerne and Jura neuchâtelois; Germany: Dillingen near Saarlouis, Günzburg, Dinkelsbühl; E France: dep. Savoie: environs of Annecy, Chambéry, Aix-les-Bains, Mouxy, Albertville; dep. Isère: vicinity of Grenoble, Sassenage, Saint-Martin-le-Vinoux, Allevard-les-Bains, Grande-Chartreuse, Sappey, Voreppe; dep. Hautes-Alpes: Barcelonnette; dep. Rhône: environs de Lyon, alluvions de Rhône N Lyon, Brotteaux, Sathonay, Pape; dep. Ain: Laumusse, Bugey, alluvions of Suran; dep. Jura: Bief-du-Fourg, Saint-Claude, Poligny; dep. Côte-d'Or: Châtillon-sur-Seine; environs of Paris; Bionville near Metz; dep. Finistère: Brest].

1894 *Helix (Trichia) britannica* Westerlund, Nachrichtsbl. dtsch. malakozool. Ges.: 26 (9/10): 164–165 [London].

1894 *Helix rufescentella* Locard, Coq. terr. France: 128–129 [dep. Nord: Valenciennes and Lille].

1914 *Helix juvavensis* Geyer, Verh. k. k. zool.-bot. Ges. Wien: 65 (5/6): 276–278 [Salzburg, Schafberg].

Type specimens: [to be completed].

Description: *Trochulus striolatus* (clade14) is characterized by a pale brown, roundish-conical shell with coarse ribs. Adult shells are strong and have a strong white lip are They are usually without hairs. Shell width of the investigated specimens ranges from 7.99–11.90 mm and shell height from 4.54–7.3 mm (N = 9). All measurements can be found in the appendix (supplementary material II). The umbilicus is wide and open. The body is beige to greyish.

Distribution (Fig. 35): *Trochulus striolatus* is found Ireland, south England, Germany, northern Switzerland (Schaffhausen), north-east Austria, and Slovakia.

Habitat: The species prefers shaded and humid habitats, lives in forests, along roadsides or under scrubs (Proćków 2009; Proćków et al. 2014).

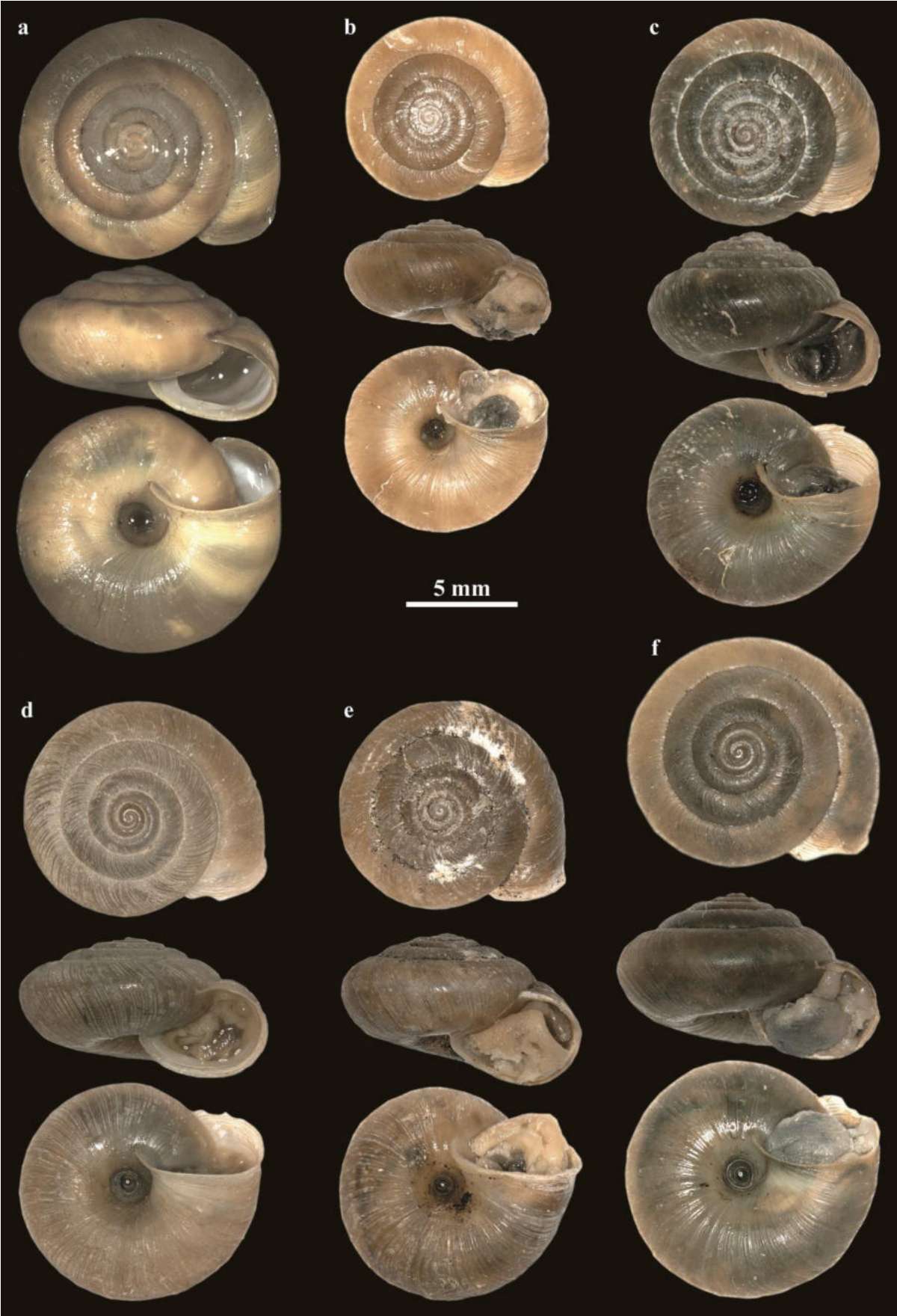


Figure 34: *Trochulus striolatus*. Clade14; (a) NMBE 571160; Germany, Dorsel; (b) MNHW_A.17.12_01; Austria, Schafberg; (c) MNHW_I.16.12_01; Ireland, Maam; (d) MNHW_F.18.10_06; France, Blecquenecques n. Marquise; (e) MNHW_GB.Br_01; United Kingdom, Bramley near Basingstoke; (f) MNHW_SK.19.71_01; Slovakia, Varín.

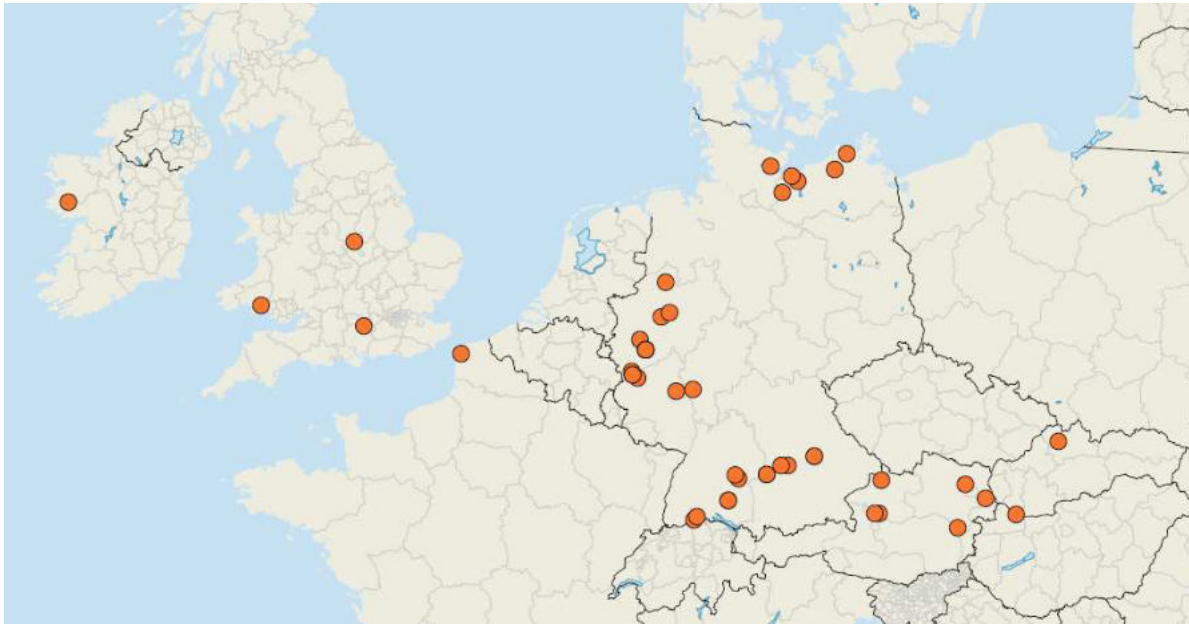


Figure 35: Distribution map of the investigated *T. striolatus* specimens.

Trochulus becasis (Rambur, 1868) [clade15] Figs 36a-d

1868 *Helix becasis* Rambur, Journal de Conchyliologie: 16 (3): 267–268 [Ad basin montis “Canigou” dicti, Galliae].

1869 *Helix vendeana* Letourneux, Revue et Magasin de Zoologie: 21: 60 [Bois-Plat, près de Fontenay-le-Comte].

1877 *Helix steneligma* Mabilie, Bull. Soc. zool. France: 305 [Pyrenees; dep. Oise: in silvis pagi Compendiaci [= probably Compiègne].

1881 *Helix deobrigana* Servain, Moll. Espagne Portugal: 59–60 [fontaine ferrugineuse de Luchon sur le chemin de l’Hospice].

1882 *Helix microgyra* Bourguignat in Locard, Prodr. malac. française: 1: 79, 319 [Val du pic du Gers, B. Pyr.].

1883 *Helix ataxiaca* Fagot, Bull. Soc. Hist. nat. Toulouse: 17: 220 [Quillau, Fanges forest].

1888 *Helix globulosa* Locard, Ann. Soc. Linn. Lyon, (N.S.): 34 [“1887”]: 337 [de l’île de Jersey].

1894 *Helix alixae* Locard, Coq. terr. France: 120 [Loudres].

1894 *Helix pictavica* Bourguignat, Coq. terr. France: 127 [Clain].

Type specimens: [to be completed].

Description: The investigated specimens of *T. becasis* have a roundish-conical shell with fine strips. The shell contains short, straight hair. The mummy in Figure 20a lost its hairs, but hair scars are still visible. Shell width ranges from 8.41–10.67 mm and shell height from 5.31–6.26 mm (N = 4). All measurements can be found in the appendix (supplementary material II). The umbilicus is wide and open. The body is beige with dark spots.

Distribution (Fig. 37): *Trochulus becasis* is found north of the Pyrenees, in Perreux in south-east France and near Orléans in Central France.

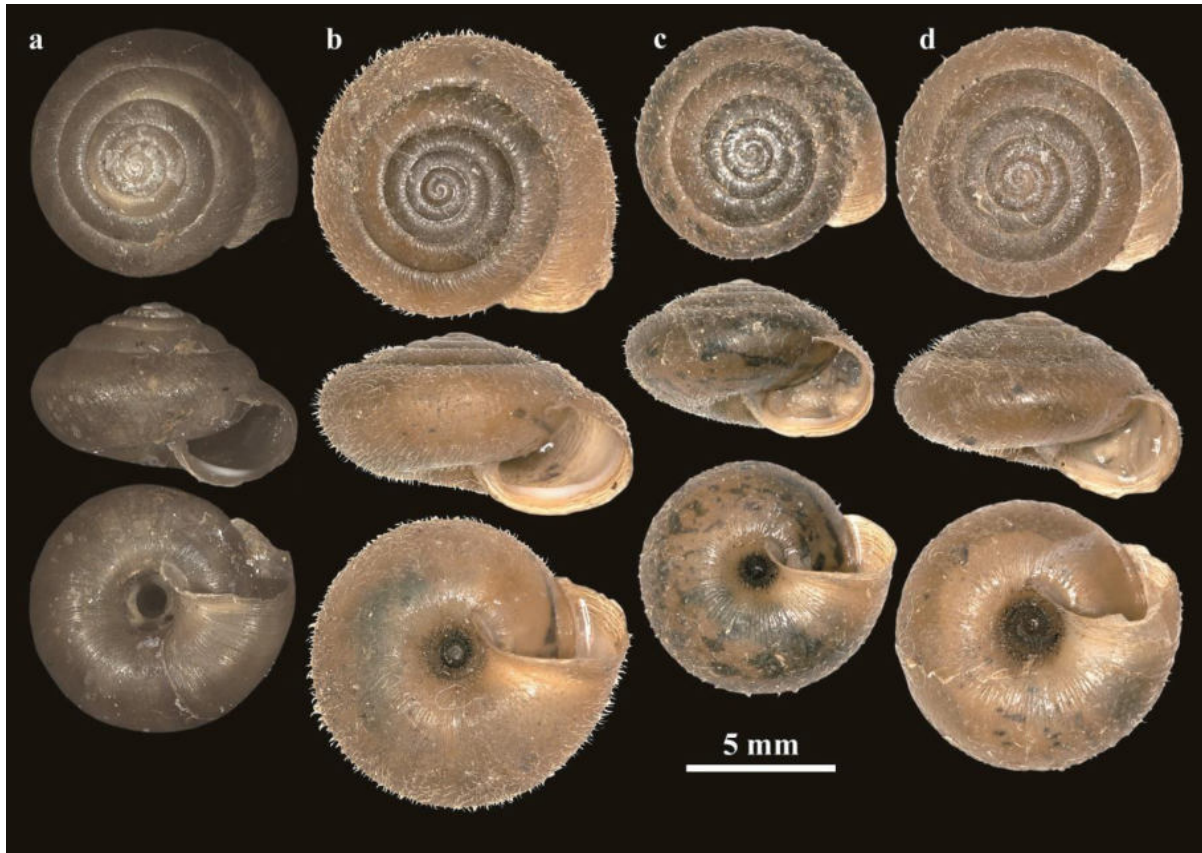


Figure 36: *Trochulus becasis*. Clade15; (a) NMBE 571128; United Kingdom, Jersey; (b) MNHW_F.18.37_301; France, Forêt de Beleste; (c) MNHW_F.18.35_300; France, Le Chandelier; (d) MNHW_F.18.30_299; France, Forêt Bac Estable 2.

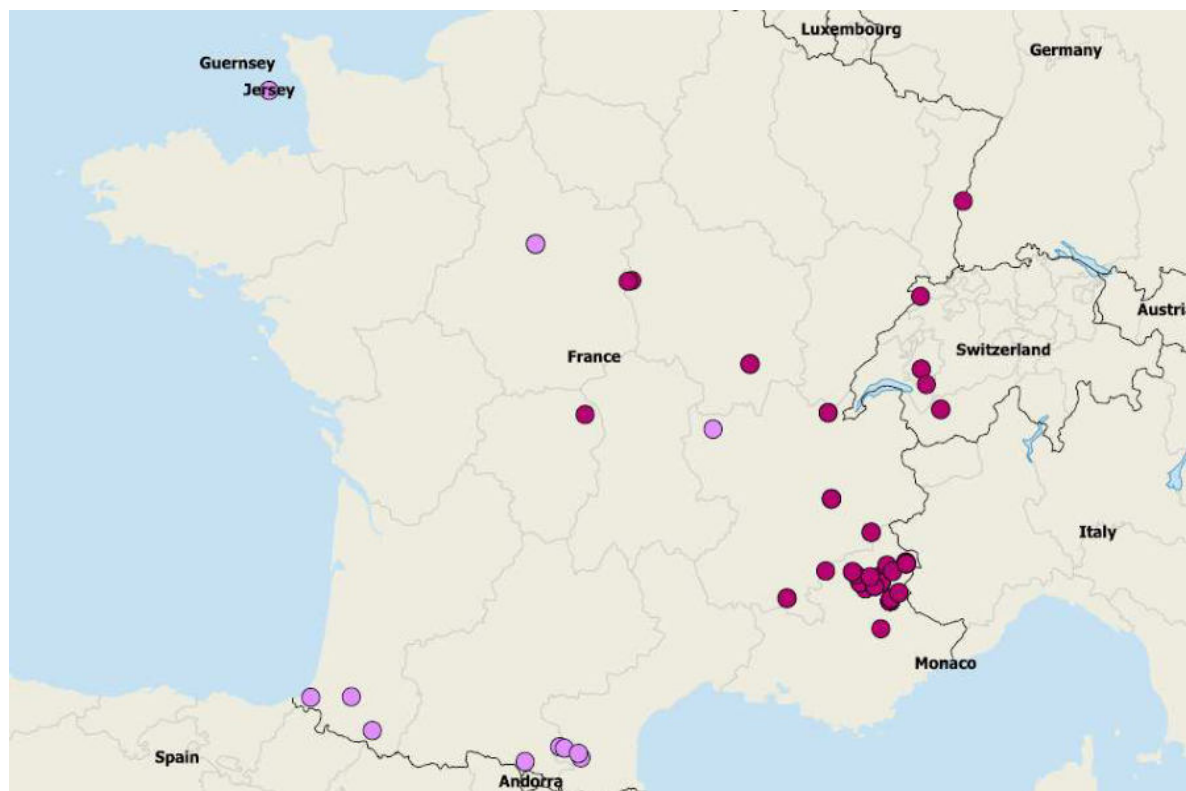


Figure 37: Distribution map of the investigated *T.s becasis* (lilac circles) and *T. plebeius* (bordeaux circles) specimens.

Trochulus plebeius (Draparnaud, 1805) [clade16] Figs 38a-e

1805 *Helix plebeium* Draparnaud, Hist. nat. Moll. terr. fluv. France: 105, pl. 7 fig. 5 [unknown].

1820 *Glischrus (Helix) rudis* Studer, Syst. Verz. Schweizer-Conchylien: 12 [not mentioned; Remark (1): refers to *Helix plebeium* Draparnaud, 1805, pl. 7 fig. 5. Remark (2): name to be treated as a nomen novum? Remark (3): also mentioned by Hartmann, 1821, in: Steinmüller, Neue Alpina, 1: 237, 238; but he refers to Draparnaud, 1805: 104, pl. 7 fig. 21 sub *Helix hispida* var. β].

1826 *Helix prevostiana* Risso: IV: 73 [nos collines [in Dep. Alpes-Maritimes]].

1832 *Helix hispidula* De Cristofori & Jan, Mantissa: 2 [Ital. bor. [northern Italy]].

1855 *Helix hispida* Dumont, Bull. Inst. natn. genevois: 3: 355 [des Alpes; junior homonym of *Helix hispida* Linnaeus, 1758].

1855 *Helix depressula* Dumont, Bull. Inst. natn. genevois: 3: 356 [Mont-Saxonnet, sous l'Eglise, 900 m"; "Brizon, 1100 m"; "St.-Pierre-d'Entremont, 800 m"; "Grande-Chartreuse, 950 m"; "environs de Montiers, 488 m"; "Bramant, 1300 m"; "Mont-Cenis"; "Lanslevillard, de 1500 à 1700 m; junior homonym of *Helix depressula* E. A. Rossmäessler, Iconographie II (3 & 4) Sept. 1839, 6.].

1864 *Helix bourniana* Bourguignat, Malac. Grande-Chartreuse: 54-55, pl. 7 figs 13–17 [le long du sentier de Chartreuse].

1869 *Helix gratianopolitana* Rambur, Journal de Conchyliologie: 17: 267 [dans les environs de Grenoble].

1879 *Helix hemisphaerica* Lessona, Atti r. Accad. Sci. Torino: 15 (2): 295, pl. 7 figs 19-21 [Brossasco].

- 1879 *Helix ripularum* Lessona, Atti r. Accad. Sci. Torino: 15 (2): 293, 294, 296, pl. 6 figs 1-5 [Rivoli (V. della Doria Riparia)].
- 1879 *Helix subcoelata* Lessona, Atti r. Accad. Sci. Torino: 15 (2): 294, pl. 6 fig. 9 [Susa].
- 1879 *Helix subplebeia* Lessona, Atti r. Accad. Sci. Torino: 15 (2): 295, 296, pl. 6 figs 6-8 [Tornino].
- 1879 *Helix trochiformis* Lessona, Atti r. Accad. Sci. Torino: 15 (2): 294, 295, 296, pl. 7 figs 22-24 [Tornino; junior homonym of *trochiformis* *Helix*, Grateloup, Bull. H. N. Soc. Linn. Bordeaux, II (7) 1827].
- 1879 *Helix vulgaris* Lessona, Atti r. Accad. Sci. Torino: 15 (2): 292, 294, 295, pl. 6 figs 16-18 [Tornino; junior homonym of *Helix vulgaris*, E. M. da Costa, Brit. Conch. 1778, 72].
- 1879 *Helix globus* Lessona, Atti r. Accad. Sci. Torino: 15 (2): 296, pl. 7 figs 28-30 [Tornino].
- 1882 *Helix subbadiella* Bourguignat in Locard, Prodr. malac. française: 1: 74, 317 [Alpes Maritimes: Monton].
- 1882 *Helix vendoperanensis* Bourguignat in Locard, Prodr. malac. française: 1: 76, 317 [dep. Aube: Vendeuvre-sur Barse and Viélaines near Rosières; environs de Lyon].
- 1882 *Helix cularensis* Bourguignat in Locard, Prodr. malac. française: 1: 79, 319 [Sassenage près Grenoble].
- 1886 *Helix vagienna* Pollonera, Boll. Mus. Zool. Anat. comp. Univ. Torino: 1 (17): 3 [Purriac, Valle Stura di Cuneo tra 2100 e 2500m].
- 1894 *Helix barcelonnettensis* Bourguignat, Coq. terr. France: 125 [Hauteville (Ain), Albertville (Savoie), Barcelonnette (H. Alpes); photographed specimen from Barcelonnette].
- 1909 *Helix* [*Capillifera*] *maynardi* Caziot, Bull. Soc. zool. France: 34 (5/6): 90, fig. 21 [Mont-Mounier (2.800m); sur le plateau du Demant (2400m)].
- 1910 *Helix* [*Capillifera*] *orzszkoi* Caziot, Moll. terr. fluv. Monaco: 117 [fréquente dans les alluvions du Loup].
- 1910 *Helix* [*Capillifera*] *subniverniaca* Caziot, Moll. terr. fluv. Monaco: 115 [Dans les prés, à l'Est du champ de courses du Var, près du bord de la mer].

Type specimens: The collection of Draparnaud is located in the Natural History Museum Vienna. Under the number NHMW 14828 a syntype of *H. plebeium* is preserved. Investigation of this specimen revealed that it is a specimen of *Urticiola umbrosa*; the original specimen of Draparnaud is not preserved. For this reason, we herewith designate NMBE 569666 (D = 7.86 mm; France, Forest-Saint-Julien; Fig. 38e) as neotype to stabilize the application of the name.

Description: The investigated specimens of *T. plebeius* have a pale brown shell with short, slightly curved hairs. The shell is finely striated. Shell width ranges from 7.51–9.01 mm and shell height from 4.32–4.99 mm (N = 5). All measurements can be found in the appendix (supplementary material II). The specimens have 5.5 whorls. The body is beige with dark spots.

Distribution (Fig. 37): *Trochulus plebeius* is found in the northern area of the province Provence-Alpes-Côte d'Azur and Rhône-Alpes in south-east France, in Central France, and in western Switzerland.



Figure 38: *Trochulus plebeius*. Clade16; (a) MNHW_F-Com_227; France, Chameyer; (b) MNHN-IM-2013-76890; France, Guillestre; (c) MNHW_F-Ech_02; France, Échallon; (d) NMBE 569626; France, Avonçon; (e) neotype NMBE 569666; France, Forest-Saint-Julien.

Trochulus villosulus (Rossmässler, 1838) [clade17] Figs 39a-h

1838 *Helix villosula* Rossmässler, Iconographie: (1) 2 (1/2): 1 [Hungary; name attributed to Ziegler.].

1914 *Fruticicola (Trichia) elatior* Polinski, Spraw. Kom. Fizyogr.: 48: 28 [Ojców].

Type specimens: [to be completed].

Description: *Trochulus villosulus* is characterized by a flattened shell with long hairs. The umbilicus is wide and open and accounts for about 1/5 of the shell diameter. Shell width of the investigated specimens ranges from 6.87–8.92 mm and shell height from 3.96–5.37 mm (N = 9). All measurements can be found in the appendix (supplementary material II). The body is grey with few dark spots.

Distribution (Fig. 40): *Trochulus villosulus* is found in Poland, eastern Czech Republic, Slovakia and Ukraine.

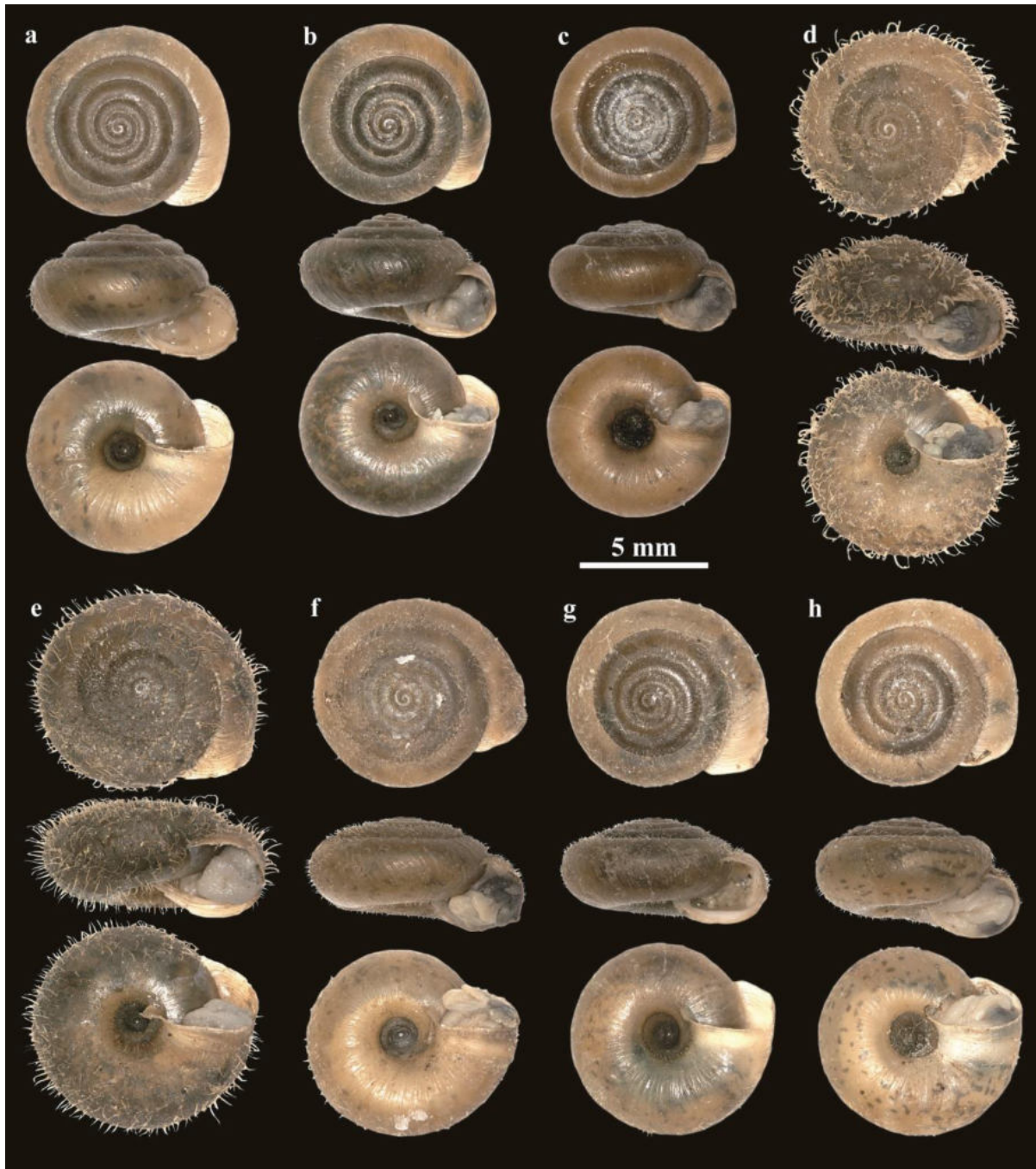


Figure 39: *Trochulus villosulus*. Clade17; (a) MNHW_PL.19.09_257; Poland, Barcin-Górne Wolice; (b) MNHW_PL.20.05_249; Poland, Cisowy Jar; (c) MNHW_PL.20.13_253; Poland, Gamlówka; (d) MNHW_PL.20.16_306; Poland, Wapowce; (e) MNHW_PL.20.32_307; Poland, Muszyna 2 ; (f) MNHW_UA.18.55_264; Ukraine, Bibrka; (g) MNHW_UA.18.56_265; Ukraine, Swirz; (h) MNHW_UA.18.58_267; Ukraine, Mikuliczyn.

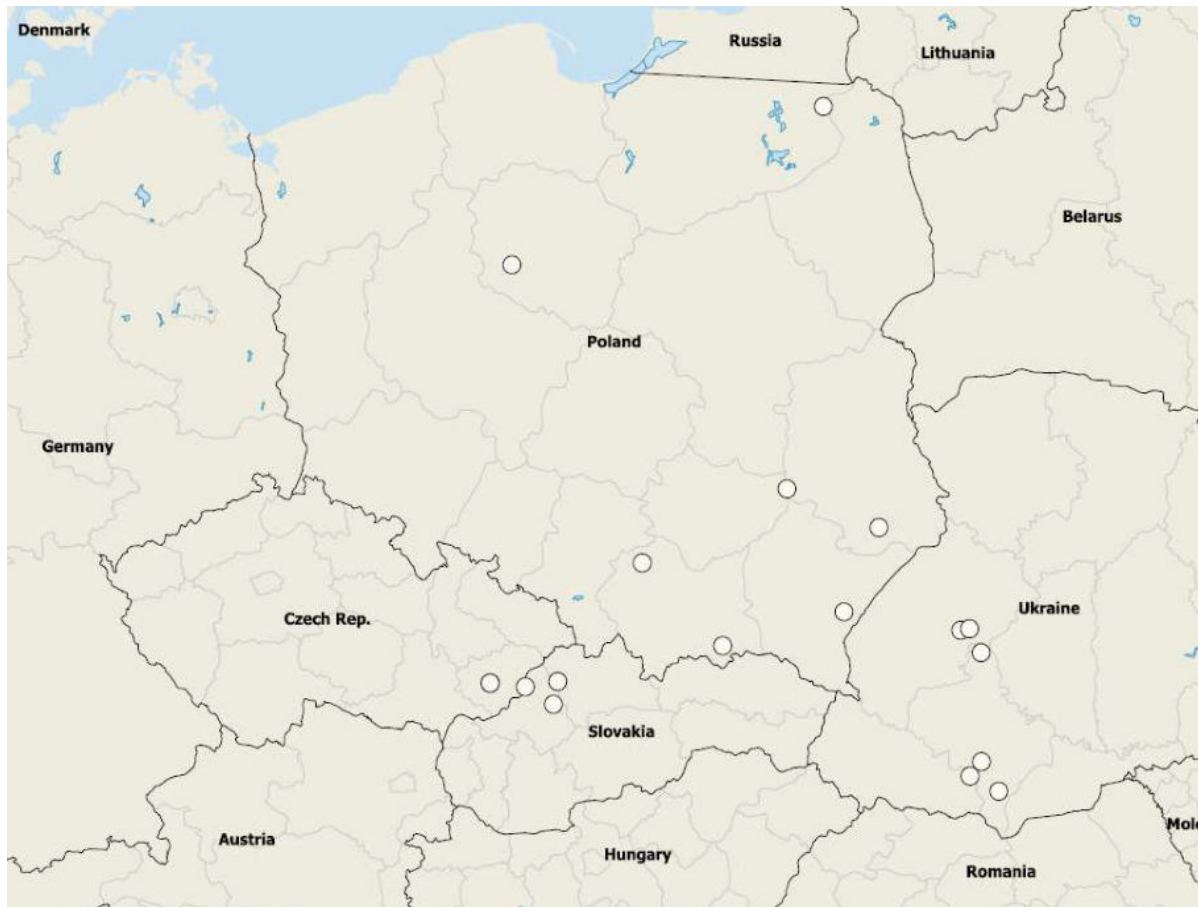


Figure 40: Distribution map of the investigated *T. villosulus* specimens.

Trochulus sp. 3 (sp. nov.?) [clade18] Figs 41a-d

Type specimens: [to be completed].

Description: The shell of the investigated specimens is roundish-conical. Shell width of the investigated specimens ranges from 6.5–9.6 mm and shell height from 3.73–5.99 mm (N = 4). All measurements can be found in the appendix (supplementary material II). The shell comprises of short straight hairs. The umbilicus is wide and open.

Distribution (Fig. 42): The species is found in eastern France in the Alsace, in northern Switzerland, at the Baltic Sea, in the southern Black Forest and southern Bavaria in Germany, and in Vorarlberg and along the Danube near Linz in Austria.

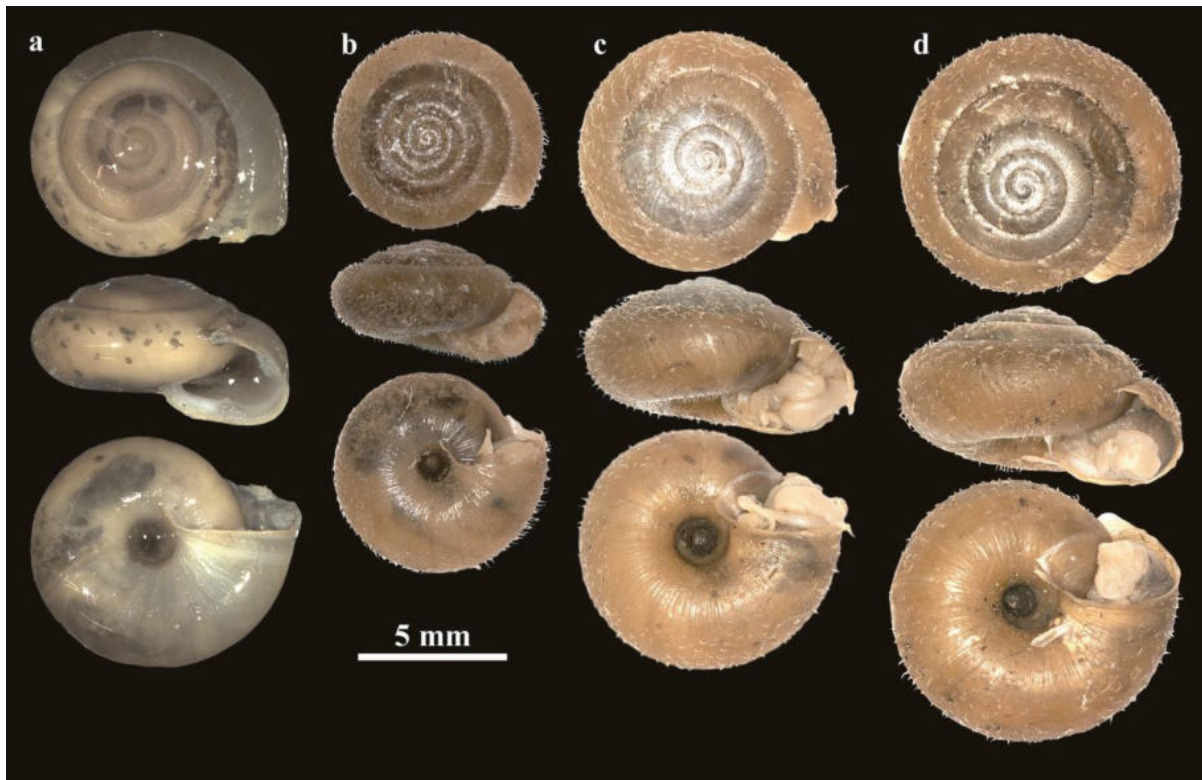


Figure 41: *Trochulus* sp. 3. Clade18; (a) NMBE 571152; Germany, Kelheim; (b) MNHW_A.Schw_202; Austria, Schwarzenberg-Loch; (c) MNHW_F.15.09_09; France, between Aubure & La Petite Verrerie; (d) MNHW_F.15.09_10; France, between Aubure and La Petite Verrerie.

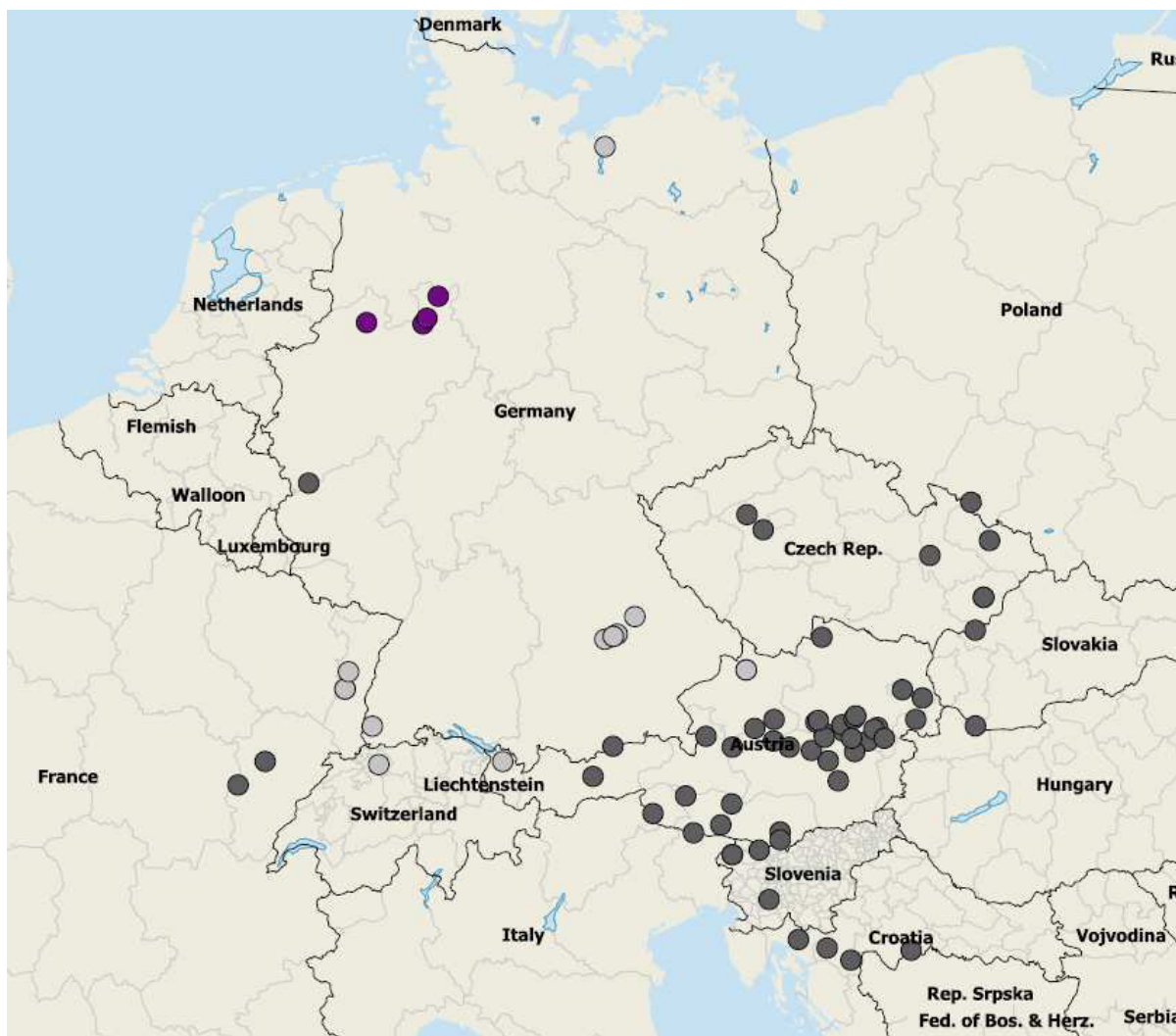


Figure 42: Distribution map of the investigated *Trochulus* sp. 3 (pale grey circles), *T. sp. 4* (dark grey circles), and *T. sp. 5* (purple circles) specimens.

Trochulus sp. 4 (sp. nov.?) [clade19] Figs 43a-d

Type specimens: [to be completed].

Description: The investigated specimens have a pale brown shell with short straight hairs. The shell is flattened and the umbilicus wide and open. Shell width ranges from 7.31–9.17 mm and shell height from 3.93–5.27 mm (N = 4). All measurements can be found in the appendix (supplementary material II). The specimens have 5.5 whorls. The body is beige with black spots.

Distribution (Fig. 42): The species is found throughout Austria except Vorarlberg, in Czech Republic, western Slovakia, Slovenia, and northern Croatia.

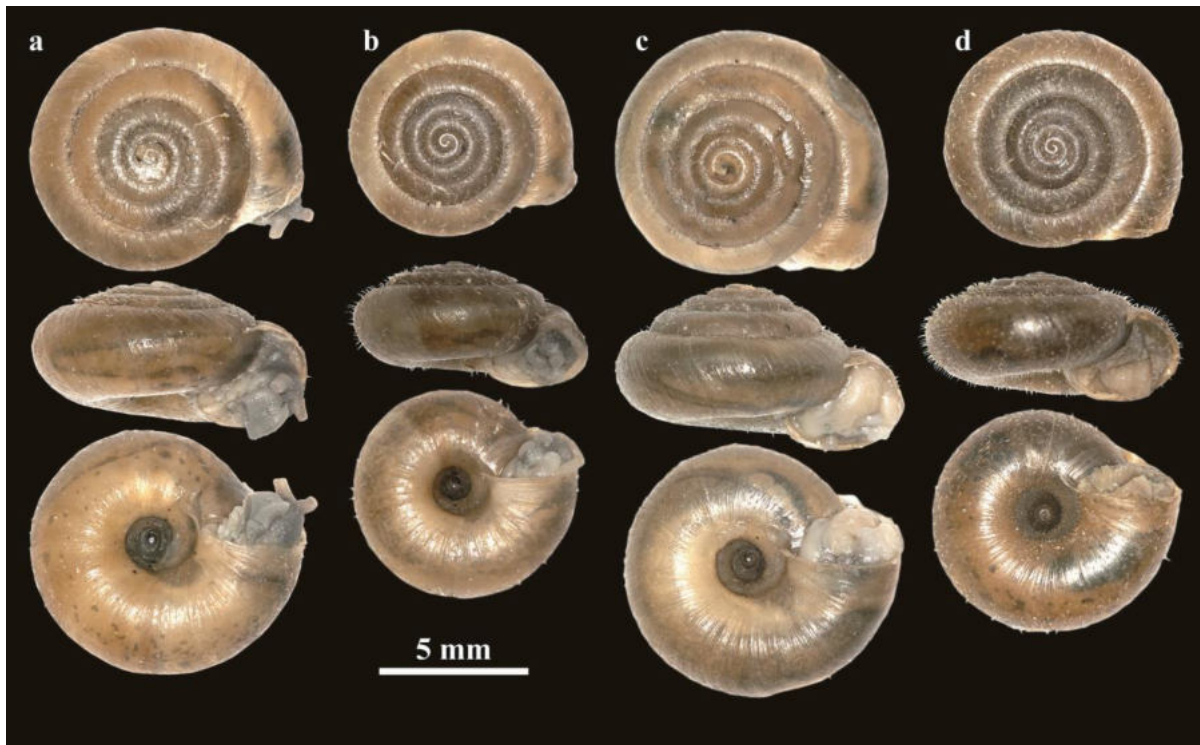


Figure 43: *Trochulus* sp. 4. Clade19; (a) MNHW_CZ.19.78_218; Czech Republic, Pitárné; (b) MNHW_CZ.19.35_213; Czech Republic, Srbsko 3; (c) MNHW_SK.19.63_262; Slovakia, Medved'ov; (d) MNHW_SLO.17.140_260; Slovenia, Vintgar Gorge.

Trochulus villosus (Draparnaud, 1805) [clade20] Figs 44a-f

1805 *Helix villosa* Draparnaud, Hist. nat. Moll. terr. fluv. France: 104-105, pl. 7 fig. 18 [“dans les montagnes de Savoie”; refers to Draparnaud, 1801, Tabl. moll. terr. fluv. France: 85 sub *Helix sericea* var. b].

1812 *Helix pilosa* von Alten, Systemat. Abhandl. Erd-und Flussconchyl. Augsburg: 46-47, pl. 4 fig. 7 [“Man findet sie an schattigen Orten in Waldungen, auf verschiedenen Pflanzen, wie auch auf Erlen, besonders auf Weidensträuchen, an den Lechkanälen auf dem Siebenbrunnenfeld, wie auch in der Gegend von Steßling”].

1821 *Helix detrita* W. Hartmann, Neue Alpina: 1: 235 [in bergigten Gegenden der Schweiz, Deutschland und Frankreich; Remark: see also Hartmann, 1824, in: Sturm, Deutschlands Fauna, 6 (7): 13, figs 13a-b.].

1871 *Helix* [*Fruticiola*] *rubra* Clessin, Ber. Naturh. Ver. Augsburg: 21: 93 [bei Günzburg].

1914 *Fruticicola alpicola* Eder, Archiv für Molluskenkunde: 53 (5): 228-231 [in den Churfürsten”; “im Alpsteingebirge (Hoher Kasten, Ebenalp)”; “In Unterwalden von ca. 1700 m. bis 2200 m. zu beiden Seiten des Bannalppasses].

Type specimens: [not yet researched, to be found in Vienna].

Description: *Trochulus villosus* is characterized by a flat shell with very long, strong hairs. The shell is strong and contains a strong lip. Shell width of the investigated specimens ranges from 9.61–13.48 mm and shell height from 5.21–9.73 mm (N = 14). All measurements can be found in the appendix (supplementary material II). The body whorl height accounts for about 85-90% of the shell height. The body is beige with dark spots.

Distribution (Fig. 45): *Trochulus villosus* is found north of the Swiss alps, in southern Germany (Black Forest and Bavaria) and Vorarlberg in western Austria.

Habitat: The species lives in humid and shaded montane areas, in alpine pastures and in forests (Proćków 2009).

Remark: Some *T. alpicola* specimens were collected and examined near Torgon in the Valais, Beatenberg and on the mountain Säntis. There is no genetic difference in the genes studied between *T. villosus* and *T. alpicola*. The latter is most likely a smaller altitudinal form of *T. villosus*, which is why it is synonymised with *T. villosus*.

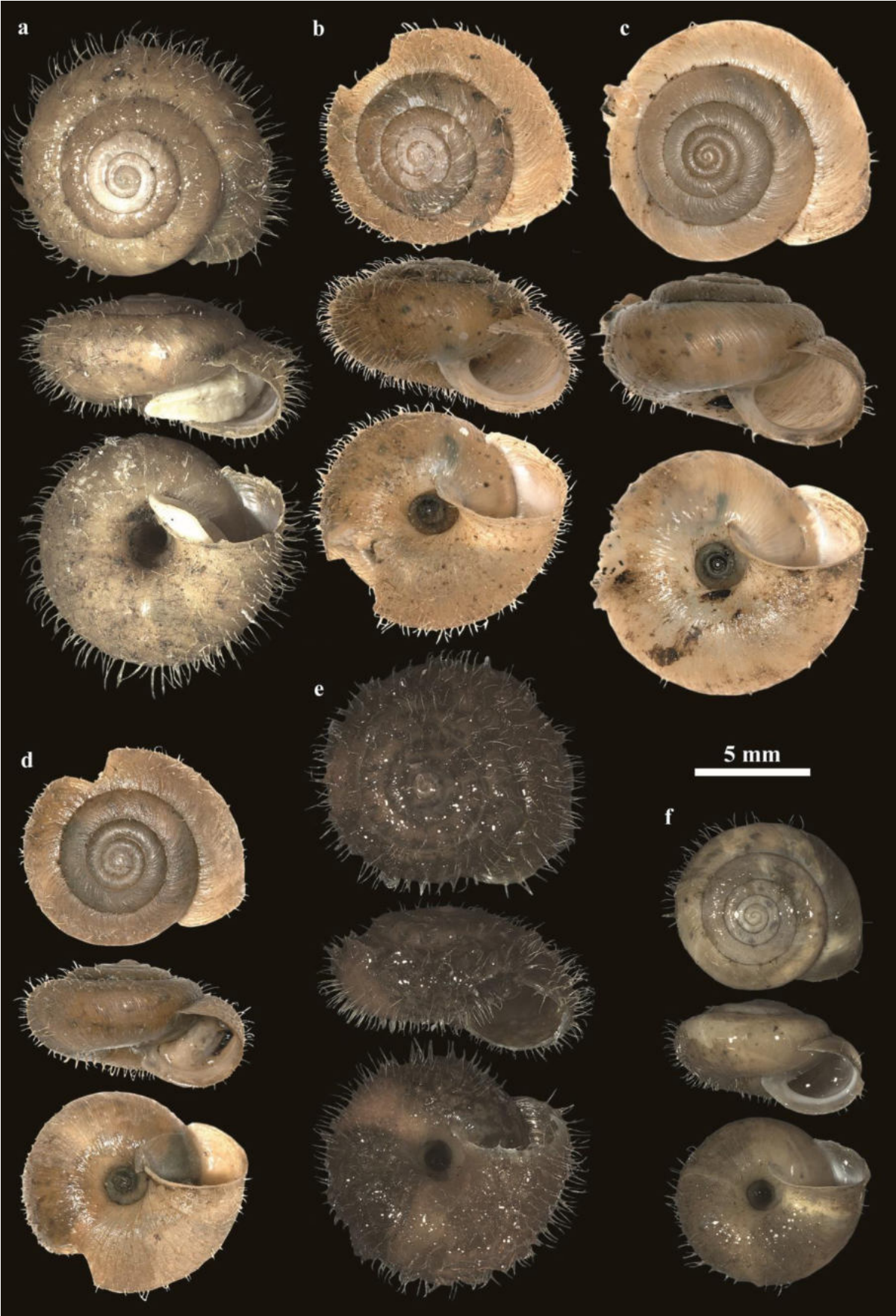


Figure 44: *Trochulus villosus*. Clade20; (a) NMBE 569640; Switzerland, Bürgenstock; (b) MNHW_S.15.29_100; Switzerland, Montagne De Cernier; (c) MNHW_G.15.52_109; Germany, Geisingen; (d) MNHW_A.MtK_105; Austria, Mt Kojenkopf; (e) NMBE 569639; Switzerland, Stansstad; (f) NMBE 571203; Switzerland, Säntis, Meglisalp.

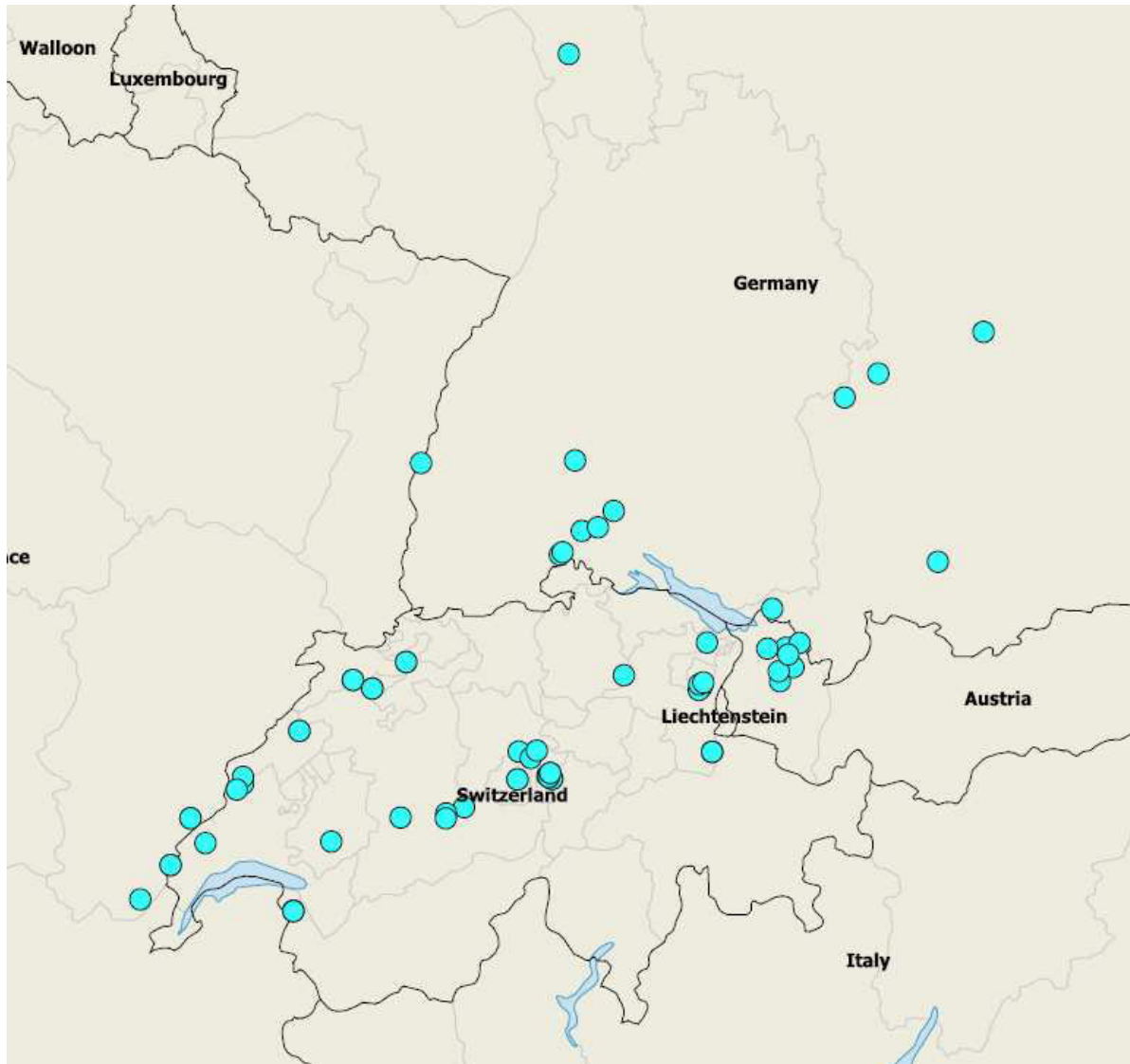


Figure 45: Distribution map of the investigated *Trochulus villosus* specimens.

Trochulus sp. 5 (sp. nov.?) [clade22] Figs 46a-b

Type specimens: [to be completed].

Description: The investigated specimens have a roundish-conical shell which is pale brown and shiny. The shell contains short, slightly curved hairs. The aperture is lunate. The umbilicus is wide and open. The body is beige with black spots.

Distribution (Fig. 42): The species is found in a small area around Bielefeld in North Rhine-Westphalia in northern Germany.



Figure 46: *Trochulus* sp. 5. Clade22; (a) NMBE 571329; Germany, Kreis Herford, Enger, Belke-Steinbeck, Brandbach; (b) NMBE 571333; Germany, Kreis Minden-Lübbecke, Hille, Mindenerwald.

Discussion

This study is the first that comprehensively examines specimens from almost the entire distribution range of the genus *Trochulus*. A total of 551 specimens was collected and studied with an integrative approach including a genetic and morphometric survey. In the phylogenetic part, three different methods were used to calculate trees (Bayesian Inference and two Maximum Likelihood methods) based on the concatenated data set of COI, 16S and 5.8S rRNA+ITS2. These studies yielded 21 stable clades, with some of them detected for the first time. The trees include the data of previous studies. The phylogenies of these studies were largely retrieved in clade structures. To facilitate their recognition, we provide a table supplying the corresponding data (Appendix, supplementary material III). Due to the lack of some markers, the resolution within the clades is poor and some nodes are not supported. During the investigation, a saturation in clade recognition could be observed, i.e. additional specimens sorted well into the clade structure, and only randomly a new clade was encountered. For this reason, we conclude that these clades represent species; however, at the current state a sound phylogenetic statement is impossible due to missing node support and presence of an unravelled polytomy in the BI analysis (Fig. 3), which is reflected in the ML analysis by a group of less related clades (Fig. 4). Also, the position of some clades varies to some extent, while their specimen composition stays stable. To overcome this

weakness of the Sanger analysis, a subset of 100 specimens representing all clades recovered so far is currently analysed by using a ddRADseq approach.

However, the basic split in the tree, which is rather well supported in both ML analyses and also present in the BI tree (not supported), separates the genus into two geographically well sorted groups. The first is the subgroup living in the Jurassic Mountains and the Franche-Comté in France and is composed of *T. circinnatus*, *T. montanus*, *T. clandestinus*, *T. caelatus*, *T. plebicola*, *T. pascali*, *T. albulus*, and *T. villosus*. The other one comprises the remaining clades from the distribution area of the genus in Europe. The Jurassic species may have retreated to refuges in unglaciated parts of the Jura Mountains during the Last Glacial Maximum (LGM; e.g., Graf et al. 2015; Claude et al. 2019). After the ice layers have retreated from the Swiss midlands, these species, except *T. clandestinus*, *T. albulus*, and *T. villosus*, could not spread that far (see Fig. 1). In contrast, the species of the European group such as *T. hispidus* and *T. villersii*, had greater dispersal potential and were able to occupy empty niches rather fast.

Our unbiased approach ignoring *a priori* determinations of specimens resolves the paraphyletic situation as reported by previous authors (e.g., Kruckenhauser et al. 2014; Duda et al. 2014, 2017; Proćków et al. 2013, 2017a, 2021), which may be demonstrated by the example of *T. hispidus*. This species was considered to live widespread in Europe. Restriction of the type locality for this species to Linnaeus' Garden in Uppsala recovers clade10 as *T. hispidus*. This lineage now denominates a boreal group with genetic records from Sweden, Ireland, and north-eastern France. Certainly, the British Isles are also inhabited by that species as well as we infer its presence in the western and more coastal parts of Belgium, The Netherlands, Germany and Denmark. But contrary to all previous determinations, *T. hispidus* is not recorded from Switzerland, nor from southern Germany or Austria. Thus, our concept of *T. hispidus* is radically different to the papers referenced so far, including the mainstream opinions of the last two centuries. Although the framework seems to be settled, rather large sampling gaps in western France and northern and central Germany hamper a final re-grouping of the genus. It may well be that such gaps harbour more small-range endemic lineages like *Trochulus* sp. 5 n. sp., which unexpectedly occurred in a small area in North Rhine-Westphalia, Germany. Since we unfortunately do not have any specimens from Lower Saxony, we do not know exactly how widespread this species is in the north of German. Still, there are single specimens from France that do not fit into the established clades (MNHN-IM-2013-77397 and MNHN-IM-2013-77398 in Fig. 3, 4 and 5), and probably represent uncovered lineages in an ill-sampled area. Future sampling efforts in deficit regions could further clarify the distribution of individual species and possibly reveal new cryptic taxa.

Several of our clades could relate to a name. A prerequisite for this is that ideally topotypic specimens were included in the analysis adjusting the application of a given name. We were able to identify 16 clades with validly described taxa. Given that still almost 100 names need to be evaluated under a taxonomical and nomenclatorial point of view, we refrain to describe the remaining five taxa as new species. No statistical differences in the morphology of the shells of *Trochulus* sp. 1 n. sp. and *Trochulus* sp. 2 n. sp. could be detected. *Trochulus* sp. 3 n. sp. and *Trochulus* sp. 4 n. sp. form sister lineages in the phylogenies (Figs. 3, 4, and 5). They are widespread in Europe, with *Trochulus* sp. 4 appearing to have its radiation hotspot in Austria. So far it was not possible to allocate a name for this lineage.

Nonetheless, the second aim was to investigate the presence of synapomorphic morphological traits differentiating the clades from each other; these could serve as identification features beyond the molecular methods and serve all applied field biologists. Several geometric morphometric methods were tested. Even though we have tried to capture the shape of adult shells as well as possible with landmarks, we have not succeeded in statistically separating all clades from each other. There are several cases, where genetically well supported species also form clear geographical entities, while they remain inseparable by shell morphometry (Fig. 6, 7, and 8). The shape of the shell is very similar for most species and only slight trends are discernible (Fig. 11 and 12), but no clear delineation. Of the specimens examined in the GMM, only *T. caelatus* can be morphologically determined with certainty. But here the type specimen stands out. This could be, since the shell is slightly tilted forward on the frontal picture and therefore the first whorls appear higher than they actually are. The exact orientation of the shells can have a big influence on the landmark analyses. The number of individuals also differs greatly within the clades. Most animals were examined in *T. clandestinus* (N = 36) and the fewest in *T. plebicola*, *T. caelatus* and *Trochulus* sp. 5 (N = 2). This also has an influence on the analyses because with a small number of individuals, it is difficult to estimate the intraspecific variability.

For the other species than *T. caelatus*, several combinations of characteristics are needed to identify the species morphologically. For example, *T. villosus* can be clearly identified by its size and long hairs. Since most cryptic species are not syntopic, they can be identified relatively well by their distribution or ecology.

Trochulus species colonize a wide range of habitats: from rocky alpine sites to lowlands, forests, near rivers, and nettle fields, to tall grasses in open areas (e.g., Duda et al. 2014; Proćków et al. 2017b). *Trochulus* species seem to be very adaptable and were able to colonize different habitats. At the moment, best practice to identify a species is to use our distribution maps reporting genetically identified clades or species, identify sympatric species

also occurring in the area, and exclude all other species. In all cases, a simple barcode can help to correctly identify the animals. This reduces the number of misidentifications.

Outlook

Although we have tried to cover the entire distribution range of the genus *Trochulus*, we are still missing some regions that may harbour new species. We still have collection gaps in western France and in central and northern Germany. Only by conscientiously sampling these regions and examining the specimens, will we get a complete picture. Even though we have collected over 180 *Trochulus* names, we have discovered five new species which will be described in a future paper. The phylogeny will be clarified by results of an ongoing ddRADseq approach; the data were not yet available.

Acknowledgements

We are grateful to Damien Combrisson, Armin Deutsch, Issaad Kawther Ezzine, Ralf Hannefort, René Heim, David Herbert, Fabian Heussler, Neele Höhne, Michal Horsák, Thomas Inäbnit, Adrienne Jochum, Bettina Kneubühler, Peter Landert, Katja Lassauer, Silvan Meister, Holger Menzel-Harloff, Andreas Pardey, Ben Rowson, Jörg Rüetschi, Julien Ryelandt, Vivianne Schallenberg, Ueli Schneppat, Jonas Schulz, Karin Urfer, Svenja Zehnder, Yvonne Zürcher for their tremendous collecting efforts. We sincerely thank Ruud A. Bank for the help in solving nomenclatural problems. We thank the Swiss Federal Office of Environment (FOEN) for financial support (contracts no. 110010344 / 8T30/00.5147.PZ/0006 and XXXXX).

References

- Adams D.C., Collyer M.L., Kaliontzopoulou A. & Baken E. 2020. Geomorph: software for geometric morphometric analyses. R package version 3.2.1. Available at <https://cran.r-project.org/package=geomorph>
- Altekar G., Dwarkadas S., Huelsenbeck J.P. & Ronquist, F. 2004. Parallel Metropolis-coupled Markov chain Monte Carlo for Bayesian phylogenetic inference. *Bioinformatics* 20 (3): 407–415. <https://doi.org/10.1093/bioinformatics/btg427>
- Alten JW von 1812. Systematische Abhandlung über die Erd- und Flussconchilien welche um Augsburg und der umliegenden Gegend gefunden werden, als ein Beytrag zur vaterländischen Naturgeschichte. 120 pp.
- Bamberger S., Duda M., Tribsch A., Haring E., Sattmann H., Macek O., Affenzeller M. & Kruckenhauser L. 2020. Genome-wide nuclear data confirm two species in the Alpine

endemic land snail *Noricella oreinos* s.l. (Gastropoda, Hygromiidae). *Journal of Zoological Systematics and Evolutionary Research* 58 (4): 982–1004. <https://doi.org/10.1111/jzs.12362>

Baudon A. 1862: Nouveau catalogue des Mollusques du département de l'Oise.- Mém. Soc. acad. Archéol. Sci. Arts Dép. Oise, 5: 171–211. Beauvais. [Separatum: pp. 1-43, Paris et Beauvais.]

Bickford D., Lohman D.J., Sodhi N.S., Ng P.K.L., Meier R., Winker K., Ingram K.K & Das I. 2007. Cryptic species as a window on diversity and conservation. *Trends in Ecology & Evolution*, 22 (3), 148–155. <https://doi.org/10.1016/j.tree.2006.11.004>

Bischof E.A., Schlüter N., Korn D. & Lehmann J. 2021. Ontogeny of highly variable ceratitid ammonoids from the Anisian (Middle Triassic) *PeerJ* 9:e10931 <https://doi.org/10.7717/peerj.10931>

Bischof E.A., Schlüter N. & Lehmann J. 2022. Geometric morphometric analysis of morphologic disparity, intraspecific variation and ontogenetic allometry of beyrichitine ammonoids. *PLoS ONE* 17(2): e0263524. <https://doi.org/10.1371/journal.pone.0263524>

Bookstein F. 1991. Morphometric tools for landmark data: geometry and biology. New York: Cambridge University Press, 435.

Bourguignat J.-R. 1864. Malacologie de la Grande-Chartreuse, 1–103, 9 unnumbered pls (panoramic landscapes) + pls 1-8 (duplicate plates: both in b/w and in colour), Paris (F. Savy).

Broeck, van den, 1872. ***** . *Bull. Soc. Malac. Belgique*, 6 [“1871”]: *-*.

Broeck, van den, 1873. ***** . *Ann. Soc. Malac. Belgique*, 7:

Brown, J 1841. ***** . *Ann. Mag. nat. Hist.*:

Caziot E. 1910. Étude sur les mollusques terrestres et fluviatiles de la Principauté de Monaco et du Département des Alpes-Maritimes. 559 + [1] (= Errata) + [7] (= Ouvrages scientifiques du même auteur) pp., pl. 1-10. Monaco (Collection de Mémoires et Documents).

Caziot E. & Margier E. 1909. Étude historique de la classification des Pupa du système européen. *Bulletin de la Société Zoologique de France*. 34: 134–147. Paris.

Chiba S. 1999. Accelerated evolution of land snails *Mandarina* in the oceanic Bonin Islands: evidence from mitochondrial DNA sequences. *Evolution*, 460–471. <https://doi.org/10.2307/2640782>

Claude A., Akçar N., Ivy-Ochs S., Schlunegger F., Kubik P.W., Christl M., Vockenhuber C., Kuhlemann J., Rahn M. & Schlüchter C. 2019. Changes in landscape evolution patterns in the northern Swiss Alpine Foreland during the mid-Pleistocene revolution. *GSA Bulletin*, 131(11–12), 2056–2078. <https://doi.org/10.1130/b31880.1>

- Clessin S. 1871. Die Mollusken-Fauna der Umgegend von Augsburg. *Bericht des Naturhistorischen Vereins in Augsburg*. 21: 81–126.
- Clessin S. 1874. Studien über die *Helix*-Gruppe *Fruticicola* Held. *Jahrbücher der Deutschen Malakozoologischen Gesellschaft*. 1: 305–336, pls. 12, 13.
- Clessin S. 1878. Vom Pleistocaen zur Gegenwart. Eine conchyliologische Studie. (Fortsetzung). *Correspondenzblatt des Zoologisch-Mineralogischen Vereines in Regensburg*, 32: 42–64. Regensburg.
- Colbeau J. 1868. Liste generale des mollusques vivants de la Belgique. *Annales de la Societe Royal Zoologique et Malacologique de Belgique*. 3: 85–111.
- Cristofori, De G. & Jan G. 1832. Mantissa in secundam partem catalogi Testaceorum exstantium in collectione quam possident De Cristofori et Jan, exhibens characteres essentielles specierum molluscorum terrestrium et fluviatilium ab eis enunciatarum in prima parte ejusdem catalogi. 4 pp.
- Dépraz A., Hausser J. & Pfenninger M. 2009. A species delimitation approach in the *Trochulus sericeus/hispidus* complex reveals two cryptic species within a sharp contact zone. *BMC Evolutionary Biology* 9: 171. <https://doi.org/10.1186/1471-2148-9-171>
- Draparnaud J.-P.-R. 1805. Histoire naturelle des mollusques terrestres et fluviatiles de la France. 2 pp. (Avertissement a sa Majesté l'Impératrice), 2 pp. Rapport, i–viii (Préface), 1–164, pl. 1–13, 1 p. Errata. [< 22 September]. Paris (Levrault & Schoell).
- Duda M., Kruckenhauser L., Sattmann H., Harl J., Jaksch K. & Haring E. 2014. Differentiation in the *Trochulus hispidus* complex and related taxa (Pulmonata: Hygromiidae): Morphology, ecology and their relation to phylogeography. *Journal of Molluscan Studies* 80 (4): 371–387. <https://doi.org/10.1093/mollus/eyu023>
- Duda M., Schindelar J., Macek O., Eschner A. & Kruckenhauser L. 2017. First record of *Trochulus clandestinus* (Hartmann, 1821) in Austria (Gastropoda: Eupulmonata: Hygromiidae). *Malacologica Bohemoslovaca* 16: 37–43.
- Dumont F. & Mortillet G. de 1852–1855. Histoire des Mollusques terrestres et d'eau douce, vivants et fossiles, de la Savoie et du bassin du Léman. *Bulletin de la Société d'Histoire Naturelle de Savoie*, 3: 14–142 (1852); 4: 1–78 (1853); 5: 81–152 (1854), 239–248 (1855).
- Eder L. 1917. Eine neue Schweizer Helicide. *Revue Suisse de Zoologie* 25 (15): 442–452.
- Fagot P. 1883. Diagnoses d'espèces nouvelles pour la faune française. I. Nova *Xerophila Lauragaisiana*. II. Mollusca nova Gallica. *Bulletin de la Société d'Histoire Naturelle de Toulouse*. 17: 207–224. Toulouse.
- Falkner G., Ripken T.E.J. & Falkner M. 2002. Mollusques continentaux de France. Liste de référence annotée et bibliographique. *Patrimoines Naturels*, 52: 1–350. Paris [22 March].

- Folmer O., Black M., Hoe W., Lutz R. & Vrijenhoek R. 1994. DNA primers for amplification of mitochondrial cytochrome c oxidase subunit I from diverse metazoan invertebrates. *Molecular Marine Biology and Biotechnology* 3 (5): 294–299.
- Forcart L. 1966. Die Schneckenfauna des Isteiner Klotzes im Wandel der Zeiten. in: Der Isteiner Klotz. Zur Naturgeschichte einer Landschaft am Oberrhein. *Die Natur- und Landschaftsschutzgebiete Baden-Württembergs*, Bnd. 4 (Ed.: H.Schäfer & O.Wittmann): 369–408.
- Fruciano C. 2019. Geometric morphometrics mix: miscellaneous functions useful for geometric morphometrics. R package version 0.0.7.9000.
- Gerber S. 2017. The geometry of morphospaces: lessons from the classic Raup shell coiling model. *Biological Reviews* 92 (2): 1142–1155. <https://doi.org/10.1111/brv.12276>
- Geyer D. 1914. ***** . Verh. k. k. zool.-bot. Ges. Wien, 65 (5/6): XX-XX.
- Graf A., Akçar N., Ivy-Ochs S., Strasky S., Kubik P.W., Christl M., Burkhard M., Wieler R. & Schlüchter C. 2015. Multiple advances of Alpine glaciers into the Jura Mountains in the Northwestern Switzerland. *Swiss Journal of Geosciences* 108 (2–3), 225–238. <https://doi.org/10.1007/s00015-015-0195-y>
- Guindon S., Dufayard J.F., Lefort V., Anisimova M., Hordijk W. & Gascuel O. 2010. New Algorithms and Methods to Estimate Maximum-Likelihood Phylogenies: Assessing the Performance of PhyML 3.0, *Systematic Biology* 59 (3): 307–321, <https://doi.org/10.1093/sysbio/syq010>
- Gunz P. & Mitteroecker P. 2013. Semilandmarks: a method for quantifying curves and surfaces. *Hystrix, The Italian Journal of Mammalogy* 24 (1): 103–109. <https://doi.org/10.4404/hystrix-24.1-6292>
- Hartmann J.D.W. 1840–1844. Erd- und Süßwasser-Gasteropoden der Schweiz. Mit Zugabe einiger merkwürdigen exotischen Arten, i–xx, 1–36, pl. 1–2 [30-06-1840]; 37–116, pl. 13–36 [1841]; 117–156, pl. 37–60 [1842]; 157–204, pl. 61–72 [1843]; 205–227, pl. 73–84 [1844]. St. Gallen.
- Hartmann J.D.W. 1821. System der Erd- und Flußschnecken der Schweiz. Mit vergleichender Aufzählung aller auch in den benachbarten Ländern, Deutschland, Frankreich und Italien sich vorfindenden Arten. In: J.R. Steinmüller (ed.). *Neue Alpina*. Eine Schrift der Schweizerischen Naturgeschichte, Alpen- und Landwirthschaft gewidmet, Erster Band: 194–268, pl. 1–2. Winterthur.
- Hoang D.T., Chernomor O., Haeseler, von A., Minh B.Q. & Vinh L.S. 2018. UFBoot2: Improving the ultrafast bootstrap approximation. *Molecular Biology and Evolution* 35 (2): 518–522. <https://doi.org/10.1093/molbev/msx281>

- Huelsenbeck J.P. & Ronquist F. 2001. MRBAYES: Bayesian inference of phylogeny. *Bioinformatics* 17 (8): 754–755. <https://doi.org/10.1093/bioinformatics/17.8.754>
- Jeffreys J.G. 1830. A synopsis of the testaceous pneumonobranchous Mollusca of Great Britain. *Transactions of the Linnean Society of London* 16: 323–392.
- Jeffreys J.G. 1862–1869. British conchology. Vol. 1: pp. cxiv + 341 [1862]. Vol. 2: pp. 479 [1864]. Vol. 3: pp. 394 [1865]. Vol. 4: pp. 487 [1867]. Vol. 5: pp. 259 [1869]. London, van Voorst.
- Jörger K.M. & Schrödl M. 2013. How to describe a cryptic species? Practical challenges of molecular taxonomy. *Frontiers in Zoology* 10 (1), 59. <https://doi.org/10.1186/1742-9994-10-59>
- Kerney M.P., Cameron R.A.D. & Jungbluth J-H. 1983. Die Landschnecken Nord- und Mitteleuropas. Ein Bestimmungsbuch für Biologen und Naturfreunde, 384 pp., 24 plates. Hamburg / Berlin (Paul Parey).
- Klemm W. 1974. Die Verbreitung der rezenten Land-Gehäuse-Schnecken in Österreich. Denkschriften der österreichischen Akademie der Wissenschaften, mathematisch-naturwissenschaftliche Klasse, 117: 503 pp., III + 153 maps. Wien.
- Klöti-Hauser E. 1920. Beiträge zur Anatomie des Geschlechtsapparates einiger schweizerischen *Trichia* (*Fruticicola*-, *Helix*-) Arten. Dissertation Zürich.
- Kneubühler J., Baggenstos M., Neubert E. 2022. On the verge of extinction – revision of a highly endangered Swiss alpine snail with description of a new genus, *Raeticella* gen. nov. (Gastropoda, Eupulmonata, Hygromiidae). *ZooKeys* 1104: 69–91. <https://doi.org/10.3897/zookeys.1104.82866>
- Kruckenhauser L., Duda M., Bartel D., Sattmann H., Harl J., Kirchner S. & Haring E. 2014. Paraphyly and budding speciation in the hairy snail (Pulmonata, Hygromiidae). *Zoologica Scripta* 43 (3): 273–288. <https://doi.org/10.1111/zsc.12046>
- Kumar S., Stecher G., Li M., Knyaz C. & Tamura K. 2018. MEGA X: Molecular Evolutionary Genetics Analysis across computing platforms. *Molecular Biology and Evolution* 35 (6): 1547–1549. <https://doi.org/10.1093/molbev/msy096>
- Lanfear R., Frandsen P.B., Wright A.M., Senfeld T. & Calcott B. 2016. PartitionFinder 2: new methods for selecting partitioned models of evolution for molecular and morphological phylogenetic analyses. *Molecular Biology and Evolution* 34 (3): 772–773. <https://doi.org/10.1093/molbev/msw260>.
- Lessona M. 1879. Sulla *Helix hispida* LINN. in Piemonte.- Atti r. Accad. Sei. Torino, 15 (2): 291–297, tavv. 6-7. Torino.

Letourneux A. 1869. Catalogue des Mollusques terrestres et fluviatiles recueillis dans le département de la Vendée, et particulièrement dans l'arrondissement de Fontenay-le-Comte. *Revue et Magasin de Zoologie*, (2) 21 (2): 49–64, (3): 105–109, (4):145–148, (5): 193–203. Paris.

Linnaeus C. 1758. *Systema Naturae per regna tria naturae, secundum classes, ordines, genera, species, cum characteribus, differentiis, synonymis, locis*. Editio decima, reformata [10th revised edition], vol. 1: 824 pp. Laurentius Salvius: Holmiae.

Locard A. 1882. *Prodrome de malacologie française*. [I]. Catalogue général des mollusques vivants de France. Mollusques terrestres, des eaux douces et des eaux saumâtres. – Lyon (HENRI GEORG): VI + 462 pp. [June 1882 mentioned on page 451; *Nat. Novit.*, 4 (17): 157 = August 1882; *Journal de Conchyliol.*, 30 (3): 221 = 13 December 1882; *Zool. Anz.*, 5: 678 = 25 December 1882]. Note: published later under the title “*Prodrome de malacologie française*” in the *Annales de la Société d'Agriculture, Histoire naturelle et Arts utiles de Lyon*, (5) 4 [“1881”]: 189–748. Lyon (1882) [*Nat. Novit.*, 4 (25): 229 = December 1882; *Zool. Anz.*, 7: 50 = 4 February 1884]. The preprint appeared earlier.

Locard A. 1888. *Contributions à la faune malacologique française*. XII. Études critiques sur les *Helix* du groupe de l'*Helix rufescens* Pennant (*Helix striolata*, *H. rufescens*, *H. montana*, *H. caelata*, *H. circinata*, *H. clandestina*). *Annales de la Société Linnéenne de Lyon*, (N.S.) 34 [“1887”]: 309–368. Lyon.

Locard A. 1894. *Conchyliologie française*. [II]. Les coquilles terrestres de France. Description des familles, genres et espèces, 1–370. Paris (J.-B. Baillière).

Mabille J. 1877. Testarum novarum diagnoses. *Bulletin de la Société Zoologique de France*, 2 (3/4): 304–306. Paris [October]

Malzine F. de 1867. *Essai sur la faune malacologique de la Belgique ou catalogue des mollusques qui se trouvent dans ce pays*. 99 pp, 1 pl.

Mayr E. 1942. *Systematics and the Origin of Species*. By Ernst Mayr. New York, Columbia University Press. 334 pp. 29 figures.

Mikula E. 1957. *Trochulus hispidus* scheerpeltzi n. subsp. *Archiv für Molluskenkunde*, 86 (1): 91–93.

Minh B.I., Nguyen M.A.T. & Haeseler, von A. 2013. Ultrafast Approximation for Phylogenetic Bootstrap. *Molecular Biology and Evolution* 30 (5): 1188–1195. <https://doi.org/10.1093/molbev/mst024>

Moquin-Tandon A. 1855–1856. *Histoire naturelle des mollusques terrestres et fluviatiles de France*, Tome premier (1): i–viii, 1–14 + Atlas: 1–16, pl. 1–9 (12 April 1855); (2): 145–256 + Atlas: 17–32, pl. 10–18 (4 May 1855); (3): 257–416 + Atlas: 33–48, pl. 19–27 (1 August

1855). Tome second (4): i–iii, 1–176 + Atlas: 49–64, pl. 28–36 (10 September 1855); (5): 177–368 + Atlas: 65–80, pl. 37–45 (2 January 1856); (6): 369–646 + Atlas: i–iii, 81–92, pl. 46–54 (9 April 1856). Paris (J.-B. Baillière).

Müller O.F. 1773–1774. Vermium terrestrium et fluviatilium, seu animalium infusoriorum, helminthicorum, et testaceorum, non marinorum, succincta historia. Havniæ et Lipsiæ. Vol. 1, Pars Ima: 1–136 [1773]; Pars Altera: 1–72 + index 8 pp. [1774]. Havniæ (Copenhagen) & Lipsiæ (Leipzig), Heineck & Faber.

Neige P. 1999. The use of landmarks to describe ammonite shape. In: Olóriz F., Rodríguez-Tovar F.J., eds. Advancing research on living and fossil cephalopods. New York: Kluwer Academic/Plenum, 263–272.

Nguyen L.T., Schmidt H.A., Haeseler, von A. & Minh B.Q. 2015. IQ-TREE: A fast and effective stochastic algorithm for estimating maximum likelihood phylogenies. *Molecular Biology and Evolution* 32 (1): 268–274. <https://doi.org/10.1093/molbev/msu300>

Nordsieck H. 1993. Das System der paläarktischen Hygromiidae (Gastropoda: Stylommatophora: Helicoidea). *Archiv für Molluskenkunde*, 122 (Zilch-Festschrift): 1–23. Frankfurt am Main [28 February].

Pfeiffer C. 1821–1828. Naturgeschichte deutscher Land- und Süßwasser-Mollusken. Weimar. Abt. 1: i–x, 1–134, pls 1–8 [1821]; Abt. 2: i–viii, 1–40, pls 1–8 [1825]; Abt. 3: i–vi, 1–84, pls 1–8 [1828].

Pfeiffer L. 1841. Symbolae ad historiam Heliceorum. Sectio prima [vol. 1]. Kassel: Th. Fischer. 88 pp.

Pfenninger M. & Pfenninger A. 2005. A new *Trochulus* species from Switzerland (Gastropoda: Pulmonata: Hygromiidae). *Archiv Für Molluskenkunde: International Journal of Malacology*, 134 (2), 26/*-+9. <https://doi.org/10.1127/arch.moll/0003-9284/134/261-269>

Pfenninger M. & Schwenk K. 2007. Cryptic animal species are homogeneously distributed among taxa and biogeographical regions. *BMC Evolutionary Biology* 7, 121. <https://doi.org/10.1186/1471-2148-7-121>

Pfenninger M., Hrabáková M., Steinke D. & Dépraz A. 2005. Why do snails have hairs? A Bayesian inference of character evolution. *BMC Evolutionary Biology* 5, 59. <https://doi.org/10.1186/1471-2148-5-59>

Picard C. 1840. Histoire des Mollusques terrestres et fluviatiles qui vivent dans le département de la Somme.- *Bull. Soc. linn. Nord France*, 1 (3): 149–328. Abbeville.

Polinski W. 1914. Slimaki Ojcowa. Spraw. Kom. Fizyogr. 48: 16–50, Kraków.

Pollonera C. 1886. Aggiunte alla Malacologia terrestre del Piemonte. Bollettino dei Musei di Zoologia ed Anatomia Comparata della R. Università di Torino 1: 1–4

Polly P.D. & Motz G.J. 2016. Patterns and processes in morphospace: geometric morphometrics of three-dimensional objects. *The Paleontological Society Papers* 22: 71–99. <https://doi.org/10.1017/scs.2017.9>

Proćków M. 2009. The genus *Trochulus* Chemnitz, 1786 (Gastropoda: Pulmonata: Hygromiidae) – a taxonomic revision. *Folia Malacologica* 17: 101–176. <https://doi.org/10.2478/v10125-009-0013-0>

Proćków M., Kuźnik-Kowalska E. & Mackiewicz P. 2017a. Phenotypic plasticity can explain evolution of sympatric polymorphism in the hairy snail *Trochulus hispida* (Linnaeus, 1758). *Current zoology* 63 (4): 389–402. <https://doi.org/10.1093/cz/zow082>

Proćków M., Kuźnik-Kowalska E., & Mackiewicz P. 2017b. The influence of climate on shell variation in *Trochulus striolatus* (C. Pfeiffer, 1828) (Gastropoda: Hygromiidae) and its implications for subspecies taxonomy. *Annales Zoologici*, 67: 199–220. <https://doi.org/10.3161/00034541an.z2017.67.2.002>

Proćków M., Kuźnik-Kowalska E., Pieńkowska J.R., Żeromska A. & Mackiewicz P. 2021. Speciation in sympatric species of land snails from the genus *Trochulus* (Gastropoda, Hygromiidae). *Zoologica Scripta* 50: 16–42. <https://doi.org/10.1111/zsc.12458>

Proćków M., Mackiewicz P. & Pieńkowska J.R. 2013. Genetic and morphological studies of species status for poorly known endemic *Trochulus phorochaetius* (Bourguignat, 1864) (Gastropoda: Pulmonata: Hygromiidae), and its comparison with closely related taxa. *Zoological Journal of the Linnean Society*, 169 (1): 124–143. <https://doi.org/10.1111/zoj.12048>

Proćków M., Strzała T., Kuźnik-Kowalska E. & Mackiewicz P. 2014. Morphological similarity and molecular divergence of *Trochulus striolatus* and *T. montanus*, and their relationship to sympatric congeners (Gastropoda: Pulmonata: Hygromiidae). *Systematics and Biodiversity* 12: 366–384. <https://doi.org/10.1080/14772000.2014.925986>

Proćków M., Strzała T., Kuźnik-Kowalska E., Proćków J. & Mackiewicz P. 2017c. Ongoing Speciation and Gene Flow between Taxonomically Challenging *Trochulus* Species Complex (Gastropoda: Hygromiidae). *PLoS ONE* 12(1): e0170460. <https://doi.org/10.1371/journal.pone.0170460>

R Core Team 2021. R: A language and environment for statistical computing. R Foundation for Statistical Computing, Vienna, Austria. <https://www.R-project.org>

Rambur P. 1868. Diagnoses d'Helices nouvelles. *Journal de Conchyliologie*, 16 (3): 265–268. Paris [15 July].

- Rambur P. 1869. Description de plusieurs hélices inédites, de France et d'Espagne, suivie d'observations et de rectifications concernant deux autres espèces. *Journal de Conchyliologie*, 17: 252–269, pl. 9. Paris.
- Risso A. 1826. Histoire Naturelle des Principales Productions de l'Europe Méridionale et Particulièrement de Celles des Environs de Nice et des Alpes Maritimes. Tome V. F.-G. Levrault, Paris. i- viii + 1–400 pp., 10 pls. [maybe 1827].
- Rohlf F. 2010. TPSDig2: a program for landmark development and analysis. Available at <http://sbmophometrics.org/soft-dataacq.html> (last access 06.07.2022).
- Ronquist F. & Huelsenbeck J.P. 2003. MRBAYES 3: Bayesian phylogenetic inference under mixed models. *Bioinformatics* 19: 1572–1574. <https://doi.org/10.1093/bioinformatics/btg180>
- Rossmässler E.A. 1838–1844. Iconographie der Land- & Süßwasser- Mollusken, mit vorzüglicher Berücksichtigung der europäischen noch nicht abgebildeten Arten. (1) 2 (1/2) [7/8]: 4 + 1–44. pl 31–40 [≥ June 1838]; (1) 2 (3/4) [9–10]: I–IV + 1–46. pl. 41–50 [≥ Sept. 1839]; (1) 2 (5) [11]: I–IV + 1–15. pl. 51–55 [≥ June 1842]; (1) 2 (6) [12]: I–IV + 1–37. pl. 56–60 [≥Sept. 1844]. [Dresden und Leipzig (Arnoldische Buchhandlung)].
- Schlager S. 2017. In: Zheng G., Li S., Székely G., eds. Morpho and Rvcg–shape analysis in R: R-Packages for geometric morphometrics, shape analysis and surface manipulations. San Diego: Academic Press, 217–256.
- Servain G. 1881. [± February]: Étude sur les mollusques recueillis en Espagne et en Portugal. – Saint-Germain (D. BARDIN) [“1880”]: 172 pp. Note: page 171 dated July 1880; wrapper dated August 1880; Bibliographie de la France: 26 March 1881 # 3137; *Naturae Novitates*, 3 (12): 99 = June 1881.
- Simon C., Frati F., Beckenbach A., Crespi B., Liu H. & Flook P. 1994. Evolution, weighting, and phylogenetic utility of mitochondrial gene sequences and a compilation of conserved polymerase chain reaction primers. *Annals of the entomological Society of America*, 87 (6), 651–701. <https://doi.org/10.1093/aesa/87.6.651>
- Stamatakis A. 2014. RAxML Version 8: A tool for Phylogenetic Analysis and Post-Analysis of Large Phylogenies. *Bioinformatics*, 30 (9): 1312–1313. <https://doi.org/10.1093/bioinformatics/btu033>
- Studer S. 1820. Kurzes Verzeichnis der bis jetzt in unserm Vaterlande entdeckten Conchylien. Naturwissenschaftlicher Anzeiger der Allgemeinen Schweizerischen Gesellschaft für die Gesamten Naturwissenschaften, 3 (11): 83–90; (12): 91–94. Bern [1 May; 1 June]. [reprinted as a separate work under the title: Systematisches Verzeichniss der bis jetzt bekannt gewordenen Schweizer-Conchylien. Bern (Stämpfli: 32 pp. > 5 April)]

Wade C.M. & Mordan P.B. 2000. Evolution within the gastropod molluscs; using the ribosomal RNA gene-cluster as an indicator of phylogenetic relationships. *Journal of Molluscan Studies* 66 (4): 565–570. <http://dx.doi.org/10.1093/mollus/66.4.565>

Wagner A.J. 1915. Beiträge zur Anatomie und Systematik der Stylomatophoren aus dem Gebiete der Monarchie und der angrenzenden Balkanländer. *Denkschriften der Kaiserlichen Akademie der Wissenschaften in Wien, Mathematisch-naturwissenschaftliche Klasse*. 91: 429–498, pl. 1–24. Wien.

Weinland, 1876. ***** . Jahresh. Ver. Vaterl. Naturk. Württemberg, 32: XX-XX.

Westerlund C.A. 1871. Fauna molluscorum terrestrium et fluviatiliium Sveciae, Norvegiae et Daniae. I. Landmolluskerna. Adolf Bonnier, Stockholm. 1–296.

Westerlund C.A. 1894. Specilegium Malacologicum. Neue Binnen-Conchylien aus der paläarktischen Region. V. *Nachrichtenblatt der Deutschen Malakozoologischen Gesellschaft*. 26 (9/10): 163–177; 190–205. Frankfurt am Main [September/October].

Appendix

Supplementary material I: Database number, country of origin, geographical data, and GenBank accession numbers for the investigated *Trochulus*, *Raeticella* and *Edentiella* specimens. Specimens with † where used in the landmark analysis. Specimens with * where used in the ddRADseq analysis.

Species	Data base nr°	Country	Locality	Lat	Long	Alt	GenBank accession number COI	GenBank accession number 16S	GenBank accession number ITS2
<i>T. circinnatus</i>	NMBE 564589	Switzerland	Chasseron	46.85	6.54	1606	MW703573	MW709376	-
<i>T. clandestinus</i>	NMBE 564590	Switzerland	Villeret, Combe Grède	47.14	7.03	911	MW703574	MW709329	-
<i>T. montanus</i>	NMBE 564591	Switzerland	Moutier, Gorges de Moutier	47.28	7.37	515	MW703575	MW709377	-
<i>T. clandestinus</i>	NMBE 564592	Switzerland	Villeret, Combe Grède	47.14	7.03	911	MW703576	MW709330	MW709295
<i>T. montanus</i>	NMBE 564593	Switzerland	Sornetan, Gorges du Pichoux	47.29	7.23	643	MW703577	MW709378	MW709296
<i>T. montanus</i>	NMBE 564594	Switzerland	Montoz	47.22	7.27	1327	MW703578	MW709331	MW709297
<i>T. clandestinus</i>	NMBE 564595	Switzerland	Beinwil, Hohe Winde	47.34	7.58	1204	MW703579	MW709379	MW709298
<i>T. clandestinus</i>	NMBE 564596	Switzerland	Vechigen, Boll	46.95	7.54	570	MW703580	MW709380	MW709299
<i>T. clandestinus</i> *	NMBE 564597	Switzerland	Malix	46.81	9.54	1130	MW703581	MW709332	MW709300
<i>T. clandestinus</i>	NMBE 25267	Switzerland	Andermatt, Teufelsbrücke	46.65	8.59	1405	MW703551	MW709353	MW709283
<i>T. clandestinus</i>	NMBE 509933	Switzerland	Leissigen, Meielisalp	46.65	7.79	800	MW703553	MW709355	MW709285
<i>T. clandestinus</i>	NMBE 564598	Switzerland	Bolligen, Ferenberg	46.97	7.53	722	-	MW709381	MW709301
<i>T. clandestinus</i> *	NMBE 564599	Switzerland	Vechigen, Sinneringen	46.95	7.53	570	MW703582	MW709382	MW709302
<i>T. sericeus</i>	NMBE 509907	Switzerland	Zerne, Val Laschadura	46.70	10.16	2100	MW703552	MW709354	MW709284
<i>T. striolatus</i> *	NMBE 564600	Switzerland	Hallau, Lochgraben	47.69	8.41	350	MW703583	MW709383	-
<i>T. sericeus</i>	NMBE 564601	Switzerland	Zerne	46.70	10.09	1473	ON477942	ON479903	ON479896
<i>T. sericeus</i>	NMBE 564602	Switzerland	Zerne, Inn	46.70	10.09	1400	MW703585	MW709334	MW709304
<i>T. montanus</i>	NMBE 564604	Switzerland	Selzach, Hasenmatt	47.24	7.45	1444	MW703586	MW709335	-
<i>T. clandestinus</i>	NMBE 564605	Switzerland	St-Brais	47.31	7.11	967	-	MW709385	-
<i>T. montanus</i> *	NMBE 564607	Switzerland	Mervelier, Scheltental	47.34	7.52	615	ON477943	ON479904	ON479897
<i>T. clandestinus</i> *	NMBE 564608	Switzerland	Vallorbe, Grotte de l'Orbe	46.70	6.35	760	MW703589	MW709336	MW709307
<i>T. circinnatus</i> *	NMBE 564609	Switzerland	Bullet, Le Chasseron	46.85	6.54	1606	ON477944	ON479905	ON479898
<i>T. clandestinus</i>	NMBE 564610	Switzerland	Villeret, Combe Grède	47.14	7.03	911	MW703591	MW709389	MW709309
<i>T. clandestinus</i>	NMBE 564606	Switzerland	Chasseral	47.13	7.06	1607	MW703587	MW709386	MW709305
<i>T. clandestinus</i>	NMBE 564567	Switzerland	Areuse, Gorges de l'	46.96	6.81	516	-	MW709357	MW709287
<i>T. montanus</i> *	NMBE 564568	Switzerland	Günsberg, Chamben	47.27	7.57	1250	MW703555	MW709358	-
<i>T. albulus</i>	NMBE 564569	Switzerland	Reichenbach i. K., Kiental, Gamchi	46.53	7.78	1650	MW703556	MW709359	-
<i>T. albulus</i>	NMBE 564570	Switzerland	Sigriswil, Justistal, 1100m	46.71	7.77	1100	-	MW709360	MW709288
<i>T. sericeus</i>	NMBE 564571	Switzerland	Scuol, Puors	46.81	10.30	1559	MW703557	MW709361	MW709289
<i>T. albulus</i>	NMBE 564572	Switzerland	Brienz, Brienzler Rothorn	46.79	8.05	2349	MW703558	MW709328	-
<i>T. albulus</i>	NMBE 564573	Switzerland	Alpnach, Pilatus,	46.97	8.24	2128	MW703559	MW709362	MW709290

			Tomlishorn						
<i>T. villosus</i>	NMBE_564574	Switzerland	Pohlern, Chrümmelwä ge	46.71	7.52	1467	MW703560	MW709363	-
<i>T. villosus</i>	NMBE_564575	Switzerland	Chasseron	46.85	6.54	1606	MW703561	MW709364	MW709291
<i>T. sericeus</i> *	NMBE_564576	Switzerland	Heiden	47.44	9.52	794	MW703562	MW709365	-
<i>T. plebeius</i>	NMBE_564577	Switzerland	Soubey	47.31	7.05	476	MW703563	MW709366	-
<i>T. sp.3</i>	NMBE_564578	Switzerland	Langenbruck, Chilchzimmer sattel	47.36	7.80	990	MW703564	MW709367	-
<i>T. sericeus</i>	NMBE_564579	Switzerland	Goldach	47.47	9.47	447	MW703565	MW709368	-
<i>T. albulus</i>	NMBE_564580	Switzerland	Erlenbach, Stockhorn	46.69	7.54	2190	MW703566	MW709369	-
<i>T. pascali</i> *	NMBE_543063	Switzerland	St-Cergue, Route de Cuvaloup	46.45	6.12	1208	ON477941	ON479902	ON479895
<i>T. albulus</i>	NMBE_564581	Switzerland	Leukerbad, Allmei	46.39	7.63	1600	MW703567	MW709370	MW709292
<i>T. pascali</i> *	NMBE_564582	Switzerland	Chardonne, Mont Pélerin	46.49	6.83	1032	-	MW709371	MW709293
<i>T. caelatus</i> *	NMBE_564584	Switzerland	Bettlach, Wandflue	47.23	7.40	1300	MW703569	MW709372	MW709294
<i>T. caelatus</i> *	NMBE_564585	Switzerland	Oberdorf, Weissenstein	47.25	7.50	1280	MW703570	MW709373	-
<i>T. caelatus</i> *	NMBE_564586	Switzerland	Moutier, Gorges de Moutier	47.28	7.37	515	MW703571	MW709374	-
<i>T. sericeus</i>	NMBE_564587	Switzerland	Steinach, Obersteinach	47.49	9.44	417	MW703572	MW709375	-
<i>T. sericeus</i>	NMBE_24820	Germany	Blumberg, Eichberg/Bad en- Württemberg	47.85	8.52		MW703549	MW709351	MW709281
<i>T. sericeus</i>	NMBE_24833	Germany	Neuschwaig/ Bayern	48.65	10.68		MW703550	MW709352	MW709282
<i>E. edentula</i>	MNHW_S- Er_50	Switzerland	Erschwil	47.37	7.56		MW440986	MW621003	MW440679
<i>E. edentula</i>	MNHW_S- Er_51	Switzerland	Erschwil	47.37	7.56		MW440987	MW621004	MW440680
<i>E. edentula</i> *	MNHW_F- Ech_50	France	Échallon	46.20	5.75		-	MW772316	MW775782
<i>E. edentula</i>	MNHW_F.15.36 51	France	Bonnevaux	46.82	6.21		-	MW772295	MW775759
<i>E. edentula</i>	MNHW_F.15.36 50	France	Bonnevaux	46.82	6.21		-	MW772294	MW775758
<i>E. edentula</i>	MNHW_F.15.37 50	France	Cascade du Moulin du SAustria	46.76	6.02		-	MW772298	MW775760
<i>E. edentula</i>	MNHW_F.15.37 51	France	Cascade du Moulin du SAustria	46.76	6.02		-	MW772299	MW775761
<i>T. albulus</i>	MNHW_F- ChJ_38	France	Château de Joux	46.87	6.37		MW774498	-	MW775776
<i>T. albulus</i>	MNHW_S.15.17 12	Switzerland	Gorges de Court	47.26	7.34		MW774513	MW772329	MW775793
<i>T. albulus</i> †	MNHW_S.15.19 10	Switzerland	Gorges de Court 3	47.25	7.34		-	MW772330	-
<i>T. albulus</i> †	MNHW_S.15.19 11	Switzerland	Gorges de Court 3	47.25	7.34		MW774518	MW772331	MW775797
<i>T. albulus</i>	MNHW_S.15.25 04	Switzerland	Frinvillier	47.17	7.25		MW774538	MW772344	-
<i>T. albulus</i> †	MNHW_S.15.21 13	Switzerland	Gorges de Moutier	47.29	7.38		MW774524	MW772338	MW775803
<i>T. albulus</i> †	MNHW_S.15.21 14	Switzerland	Gorges de Moutier	47.29	7.38		MW774525	MW772339	MW775804
<i>T. plebeius</i> †	MNHW_F- Ech_02	France	Échallon	46.20	5.75		MW774499	MW772312	MW775779
<i>T. plebeius</i>	MNHW_F- Ech_03	France	Échallon	46.20	5.75		MW774500	MW772313	MW775780
<i>T. albulus</i> †	MNHW_S.15.27 12	Switzerland	Twannbachsc hlucht	47.10	7.14		MW440984	MW621002	MW440677

<i>T. albulus</i>	MNHW_S.15.27 13	Switzerland	Twannbachsc hlucht	47.10	7.14		MW774543	MW772345	MW775821
<i>T. albulus</i>	MNHW_S.15.27 14	Switzerland	Twannbachsc hlucht	47.10	7.14		MW774544	MW772346	MW775822
<i>T. albulus</i>	MNHW_S- Me_05	Switzerland	Mervelier	47.34	7.51		MW774561	-	MW775842
<i>T. clandestinus</i> †	MNHW_S.15.20 01	Switzerland	Gorges de Court 4	47.25	7.35		MW774519	MW772332	MW775798
<i>T. clandestinus</i> †	MNHW_S.15.20 02	Switzerland	Gorges de Court 4	47.25	7.35		-	MW772333	-
<i>T. montanus</i>	MNHW_S.15.19 08	Switzerland	Gorges de Court 3	47.25	7.34				
<i>T. clandestinus</i>	MNHW_S.15.19 09	Switzerland	Gorges de Court 3	47.25	7.34		MW774516	MW776381	MW775796
<i>T. montanus</i>	MNHW_S.15.25 01	Switzerland	Frinvillier	47.17	7.25		MW774517	MW776382	-
<i>T. montanus</i> *	MNHW_S.15.25 03	Switzerland	Frinvillier	47.17	7.25		MW774536	MW776388	-
<i>T. clandestinus</i> †*	MNHW_S.15.26 02	Switzerland	Frinvillier 2	47.17	7.25		MW774537	MW776389	MW775815
<i>T. montanus</i> †	MNHW_S.15.26 03	Switzerland	Frinvillier 2	47.17	7.25		MW774539	MW776390	MW775816
<i>T. clandestinus</i>	MNHW_S.15.27 04	Switzerland	Twannbachsc hlucht	47.10	7.14		MW774540	MW776391	MW775817
<i>T. clandestinus</i>	MNHW_S.15.27 05	Switzerland	Twannbachsc hlucht	47.10	7.14		MW774541	MW776392	MW775818
<i>T. clandestinus</i>	MNHW_S.15.27 06	Switzerland	Twannbachsc hlucht	47.10	7.14		-	MW776394	MW775820
<i>T. clandestinus</i> †	MNHW_S.15.28 06	Switzerland	Saint- Imier/Les Pontins	47.14	6.99		MW774545	MW776395	MW775823
<i>T. villosus</i>	MNHW_S.15.22 a_100	Switzerland	Gorges du Pichoux	47.29	7.22		MW774530	-	MW775809
<i>T. villosus</i>	MNHW_S.15.22 a_101	Switzerland	Gorges du Pichoux	47.29	7.22		MW774531	MW776384	MW775810
<i>T. villosus</i> †	MNHW_S.15.29 100	Switzerland	Montagne De Cernier	47.08	6.89		MW774549	MW776396	MW775827
<i>T. villosus</i> †	MNHW_S.15.29 101	Switzerland	Montagne De Cernier	47.08	6.89		MW440985	MW447773	MW440678
<i>T. villosus</i> *	MNHW_F.15.33 100	France	Les Rousses- d'Amont	46.51	6.09		MW774474	MW776373	MW775747
<i>T. villosus</i>	MNHW_F.15.33 101	France	Les Rousses- d'Amont	46.51	6.09		MW774475	MW772284	MW775748
<i>T. villosus</i>	MNHW_F.15.35 100	France	Mouthe, Source du Doubs	46.71	6.21		MW774481	MW772290	MW775754
<i>T. villosus</i>	MNHW_F.15.35 101	France	Mouthe, Source du Doubs	46.71	6.21		MW774482	MW772291	MW775755
<i>T. villosus</i>	MNHW_F.15.44 100	France	Grand Colombier				MW774495	MW776377	MW775772
<i>T. villosus</i>	MNHW_S- Er_100	Switzerland	Erschwil	47.37	7.56		MW774558	MW776398	MW775838
<i>T. villosus</i>	MNHW_S- Er_101	Switzerland	Erschwil	47.37	7.56		MW774559	MW772359	MW775839
<i>T. villosus</i>	MNHW_S- Bu_100	Switzerland	Buttes	46.88	6.54		MW774557	MW772356	MW775835
<i>T. villosus</i> *	MNHW_S.15.17 100	Switzerland	Gorges de Court	47.26	7.34		MW774514	MW776379	MW775794
<i>T. villosus</i>	MNHW_S.15.17 101	Switzerland	Gorges de Court	47.26	7.34		MW774515	MW776380	MW775795
<i>T. montanus</i> *	MNHW_S.15.23 01	Switzerland	Gorges du Pichoux 2	47.29	7.22		MW774532	MW776385	MW775811
<i>T. montanus</i>	MNHW_S.15.23 02	Switzerland	Gorges du Pichoux 2	47.29	7.22		MW774533	MW776386	MW775812
<i>T. montanus</i>	MNHW_S- Me_14	Switzerland	Mervelier	47.34	7.51		MW774562	MW772362	MW775843
<i>T. montanus</i>	MNHW_S- Mell_12	Switzerland	Mervelier 2	47.34	7.51		-	MW772363	MW775844
<i>T. montanus</i>	MNHW_S- Mell_13	Switzerland	Mervelier 2	47.34	7.51		MW774563	MW772364	
<i>T. montanus</i>	MNHW_S- Er_05	Switzerland	Erschwil	47.37	7.56		-	MW772357	MW775836

<i>T. montanus</i>	MNHW_S-Er_08	Switzerland	Erschwil	47.37	7.56		-	MW772358	MW775837
<i>T. caelatus</i> †	MNHW_S.15.21_01	Switzerland	Gorges de Moutier	47.29	7.38		MW774522	MW772336	MW775801
<i>T. caelatus</i> †	MNHW_S.15.21_02	Switzerland	Gorges de Moutier	47.29	7.38		MW440982	MW621001	MW440675
<i>T. caelatus</i>	MNHW_S.15.21_04	Switzerland	Gorges de Moutier	47.29	7.38		MW774523	MW772337	MW775802
<i>T. montanus</i> †	MNHW_S.15.22_a_10	Switzerland	Gorges du Pichoux	47.29	7.22		MW774528	MW772341	MW775807
<i>T. albulus</i>	MNHW_S.15.22_a_11	Switzerland	Gorges du Pichoux	47.29	7.22		MW774529	MW772342	MW775808
<i>T. clandestinus</i>	MNHW_S.15.32_01	Switzerland	Sources de l'Orbe	46.70	6.34		MW774553	MW772351	MW775830
<i>T. clandestinus</i>	MNHW_S.15.32_02	Switzerland	Sources de l'Orbe	46.70	6.34		MW774554	MW772352	MW775831
<i>T. clandestinus</i>	MNHW_S.15.32_03	Switzerland	Sources de l'Orbe	46.70	6.34		-	MW772353	MW775832
<i>T. pascali</i> †	MNHW_F.15.33_04	France	Les Rousses-d'Amont	46.51	6.09		MW774471	MW772283	MW775744
<i>T. pascali</i> †	MNHW_F.15.33_05	France	Les Rousses-d'Amont	46.51	6.09		MW774472	MW776371	MW775745
<i>T. pascali</i> †	MNHW_F.15.33_06	France	Les Rousses-d'Amont	46.51	6.09		MW774473	MW776372	MW775746
<i>T. pascali</i> †	MNHW_F.15.39_01	France	Cascades du Hérisson	46.62	5.86		MW774488	MW772302	MW775764
<i>T. pascali</i> †	MNHW_F.15.39_02	France	Cascades du Hérisson	46.62	5.86		-	MW772303	MW775765
<i>T. pascali</i> †	MNHW_F.15.39_a_01	France	Cascades du Hérisson	46.62	5.86		MW774489	MW776374	MW775766
<i>T. plebicola</i>	MNHW_F.15.41_05	France	HAustriaville-Lompnes 2	45.97	5.58		MW774490	MW772304	MW775767
<i>T. plebicola</i> †	MNHW_F.15.42_a_03	France	Arandas	45.89	5.49		MW774491	MW772305	MW775768
<i>T. plebicola</i> †	MNHW_F.15.42_a_04	France	Arandas	45.89	5.49		MW774492	MW772306	MW775769
<i>T. plebicola</i> *	MNHW_F.15.43_01	France	Virieu-Le-Petit	45.91	5.74		MW774493	MW776375	MW775770
<i>T. plebicola</i>	MNHW_F.15.43_02	France	Virieu-Le-Petit	45.91	5.74		MW774494	MW776376	MW775771
<i>T. pascali</i> †*	MNHW_F.15.47_04	France	Jalinard	46.06	5.65		-	MW772307	MW775773
<i>T. pascali</i> †	MNHW_F.15.47_05	France	Jalinard	46.06	5.65		MW774496	MW776378	MW775774
<i>T. montanus</i>	MNHW_F-Ech_09	France	Échallon	46.20	5.75		MW774501	MW772315	MW775781
<i>T. montanus</i> †	MNHW_S.15.17_01	Switzerland	Gorges de Court	47.26	7.34		MW774511	MW772326	MW775791
<i>T. clandestinus</i> †	MNHW_S.15.17_02	Switzerland	Gorges de Court	47.26	7.34		MW774512	MW772327	MW775792
<i>T. montanus</i> †	MNHW_S.15.20_17	Switzerland	Gorges de Court 4	47.25	7.35		MW774520	MW772334	MW775799
<i>T. clandestinus</i> †	MNHW_S.15.20_18	Switzerland	Gorges de Court 4	47.25	7.35		MW774521	MW772335	MW775800
<i>T. clandestinus</i>	MNHW_S.15.22_06	Switzerland	Gorges du Pichoux	47.29	7.22		MW774527	MW776383	MW775806
<i>T. clandestinus</i>	MNHW_S.15.22_05	Switzerland	Gorges du Pichoux	47.29	7.22		MW774526	MW772340	MW775805
<i>T. clandestinus</i> †	MNHW_S.15.24_01	Switzerland	Undervelier	47.32	7.22		MW774534	MW776387	MW775813
<i>T. montanus</i> *	MNHW_S.15.24_07	Switzerland	Undervelier	47.32	7.22		MW774535	MW772343	MW775814
<i>T. clandestinus</i> †*	MNHW_S.15.28_07	Switzerland	Saint-Imier/Les Pontins	47.14	6.99		MW774546	MW772347	MW775824
<i>T. clandestinus</i> †	MNHW_S.15.28_08	Switzerland	Saint-Imier/Les Pontins	47.14	6.99		MW774547	-	MW775825
<i>T. clandestinus</i> †	MNHW_S.15.29_01	Switzerland	Montagne De Cernier	47.08	6.89		MW774548	MW772348	MW775826
<i>T. clandestinus</i> †	MNHW_S.15.29_02	Switzerland	Montagne De Cernier	47.08	6.89		MW440983	MW447772	MW440676

<i>T. clandestinus</i>	MNHW_S.15.30 01	Switzerland	Gorges de L'Areuse	46.96	6.82		MW774550	MW772349	MW775828
<i>T. circinnatus</i> †	MNHW_S.15.30 02	Switzerland	Gorges de L'Areuse	46.96	6.82		MW774551	MW772350	MW775829
<i>T. circinnatus</i> *	MNHW_S.15.30 03	Switzerland	Gorges de L'Areuse	46.96	6.82		MW774552	MW776397	-
<i>T. clandestinus</i>	MNHW_F.15.31 01	France	Mont d'Or	46.74	6.35		MW774468	MW772280	MW775741
<i>T. clandestinus</i> †	MNHW_F.15.31 02	France	Mont d'Or	46.74	6.35		MW774469	MW772281	MW775742
<i>T. clandestinus</i> †	MNHW_F.15.31 03	France	Mont d'Or	46.74	6.35		MW774470	MW772282	MW775743
<i>T. circinnatus</i> †	MNHW_F.15.34 01	France	La Chevry	46.65	6.05		MW774476	MW772285	MW775749
<i>T. circinnatus</i> †*	MNHW_F.15.34 03	France	La Chevry	46.65	6.05		MW774477	MW772286	MW775750
<i>T. circinnatus</i> †	MNHW_F.15.34 05	France	La Chevry	46.65	6.05		MW774478	MW772287	MW775751
<i>T. circinnatus</i> †	MNHW_F.15.35 01	France	Mouthe, Source du Doubs	46.71	6.21		MW774479	MW772288	MW775752
<i>T. clandestinus</i>	MNHW_F.15.35 02	France	Mouthe, Source du Doubs	46.71	6.21		MW774480	MW772289	MW775753
<i>T. circinnatus</i> †*	MNHW_F.15.36 01	France	Bonnevaux	46.82	6.21		MW774483	MW772292	MW775756
<i>T. montanus</i>	MNHW_F.15.36 02	France	Bonnevaux	46.82	6.21		MW774484	MW772293	MW775757
<i>T. circinnatus</i> †	MNHW_F.15.37 05	France	Cascade du Moulin du SAustria	46.76	6.02		-	MW772296	-
<i>T. circinnatus</i> †	MNHW_F.15.37 06	France	Cascade du Moulin du SAustria	46.76	6.02		MW774485	MW772297	-
<i>T. pascali</i> †	MNHW_F.15.38 05	France	Chaux-des- Crottenay	46.65	5.99		MW774486	MW772300	MW775762
<i>T. circinnatus</i> †*	MNHW_F.15.38 06	France	Chaux-des- Crottenay	46.65	5.99		MW774487	MW772301	MW775763
<i>T. clandestinus</i>	MNHW_S- Gr_10	Switzerland	Grindel	47.39	7.51		-	MW772360	MW775840
<i>T. clandestinus</i>	MNHW_S- Gr_11	Switzerland	Grindel	47.39	7.51		MW774560	MW772361	MW775841
<i>T. circinnatus</i>	MNHW_F- Pr_17	France	Pretin	46.93	5.85		MW774502	MW772317	MW775783
<i>T. circinnatus</i>	MNHW_F- Pr_18	France	Pretin	46.93	5.85		MW774503	MW772318	MW775784
<i>T. circinnatus</i>	MNHW_F-An- M_06	France	Andelot-en- Montagne	46.88	5.95		-	MW772308	MW775775
<i>T. circinnatus</i>	MNHW_F-An- M_09	France	Andelot-en- Montagne	46.88	5.95		MW774497	MW772309	-
<i>T. clandestinus</i>	MNHW_S- Bu_05	Switzerland	Buttes	46.88	6.54		MW774556	-	-
<i>T. clandestinus</i>	MNHW_F- ChJ_43	France	Château de Joux	46.87	6.37		-	MW772310	MW775777
<i>T. clandestinus</i>	MNHW_F- ChJ_44	France	Château de Joux	46.87	6.37		-	MW772311	MW775778
<i>T. villosus</i>	NMBE_565855	Switzerland	Chrüzhütte 1746m	46.89	8.44	1746	MW703604	MW709348	MW709322
<i>T. villosus</i>	NMBE_565856	Switzerland	Chrüzhütte 1746m	46.89	8.44	1746	MW703605	MW709390	MW709323
<i>T. albulus</i>	NMBE_565858	Switzerland	Schwanden 1459m	46.88	8.45	1460	MW703606	MW709391	MW709324
<i>T. albulus</i> *	NMBE_565860	Switzerland	Schwanden 1459m	46.88	8.45	1460	MW703608	MW709392	MW709326
<i>T. villosus</i>	NMBE_565862	Switzerland	Grünenboden 2015m	46.87	8.47	2015	MW703609	MW709350	MW709327
<i>T. villosus</i>	NMBE_565859	Switzerland	Grünenboden 2015m	46.87	8.47	2015	MW703607	MW709349	MW709325
<i>T. villosus</i> *	NMBE_565821	Switzerland	Schonegg 2234m	46.87	8.25	2234	ON477945	ON479906	ON479899
<i>T. villosus</i>	NMBE_565822	Switzerland	Schonegg 2234m	46.87	8.25	2234	MW703593	MW709338	MW709311

<i>T. villosus</i>	NMBE_565824	Switzerland					-	MW709339	MW709312
			Lang Band? 1636m insgäu bach	46.88					
<i>T. villosus</i>	NMBE_565825	Switzerland			8.44	1640	MW703594	MW709340	MW709313
<i>T. villosus</i>	NMBE_565832	Switzerland	Lombachalp	46.75	7.92	1600	MW703600	MW709344	MW709319
<i>T. clandestinus</i>	NMBE_565831	Switzerland	Churwalden	46.81	9.53	1120	MW703599	MW709343	MW709318
<i>T. villosus</i>	NMBE_565828	Switzerland	Jura	46.83	6.50	1120	MW703596	-	MW709315
<i>T. clandestinus</i>	NMBE_565829	Switzerland	Jura	46.80	6.50	1330	MW703597	MW709341	MW709316
<i>T. villosus</i>	NMBE_565830	Switzerland	Pilatus	46.99	8.26	1308	MW703598	MW709342	MW709317
<i>T. villosus</i>	NMBE_565827	Switzerland	Mont Tendre	46.60	6.30	1630	MW703595	-	MW709314
<i>T. villosus</i>	NMBE_565833	Switzerland	Beatenberg	46.73	7.80	1800	MW703601	MW709345	MW709320
<i>T. villosus</i>	NMBE_565834	Switzerland	Beatenberg, 1728m	46.70	7.80	1730	MW703602	MW709346	-
<i>T. albulus</i>	NMBE_565836	Switzerland	Beatenberg, 1751m	46.70	7.80	1730	MW703603	MW709347	MW709321
<i>T. villosus</i>	NMSG-IM- 28906	Switzerland	Bad Ragaz/Pizol SG	46.99	9.46				
<i>T. albulus</i>	NMSG-IM- 28907	Switzerland	Mittelsass Kurve in den Wald SG	47.00	9.46				
<i>T. villosus</i>	NMSG-IM- 28908	Switzerland	Wiese Pardiell SG	46.99	9.46				
<i>T. villosus</i>	NMSG-IM- 28909	Switzerland	oberhalb Pardiell SG	46.99	9.46				
<i>R. biconica</i>	NMBE_567164	Switzerland	Bannalp Schonegg	46.87	8.47	2234	MW435154	MW433778	MW433799
<i>R. biconica</i>	NMBE_567165	Switzerland	Bannalp Schonegg	46.87	8.47	2234	MW435155	MW433779	MW433800
<i>R. biconica</i> *	NMBE_567167	Switzerland	Chaiserstuel	46.88	8.47	2263	MW435156	MW433780	MW433801
<i>R. biconica</i>	NMBE_567168	Switzerland	Chaiserstuel	46.88	8.47	2263	MW435157	MW433781	MW433802
<i>R. biconica</i>	NMBE_567149	Switzerland	Wissberg I	46.81	8.47	2335	MW435158	MW433782	MW433803
<i>R. biconica</i> *	NMBE_567150	Switzerland	Wissberg I	46.81	8.47	2335	MW435159	MW433783	MW433804
<i>R. biconica</i>	NMBE_567152	Switzerland	Wissberg II	46.81	8.36	2355	MW435160	MW433784	MW433805
<i>R. biconica</i>	NMBE_567153	Switzerland	Wissberg II	46.81	8.36	2355	MW435161	MW433785	MW433806
<i>R. biconica</i>	NMBE_567155	Switzerland	Widderfeld I	46.84	8.33	2120	MW435162	MW433786	MW433807
<i>R. biconica</i> *	NMBE_567156	Switzerland	Widderfeld I	46.84	8.33	2120	MW435163	MW433787	MW433808
<i>R. biconica</i>	NMBE_567159	Switzerland	Widderfeld II	46.83	8.33	2290	MW435164	MW433788	MW433809
<i>R. biconica</i>	NMBE_567161	Switzerland	Brisen I	46.90	8.45	2045	MW435165	MW433789	MW433810
<i>R. biconica</i>	NMBE_567137	Switzerland	Brisen I	46.90	8.45	2045	MW435166	MW433790	MW433811
<i>R. biconica</i>	NMBE_567139	Switzerland	Brisen II	46.90	8.46	2130	MW435167	MW433791	MW433812
<i>R. biconica</i>	NMBE_567140	Switzerland	Brisen II	46.90	8.46	2130	MW435168	MW433792	MW433813
<i>R. biconica</i>	NMBE_567142	Switzerland	Brisen III	46.91	8.47	2090	MW435169	MW433793	MW433814
<i>R. biconica</i>	NMBE_567143	Switzerland	Brisen III	46.91	8.47	2090	MW435170	MW433794	MW433815
<i>R. biconica</i>	NMBE_567145	Switzerland	Gitschen I	46.88	8.57	1890	MW435171	MW433795	MW433816
<i>R. biconica</i>	NMBE_567146	Switzerland	Gitschen I	46.88	8.57	1890	MW435172	MW433796	MW433817
<i>R. biconica</i> *	NMBE_567148	Switzerland	Gitschen II	46.88	8.57	1970	MW435173	MW433797	MW433818
<i>R. biconica</i>	NMBE_567162	Switzerland	Gitschen II	46.88	8.57	1970	MW435174	MW433798	MW433819
<i>T. villosus</i>	NMBE_568160	Switzerland	Torgon, La Cheurgne	46.31	6.85	1282			
<i>T. albulus</i>	NMBE_568161	Switzerland	Torgon, La Cheurgne	46.31	6.85	1282			
<i>T. villosus</i>	NMBE_568164	Switzerland	Torgon, La Cheurgne	46.31	6.85	1318			
<i>T. villosus</i>	NMBE_568167	Switzerland	Torgon, La Cheurgne	46.31	6.85	1342			
<i>T. hispidus</i>	NMBE_568099	Sweden	prov. Uppland, Uppsala, Linnaeus Garden	59.86	17.63				
<i>T. hispidus</i> *	NMBE_568100	Sweden	prov. Uppland, Uppsala, Linnaeus Garden	59.86	17.63		ON477947	-	-

<i>T. hispidus</i>	NMBE_568107	Sweden	prov. Västergötland, Borås, Rya asar	57.74	12.92				
<i>T. villersii</i> *	NMBE_568108	Sweden	prov. Västergötland, Borås, Rya asar	57.74	12.92				
<i>T. hispidus</i> *	NMBE_568103	Sweden	prov. Östergötland, Väst	58.33	15.73		ON477948	ON479908	ON479901
<i>T. villersii</i>	NMBE_568104	Sweden	prov. Östergötland, Väst	58.33	15.73				
<i>T. villosus</i>	MNHW_A.EE_100	Austria	Ebenwald-Egg	47.43	9.92		MW774452	MW772262	-
<i>T. villosus</i> †	MNHW_A.Me_101	Austria	Mellau	47.35	9.97		MW774457	MW772268	-
<i>T. villosus</i>	MNHW_A.Dor_102	Austria	Dornbündt	47.45	10.01		MW774451	MW772261	-
<i>T. villosus</i>	MNHW_A.Bo_103	Austria	Bödele	47.42	9.81		MW774448	MW772258	MW775722
<i>T. villosus</i>	MNHW_A.Da_104	Austria	Damüls	47.29	9.89		MW774449	MW772259	MW775723
<i>T. villosus</i> †	MNHW_A.MtK_105	Austria	Mt Kojenkopf	47.33	9.88		MW774459	MW772270	MW775731
<i>T. villosus</i> †	MNHW_A.MtB_106	Austria	Mt Baumgarten	47.40	9.94		MW774458	MW772269	MW775730
<i>T. villosus</i>	MNHW_G.15.51_107	Germany	Fützen	47.82	8.51		MW774505	MW772320	MW775786
<i>T. villosus</i> †	MNHW_G.15.50a_108	Germany	Buchberg 2	47.83	8.53		MW774504	MW772319	MW775785
<i>T. villosus</i> †	MNHW_G.15.52_109	Germany	Geisingen	47.92	8.65		MW774506	MW772321	MW775787
<i>T. villosus</i>	MNHW_G.15.53_110	Germany	Willingendorf	48.21	8.61		MW774507	MW772322	MW775788
<i>T. villosus</i>	MNHW_G.Bi_111	Germany	Bittenbrunn	48.74	11.16		MW774508	MW772323	MW775789
<i>T. villosus</i>	MNHW_G.Im_112	Germany	Immendingen	47.93	8.75		MW774510	MW772325	MW775790
<i>T. villosus</i> *	MNHW_G.Dil_113	Germany	Dillingen a.d. Donau	48.57	10.50		MW774509	MW772324	
<i>T. villosus</i>	MNHW_S.15.4901	Switzerland	Brisen	46.90	8.45		-	MW772354	MW775833
<i>T. villosus</i>	MNHW_S.15.4902	Switzerland	Brisen	46.90	8.45		MW774555	MW772355	MW775834
<i>T. albulus</i>	MNHW_A.Dor_102	Austria	Dornbündt	47.45	10.01		-	MW772260	-
<i>T. sericeus</i>	MNHW_A.Kap_103	Austria	Kapf n. Egg	47.42	9.95		MW774455	MW772265	-
<i>T. sericeus</i>	MNHW_A.Kap_104	Austria	Kapf n. Egg	47.42	9.95		MW774456	MW772266	MW775727
<i>T. clandestinus</i> †	MNHW_A.Me_05	Austria	Mellau	47.35	9.97		-	MW772267	MW775728
<i>T. clandestinus</i>	MNHW_A.FA_07	Austria	Forst-Au	47.33	9.97		MW774453	MW772263	MW775725
<i>T. clandestinus</i>	MNHW_A.FA_08	Austria	Forst-Au	47.33	9.97		MW774454	MW772264	MW775726
<i>T. sp.3</i> †	MNHW_F.15.0909	France	between Aubure & La Petite Verrerie	48.21	7.25		MW774460	MW772271	MW775732
<i>T. sp.3</i> †	MNHW_F.15.0910	France	between Aubure & La Petite Verrerie	48.21	7.25		MW774461	MW772272	MW775733
<i>T. clandestinus</i> †*	MNHW_F.15.1111	France	Tellure	48.21	7.13		MW774462	MW772273	MW775734
<i>T. clandestinus</i> †	MNHW_F.15.1112	France	Tellure	48.21	7.13		-	MW772274	MW775735
<i>T. clandestinus</i> †	MNHW_F.15.1413	France	Source de la Moselle n. Bussang	47.89	6.88		MW774463	MW772275	MW775736

<i>T. clandestinus</i> †	MNHW_F.15.14 14	France	Source de la Moselle n. Bussang	47.89	6.88		MW774464	MW772276	MW775737
<i>T. clandestinus</i> †	MNHW_F.15.15 15	France	Bussang	47.87	6.83		MW774465	MW772277	MW775738
<i>T. clandestinus</i> †	MNHW_F.15.15 16	France	Bussang	47.87	6.83		MW774466	MW772278	MW775739
<i>T. clandestinus</i> †	MNHW_F.15.15 17	France	Bussang	47.87	6.83		MW774467	MW772279	MW775740
<i>T. albulus</i>	NMBE_568077	Switzerland	Vex	46.19	7.41	654			
<i>T. albulus</i>	NMBE_568079	Switzerland	Bex, Mines de Sel	46.28	7.03	598			
<i>T. albulus</i> †	NMBE_568084	Switzerland	St. Maurice, Grotte aux Fées	46.22	7.00	455			
<i>T. albulus</i>	NMBE_568086	Switzerland	Martigny, Amphitheater	46.09	7.07	497			
<i>T. albulus</i>	NMBE_568087	Switzerland	Martigny, Amphitheater	46.09	7.07	497			
<i>T. albulus</i>	NMBE_568089	Switzerland	Vex, Römerbrücke	46.19	7.41	670			
<i>T. plebeius</i>	NMBE_568094	Switzerland	Lac du Mont d'Orge	46.23	7.33	624	ON477946	ON479907	ON479900
<i>T. plebeius</i>	NMBE_568095	Switzerland	Lac du Mont d'Orge	46.23	7.33	624			
<i>T. clandestinus</i> †	NMBE_569597	Switzerland	Bern-Bümpliz, Schlosspark	46.94	7.39	540			
<i>T. clandestinus</i> †	NMBE_569598	Switzerland	Bern-Bümpliz, Schlosspark	46.94	7.39	540			
<i>T. albulus</i>	NMBE_569671	Switzerland	Münsingen	46.87	7.54				
<i>T. villosus</i> †	NMBE_569638	Switzerland	Broc, Waldlichtung	46.61	7.09	744			
<i>T. plebeius</i>	NMBE_569672	Switzerland	Bulle, Schlosspark	46.62	7.06	777			
<i>T. plebeius</i>	NMBE_569673	Switzerland	Bulle, Schlosspark	46.62	7.06	777			
<i>T. clandestinus</i>	NMBE_569674	Switzerland	Châtel-sur-Montsalvens, Staumauer	46.61	7.14	847			
<i>T. albulus</i>	NMBE_569675	Switzerland	Châtel-sur-Montsalvens, Staumauer	46.61	7.14	847			
<i>T. striolatus</i>	NMBE_569618	Germany	Stormsdorf, NSG Reppeliner Bachtal	54.07	12.45				
<i>T. sericeus</i>	NMBE_569620	Germany	Insel Poel	54.00	11.38				
<i>T. striolatus</i>	NMBE_569641	Germany	Gross Woltersdorf	53.87	11.39				
<i>T. sericeus</i>	NMBE_569643	Germany	Beidendorf	53.82	11.39				
<i>T. sp.3 *</i>	NMBE_569645	Germany	Greese	53.87	11.54				
<i>T. striolatus</i>	NMBE_569647	Germany	Tarnewitzer Bach	53.95	11.22				
<i>T. sericeus *</i>	NMBE_569649	Germany	Wüstenmark	53.77	11.25				
<i>T. striolatus *</i>	NMBE_569651	Germany	Flemendorf, Kirche	54.33	12.80				
<i>T. sp.2 *</i>	NMBE_569655	Germany	Rügen	54.50	13.57				
<i>T. sericeus</i>	MNHW_Ka-3	Germany	Kaisheim	48.73	10.87	401			
<i>T. sericeus</i>	MNHW_La-7	Germany	Lauingen	48.56	10.42	443			
<i>T. sericeus</i>	MNHW_G-Gu9	Germany	Günzburg, Reisensburg	48.47	10.30	436			
<i>T. sericeus</i>	MNHW_Gm-1	Germany	Gremheim	48.63	10.65	445			
<i>T. villosulus</i>	MNHW_SK.19. 54_308	Sloveniavak ia	Hlboké 2	49.12	18.12	522			
<i>T. villosulus</i> †	MNHW_PL.20.4 5_305	Poland	Pieskowa Skala (PN)	50.24	19.78	435			
<i>T. villosulus</i> †	MNHW_PL.20.3 2_307	Poland	Muszyna 2	49.50	20.92	477			
<i>T. villosulus</i> †*	MNHW_PL.20.1 6_306	Poland	Wapowce	49.80	22.65	213			

<i>T. plebeius</i>	MNHW_S.15.48 309	Switzerland	Chateau- D'Oex	46.47	7.13	933			
<i>T. albulus</i>	MNHW_S.15.48 311	Switzerland	Chateau- D'Oex	46.47	7.13	933			
<i>T. albulus</i>	MNHW_S.15.48 310	Switzerland	Chateau- D'Oex	46.47	7.13	933			
<i>T. sericeus</i>	MNHW_Ei6	Germany	Eichberg	47.85	8.51	829			
<i>T. becasis</i>	MNHW_F.18.48 302	France	Arties near Auzat	42.74	1.48	984			
<i>T. becasis</i> †*	MNHW_F.18.30 299	France	Forêt Bac Estable 2	42.78	2.26	1391			
<i>T. becasis</i> †	MNHW_F.18.37 301	France	Forêt de Beleste	42.89	1.97	844			
<i>T. becasis</i> †	MNHW_F.18.35 300	France	Le Chandelier	42.88	2.03	826			
<i>T. becasis</i>	MNHW_F.18.52 303	France	Saint-Martin- Lys	42.83	2.23	333			
<i>T. clandestinus</i> †	MNHW_F.VM_ 295	France	Vallon du Moulinot	47.18	5.95				
<i>T. clandestinus</i> †	MNHW_F.RP_2 97	France	La Roche des Pins	47.11	6.15				
<i>T. clandestinus</i> †	MNHW_F.VM_ 294	France	Vallon du Moulinot	47.18	5.95				
<i>T. clandestinus</i> †	MNHW_F.ML_2 96	France	Mont de Lune	47.15	5.95				
<i>T. striolatus</i>	MNHW_S.Sch_ 07	Switzerland	Schleitheim	47.76	8.50	508			
<i>T. striolatus</i> †	MNHW_A.17.12 01	Austria	Schafberg	47.78	13.43	1767			
<i>T. striolatus</i> †	MNHW_I.16.12 01	Ireland	Maam	53.51	-9.53	20			
<i>T. striolatus</i> †*	MNHW_SK.19. 71_01	Slovakia	Varín	49.20	18.87	406			
<i>T. striolatus</i> †*	MNHW_F.18.10 _06	France	Blecquenecqu es n. Marquise	50.82	1.73	26			
<i>T. striolatus</i>	MNHW_SK.19. 63_01	Slovakia	Medved'ov	47.80	17.65	115			
<i>T. striolatus</i> †	MNHW_GB.Br_ 01	United Kingdom	Bramley near Basingstoke	51.33	-1.06	62			
<i>T. striolatus</i>	MNHW_G.Ri_0 2	Germany	Riedensheim	48.74	11.11	387			
<i>T. albulus</i> *	MNHW_F.LaD_ 24	France	Là Diat	45.34	5.80	722			
<i>T. albulus</i>	MNHW_F.LeP_ 34	France	Le Pont du Lac	45.43	5.88	750			
<i>T. albulus</i>	MNHW_F.Sa_3 4	France	Sassenage	45.21	5.65	252			
<i>T. hispidus</i> †	MNHW_F.18.25 279	France	Escames	49.55	1.81	134			
<i>T. hispidus</i> †	MNHW_F.18.07 278	France	Beaucamps- Le-Jeune	49.82	1.77	199			
<i>T. sp.3</i>	MNHW_F.15.13 276	France	Hoft Cascade du Hohwald	48.40	7.30	676			
<i>T. hispidus</i> †	MNHW_F.18.05 277	France	Fouquénies	49.46	2.06	29			
<i>T. sp.4</i>	MNHW_F.CC_2 84	France	Combe aux Cordiers	47.40	5.93				
<i>T. sp.4</i> *	MNHW_F.SF_2 82	France	Source de la Foulotière	47.13	5.48				
<i>T. albulus</i> †	MNHW_F.LE_2 80	France	Les Essarts	46.93	5.32				
<i>T. montanus</i>	MNHW_F.CP_2 91	France	Colline Planoise	47.21	5.98				
<i>T. montanus</i> †	MNHW_F.LR_2 90	France	La Ruchotte	47.14	5.49				
<i>T. montanus</i>	MNHW_F.Soy_ 292	France	Soyère	47.31	6.81				
<i>T. villersii</i>	MNHW_F.BS_2 93	France	Bord de Saône	47.47	5.65				
<i>T. albulus</i>	MNHW_So4	Germany	Sommerau	47.81	8.27	878			
<i>T. sericeus</i> †	MNHW_Re5	Germany	Reischenau	48.32	10.59	468			

<i>T. albulus</i> †*	MNHW_G.15.0 5_285	Germany	Ketsch	49.37	8.52	107			
<i>T. sericeus</i>	MNHW_G.17.1 9_286	Germany	Ramsau b. Berchtesgaden	47.61	12.94	621			
<i>T. albulus</i>	MNHW_S.Ros_ 288	Switzerland	Rosern	47.50	7.68	531			
<i>T. albulus</i>	MNHW_S.Fr_2 87	Switzerland	Froburg	47.38	7.89	833			
<i>T. albulus</i> †	MNHW_RF4	Switzerland	Ruine Farnsburg	47.49	7.87	721			
<i>T. sp.1</i> †	MNHW_St-14	Germany	Staubing	48.89	11.81	355			
<i>T. sericeus</i> †	MNHW_G.17.0 5_298	Germany	Pfatter	48.97	12.39	283			
<i>T. sp.3</i>	MNHW_KI-2	Germany	Kleinmehring	48.76	11.54	378			
<i>T. sp.3</i> *	MNHW_Kle-8	Germany	Kleinprüfenin g	49.01	12.03	326			
<i>T. albulus</i> †*	MNHW_Sau1	Austria	Sausteig	47.44	10.02	994			
<i>T. albulus</i>	MNHW_Sau2	Austria	Sausteig	47.44	10.02	994			
<i>T. sp.4</i>	MNHW_A.17.15 271	Austria	Schlenken 2	47.68	13.21	1398			
<i>T. sp.2</i> †	MNHW_CZ.Vit_ 274	Czech Republic	Vitkovice	50.69	15.53	614			
<i>T. sp.2</i> †*	MNHW_CZ.Lan 273	Czech Republic	Lánov	50.64	15.67	593			
<i>T. sp.2</i> †*	MNHW_CZ.CD 272	Czech Republic	Černý Důl	50.65	15.71	667			
<i>T. villersii</i> †	MNHW_CZ.19. 51_275	Czech Republic	Radňovice	49.56	16.02	610			
<i>T. montanus</i> †	MNHW_F.SF_2 83	France	Source de la Foulotière	47.13	5.48				
<i>T. clandestinus</i>	MNHW_F.LE_2 81	France	Les Essarts	46.93	5.32				
<i>T. montanus</i> †	MNHW_F.Lcr_2 89	France	La croix rouge	47.23	6.74				
<i>T. villersii</i> †	MNHW_PL.20.0 9_252	Poland	Leśna Podlaska	52.12	23.05	143			
<i>T. villosulus</i>	MNHW_PL.19.1 8_254	Poland	Jakubowice near AnnoPoland	50.90	21.84	164			
<i>T. villosulus</i> †	MNHW_PL.20.1 3_253	Poland	Gamlówka	50.56	23.14				
<i>T. villersii</i> †*	MNHW_PL.20.0 7_251	Poland	Budy Leśne n. Białowieża	52.72	23.72	167			
<i>T. villersii</i> †	MNHW_PL.19.1 0_250	Poland	Mątki near Sztum	53.85	19.00	62			
<i>T. villersii</i> †	MNHW_PL.Ro_ 247	Poland	Puszczą Romincka	54.34	22.68				
<i>T. villersii</i> †	MNHW_PL.20.0 4_248	Poland	Rapa	54.31	22.02	107			
<i>T. villosulus</i> †*	MNHW_PL.20.0 5_249	Poland	Cisowy Jar	54.16	22.35	265			
<i>T. sp.4</i>	MNHW_HR.17. 134_209	Croatia	Lokve	45.36	14.73	721			
<i>T. sp.4</i> *	MNHW_HR.17. 108_206	Croatia	Rosulje near Croatiaatska Kostajnica	45.23	16.59	91			
<i>T. sp.4</i>	MNHW_HR.17. 126_208	Croatia	Ogulin (Dobra river)	45.26	15.21	327			
<i>T. sp.4</i>	MNHW_HR.17. 110_207	Croatia	Slunij	45.12	15.60	267			
<i>T. sp.4</i>	MNHW_CZ.17. 33_210	Czech Republic	Špraněk Brook valley	49.67	16.90	430			
<i>T. sp.4</i> †*	MNHW_CZ.19. 78_218	Czech Republic	Pitárné	50.24	17.58	405			
<i>T. villersii</i> †	MNHW_CZ.17. 145_212	Czech Republic	Závist	49.38	16.58	403			
<i>T. sp.4</i> †	MNHW_CZ.19. 35_213	Czech Republic	Srbsko 3	49.94	14.15	280			
<i>T. sp.4</i>	MNHW_CZ.19. 40_215	Czech Republic	Brejil	50.10	13.88	337			

<i>T. sp.4</i>	MNHW_CZ.19.77_217	Czech Republic	Skřipov	49.83	17.89	409			
<i>T. sp.1 †*</i>	MNHW_CZ.19.38_214	Czech Republic	Štěchovice (Maják)	49.85	14.39	198			
<i>T. villersii †</i>	MNHW_CZ.19.43_216	Czech Republic	Debrník	49.12	13.24	725			
<i>T. villersii</i>	MNHW_CZ.17.34_211	Czech Republic	Březina	49.67	16.92	402			
<i>T. villersii †</i>	MNHW_PL.19.27_242	Poland	Bedzin	50.35	19.17	258			
<i>T. villersii</i>	MNHW_PL.Lo_240	Poland	Łopuszna	49.50	20.13	720			
<i>T. villersii</i>	MNHW_PL.19.24_241	Poland	Lipnica Dolna 2	49.86	20.55	280			
<i>T. villersii *</i>	MNHW_UK.En-HW_19	United Kingdom	Hayley Wood	52.16	-0.12	84			
<i>T. villersii †</i>	MNHW_UK.En-D_5	United Kingdom	Downside	51.39	-2.72	160			
<i>T. sp.4</i>	MNHW_A.17.144_205	Austria	Oberdorf	47.41	15.22	504			
<i>T. sericeus</i>	MNHW_A.Dor_200	Austria	Dornbündt	47.45	10.01	880			
<i>T. sericeus †</i>	MNHW_A.Gens_201	Austria	Genabend-Sibratsgfäll	47.44	10.01	1042			
<i>T. sp.2 †*</i>	MNHW_A.17.28_203	Austria	Durnbachtal	47.85	16.02	613			
<i>T. sp.3 †*</i>	MNHW_A.Schw_202	Austria	Schwarzenberg-Loch 2	47.40	9.85	619			
<i>T. sp.4</i>	MNHW_A.17.21_204	Austria	Präbichl 2	47.52	14.95	1235			
<i>T. villersii</i>	MNHW_PL.19.87_238	Poland	Chwalisław	50.43	16.83	444			
<i>T. villersii</i>	MNHW_PL.JW_31	Poland	Wrocław-Jarnołtów	51.12	16.84	112			
<i>T. villersii</i>	MNHW_PL.17.03_239	Poland	Ratnowice near Otmuchów	50.43	17.13	219			
<i>T. villersii</i>	MNHW_PL.JW_33	Poland	Wrocław-Jarnołtów	51.12	16.84	112			
<i>T. villersii</i>	MNHW_PL.JW_32	Poland	Wrocław-Jarnołtów	51.12	16.84	112			
<i>T. villersii †</i>	MNHW_PL.19.82_236	Poland	Wojcieszów Górny	50.93	15.92	391			
<i>T. villersii</i>	MNHW_PL.19.84_237	Poland	Sokolec	50.66	16.48	513			
<i>T. villersii †*</i>	MNHW_NL.19.03_234	Netherlands	Veere 2	51.55	3.65	6			
<i>T. villersii †</i>	MNHW_NL.Ost_233	Netherlands	Oestgeest near Leiden	52.18	4.46	1			
<i>T. villersii</i>	MNHW_NL.03_235	Netherlands	Veere 2	51.55	3.65	6			
<i>T. hispidus †</i>	MNHW_F.18.14_225	France	Larré	50.68	2.06	65			
<i>T. hispidus †</i>	MNHW_F.18.24_223	France	Le Mont Gournoy 2 (Forêt Indivise d'Eu)	49.80	1.59	217			
<i>T. hispidus *</i>	MNHW_F.18.20_222	France	Froise	50.28	1.63	86			
<i>T. pascali †</i>	MNHW_F.Col_228	France	Col. De Vac.	46.27	5.55				
<i>T. hispidus †</i>	MNHW_F.18.08_221	France	Eaucourt-Sur-Somme	50.06	1.88	11			
<i>T. plebeius †</i>	MNHW_F.Com_227	France	Chameyer	44.62	6.50				
<i>T. villersii †*</i>	MNHW_F.18.12_224	France	Licques	50.80	1.94	81			
<i>T. villersii</i>	MNHW_F.18.17_226	France	Cap Gris-Nez	50.87	1.58	58			
<i>T. villersii †</i>	MNHW_F.15.07_219	France	Bertrange	49.32	6.17	164			
<i>T. hispidus †</i>	MNHW_I.16.8_231	Ireland	Lough Gur	52.52	-8.52	66			

<i>T. hispidus</i> †	MNHW_I.16.4_230	Ireland	Rock of Cashel	52.52	-7.89	116			
<i>T. hispidus</i> †	MNHW_I.16.3_229	Ireland	Monastery	53.20	-6.17	126			
<i>T. hispidus</i> †*	MNHW_I.16.10_232	Ireland	Bealaclogga	53.13	-9.07	31			
<i>T. plebeius</i>	MNHW_F.GrCh t 42	France	Grande Chartreuse	45.37	5.79	851			
<i>T. plebeius</i>	MNHW_F.GrCh t 43	France	Grande Chartreuse	45.37	5.79	851			
<i>T. plebeius</i>	MNHW_F.GrCh t 41	France	Grande Chartreuse	45.37	5.79	851			
<i>T. plebeius</i>	MNHW_F.GrCh t 44	France	Grande Chartreuse	45.37	5.79	851			
<i>T. villosulus</i>	MNHW_UA.18.57_266	Ukraine	Podwysokie	49.43	24.59	261			
<i>T. villosulus</i> *	MNHW_UA.18.68_269	Ukraine	Lazeschyna	48.30	24.44	839			
<i>T. villosulus</i> †	MNHW_UA.18.55_264	Ukraine	Bibrka	49.64	24.30	301			
<i>T. villosulus</i> †	MNHW_UA.18.58_267	Ukraine	Mikuliczyn	48.43	24.60	569			
<i>T. villosulus</i> †	MNHW_UA.18.56_265	Ukraine	Swirz	49.65	24.43	315			
<i>T. villosulus</i>	MNHW_UA.18.65_268	Ukraine	Wierchowina	48.15	24.84	604			
<i>T. sericeus</i> †*	MNHW_G.17.17_228	Germany	Thannlehen b. Berchtesgaden	47.64	13.09	1065			
<i>T. sericeus</i> †*	MNHW_G.Ott_227	Germany	Ottendorf	50.94	14.29	271			
<i>T. dubia</i> †	MNHW_G-Mo5	Germany	Moosburg a.d. Isar	48.48	11.93	376			
<i>T. sericeus</i>	MNHW_RW2	Germany	Ruine Waldau	48.16	8.41	751			
<i>T. sericeus</i>	MNHW_RW3	Germany	Ruine Waldau	48.16	8.41	751			
<i>T. sericeus</i>	MNHW_RW1	Germany	Ruine Waldau	48.16	8.41	751			
<i>T. villersii</i> †	MNHW_PL.19.08_256	Poland	Ostrów	52.69	17.66	128			
<i>T. villosulus</i> †	MNHW_PL.19.09_257	Poland	Barcin-Górne Wolice	52.84	17.93	95			
<i>T. villersii</i> †	MNHW_PL.20.01_255	Poland	Siemianice n. Kępno	51.18	18.17	174			
<i>T. villersii</i>	MNHW_PL.19.15_258	Poland	Grabce Józefowskie	51.99	20.50	169			
<i>T. sp.1</i> †*	MNHW_SK.19.62_261	Slovakia	Čičov (Čičovský les)	47.78	17.70	137			
<i>T. sp.4</i> †*	MNHW_SK.19.63_262	Slovakia	Medveďov	47.80	17.65	115			
<i>T. villersii</i> *	MNHW_SK.19.73_263	Sloveniavakia	Belá	49.22	18.96	588			
<i>T. villersii</i> †	MNHW_PL.20.23_246	Poland	Równia	49.41	22.59	498			
<i>T. villersii</i> †	MNHW_PL.20.22_245	Poland	Stebnik	49.46	22.66	419			
<i>T. sp.4</i> *	MNHW_SLO.17.137_259	Slovenia	Planina	45.82	14.25	458			
<i>T. sp.4</i> †	MNHW_SLO.17.140_260	Slovenia	Vintgar Gorge	46.39	14.08	585			
<i>T. villersii</i> †	MNHW_PL.20.34_243	Poland	Szlachtowa 2	49.41	20.54	564			
<i>T. villersii</i> †	MNHW_PL.20.44_244	Poland	Owczary	50.17	19.93	352			
<i>T. clandestinus</i> †	NMBE_569600	Switzerland	Schwarzwasser, Ufer	46.86	7.37	608			
<i>T. clandestinus</i>	NMBE_569601	Switzerland	Schwarzwasser, Ufer	46.86	7.37	608			
<i>T. albulus</i> †	NMBE_569677	Switzerland	Schwarzwasser, Ufer	46.86	7.37	608			
<i>T. clandestinus</i>	NMBE_569603	Switzerland	Schwarzwasser, Brücke	46.84	7.37	617			
<i>T. clandestinus</i> †	NMBE_569604	Switzerland	Schwarzwasser	46.84	7.37	617			

			er, Brücke						
<i>T. albulus</i>	NMBE_569679	Switzerland	Schwarzwasser, Brücke	46.84	7.37	617			
<i>T. albulus</i>	NMBE_569606	Switzerland	Zürich	47.39	8.52	400			
<i>T. albulus</i> †	NMBE_569607	Switzerland	Zürich	47.39	8.52	400			
<i>T. albulus</i> †	NMBE_569680	Switzerland	Brugg, Friedhof, unterhalb Austriaobahnbrücke	47.48	8.21	349			
<i>T. albulus</i> †	NMBE_569681	Switzerland	Brugg, Friedhof, unterhalb Austriaobahnbrücke	47.48	8.21	349			
<i>T. clandestinus</i> †	NMBE_569609	Switzerland	Aarau, Parkanlage Grossratsgebäude	47.39	8.05	348			
<i>T. albulus</i>	NMBE_569683	Switzerland	Brugg, Aareufer	47.48	8.21	330			
<i>T. albulus</i> †	NMBE_569684	Switzerland	Brugg, Aareufer	47.48	8.21	330			
<i>T. clandestinus</i> †	NMBE_569611	Switzerland	Sursee, Surepärkli	47.17	8.11	483			
<i>T. albulus</i> †	NMBE_569686	Switzerland	Hallwil, Schloss	47.32	8.20	446			
<i>T. albulus</i> †	NMBE_569689	Switzerland	Stansstad, Kieswerk, Flusssufer	46.96	8.33	462			
<i>T. albulus</i>	NMBE_569690	Switzerland	Stansstad, Kieswerk, Flusssufer	46.96	8.33	462			
<i>T. villosus</i> †	NMBE_569639	Switzerland	Stansstad, Kieswerk, Flusssufer	46.96	8.33	462			
<i>T. albulus</i> †	NMBE_569616	Switzerland	Zürich, Beckenhof	47.38	8.54	430			
<i>T. villosus</i> †	NMBE_569640	Switzerland	Stans, Bürgenberg, Bürgenstock	46.99	8.37	900			
<i>T. plebeius</i>	NMBE_569635	France	Villard d'arène	45.04	6.35				
<i>T. plebeius</i>	NMBE_569636	France	Villard d'arène	45.04	6.35				
<i>T. plebeius</i>	NMBE_569632	France	Rousset	44.48	6.27				
<i>T. plebeius</i>	NMBE_569629	France	Avonçon	44.54	6.20				
<i>T. plebeius</i>	NMBE_569630	France	Avonçon	44.54	6.20				
<i>T. plebeius</i> †	NMBE_569626	France	Avonçon	44.54	6.20				
<i>T. plebeius</i>	NMBE_569627	France	Avonçon	44.54	6.20				
<i>T. plebeius</i>	NMBE_569660	France	Chateauroux les alpes	44.54	6.49				
<i>T. plebeius</i>	NMBE_569661	France	Chateauroux les alpes	44.54	6.49				
<i>T. plebeius</i>	NMBE_569664	France	Crots	44.54	6.48				
<i>T. plebeius</i> †	NMBE_569666	France	Forest-Saint-Julien	44.62	6.14				
<i>T. plebeius</i>	NMBE_569667	France	Forest-Saint-Julien	44.62	6.14				
<i>T. plebeius</i>	NMBE_569668	France	Chateauroux les alpes	44.54	6.49				
<i>T. plebeius</i>	NMBE_569669	France	Chateauroux les alpes	44.54	6.49				
<i>T. plebeius</i>	NMBE_569623	France	Savines-le-Lac	44.50	6.40				
<i>T. plebeius</i>	NMBE_569624	France	Savines-le-Lac	44.50	6.40				
<i>T. villosus</i>	NMSG-IM-28911	Switzerland	Bad Ragaz, Schammboden, Jonaweg	47.31	8.91				
<i>T. albulus</i>	NMBE_571090	Switzerland	Aarburg, Born-Gratweg	47.32	7.89				

<i>T. albulus</i>	NMBE_571088	Switzerland	Aarburg, Tschärpissstra sse	47.32	7.88			
<i>T. pascali</i> *	NMBE_571084	Switzerland	Könizbergwal d	46.93	7.39	630		
<i>T. albulus</i> †	NMBE_571095	Switzerland	Grimentz	46.18	7.57	1620		
<i>T. sp.3</i>	NMBE_571097	Germany	Badenweiler, Vogelbachtal	47.79	7.70			
<i>T. albulus</i>	NMBE_571102	Switzerland	Mümliswil- Ramiswil, Naturpark Thal	47.37	7.69	1000		
<i>T. striolatus</i> *	NMBE_571105	Germany	Kelkheim- Eppenhain, Naturpark Taunus	50.17	8.38	350		
<i>T. striolatus</i> †	NMBE_571107	Germany	Rheinland- Palatinate, Welterod	50.13	7.90			
<i>T. dubia</i> †*	NMBE_571108	Germany	Diessen am Ammersee	47.95	11.11	544		
<i>T. villosus</i>	NMBE_571110	Germany	Schongau, Heidewiese	47.79	10.87	730		
<i>T. sericeus</i> †*	NMBE_571112	Denmark	Hovedstaden, Fureso Kommune	55.78	12.44	22		
<i>T. dubia</i> †*	NMBE_571125	United Kingdom	Carmel, near Swansea	51.83	-4.05			
<i>T. striolatus</i> *	NMBE_571126	United Kingdom	Pontlliw	51.70	-4.01			
<i>T. beccasis</i> †	NMBE_571128	United Kingdom	Jersey	49.21	-2.13			
<i>T. albulus</i>	NMBE_571130	Switzerland	Waldstatt	47.36	9.30	416		
<i>T. albulus</i>	NMBE_571132	Switzerland	Oberriet	47.33	9.50	867		
<i>T. clandestinus</i> †	NMBE_571134	Switzerland	Flühli	46.81	7.98	1283		
<i>T. albulus</i>	NMBE_571141	Switzerland	Davos	46.80	9.84			
<i>T. clandestinus</i> †	NMBE_571142	Switzerland	Bergün Dorf	46.63	9.75			
<i>T. clandestinus</i> †	NMBE_571234	Switzerland	Amriswil, Kronberg	47.56	9.29			
<i>T. clandestinus</i> †	NMBE_571235	Switzerland	Bürglen, Schloss	47.55	9.15			
<i>T. striolatus</i>	NMBE_571137	Germany	Dortmund	51.49	7.48			
<i>T. clandestinus</i> †	NMBE_571145	Switzerland	Twannbachsc hlucht	47.10	7.14			
<i>T. villosus</i>	NMBE_571139	Germany	Weil, Rheinauen	48.20	7.65			
<i>T. sp.3</i> †	NMBE_571152	Germany	Kelheim,	48.81	11.74			
<i>T. plebeius</i>	NMBE_571154	Germany	Weil, Rheinauen	48.20	7.65			
<i>T. striolatus</i>	NMBE_571156	Germany	Unna	51.57	7.71			
<i>T. striolatus</i> †	NMBE_571158	Germany	Mettmann,	51.08	6.86			
<i>T. striolatus</i> †	NMBE_571160	Germany	Dorsel,	50.38	6.80			
<i>T. albulus</i>	NMBE_571164	Germany	Weil, Rheinauen	48.20	7.65			
<i>T. albulus</i>	NMBE_571166	Switzerland	Bettlingen,	47.57	7.68			
<i>T. sericeus</i>	NMBE_571168	Italia	Südtirol, Wolkenstein Gröden	46.56	11.78			
<i>T. sp.2</i>	NMBE_571172	Germany	Ilmkreis, Gehren, Schlosspark	50.65	11.01			
<i>T. striolatus</i>	NMBE_571174	Germany	Ostholstein bei Oldenburg	54.12	10.61			
<i>T. sp.4</i>	NMBE_571180	Germany	Euskirchen, Blankenheim, Burg	50.44	6.65			
<i>T. villosus</i>	NMBE_571201	Switzerland	Sântis	47.26	9.40			
<i>T. villosus</i> †*	NMBE_571203	Switzerland	Sântis	47.25	9.38			
<i>T. villosus</i> †	NMBE_571206	Switzerland	Sântis,	47.27	9.38			

			Schäfler						
<i>T. villosus</i> †	NMBE_571208	Switzerland	Säntis, Ebenalp	47.28	9.41				
<i>T. striolatus</i>	NMBE_571328	Germany	Nettersheim	50.50	6.63	470			
<i>T. striolatus</i>	NMBE_571319	Germany	Blankenheim	50.44	6.65	495			
<i>T. striolatus</i>	NMBE_571325	Germany	Mechernich	50.44	6.65				
<i>T. villersii</i>	NMBE_571321	Belgium	Fonds de Lesse bei Dinant	50.23	4.90	105			
<i>T. villosus</i>	NMBE_571305	Germany	Scheidegg	47.59	9.84	695			
<i>T. villosus</i>	NMBE_571323	Germany	Griesheim	49.87	8.57				
<i>T. albulus</i>	NMBE_571312	Germany	Rheinaue	49.82	8.44				
<i>T. clandestinus</i>	NMBE_571316	Germany	Badenweiler	47.81	7.70				
<i>T. villosus</i> †	NMBE_571237	Switzerland	Untereggen, Altrüti SG	47.45	9.43	570			
<i>T. albulus</i>	NMBE_571238	Switzerland	Homburg, Mosraa TG	47.64	8.98	570			
<i>T. sericeus</i>	NMBE_571239	Switzerland	Untereggen, Altrüti SG	47.45	9.43	570			
<i>T. villersii</i>	NMBE_571211	Germany	Berlin, Wannseebadweg	52.45	13.18	30			
<i>T. dubia</i> *	NMBE_571212	Germany	Potsdam, Schlaatz, Milanhorst	52.38	13.09	34			
<i>T. villersii</i> *	NMBE_571213	Germany	Potsdam, Wildpark	52.38	12.97	34			
<i>T. villersii</i>	NMBE_571216	Germany	Klein Woltersdorf	53.89	11.41	10			
<i>T. striolatus</i> †	NMBE_571218	Germany	Dutzower See, Nordspitze	53.67	10.95	40			
<i>T. villosulus</i>	NMBE_571220	Czech Republic	Moravia, Bohuslavice u Zlina	49.16	17.62	240			
<i>T. villosulus</i> *	NMBE_571222	Czech Republic	Moravia, Bohuslavice u Zlina	49.16	17.62	240			
<i>T. sp.4</i>	NMBE_571224	Czech Republic	Moravia, Zadverice	49.22	17.79	260			
<i>T. sp.4</i>	NMBE_571225	Czech Republic	Moravia, Zadverice	49.22	17.79	260			
<i>T. striolatus</i>	MNHW_GB.19.01_01	United Kingdom	Diseworth	52.82	-1.33				
<i>T. sp.5</i>	MNHW_G.Gre_01	Germany	Greven	52.11	7.60				
<i>T. striolatus</i>	MNHW_G.Gre_02	Germany	Greven	52.11	7.60				
<i>T. striolatus</i>	MNHW_G.Col_01	Germany	Köln-Westhoven/Ensen	50.90	7.03				
<i>T. striolatus</i>	MNHW_G.Col_02	Germany	Köln-Westhoven/Ensen	50.90	7.03				
<i>T. striolatus</i>	MNHW_G.Col_04	Germany	Köln-Westhoven/Ensen	50.90	7.03				
<i>T. striolatus</i>	MNHW_G.Col_20	Germany	Köln-Westhoven/Ensen	50.90	7.03				
<i>T. striolatus</i>	MNHW_G.Col_21	Germany	Köln-Westhoven/Ensen	50.90	7.03				
<i>T. sp.4</i>	NMBE_571229	Czech Republic	Moravia, Vápenky	48.86	17.65	820			
<i>T. albulus</i>	NMBE_571231	Switzerland	Appenzell, Rufen	47.34	9.49	718			
<i>T. sp.6</i>	MNHN-IM-2013-77397	France	Gonds	45.70	-0.59				
<i>T. becasis</i>	MNHN-IM-2013-76972	France	Saint-Martin-Bideren	43.40	-0.97				

<i>T. albulus</i> †	MNHN-IM-2013-76922	France	Saint-Laurent-du-Pont	45.35	5.76				
<i>T. hispidus</i> *	MNHN-IM-2013-76909	France	Bèze	47.47	5.27				
<i>T. sp.6</i> *	MNHN-IM-2013-77398	France	Gonds	45.70	-0.59				
<i>T. pascali</i> *	MNHN-IM-2013-76928	France	Bonlieu	46.58	5.87				
<i>T. plebeius</i> *	MNHN-IM-2013-76924	France	Aubres	44.39	5.17				
<i>T. hispidus</i>	MNHN-IM-2013-76932	France	Neuville	50.50	3.07				
<i>T. plebeius</i>	MNHN-IM-2013-77045	France	Molines-en-Queyras	44.73	6.84				
<i>T. albulus</i>	MNHN-IM-2013-77391	France	Avon	48.41	2.73				
<i>T. plebeius</i> *	MNHN-IM-2013-77107	France	Château-Ville-Vieille	44.74	6.84				
<i>T. albulus</i>	MNHN-IM-2013-77259	France	Villard-de-Lans	45.07	5.53				
<i>T. becasis</i> *	MNHN-IM-2013-77000	France	Lourdios-Ichère	43.06	-0.68				
<i>T. becasis</i> *	MNHN-IM-2013-76902	France	Ahetze	43.39	-1.54				
<i>T. albulus</i>	MNHN-IM-2013-77392	France	Avon	48.41	2.73				
<i>T. albulus</i> *	MNHN-IM-2013-86901	France	Saint-Projet	44.30	1.79				
<i>T. plebeius</i> *	MNHN-IM-2013-77379	France	Lussat	46.18	2.32				
<i>T. plebeius</i> *	MNHN-IM-2013-77128	France	Myennes	47.45	2.93				
<i>T. dubia</i> *	MNHN-IM-2013-77383	France	Lussat	46.18	2.32				
<i>T. albulus</i>	MNHN-IM-2013-86900	France	Saint-Projet	44.30	1.79				
<i>T. hispidus</i>	MNHN-IM-2013-76914	France	Châtillon-sur-Seine	47.86	4.58				
<i>T. hispidus</i>	MNHN-IM-2013-76911	France	Bèze	47.47	5.27				
<i>T. albulus</i>	MNHN-IM-2013-77261	France	Villard-de-Lans	45.07	5.53				
<i>T. pascali</i>	MNHN-IM-2013-76918	France	Saint-Claude	46.40	5.88				
<i>T. plebeius</i>	MNHN-IM-2013-76907	France	Champcella	44.71	6.57				
<i>T. plebeius</i>	MNHN-IM-2013-77046	France	Molines-en-Queyras	44.73	6.84				
<i>T. albulus</i> †	MNHN-IM-2013-77127	France	Myennes	47.45	2.93				
<i>T. becasis</i>	MNHN-IM-2013-77376	France	Beaugency	47.80	1.62				
<i>T. villosus</i>	MNHN-IM-2013-76921	France	Septmoncel les Molunes	46.36	5.90				
<i>T. pascali</i>	MNHN-IM-2013-76929	France	Bonlieu	46.58	5.87				
<i>T. plebeius</i>	MNHN-IM-2013-76904	France	Champcella	44.71	6.57				
<i>T. plebeius</i>	MNHN-IM-2013-76899	France	Laye	44.65	6.09				
<i>T. becasis</i>	MNHN-IM-2013-76896	France	Perreux	46.04	4.12				
<i>T. pascali</i>	MNHN-IM-2013-76919	France	Saint-Claude	46.40	5.88				
<i>T. becasis</i> *	MNHN-IM-2013-77378	France	Beaugency	47.80	1.62				
<i>T. hispidus</i>	MNHN-IM-2013-76915	France	Châtillon-sur-Seine	47.86	4.58				
<i>T. albulus</i>	MNHN-IM-2013-76884	France	Paris	48.84	2.36				
<i>T. albulus</i> *	MNHN-IM-2013-76886	France	Paris	48.84	2.36				

<i>T. plebeius</i>	MNHN-IM-2013-77108	France	Château-Ville-Vieille	44.74	6.84				
<i>T. plebeius</i>	MNHN-IM-2013-77154	France	Réallon	44.60	6.34				
<i>T. plebeius</i>	MNHN-IM-2013-77177	France	Fley	46.67	4.65				
<i>T. plebeius</i>	MNHN-IM-2013-77178	France	Fley	46.67	4.65				
<i>T. hispidus</i>	MNHN-IM-2013-76935	France	Neuville	50.50	3.07				
<i>T. plebeius</i>	MNHN-IM-2013-76925	France	Aubres	44.39	5.17				
<i>T. plebeius</i>	MNHN-IM-2013-76900	France	Laye	44.65	6.09				
<i>T. plebeius</i> †	MNHN-IM-2013-76890	France	Guillestre	44.65	6.65				
<i>T. plebeius</i>	MNHN-IM-2013-76891	France	Guillestre	44.65	6.65				
<i>T. albulus</i>	MNHN-IM-2013-76894	France	Perreux	46.04	4.12				
<i>T. sp.5</i> *	NMBE_571337	Germany	Bielefeld	52.10	8.53	129			
<i>T. sp.5</i> †	NMBE_571329	Germany	Herford	52.15	8.60	75			
<i>T. sp.5</i> †*	NMBE_571333	Germany	Minden	52.38	8.79	59			
<i>T. clandestinus</i>	NMBE_571315	Austria	Feldkirch, Schlattenburg	47.24	9.60				
<i>T. plebeius</i>	NMBE_569657	France	Freissinières	44.74	6.49				
<i>T. plebeius</i>	NMBE_569658	France	Freissinières	44.74	6.49				

Supplementary material II: Shell measurements and ratios of the genetically investigated adult specimens. Abbreviations used: W = shell width, H = shell height, bwH = body whorl height, h = aperture height, w = aperture width, D = shell diameter, U = major umbilicus width, u = minor umbilicus width, whl = number of whorls. All measurements are in millimetres.

Data base nr°	locality	W	H	bwH	h	w	D	U	u	whl	H/W	U/D	u/U	bwH/H	h/w
MNHW_S.15.19_10	Gorges de Court 3	8.46	5.21	4.22	2.87	4.57	8.66	0.92	0.82	5.5	0.62	0.11	0.89	0.81	0.63
MNHW_S.15.19_11	Gorges de Court 3	8.33	5.92	4.71	3.00	4.62	8.35	0.90	1.05	5.6	0.71	0.11	1.16	0.79	0.65
MNHW_S.15.21_13	Gorges de Moutier	7.60	5.10	4.22	2.92	4.21	8.16	1.11	0.96	5.3	0.67	0.14	0.86	0.83	0.69
MNHW_S.15.21_14	Gorges de Moutier	8.47	5.31	4.43	3.08	4.75	8.09	0.97	0.71	5.2	0.63	0.12	0.73	0.83	0.65
MNHW_F-Ech_02	Échallon	9.01	4.62	3.96	2.97	4.07	8.90	2.20	1.98	5.8	0.51	0.25	0.90	0.86	0.73
MNHW_S.15.27_12	Twannbachschlucht	8.51	5.10	4.35	3.27	4.64	8.36	0.98	0.84	5.6	0.60	0.12	0.86	0.85	0.70
MNHW_S.15.20_01	Gorges de Court 4	10.79	5.94	5.14	3.53	5.63	11.51	2.25	2.10	6	0.55	0.20	0.94	0.86	0.63
MNHW_S.15.20_02	Gorges de Court 4	11.43	6.23	5.16	3.98	6.07	12.56	2.31	1.84	6	0.54	0.18	0.80	0.83	0.66
MNHW_S.15.26_02	Frinvillier 2	11.90	6.67	5.45	3.89	5.94	12.36	2.40	2.15	5.75	0.56	0.19	0.89	0.82	0.65
MNHW_S.15.26_03	Frinvillier 2	12.40	6.44	5.70	3.90	6.75	13.40	2.28	1.96	6	0.52	0.17	0.86	0.88	0.58
MNHW_S.15.28_06	Saint-Imier/Les Pontins	11.23	6.96	5.51	3.80	5.52	11.70	2.28	1.69	6	0.62	0.19	0.74	0.79	0.69
MNHW_S.15.29_100	Montagne De Cernier	12.89	8.28	7.08	4.51	7.14	13.26	2.74	2.33	5.5	0.64	0.21	0.85	0.86	0.63
MNHW_S.15.29_101	Montagne De Cernier	11.42	7.21	6.06	4.23	5.89	11.63	2.18	1.81	5.9	0.63	0.19	0.83	0.84	0.72
MNHW_S.15.21_01	Gorges de Moutier	8.93	4.52	3.94	2.87	4.35	8.29	1.55	1.46	5.5	0.51	0.19	0.94	0.87	0.66
MNHW_S.15.21_02	Gorges de Moutier	7.80	3.67	3.35	2.69	4.06	8.14	1.48	1.55	5	0.47	0.18	1.05	0.91	0.66
MNHW_S.15.22a_10	Gorges du Pichoux	10.04	6.04	5.18	3.79	5.84	9.27	0.97	0.84	5.6	0.60	0.10	0.87	0.86	0.65
MNHW_F.15.33_04	Les Rousses-d'Amont	10.19	6.46	5.26	3.69	5.34	10.57	1.45	1.28	6	0.63	0.14	0.88	0.81	0.69
MNHW_F.15.33_05	Les Rousses-d'Amont	10.97	6.83	5.74	4.08	6.18	11.90	1.70	1.58	5.75	0.62	0.14	0.93	0.84	0.66
MNHW_F.15.33_06	Les Rousses-d'Amont	9.87	6.57	5.27	3.67	5.25	10.43	1.22	0.99	5.5	0.67	0.12	0.81	0.80	0.70
MNHW_F.15.39_01	Cascades du Hérisson	10.82	6.84	5.67	4.10	6.26	11.62	1.24	1.07	5.8	0.63	0.11	0.86	0.83	0.66
MNHW_F.15.39_02	Cascades du Hérisson	9.91	7.19	5.31	3.21	5.26	10.80	1.48	1.41	6.25	0.73	0.14	0.95	0.74	0.61
MNHW_F.15.39a_01	Cascades du Hérisson	10.89	7.06	5.55	4.10	6.08	11.48	1.38	1.34	6	0.65	0.12	0.97	0.79	0.67
MNHW_F.15.42a_03	Arandas	9.89	6.75	5.18	3.82	5.61	10.03	1.09	0.79	6	0.68	0.11	0.72	0.77	0.68
MNHW_F.15.42a_04	Arandas	9.19	6.23	5.00	3.21	5.07	9.55	1.11	0.96	6	0.68	0.12	0.86	0.80	0.63
MNHW_F.15.47_04	Jalinard	9.47	5.73	4.82	3.45	5.19	10.16	1.30	1.04	5.5	0.60	0.13	0.79	0.84	0.66
MNHW_F.15.47_05	Jalinard	9.65	5.45	4.67	3.60	4.85	9.66	1.28	1.12	5.6	0.56	0.13	0.88	0.86	0.74
MNHW_S.15.17_01	Gorges de Court	10.85	6.34	5.27	3.79	6.01	11.52	1.58	1.40	5.75	0.58	0.14	0.89	0.83	0.63
MNHW_S.15.17_02	Gorges de Court	8.43	5.12	4.26	3.28	4.73	9.17	1.24	1.04	5.25	0.61	0.13	0.84	0.83	0.69
MNHW_S.15.20_17	Gorges de Court 4	9.51	6.20	4.83	3.05	4.86	9.99	1.72	1.47	5.9	0.65	0.17	0.86	0.78	0.63
MNHW_S.15.20_18	Gorges de Court 4	9.77	6.28	5.03	3.62	5.02	9.82	1.52	1.42	6	0.64	0.15	0.93	0.80	0.72
MNHW_S.15.24_01	Undervelier	10.16	5.76	4.75	3.51	5.43	10.35	1.51	1.31	5.7	0.57	0.15	0.87	0.82	0.65
MNHW_S.15.28_07	Saint-Imier/Les Pontins	10.02	6.07	4.84	3.46	5.33	10.72	1.60	1.30	5.6	0.61	0.15	0.82	0.80	0.65
MNHW_S.15.28_08	Saint-Imier/Les Pontins	11.09	6.45	5.35	3.72	5.92	11.86	1.82	1.55	6.1	0.58	0.15	0.85	0.83	0.63

Kneubühler et al.: The *Trochulus* enigma

MNHW_S.15.29_01	Montagne De Cernier	11.99	7.14	5.85	4.43	6.44	12.82	2.22	1.75	6.25	0.60	0.17	0.79	0.82	0.69
MNHW_S.15.29_02	Montagne De Cernier	11.54	5.96	5.03	3.61	5.97	11.62	1.79	1.62	5.5	0.52	0.15	0.91	0.85	0.60
MNHW_S.15.30_02	Gorges de L'Areuse	9.48	5.63	4.73	3.64	5.22	10.26	1.64	1.29	5.6	0.59	0.16	0.79	0.84	0.70
MNHW_F.15.31_02	Mont d'Or	9.05	5.61	4.53	3.13	4.60	9.45	1.72	1.51	5.75	0.62	0.18	0.88	0.81	0.68
MNHW_F.15.31_03	Mont d'Or	10.22	5.69	4.92	3.89	5.46	10.00	1.67	1.30	5.5	0.56	0.17	0.78	0.87	0.71
MNHW_F.15.34_01	La Chevry	11.98	7.10	6.04	4.73	6.49	13.08	2.05	1.66	6	0.59	0.16	0.81	0.85	0.73
MNHW_F.15.34_03	La Chevry	10.58	5.48	4.66	3.43	5.21	10.85	2.07	1.71	5.6	0.52	0.19	0.83	0.85	0.66
MNHW_F.15.34_05	La Chevry	10.35	5.62	4.63	3.35	5.25	9.87	1.94	1.57	5.25	0.54	0.20	0.81	0.82	0.64
MNHW_F.15.35_01	Mouthe, Source du Doubs	10.18	6.10	5.21	3.88	5.36	10.56	1.64	1.45	6	0.60	0.16	0.88	0.85	0.72
MNHW_F.15.36_01	Bonnevaux	9.97	6.00	4.78	3.37	5.27	10.91	1.79	1.38	5.5	0.60	0.16	0.77	0.80	0.64
MNHW_F.15.37_05	Cascade du Moulin du Saut	10.87	6.58	5.25	3.65	5.67	11.46	2.08	1.75	6	0.61	0.18	0.84	0.80	0.64
MNHW_F.15.37_06	Cascade du Moulin du Saut	10.26	6.27	5.02	3.39	5.29	11.00	1.82	1.50	5.6	0.61	0.17	0.82	0.80	0.64
MNHW_F.15.38_05	Chaux-des-Crotenay	10.46	5.93	4.78	3.74	5.50	10.34	1.61	1.32	5.7	0.57	0.16	0.82	0.81	0.68
MNHW_F.15.38_06	Chaux-des-Crotenay	11.03	6.63	5.40	3.80	5.79	10.87	1.91	1.46	6	0.60	0.18	0.76	0.81	0.66
MNHW_A.Me_101	Austria, Mellau	12.79	7.56	6.72	4.61	7.06	11.78	2.15	1.93	5.5	0.59	0.18	0.90	0.89	0.65
MNHW_A.MtK_105	Austria, Mt Kojenkopf	11.08	6.48	5.66	3.81	5.76	11.47	2.20	1.93	5.52	0.58	0.19	0.88	0.87	0.66
MNHW_A.MtB_106	Austria, Mt Baumgarten	10.40	6.14	5.33	3.90	5.59	10.67	2.02	1.70	5	0.59	0.19	0.84	0.87	0.70
MNHW_G.15.50a_108	Germany, Buchberg 2	13.48	9.73	7.57	4.84	7.95	14.39	2.35	2.16	6.25	0.72	0.16	0.92	0.78	0.61
MNHW_G.15.52_109	Germany, Geisingen	13.10	8.51	7.13	4.73	6.97	13.60	2.59	2.34	6	0.65	0.19	0.91	0.84	0.68
MNHW_A.Me_05	Austria, Mellau	9.72	5.58	4.69	3.41	5.27	10.03	1.79	1.36	5.25	0.57	0.18	0.76	0.84	0.65
MNHW_F.15.09_09	France, between Aubure & La Petite Verrerie	8.63	4.97	4.12	2.93	4.18	8.36	1.72	1.49	5.5	0.58	0.21	0.87	0.83	0.70
MNHW_F.15.09_10	France, between Aubure & La Petite Verrerie	9.60	5.99	4.74	3.17	4.73	9.85	1.95	1.54	5.6	0.62	0.20	0.79	0.79	0.67
MNHW_F.15.11_11	France, Tellure	10.58	6.02	4.87	3.39	5.38	10.50	1.82	1.56	5.5	0.57	0.17	0.85	0.81	0.63
MNHW_F.15.11_12	France, Tellure	9.90	6.29	5.18	3.65	5.41	9.72	1.67	1.41	5.5	0.64	0.17	0.85	0.82	0.67
MNHW_F.15.14_13	France, Source de la Moselle n. Bussang	9.64	5.99	5.01	3.63	5.07	9.64	1.28	1.12	5.5	0.62	0.13	0.88	0.84	0.72
MNHW_F.15.14_14	France, Source de la Moselle n. Bussang	9.09	5.84	4.56	3.01	4.90	9.08	1.51	1.17	5.25	0.64	0.17	0.77	0.78	0.61
MNHW_F.15.15_15	France, Bussang	10.61	6.57	5.31	3.88	5.73	10.69	1.60	1.34	6	0.62	0.15	0.83	0.81	0.68
MNHW_F.15.15_16	France, Bussang	10.18	6.29	5.05	3.80	5.40	10.23	1.56	1.19	5.5	0.62	0.15	0.76	0.80	0.70
MNHW_F.15.15_17	France, Bussang	9.88	5.80	4.79	3.36	5.08	9.79	1.76	1.43	5.5	0.59	0.18	0.82	0.83	0.66
NMBE_568084	St. Maurice, Grotte aux Fées	6.89	4.10	4.01	4.67	3.88	7.09	0.70	0.61	5	0.60	0.10	0.87	0.98	1.20
NMBE_569597	Bern-Bümpliz, Schlosspark	7.53	4.44	3.90	3.02	4.07	7.45	0.80	0.99	5.5	0.59	0.11	1.24	0.88	0.74
NMBE_569598	Bern-Bümpliz, Schlosspark	7.18	4.08	3.46	2.76	3.91	7.03	1.15	0.92	5.5	0.57	0.16	0.80	0.85	0.71
NMBE_569638	Broc, Waldlichtung	11.28	6.39	6.10	3.09	5.96	11.79	1.97	2.13	5.75	0.57	0.17	1.08	0.95	0.52
MNHW_PL.20.45_305	Poland, Pieskowa Skała (PN)	7.75	4.34	3.82	2.40	3.49	7.96	1.65	1.43	5.2	0.56	0.21	0.87	0.88	0.69
MNHW_PL.20.32_307	Poland, Muszyna 2	8.92	4.66	4.38	2.81	4.42	9.08	1.78	1.68	5.75	0.52	0.20	0.94	0.94	0.64
MNHW_PL.20.16_306	Poland, Wapowce	7.86	4.77	4.04	2.34	3.90	7.68	1.36	1.21	5	0.61	0.18	0.89	0.85	0.60
MNHW_F.18.30_299	France, Forêt Bac Estable 2	9.67	6.26	4.92	3.43	5.05	9.67	2.05	1.93	6	0.65	0.21	0.95	0.79	0.68

Kneubühler et al.: The *Trochulus* enigma

MNHW_F.18.37_301	France, Forêt de Belesté	10.67	6.13	5.15	3.54	5.51	10.79	2.05	1.77	6.2	0.57	0.19	0.86	0.84	0.64
MNHW_F.18.35_300	France, Le Chandelier	8.41	5.31	4.36	3.34	4.51	8.76	1.39	1.20	5.5	0.63	0.16	0.86	0.82	0.74
MNHW_F.VM_295	France, Vallon du Moulinot	9.46	5.76	4.63	3.13	5.02	9.33	1.17	1.07	5.75	0.61	0.13	0.91	0.81	0.62
MNHW_F.RP_297	France, La Roche des Pins	8.65	5.27	4.20	3.12	4.57	8.64	0.97	0.86	6	0.61	0.11	0.89	0.80	0.68
MNHW_F.VM_294	France, Vallon du Moulinot	8.17	5.51	4.28	2.89	4.59	8.23	0.93	0.89	5.7	0.67	0.11	0.95	0.78	0.63
MNHW_F.ML_296	France, Mont de Lune	8.36	5.70	4.30	2.93	3.83	8.42	1.48	1.10	6	0.68	0.18	0.75	0.75	0.77
MNHW_A.17.12_01	Austria, Schafberg	8.97	5.06	4.28	2.89	4.68	8.71	1.43	1.29	5.5	0.56	0.16	0.90	0.85	0.62
MNHW_I.16.12_01	Ireland, Maam	10.46	7.30	5.81	3.79	5.53	10.44	1.82	1.64	6	0.70	0.17	0.90	0.80	0.68
MNHW_SK.19.71_01	Slovakia, Varín	11.59	7.27	5.81	4.01	5.80	11.21	1.87	1.62	5.7	0.63	0.17	0.87	0.80	0.69
MNHW_F.18.10_06	France, Blecquenecques n. Marquise	10.96	6.13	5.20	3.61	5.68	10.77	1.82	1.56	5.5	0.56	0.17	0.85	0.85	0.64
MNHW_GB.Br_01	Great Britain, Bramley near Basingstoke	10.85	6.81	5.78	4.02	5.99	10.93	1.51	1.39	5.6	0.63	0.14	0.92	0.85	0.67
MNHW_F.18.25_279	France, Escames	8.03	4.82	3.99	2.75	3.72	7.89	1.24	1.10	5.25	0.60	0.16	0.89	0.83	0.74
MNHW_F.18.07_278	France, Beaucamps-Le-Jeune	8.05	5.58	4.46	2.62	4.06	8.15	1.23	1.13	5.7	0.69	0.15	0.92	0.80	0.65
MNHW_F.18.05_277	France, Fouquenies	8.08	5.58	4.40	2.59	4.07	8.15	1.19	1.11	5.7	0.69	0.15	0.93	0.79	0.64
MNHW_F.LE_280	France, Les Essarts	6.49	4.57	3.75	2.74	3.48	6.48	0.57	0.56	5	0.70	0.09	0.98	0.82	0.79
MNHW_F.LR_290	France, La Ruchotte	7.84	5.04	3.98	2.56	4.28	7.80	1.20	1.05	5.6	0.64	0.15	0.87	0.79	0.60
MNHW_Re5	Germany, Reischenau	8.02	5.38	4.51	3.08	4.18	8.02	0.99	0.99	5.25	0.67	0.12	1.00	0.84	0.74
MNHW_G.15.05_285	Germany, Ketsch	8.91	5.79	4.62	2.84	4.74	8.97	1.35	1.10	6	0.65	0.15	0.81	0.80	0.60
MNHW_RF4	Switzerland, Ruine Farnsburg	7.80	4.62	3.96	2.75	3.85	7.80	0.88	0.88	5.25	0.59	0.11	1.00	0.86	0.71
MNHW_St-14	Germany, Staubing	9.27	5.82	4.55	3.09	4.55	9.09	1.64	1.45	5.8	0.63	0.18	0.89	0.78	0.68
MNHW_G.17.05_298	Germany, Pfatter	8.74	4.96	4.29	3.24	4.59	8.89	1.76	1.51	5.6	0.57	0.20	0.86	0.87	0.71
MNHW_Sau1	Austria, Sausteig	8.24	5.16	4.29	3.19	4.40	8.13	0.99	0.88	5.4	0.63	0.12	0.89	0.83	0.73
MNHW_CZ.Vit_274	Czech Republic, Vitkovice	6.95	4.42	3.61	2.74	3.46	6.91	1.08	0.95	5.2	0.64	0.16	0.88	0.82	0.79
MNHW_CZ.Lan_273	Czech Republic, Lánov	7.03	4.92	4.01	2.63	3.56	6.99	0.75	0.70	5.25	0.70	0.11	0.94	0.82	0.74
MNHW_CZ.CD_272	Czech Republic, Černý Důl	6.87	4.29	3.69	2.63	3.57	6.79	0.67	0.50	5.6	0.62	0.10	0.75	0.86	0.74
MNHW_CZ.19.51_275	Czech Republic, Radňovice	7.63	5.12	4.13	2.82	3.71	7.69	1.19	1.11	5.5	0.67	0.15	0.93	0.81	0.76
MNHW_F.SF_283	France, Source de la Foulotière	8.78	5.23	4.41	3.04	4.61	8.77	1.10	0.87	5.5	0.60	0.12	0.79	0.84	0.66
MNHW_F.Lcr_289	France, La croix rouge	9.45	5.34	4.32	3.31	5.00	9.29	1.26	1.12	5.7	0.57	0.14	0.89	0.81	0.66
MNHW_PL.20.09_252	Poland, Leśna Podlaska	7.15	4.62	3.68	2.61	3.25	7.46	1.86	1.51	5.4	0.65	0.25	0.81	0.80	0.80
MNHW_PL.20.13_253	Poland, Gamlówka	6.87	4.02	3.38	2.07	3.02	6.74	1.63	1.59	5.5	0.59	0.24	0.98	0.84	0.69
MNHW_PL.20.07_251	Poland, Budy Leśne n. Białowieża	7.68	5.57	4.24	2.43	3.73	7.76	1.35	1.29	5.6	0.73	0.17	0.96	0.76	0.65
MNHW_PL.19.10_250	Poland, Mątki near Sztum	8.49	4.79	3.81	2.77	3.69	8.32	2.06	1.57	6	0.56	0.25	0.76	0.79	0.75
MNHW_PL.Ro_247	Poland, Puszcza Romincka	6.97	5.09	3.96	2.80	3.39	7.07	1.21	1.10	5.5	0.73	0.17	0.91	0.78	0.83
MNHW_PL.20.04_248	Poland, Rapa	7.39	5.09	4.15	2.76	3.87	7.44	1.42	1.38	5.2	0.69	0.19	0.97	0.82	0.71
MNHW_PL.20.05_249	Poland, Cisowy Jar	7.40	5.10	4.11	2.76	3.89	7.85	1.79	1.54	5.3	0.69	0.23	0.86	0.81	0.71
MNHW_CZ.19.78_218	Czech Republic, Pitárné	9.03	4.77	4.04	3.10	4.24	9.07	2.32	1.74	5.4	0.53	0.26	0.75	0.85	0.73
MNHW_CZ.17.145_212	Czech Republic, Závist	7.97	5.06	3.96	2.55	3.93	8.06	1.79	1.44	5.6	0.64	0.22	0.80	0.78	0.65

Kneubühler et al.: The *Trochulus* enigma

MNHW_CZ.19.35_213	Czech Republic, Srbsko 3	7.31	3.93	3.29	2.10	3.28	7.24	1.73	1.51	5.5	0.54	0.24	0.87	0.84	0.64
MNHW_CZ.19.38_214	Czech Republic, Štěchovice (Maják)	7.56	4.77	3.81	2.64	3.54	7.57	1.79	1.54	6.1	0.63	0.24	0.86	0.80	0.74
MNHW_CZ.19.43_216	Czech Republic, Debrník	7.60	4.68	3.74	2.77	3.98	7.70	1.35	1.20	5.6	0.62	0.18	0.89	0.80	0.70
MNHW_PL.19.27_242	Poland, Będzin	6.83	4.34	3.40	2.16	3.06	6.88	1.56	1.50	5.2	0.63	0.23	0.96	0.78	0.70
MNHW_UK.En-D_5	UK, Downside	8.46	5.49	4.18	3.08	4.18	8.35	1.43	1.10	5.6	0.65	0.17	0.77	0.76	0.74
MNHW_A.Gens_201	Austria, Genabend-Sibratsgfall	6.84	4.59	3.74	2.82	3.48	6.86	0.88	0.79	5.2	0.67	0.13	0.90	0.81	0.81
MNHW_A.17.28_203	Austria, Durnbachtal	7.30	3.65	3.06	2.60	3.40	7.32	1.51	1.41	5.5	0.50	0.21	0.93	0.84	0.76
MNHW_A.Schw_202	Austria, Schwarzenberg-Loch 2	6.50	3.73	2.96	2.24	3.21	6.49	1.05	1.01	5.6	0.57	0.16	0.96	0.79	0.70
MNHW_PL.19.82_236	Poland, Wojcieszów Górny	8.00	5.30	4.11	2.81	3.73	7.93	1.36	1.13	5.7	0.66	0.17	0.83	0.77	0.75
MNHW_NL.19.03_234	the Netherlands, Veere 2	7.63	3.99	3.45	2.72	3.88	7.55	1.32	1.01	5.1	0.52	0.17	0.77	0.87	0.70
MNHW_NL.Ost_233	the Netherlands, Oestgeest near Leiden	8.28	5.33	4.14	3.00	3.99	8.46	1.46	1.20	5.5	0.64	0.17	0.82	0.78	0.75
MNHW_F.18.14_225	France, Larré	6.72	4.26	3.43	2.23	3.34	6.60	1.14	0.97	5.1	0.63	0.17	0.85	0.80	0.67
MNHW_F.18.24_223	France, Le Mont Gourmoy 2 (Forêt Indivise d'Eu)	6.93	4.05	3.29	2.11	3.38	6.89	1.26	1.02	5.2	0.58	0.18	0.81	0.81	0.63
MNHW_F.Col_228	France, Col. De Vac.	7.49	4.07	3.45	2.70	3.85	7.40	0.90	0.85	5	0.54	0.12	0.95	0.85	0.70
MNHW_F.18.08_221	France, Eaucourt-Sur-Somme	7.95	4.67	3.83	2.61	3.41	7.87	1.52	1.10	5	0.59	0.19	0.73	0.82	0.77
MNHW_F.Com_227	Chameyer	7.85	4.99	4.09	3.07	3.80	7.91	1.52	1.30	5.5	0.64	0.19	0.86	0.82	0.81
MNHW_F.18.12_224	France, Licques	6.85	4.25	3.35	2.13	3.22	6.82	1.38	1.16	5	0.62	0.20	0.85	0.79	0.66
MNHW_F.15.07_219	France, Bertrange	7.36	4.99	3.88	2.35	3.38	7.49	1.71	1.32	5.3	0.68	0.23	0.77	0.78	0.70
MNHW_I.16.8_231	Ireland, Lough Gur	7.55	3.88	3.35	2.46	3.54	7.56	1.62	1.35	5	0.51	0.21	0.84	0.86	0.69
MNHW_I.16.4_230	Ireland, Rock of Cashel	6.85	3.99	3.31	2.16	3.18	6.84	1.32	1.14	5.7	0.58	0.19	0.86	0.83	0.68
MNHW_I.16.3_229	Ireland, Monastery	8.82	5.46	4.54	2.82	4.01	9.00	2.21	1.85	5.7	0.62	0.25	0.84	0.83	0.70
MNHW_I.16.10_232	Ireland, Bealaclogga	7.75	4.31	3.61	2.26	3.82	7.83	1.42	1.29	5.2	0.56	0.18	0.91	0.84	0.59
MNHW_UA.18.55_264	Ukraine, Bibrka	8.16	4.32	3.61	2.52	3.49	8.13	2.05	1.57	6	0.53	0.25	0.76	0.84	0.72
MNHW_UA.18.58_267	Ukraine, Mikuliczyn	7.60	4.44	3.78	2.32	3.50	7.57	1.80	1.69	5.5	0.58	0.24	0.94	0.85	0.66
MNHW_UA.18.56_265	Ukraine, Swirz	7.71	3.96	3.26	2.35	3.54	7.63	1.82	1.65	5.6	0.51	0.24	0.91	0.83	0.66
MNHW_G.17.17_228	Germany, Thannlehen b. Berchtesgaden	8.34	5.51	4.50	3.24	3.97	8.31	1.27	1.02	5.6	0.66	0.15	0.80	0.82	0.82
MNHW_G.Ott_227	Germany, Ottendorf	7.24	4.26	3.59	2.79	3.66	7.13	1.11	1.11	5	0.59	0.16	1.00	0.84	0.76
MNHW_G-Mo5	Germany, Moosburg a.d. Isar	6.92	4.18	3.52	2.42	3.41	6.70	1.32	1.21	5.2	0.60	0.20	0.92	0.84	0.71
MNHW_PL.19.08_256	Poland, Ostrów	7.41	4.74	3.85	2.74	3.51	7.45	1.63	1.35	5.3	0.64	0.22	0.83	0.81	0.78
MNHW_PL.19.09_257	Poland, Barcin-Górne Wolice	8.26	5.37	4.18	2.57	4.05	8.30	1.70	1.57	6.1	0.65	0.20	0.93	0.78	0.64
MNHW_PL.20.01_255	Poland, Siemianice n. Kępno	9.40	5.64	4.54	3.31	4.55	9.33	1.71	1.66	6	0.60	0.18	0.97	0.80	0.73
MNHW_SK.19.62_261	Slovakia, Čičov (Čičovský les)	8.82	4.60	4.02	2.78	3.90	8.71	2.00	1.63	5.6	0.52	0.23	0.82	0.87	0.71
MNHW_SK.19.63_262	Slovakia, Medved'ov	9.17	5.27	3.82	2.60	4.15	8.87	2.25	1.77	5.6	0.57	0.25	0.78	0.72	0.63
MNHW_PL.20.23_246	Poland, Równia	7.94	5.00	3.63	2.46	3.58	7.90	1.85	1.63	6.1	0.63	0.23	0.88	0.73	0.69
MNHW_PL.20.22_245	Poland, Stebnik	7.66	4.83	3.61	2.32	3.44	7.58	1.65	1.46	5.6	0.63	0.22	0.88	0.75	0.68
MNHW_SLO.17.140_260	Slovenia, Vintgar Gorge	8.50	4.29	3.62	2.95	3.95	8.30	2.11	1.80	5.6	0.50	0.25	0.85	0.84	0.75
MNHW_PL.20.34_243	Poland, Szlachtowa 2	8.61	5.85	4.29	2.59	3.77	8.80	1.74	1.53	6.2	0.68	0.20	0.88	0.73	0.69

Kneubühler et al.: The *Trochulus* enigma

MNHW_PL.20.44_244	Poland, Owczary	8.43	4.95	3.91	2.61	3.84	8.41	1.91	1.74	5.5	0.59	0.23	0.91	0.79	0.68
NMBE_569600	Schwarzwasser, Ufer	10.03	5.69	5.17	3.62	5.17	10.14	1.59	1.79	5.75	0.57	0.16	1.13	0.91	0.70
NMBE_569677	Schwarzwasser, Ufer	7.68	4.39	4.27	2.62	4.10	7.35	0.80	0.57	5	0.57	0.11	0.71	0.97	0.64
NMBE_569604	Schwarzwasser, Brücke	9.52	5.67	4.76	3.22	5.23	9.74	1.13	1.45	5.5	0.60	0.12	1.28	0.84	0.62
NMBE_569607	Zürich	7.44	3.95	3.65	2.80	3.98	7.28	0.80	1.11	4.75	0.53	0.11	1.39	0.92	0.70
NMBE_569680	Brugg, Friedhof, unterhalb Autobahnbrücke	7.53	4.68	4.28	2.95	4.08	7.39	0.68	0.70	5	0.62	0.09	1.03	0.91	0.72
NMBE_569681	Brugg, Friedhof, unterhalb Autobahnbrücke	8.17	4.73	4.29	2.77	4.67	8.00	0.74	0.58	5	0.58	0.09	0.78	0.91	0.59
NMBE_569609	Aarau, Parkanlage Grossratsgebäude	9.13	5.84	5.01	3.28	4.96	9.39	1.35	1.49	5.5	0.64	0.14	1.10	0.86	0.66
NMBE_569684	Brugg, Aareufer	6.65	4.32	3.86	2.46	3.53	6.83	0.85	0.68	5	0.65	0.12	0.80	0.89	0.70
NMBE_569611	Sursee, Surepärkli	9.65	5.77	4.96	3.45	5.30	9.76	1.36	1.48	5.5	0.60	0.14	1.09	0.86	0.65
NMBE_569686	Hallwil, Schloss	6.37	4.10	3.74	2.00	3.55	6.56	0.64	0.72	5	0.64	0.10	1.13	0.91	0.56
NMBE_569689	Stansstad, Kieswerk, Flussufer	8.85	5.80	5.29	3.34	5.19	8.63	0.75	0.80	5.25	0.66	0.09	1.07	0.91	0.64
NMBE_569639	Stansstad, Kieswerk, Flussufer	12.71	7.26	6.50	3.81	5.75	12.83	2.20	2.54	5.75	0.57	0.17	1.15	0.90	0.66
NMBE_569616	Zürich, Beckenhof	7.28	4.37	3.68	2.42	3.82	7.39	0.82	0.92	5	0.60	0.11	1.12	0.84	0.63
NMBE_569640	Stans, Bürgenberg, Bürgenstock	12.86	7.41	6.67	3.80	6.67	13.09	2.43	2.30	5.5	0.58	0.19	0.95	0.90	0.57
NMBE_569626	Avonçon	7.51	4.32	4.08	3.06	4.05	7.56	1.02	1.07	5.5	0.58	0.13	1.05	0.94	0.76
NMBE_569666	Forest-Saint-Julien	7.86	4.66	4.05	2.65	4.20	8.05	1.06	1.22	5.5	0.59	0.13	1.15	0.87	0.63
NMBE_571095	Grimentz	6.37	4.16	3.57	2.26	3.41	6.38	0.77	0.68	4.75	0.65	0.12	0.88	0.86	0.66
NMBE_571107	Rheinland-Palatinat, Welterod	8.25	4.54	4.21	2.83	3.90	8.60	1.42	1.64	5.5	0.55	0.17	1.15	0.93	0.73
NMBE_571108	Diessen am Ammersee	7.28	4.72	3.92	2.28	3.28	7.39	1.43	1.53	5.25	0.65	0.19	1.07	0.83	0.70
NMBE_571112	DK, Hovedstaden, Furesø Kommune	7.13	4.34	3.77	2.45	3.59	7.31	1.29	1.67	5.5	0.61	0.18	1.29	0.87	0.68
NMBE_571125	Carmel, near Swansea	7.73	4.98	4.27	2.40	4.03	8.09	1.27	1.40	5.5	0.64	0.16	1.10	0.86	0.60
NMBE_571128	Jersey	8.69	6.12	4.51	2.84	4.26	8.91	1.82	1.84	6	0.70	0.20	1.01	0.74	0.67
NMBE_571134	Flühli	9.86	5.33	3.21	4.63	5.47	9.84	1.52	1.73	5.25	0.54	0.15	1.14	0.60	0.85
NMBE_571142	Bergün Dorf	9.64	5.73	4.95	3.29	5.03	9.94	1.00	1.57	5.5	0.59	0.10	1.57	0.86	0.65
NMBE_571234	Amriswil, Kronberg	9.77	5.89	5.09	3.73	5.49	9.88	1.59	1.57	5.5	0.60	0.16	0.99	0.86	0.68
NMBE_571235	Bürglen, Schloss	10.07	6.29	5.17	3.74	5.46	9.88	1.30	1.34	5.5	0.62	0.13	1.03	0.82	0.68
NMBE_571145	Twann, Twannbachschlucht	11.25	6.12	5.22	4.26	5.69	11.59	1.70	2.01	5.5	0.54	0.15	1.18	0.85	0.75
NMBE_571152	Bayern, Kelheim, Neustadt, Donaubrücke	8.92	4.99	4.28	3.89	4.56	9.35	1.35	1.57	5.5	0.56	0.14	1.16	0.86	0.85
NMBE_571158	NRW, Mettmann, Monheim, Baumberg, Auwald	11.77	7.34	6.11	3.97	6.79	12.41	2.14	2.19	6	0.62	0.17	1.02	0.83	0.58
NMBE_571160	Dorsel, Dorseler Mühle	11.90	7.10	5.69	3.70	5.95	12.51	2.22	2.45	6.5	0.60	0.18	1.10	0.80	0.62
NMBE_571203	Säntis, Meglisalp	9.61	5.21	5.06	3.23	5.61	9.94	1.51	1.86	5.75	0.54	0.15	1.23	0.97	0.58
NMBE_571206	Säntis, Schäfler	11.17	6.32	5.40	3.67	5.80	11.61	2.44	2.68	6	0.57	0.21	1.10	0.85	0.63
NMBE_571208	Säntis, Ebenalp	11.41	6.73	5.83	3.83	5.98	11.91	1.78	2.44	6	0.59	0.15	1.37	0.87	0.64
NMBE_571237	Untereggen, Altrüti SG	12.56	6.76	6.25	4.05	5.82	12.78	2.7	2.2	5.5	0.54	0.21	0.81	0.92	0.70
NMBE_571218	Dutzower See, Nordspitze	7.99	4.56	3.70	2.53	4.17	8.29	1.55	1.34	6	0.57	0.19	0.86	0.81	0.61
MNHN-IM-2013-76922	Saint-Laurent-du-Pont	8.31	5.24	4.52	3.44	4.81	8.17	0.68	0.75	5	0.63	0.08	1.10	0.86	0.72

MNHN-IM-2013-77127	Myennes	7.35	4.43	3.66	2.71	3.73	7.20	1.38	1.11	4.75	0.60	0.19	0.80	0.83	0.73
MNHN-IM-2013-76890	Guillestre	7.19	4.22	3.37	2.39	3.38	6.97	1.39	1.34	5.25	0.59	0.20	0.96	0.80	0.71
NMBE_571329	NRW, Kreis Herford, Enger, Belke-Steinbeck, Brandbach	8.64	4.68	3.80	2.52	4.09	8.55	1.64	1.47	5.75	0.54	0.19	0.90	0.81	0.62
NMBE_571333	NRW, Kreis Minden-Lübbecke, Hille, Mindenerwald	7.54	4.45	3.55	2.64	3.60	7.67	1.71	1.44	5.75	0.59	0.22	0.84	0.80	0.73

Supplementary material III: Species ID, accession numbers from GenBank and BOLD, and sampling localities from sequences from external publications used in the genetic analysis.

ID	Locality	Country	Lat	Long	Species in this study	Clade/species in original publication	COI accession no.	16S accession no.	ITS2 accession no.	Publication
4287_452	Vätra Götalands Län	Sweden	57.68	11.95	<i>villersii</i>	1	KJ151495	KJ151606		Kruckenhauser et al. 2014
4293_455	Vätra Götalands Län	Sweden	58.26	13.28	<i>villersii</i>	1	KJ151499	KJ151608	KJ151747	Kruckenhauser et al. 2014
103_33	Nationalpark Donauau	Austria	48.11	16.78	sp. 4	2A	KJ151296	KJ151551	KJ151720	Kruckenhauser et al. 2014
104_104	Dürrenstein	Austria	47.84	15.02	sp. 4	2A	HQ204466.1	HQ204521.1		Kruckenhauser et al. 2014
109_102	Hallstatt	Austria	47.56	13.64	sp. 4	2A	HQ204464.1	HQ204516.1		Kruckenhauser et al. 2014
140_24	Gesäuse	Austria	47.56	14.58	sp. 4	2A	HQ204446.1	HQ204520.1	KJ151721	Kruckenhauser et al. 2014
683_5	Semmering	Austria	47.63	15.88	sp. 4	2A	HQ204476.1	HQ204529.1	KJ151723	Kruckenhauser et al. 2014
688_50	Hohe Wand	Austria	47.78	16.04	sp. 4	2A	HQ204473.1	HQ204530.1		Kruckenhauser et al. 2014
726_94	westliches Mittelgebirge	Austria	47.23	11.34	sp. 4	2A	KJ151322	KJ151562		Kruckenhauser et al. 2014

Kneubühler et al.: The *Trochulus* enigma

736_130	Bruck an der Mur	Austria	47.72	15.16	sp. 4	2A	HQ204483.1	HQ204526.1	KJ151728	Kruckenhauser et al. 2014
763_64	Gailtaler Alpen	Austria	46.68	13.45	sp. 4	2A	KJ151333	KJ151568		Kruckenhauser et al. 2014
769_66	Gurktaler Alpen	Austria	46.92	13.63	sp. 4	2A	KJ151337	KJ151572		Kruckenhauser et al. 2014
852_159	Waldviertel	Austria	48.78	15.12	sp. 4	2A	KJ151343	KJ151578	KJ151733	Kruckenhauser et al. 2014
926_140	Grazer Bergland	Austria	47.18	15.39	sp. 4	2A	HQ204450.1	HQ204504.1		Kruckenhauser et al. 2014
1294_168	Schneeberg	Austria	47.76	15.98	sp. 4	2A	HQ204478.1			Kruckenhauser et al. 2014
1331_167	Bucklige Welt	Austria	47.66	16.15	sp. 4	2A	HQ204496.1			Kruckenhauser et al. 2014
1335_93	Achensee	Austria	47.57	11.67	sp. 4	2A	KJ151355			Kruckenhauser et al. 2014
1346_60	Sattnitz	Austria	46.6	14.43	sp. 4	2A	KJ151362			Kruckenhauser et al. 2014
1472_223	Julische Alpen	Slovenia	46.34	13.64	sp. 4	2A	KJ151376			Kruckenhauser et al. 2014
1480_204	Deferegggen-Gebirge	Austria	46.81	12.33	sp. 4	2A	KJ151383			Kruckenhauser et al. 2014
1832_208	Fischbacher Alpen	Austria	47.51	15.66	sp. 4	2A	HQ204436.1	HQ204515.1		Kruckenhauser et al. 2014
1834_231	Donauinsel	Austria	48.2	16.45	sp. 4	2A	KJ151393			Kruckenhauser et al. 2014
2000_237	Warscheneck	Austria	47.63	14.32	sp. 4	2A	HQ204499.1			Kruckenhauser et al. 2014
2879_286	Pannonische Tiefebene	Austria	47.87	16.67	sp. 4	2A	KJ151413			Kruckenhauser et

Kneubühler et al.: The *Trochulus* enigma

										al. 2014
2984_306	Oberes Mürztal	Austria	47.74	15.47	sp. 4	2A	HQ204482.1			Kruckenhauser et al. 2014
2994_311	Mariazell	Austria	47.81	15.45	sp. 4	2A	HQ204469.1			Kruckenhauser et al. 2014
3004_313	Schwarzatal/Steinapiesting	Austria	47.88	15.65	sp. 4	2A	HQ204490.1			Kruckenhauser et al. 2014
3133_317	Gutensteinalpen	Austria	47.91	15.68	sp. 4	2A	HQ204493.1	HQ204531.1		Kruckenhauser et al. 2014
3137_318	Hochschwab	Austria	47.67	15.16	sp. 4	2A	HQ204470.1			Kruckenhauser et al. 2014
3203_339	Mürztal	Austria	47.66	15.61	sp. 4	2A	KJ151434			Kruckenhauser et al. 2014
3307_341	Lunz	Austria	47.86	15.06	sp. 4	2A	KJ151437			Kruckenhauser et al. 2014
3575_386	Sengengebirge	Austria	47.87	14.33	sp. 4	2A	KJ151447			Kruckenhauser et al. 2014
3907_385	Totes Gebirge	Austria	47.77	14.01	sp. 4	2A	KJ151449			Kruckenhauser et al. 2014
4263_446	Glocknergebiet	Austria	47.01	12.87	sp. 4	2A	KJ151489			Kruckenhauser et al. 2014
1455_200	Karnische Alpen	Italy	46.59	13	sp. 4	2B	KJ151369	KJ151589	KJ151740	Kruckenhauser et al. 2014
1471_223	Julische Alpen	Slovenia	46.34	13.64	sp. 4	2B	KJ151375	KJ151590		Kruckenhauser et al. 2014
4145_402	Karawanken	Austria	46.51	14.43	sp. 4	2B	KJ151469			Kruckenhauser et al. 2014
1341_86	Achensee	Austria	47.52	11.69	<i>sericeus</i>	3A	KJ151358	KJ151585	KJ151737	Kruckenhauser et al. 2014

Kneubühler et al.: The *Trochulus* enigma

1475_217	Salzkammergut	Austria	47.63	13.27	<i>sericeus</i>	3A	KJ151379	KJ151591	KJ151741	Kruckenhauser et al. 2014
2899_291	Mecsek Gebirge	Hungary	46.17	18.23	<i>sericeus</i>	3A	KJ151422	KJ151597	KJ151753 - KJ151755	Kruckenhauser et al. 2014
4155_407	Berchtesgadener_Land	Germany	47.68	13.01	<i>sericeus</i>	3A	KJ151472	KJ151600	KJ151746	Kruckenhauser et al. 2014
4165_412	Berchtesgadener_Land	Germany	47.75	12.64	<i>sericeus</i>	3A	KJ151475	KJ151601	KJ151756, KJ151757	Kruckenhauser et al. 2014
6233_549	Inntal	Austria	47.28	11.18	<i>sericeus</i>	3A	KJ151518			Kruckenhauser et al. 2014
849_545	Waldviertel	Austria	48.78	15.13	<i>sericeus</i>	3B	KJ151340	KJ151575	KJ151732	Kruckenhauser et al. 2014
5540_476	Donautal (Sauwald)	Austria	48.42	13.87	<i>sericeus</i>	4	KJ151506	KJ151611	KJ151763 - KJ151764	Kruckenhauser et al. 2014
5538_476	Donautal (Sauwald)	Austria	48.42	13.87	sp. 3	5	KJ151504	KJ151609	KJ151748	Kruckenhauser et al. 2014
101_33	Nationalpark Donauauen	Austria	48.11	16.78	sp. 1	6A	KJ151294	KJ151549	KJ151719	Kruckenhauser et al. 2014
2889_296	Duna-Dráva Nationalpark	Hungary	46.2	18.92	sp. 1	6A	KJ151419	KJ151596		Kruckenhauser et al. 2014
5588_482	Taubertal	Germany	49.71	9.55	sp. 1	6B	KJ151508	KJ151613	KJ151749	Kruckenhauser et al. 2014
6234_549	Inntal	Austria	47.28	11.18	sp. 1	6B	KJ151519			Kruckenhauser et al. 2014
4291_453	Vätra Götalands Län	Sweden	58.03	13.73	sp. 2	7	KJ151497	KJ151607		Kruckenhauser et al. 2014
6242_560	Frutigen-Niedersimmental	Switzerland	46.43	7.78	<i>albulus</i>	8A	KJ151525	KJ151614	KJ151750	Kruckenhauser et al. 2014
6249_555	Karlsruhe	Germany	49.08	8.37	<i>albulus</i>	8A	KJ151529	KJ151615		Kruckenhauser et

Kneubühler et al.: The *Trochulus* enigma

										al. 2014
2079_248	Graubünden	Switzerland	46.52	9.63	<i>albulus</i>	8B	KJ151407	KJ151593		Kruckenhauser et al. 2014
725_94	westliches Mittelgebirge	Austria	47.23	11.34	<i>dubia</i>	9	KJ151321	KJ151561	KJ151726	Kruckenhauser et al. 2014
1478_207	Deferegggen-Gebirge	Austria	47.01	12.44	<i>dubia</i>	9	KJ151381			Kruckenhauser et al. 2014
6229_550	Inntal	Austria	47.28	11.19	<i>dubia</i>	9	KJ151515			Kruckenhauser et al. 2014
6359_559	Ost-Obwalden	Switzerland	46.87	8.43	<i>R. biconica</i>	<i>biconicus</i>	KJ151532	KJ151617	KJ151752	Kruckenhauser et al. 2014
1381_199	Graubünden	Switzerland	46.81	9.53	<i>clandestinus</i>	<i>clandestinus</i>	KJ151365	KJ151586	KJ151738	Kruckenhauser et al. 2014
4044_413	Schwaben	Germany	48.47	10.29	<i>sericeus</i>	<i>coelomphala</i>	KJ151459	KJ151598	KJ151743	Kruckenhauser et al. 2014
5592_483	Bayrisches Donautal	Germany	48.97	12.39	<i>sericeus</i>	<i>coelomphala</i>	KJ151511			Kruckenhauser et al. 2014
248_33	Nationalpark Donauau	Germany	48.11	16.78	<i>striolatus</i>	<i>striolatus</i>	KJ151301	KJ151555	KJ151722	Kruckenhauser et al. 2014
251_122	Höllengebirge	Austria	47.82	13.6	<i>striolatus</i>	<i>striolatus</i>	KJ151304	KJ151557		Kruckenhauser et al. 2014
687_71	Wechsel	Austria	47.54	15.98	<i>striolatus</i>	<i>striolatus</i>	KJ151315	KJ151560	KJ151724	Kruckenhauser et al. 2014
1342_142	Stockerauer Au	Austria	48.38	16.2	<i>striolatus</i>	<i>striolatus</i>	KJ151359			Kruckenhauser et al. 2014
2077_249	Baden Württemberg	Germany	48.49	9.69	<i>striolatus</i>	<i>striolatus</i>	KJ151405	KJ151592		Kruckenhauser et al. 2014
4001_414	Schwäbische Alb	Germany	48.56	9.6	<i>striolatus</i>	<i>striolatus</i>	KJ151450			Kruckenhauser et al. 2014

Kneubühler et al.: The *Trochulus* enigma

5528_469	Donautal (Sauwald)	Austria	48.46	13.79	<i>striolatus</i>	<i>striolatus</i>	KJ151501			Kruckenhauser et al. 2014
1289_193	Žilinský kraj	Slovakia	48.96	18.52	<i>villosulus</i>	<i>villosulus</i>	KJ151350	KJ151581	KJ151735	Kruckenhauser et al. 2014
4053_428	Žilina	Slovakia	49.17	18.58	<i>villosulus</i>	<i>villosulus</i>	KJ151462			Kruckenhauser et al. 2014
4192_413	Schwaben	Germany	48.47	10.29	<i>villosus</i>	<i>villosus</i>	KJ151481	KJ151603		Kruckenhauser et al. 2014
4203_417	Schwäbische Alb	Germany	48	8.85	<i>villosus</i>	<i>villosus</i>	KJ151485	KJ151605	KJ151760 - KJ151762	Kruckenhauser et al. 2014
Hu_3	Hundersingen	Germany	48.0708	9.396	<i>striolatus</i>	<i>striolatus</i>	MT754820	MT755541	MT755442	Prockow et al. 2020
Hu_13	Hundersingen	Germany	48.0708	9.396	<i>striolatus</i>	<i>striolatus</i>	MT754819	MT755540		Prockow et al. 2020
Dil_11	Dillingen a/d Donau	Germany	48.5684	10.4999	<i>striolatus</i>	<i>striolatus</i>	MT754803	MT755524	MT755444	Prockow et al. 2020
Dil_15	Dillingen a/d Donau	Germany	48.5684	10.4999	<i>striolatus</i>	<i>striolatus</i>	MT754804	MT755525	MT755445	Prockow et al. 2020
Bi_5	Bittenbrunn	Germany	48.7394	11.1619	<i>sericeus</i>	<i>coelomphala</i>	MT754796	MT755517	MT755401	Prockow et al. 2020
Bi_6	Bittenbrunn	Germany	48.7394	11.1619	<i>sericeus</i>	<i>coelomphala</i>	MT754797	MT755518	MT755432	Prockow et al. 2020
Wa_5	Wackerstein	Germany	48.7888	11.6756	sp. 3	sp.	MT754855	MT755576	MT755422	Prockow et al. 2020
Wa_10	Wackerstein	Germany	48.7888	11.6756	sp. 3	sp.	MT754854	MT755575	MT755423	Prockow et al. 2020
Kel_4	Kehlheim	Germany	48.9151	11.8661	<i>striolatus</i>	<i>striolatus</i>	MT754823	MT755544	MT755411	Prockow et al. 2020
Kel_6	Kehlheim	Germany	48.9151	11.8661	<i>striolatus</i>	<i>striolatus</i>	MT754824	MT755545	MT755447	Prockow et al. 2020
Zu_1	Zulling	Germany	48.6668	12.6645	<i>dubia</i>	<i>hispidus</i>	MT754856	MT755577	MT755428	Prockow et al. 2020
Zu_2	Zulling	Germany	48.6668	12.6645	<i>dubia</i>	<i>hispidus</i>	MT754857	MT755578	MT755429	Prockow et al. 2020
EP_4	Erding-Pretzen	Germany	48.2804	11.9075	<i>dubia</i>	<i>hispidus</i>	MT754808	MT755529	MT755404	Prockow et al. 2020
EP_5	Erding-Pretzen	Germany	48.2804	11.9075	<i>dubia</i>	<i>hispidus</i>	MT754809	MT755530	MT755405	Prockow et al. 2020
Bo_3	Bödele	Austria	47.4235	9.8077	<i>sericeus</i>	<i>hispidus</i>	MT754799	MT755520	MT755395	Prockow et al. 2020
Bo_4	Bödele	Austria	47.4235	9.8077	<i>sericeus</i>	<i>hispidus</i>	MT754800	MT755521	MT755396	Prockow et al. 2020
Le_21	Lechsend	Germany	48.7384	10.9124	<i>striolatus</i>	<i>striolatus</i>	MT754838	MT755559	MT755453	Prockow et al. 2020
Le_2	Lechsend	Germany	48.7384	10.9124	<i>sericeus</i>	<i>coelomphala</i>	MT754837	MT755558	MT755414	Prockow et al. 2020

Kneubühler et al.: The *Trochulus* enigma

Gm_2	Gremheim	Germany	48.5846	10.5393	<i>sericeus</i>	<i>coelomphala</i>	MT754817	MT755536	MT755410	Prockow et al. 2020
ALNHM363-17	Bezau	Austria	47.3804	9.9208	<i>clandestinus</i>	<i>clandestinus</i>	ALNHM362-17.COI-5P	ALNHM362-17.16S		Duda et al. 2017
ALNHM362-17	Bezau	Austria	47.3804	9.9208	<i>clandestinus</i>	<i>clandestinus</i>	ALNHM363-17.COI-5P	ALNHM363-17.16S		Duda et al. 2017
MNHN-IM-2009-20119	Chateau Garnier	France	44.082	6.488	<i>plebeius</i>		MEMOL037-11			publ. in BOLD by Gargominy
MNHN-IM-2009-20195	Les Blancs	France	44.357	6.618	<i>plebeius</i>		MEMOL211-11			publ. in BOLD by Gargominy
MNHN-IM-2009-20196	Les Blancs	France	44.357	6.618	<i>plebeius</i>		MEMOL398-11			publ. in BOLD by Gargominy
MNHN-IM-2009-20197	Les Blancs	France	44.357	6.618	<i>plebeius</i>		MEMOL404-11			publ. in BOLD by Gargominy
MNHN-IM-2009-20198	Les Blancs	France	44.357	6.618	<i>plebeius</i>		MEMOL373-11			publ. in BOLD by Gargominy
MNHN-IM-2009-20199	Les Blancs	France	44.357	6.618	<i>plebeius</i>		MEMOL368-11			publ. in BOLD by Gargominy
MNHN-IM-2009-20200	Les Blancs	France	44.357	6.618	<i>plebeius</i>		MEMOL178-11			publ. in BOLD by Gargominy
MNHN-IM-2009-20202	Les Blancs	France	44.357	6.618	<i>plebeius</i>		MEMOL253-11			publ. in BOLD by Gargominy
MNHN-IM-2009-20204	Les Blancs	France	44.357	6.618	<i>plebeius</i>		MEMOL162-11			publ. in BOLD by Gargominy
MNHN-IM-2009-20205	Les Blancs	France	44.357	6.618	<i>plebeius</i>		MEMOL175-11			publ. in BOLD by Gargominy
MNHN-IM-2009-20236	Molines en Queyras	France	44.73	6.844	<i>plebeius</i>		MEMOL379-11			publ. in BOLD by Gargominy
MNHN-IM-2009-20237	Molines en Queyras	France	44.73	6.844	<i>plebeius</i>		MEMOL374-11			publ. in BOLD by Gargominy

Kneubühler et al.: The *Trochulus* enigma

MNHN-IM-2009-20239	Molines en Queyras	France	44.73	6.844	<i>plebeius</i>		MEMOL366-11		publ. in BOLD by Gargominy
MNHN-IM-2009-20240	Molines en Queyras	France	44.73	6.844	<i>plebeius</i>		MEMOL324-11		publ. in BOLD by Gargominy
MNHN-IM-2009-20276	Les la Croix Haute	France	44.657	5.711	<i>plebeius</i>		MEMOL400-11		publ. in BOLD by Gargominy
MNHN-IM-2009-20506	St. Hugues	France	45.299	5.81	<i>albulus</i>	<i>phorochaetia</i>	MEMOL318-11		publ. in BOLD by Gargominy
MNHN-IM-2009-20507	St. Hugues	France	45.299	5.81	<i>albulus</i>	<i>phorochaetia</i>	MEMOL540-12		publ. in BOLD by Gargominy
MNHN-IM-2009-21154	Barcelonnette	France	44.382	6.631	<i>plebeius</i>		MEMOL208-11		publ. in BOLD by Gargominy
MNHN-IM-2009-21155	Barcelonnette	France	44.382	6.631	<i>plebeius</i>		MEMOL210-11		publ. in BOLD by Gargominy
MNHN-IM-2009-21156	Barcelonnette	France	44.382	6.631	<i>plebeius</i>		MEMOL215-11		publ. in BOLD by Gargominy
MNHN-IM-2009-21157	Barcelonnette	France	44.382	6.631	<i>plebeius</i>		MEMOL181-11		publ. in BOLD by Gargominy
MNHN-IM-2009-21158	Barcelonnette	France	44.382	6.631	<i>plebeius</i>		MEMOL271-11		publ. in BOLD by Gargominy
MNHN-IM-2009-21160	Jausiers	France	44.442	6.742	<i>plebeius</i>		MEMOL258-11		publ. in BOLD by Gargominy
MNHN-IM-2009-21161	Jausiers	France	44.442	6.742	<i>plebeius</i>		MEMOL242-11		publ. in BOLD by Gargominy
MNHN-IM-2009-21162	Jausiers	France	44.442	6.742	<i>plebeius</i>		MEMOL248-11		publ. in BOLD by Gargominy
MNHN-IM-2013-76655	Coranche	France	45.0737	5.3984	<i>albulus</i>	<i>phorochaetia</i>	LPRCM336-21		publ. in BOLD by Gargominy
MNHN-IM-2013-	Coranche	France	45.0737	5.3984	<i>albulus</i>	<i>phorochaetia</i>	LPRCM337-		publ. in BOLD by

Kneubühler et al.: The *Trochulus* enigma

76656							21			Gargominy
MNHN-IM-2013-76657	Coranche	France	45.0737	5.3984	<i>albulus</i>	<i>phorochaetia</i>	LPRCM338-21			publ. in BOLD by Gargominy
M1_12_767	Heumadgupf	Austria	47.81	13.71	<i>N. scheerpeltzi</i>	<i>N. scheerpeltzi</i>	HQ204394		KJ151731	Bamberger et al. 2020
M3_765_7172	Hochmölbing	Austria	47.62	14.16	<i>N. scheerpeltzi</i>	<i>N. scheerpeltzi</i>	MN193608		MN299115	Bamberger et al. 2020
M4_367_3396	Haltersitz	Austria	47.79	14.32	<i>N. scheerpeltzi</i>	<i>N. scheerpeltzi</i>	HQ204392		KJ151742	Bamberger et al. 2020
M5_443_4108	Westgrat	Austria	47.65	14.38	<i>N. scheerpeltzi</i>	<i>N. scheerpeltzi</i>	MN193721		MN299218	Bamberger et al. 2020
M6_782_7237	Natterriegel	Austria	47.64	14.48	<i>N. oreinos</i>	<i>N. oreinos</i>	MN193670		MN299147	Bamberger et al. 2020
M7_55_707	Admonter Kalbling	Austria	47.55	14.52	<i>N. oreinos</i>	<i>N. oreinos</i>	HQ204396		KJ151725	Bamberger et al. 2020
M8_781_7227	Grosser Buchstein	Austria	47.61	14.59	<i>N. oreinos</i>	<i>N. oreinos</i>	MN193660		MN299128	Bamberger et al. 2020
M9_779_7222	Hesshütte	Austria	47.56	14.64	<i>N. oreinos</i>	<i>N. oreinos</i>	MN193657		MN299121	Bamberger et al. 2020
M11_134_999	Schiestlhaus	Austria	47.62	15.14	<i>N. oreinos</i>	<i>N. oreinos</i>	HQ204422		KJ151734	Bamberger et al. 2020
M14_79_757	Bismarcksteig	Austria	47.69	15.7	<i>N. oreinos</i>	<i>N. oreinos</i>	HQ204409		KJ151729	Bamberger et al. 2020

Chapter 4

In several side projects, I generated COI, 16S, and H3 sequences for the micro gastropod species of *Zospeum* and *Carychium*. Since these specimens are very small (< 2 mm), a new DNA extraction protocol was developed to generate enough DNA for the PCR in the first place. Still, the Alpine-Dinaric radiation of *Zospeum* is little explored. Due to the lack of historic type specimens, insufficient original description, and the lack of freshly collected specimens from western Balkan caves, the only known southern species, *Z. troglobalcanicum*, has remained an unknown entity. Based on recent collection efforts and my sequencing and phylogenetic analyses of new individuals, new species within the Dinaric genus *Zospeum* will be described soon.

For the ongoing revision and the worldwide phylogeny of the ellobiid genus *Carychium*, I provided the genetic data and assisted in the performance and interpretation of phylogenetic analyses. The phylogeny serves as the backbone for the taxonomic revision of the genus and reveals several new clades, which will be described as new species.

Discussion

Cryptic species have been revealed in various organism groups in recent years (e.g., Hebert *et al.* 2004; Funk *et al.* 2011; Weigand *et al.* 2013; Cruse *et al.* 2022). We are increasingly realising that we only see the tip of the iceberg in terms of species numbers in the World. So far, 1.2 million species have been described worldwide, but estimates suggest that up to 8.7 million eukaryotic species exist (Mora *et al.* 2011). We are still a long way from capturing all this biodiversity on Earth.

Cryptic species are a man-made concept not known by Nature. Species differ in ways that may be beyond our visual or auditory comprehension. But species have a way of distinguishing themselves and, for example, of finding the “right” partner for mating and avoiding the “wrong” ones which could lead to sterile offspring. We can only speak of cryptic species until we have fully investigated the animals using an integrative approach. In the identification of separate species, greater emphasis should be placed on the re-evaluation of morphological traits in the future. Here, the genetic findings serve as a guideline to identify possible, previously hidden convergences, which in previous work were wrongly interpreted as synapomorphies and thus, lead to paraphyly in the phylogenetic trees. The concept of integrative taxonomy follows this idea (e.g., DeSalle *et al.* 2005; Bickford *et al.* 2007; Padial *et al.* 2010; Horsáková *et al.* 2022).

Cryptic speciation is exemplified in Chapter 1 with the Spanish *Iberozospeum* radiation. The species are difficult to distinguish from shell morphology alone and show a high intraspecific variability. Among the specimens we studied, only some species such as *I. biscaiense* (Gómez

& Prieto, 1983), *I. percostulatum* (Á. Alonso, Prieto, Quiñonero-Salgado & Rolán, 2018), and *I. costulatum* Prieto & Jochum, 2022 can be well distinguished morphologically. In congeners, there is a morphological transition. An extensive sampling of northern Spanish caves and genetic methods have brought clarity now to the Spanish radiation. The investigation of a concatenated dataset with the four markers COI, 16S, H3 and ITS2, revealed a deep genetic split between the Spanish and the Alpine-Dinaric radiation. We found nine clades in the Spanish radiation, but the support values were not significant due to some missing markers for some specimens. With a reduced dataset containing only specimens with complete marker sets, we found the same nine clades, but the support values were significantly higher. This shows that the phylogeny covering all specimens available is reliable. We found three distinct clades within the hitherto existing species *I. vasconicum*. These clades are also consistent with the geographical distribution of the investigated individuals. The morphological discrimination from the eastern Alpine and Dinaric radiation of *Zospeum* could be performed with the help of histological analysis of the upper visceral complex and scanning electron microscopic (SEM) analyses of radulae. The composition and form of radular teeth is influenced by mineral composition of the environment, the diet, and other factors (Luchtel *et al.* 1997). Our observations that the columellar muscle becomes detached from the body wall from its origin on the columella are in sync with the trends in Ellobiidae (Barker 2001). These findings in particular show how important it is to carry out integrative studies and use several character states for species identification.

Chapter 2 and 3 of my doctoral thesis deal with the hairy snail genus *Trochulus*. A revision of the genus by Proćków (2009) was dominated by shell and genital anatomical analyses and raised more questions than clarity. Research in the *Trochulus* complex has been going on for years, but only small areas of the distribution range have been collected and studied (e.g., Dépraz *et al.* 2009; Duda *et al.* 2014; Kruckenhauser *et al.* 2014; Proćków *et al.* 2014, 2017a, 2021). Therefore, the general overview was missing for a thorough revision of the genus. With our extensive sampling of about 570 specimens from almost the entire distribution range of the genus, we were now able to genetically identify different clades for the first time. It turned out that many morphologically described species consist of several clades that are stable across different phylogenetic analysis methods. Some species are restricted to the Jura mountains and neighbouring areas, which could indicate, that the species retreated to refugia in the unglaciated part of the Jura mountains during the Last Glacial Maximum (LGM; e.g., Graf *et al.* 2015; Claude *et al.* 2019). These species could not spread very far after the retreat of the ice. In contrast, other species that are widespread in Europe, such as *T. hispidus*, probably had a greater potential for dispersal and could occupy different niches. The endemic species, *T. biconicus*, which we separated from the genus *Trochulus* due to its genetics, shell morphology and genital anatomical peculiarities and placed it in the monotypic genus

Raeticella, has presumably survived the LGM on nunataks (see Chapter 2). Here, the species lives in a barren landscape under stones and feeds on blue grass (*Sesleria caerulea*). *Trochulus* species, on the other hand, inhabit a wide range of habitats: from rocky alpine sites, lowlands, most often adjoining rivers, forests and nettle patches, or on tall grasses in open areas (e.g., Duda *et al.* 2014; Proćków *et al.* 2017b). *Trochulus* species seem to have great adaptability and have been able to colonise diverse habitats. Locally, genetically differentiated species have evolved, but we have so far missed them because of their morphological similarity. However, the shells have not changed much and only a few species can be identified by their shells. With our integrative approach, we have now uncovered some of these cryptic species.

In Chapter 4, I give some insights to our ongoing research on micro gastropods. Because the species of *Zospeum* and *Carychium* are so small and difficult to find, they remain either unknown or are often ignored due to the tedious effort required to find them. Many species descriptions are still based on shell morphology and anatomical characteristics (Bank & Gittenberger 1985). With the help of an integrative taxonomic approach, incorporating multiple lines of evidence, the species, *Z. kolbae* sp. n. for example, was genetically flagged in my analyses and is currently being processed in another work. This case constitutes yet another species that brings us closer to the real number of species in the World. Moreover, the global phylogeny with the inclusion of topotypic specimens brings valuable insights towards clarifying the systematics of *Carychium*. Within the species *C. minimum*, for example, we have detected various lineages that will soon be described as separate species.

In various land snail groups, I am endeavouring to reveal the diversity within cryptic species using integrative taxonomy. Only with the help of integrative studies can we manage to identify the World's biodiversity.

Outlook

In my studies these past few years, I was able to corroborate some species' concepts within certain land snail groups, leading to description of new species, but also to the synonymising of validly described taxa. This procedure requires the use of a significant number of animals from the whole known ecological and biogeographic range and the investigation of as many as possible different character states (Horsáková *et al.* 2022). All the aforementioned examples show that we cannot, in most cases, interpret so many species using only shell morphology. For future studies, it is essential to also focus on other character states than morphology and genetic data. Seldomly used traits such as mating signals, behavioural traits, bioacoustics data and biogeography may be promising. The chemical communication strategies in molluscs should also be studied more closely. Ballard *et al.* (2021) have shown

that the animals communicate with each other by means of proteins and pheromones in the trail mucus. This could be an approach for “cryptic” *Trochulus* species to identify species-specific differences. For smaller gastropod species such as *Iberozospeum*, *Zospeum* and *Carychium*, CT scans and histological analyses have proven successful. Since histological investigations are very tedious and time consuming beyond the few years of a doctoral thesis (A. Jochum, pers. comm. 2022) and CT scans constitute expensive methods, they are rarely used to the level we need. Still, their use would further enhance our knowledge of these miniscule snails especially if extended to several individuals per species to better identify morphological differences between species. It would also be interesting to examine the hairs of *Trochulus* with high-resolution SEM. The different lengths and shapes of the hairs can be determined well with a binocular microscope, but species-specific differences may be found microscopically. Microscopic examination of the love darts and spermatophores may also reveal species-specific differences. Although we have tried to cover the entire distribution range of the traditionally recognized taxonomic units, we are still missing some regions that may harbour “cryptic” species. For *Trochulus*, we still have collection gaps in western France and in central and northern Germany. Only by conscientiously sampling these regions and examining the specimens, will we get a complete picture. At least we were able to provide a deeper insight into the taxonomy of different land snail groups. In summary, some biological aspects should be added to the integrative taxonomy method. These include the fields described above, whose potential in the recognition of species, including “cryptic” species, has not yet been exploited.

Acknowledgements

I sincerely thank Dr. Eike Neubert (Natural history museum Bern & University of Bern, Switzerland) for the supervision of my doctoral thesis, for sharing his knowledge with me and having always an open door to address my questions.

I sincerely thank Prof. Dr. Christian Kropf (Natural history museum Bern & University of Bern, Switzerland) for the supervision of my doctoral thesis. I thank the employees and students of the Natural history museum, that have accompanied me during my time in the museum, for all the insightful discussions and funny conversations.

I am most grateful to Markus Baggenstos, Damien Combrisson, Armin Deutsch, Olivier Gargominy (Muséum national d'Histoire naturelle, Paris, France), Ralf Hannefort, René Heim, David Herbert, Fabian Heussler, Michal Horsák (Masaryk University, Brno, Czech Republic), Thomas Inäbnit (University of Potsdam, Germany), Peter Landert, Katja Lassauer, Holger Menzel-Harloff, Andreas Pardey, Ted von Proschwitz (Göteborgs Naturhistoriska Museum, Sweden), Ira Richling (Staatliches Museum für Naturkunde Stuttgart, Germany), Ben Rowson

(National Museum Wales, United Kingdom), Jörg Rüetschi, Julien Ryelandt, Ueli Schneppat, and Karin Urfer (Naturmuseum St. Gallen, Switzerland) for kindly providing specimens for examination.

I thank Issaad Kawther Ezzine (Natural history museum Bern, Switzerland), Neele Höhne (University of Bern, Switzerland), Bettina Kneubühler, Silvan Meister, Vivianne Schallenberg (Natural history museum Bern, Switzerland), Svenja Zehnder (University of Bern, Switzerland), and Yvonne Zürcher for their perseverance and tremendous collecting help on my snail hunting trips.

I thank Adrienne Jochum (Natural history museum Bern & University of Bern, Switzerland) for the great help in collecting snails all over the World, the linguistic revision of the doctoral thesis, and for always having an open ear and support far beyond my doctoral thesis.

I thank Małgorzata Proćków (Museum of Natural History, Wrocław, Poland) for the great support and sharing her 25 years of experience in *Trochulus* research with me and for contributing the majority of the animals studied.

I thank Marco T. Neiber and Simon Bober (Center of Natural History, Zoological Museum, University of Hamburg, Germany) for the introduction to the evaluation of RADseq data and the performance of phylogenetic analyses.

I thank Eva A. Bischof (Natural history museum Bern, Switzerland) for the introduction to Geometric morphometric analysis and the provision of various R scripts.

I thank Ruud Bank (University of Groningen, the Netherlands) for his kind assistance and expertise in solving the nomenclatural problems and for co-presiding on my dissertation committee.

I would like to thank the Federal Office of Environment for their financial support.

Special gratitude goes to my family and friends who always motivated and supported me and listened to all the weird snail stories I always had to tell. Without your support I would not be where I am now. I thank my dear Jonas Schulz for the great support in collecting snails, the motivation, the patience, the accompanying to collecting trips or congresses and for always lifting me up, when I was mentally down.

References

Adams, M., Raadik, T.A., Burrige C.P., & Georges A. (2014). Global biodiversity assessment and hyper-cryptic species complexes: more than one species of elephant in the room? *Systematic Biology* 63, 518–533. <https://doi.org/10.1093/sysbio/syu017>

- Ballard, K.R., Klein, A.H., Hayes, R.A., Wang, T., & Cummins, S.F. (2021) The protein and volatile components of trail mucus in the Common Garden Snail, *Cornu aspersum*. PLoS ONE 16(5): e0251565. <https://doi.org/10.1371/journal.pone.0251565>
- Bank, R.A. & Gittenberger, E. (1985). Notes on Azorean and European *Carychium* species (Gastropoda, Basommatophora, Ellobiidae). *Basteria*, 49(4/6), 85–100.
- Barker, G. M. (2001). *The Biology of Terrestrial Mollusks* (p. 558). CABI Publishing.
- Bickford, D., Lohman, D.J., Sodhi, N.S., Ng, P.K.L., Meier, R., Winker, K., Ingram, K.K., & Das, I. (2007). Cryptic species as a window on diversity and conservation. *Trends in Ecology & Evolution*, 22(3), 148–155. <https://doi.org/10.1016/j.tree.2006.11.004>
- Bingham, J.-P., Mitsunaga, E. & Bergeron, Z.L. (2010) Drugs from slugs—Past, present and future perspectives of ω -conotoxin research. *Chemico-Biological Interactions* 183, 1–18. <https://doi.org/10.1016/j.cbi.2009.09.021>
- Claude, A., Akçar, N., Ivy-Ochs, S., Schlunegger, F., Kubik, P.W., Christl, M., Vockenhuber, C., Kuhlemann, J., Rahn, M., & Schlüchter, C. (2019). Changes in landscape evolution patterns in the northern Swiss Alpine Foreland during the mid-Pleistocene revolution. *GSA Bulletin*, 131(11–12), 2056–2078. <https://doi.org/10.1130/b31880.1>
- Cruse, M., Telerant, R., Gallagher, T., Lee, T., & Taylor, J.W. (2002). Cryptic species in *Stachybotrys chartarum*. *Mycologia*, 94(5), 814–822. <https://doi.org/10.1080/15572536.2003.11833175>
- De Queiroz, K. (2007). Species Concepts and Species Delimitation. *Systematic Biology*, 56(6), 879–886. <https://doi.org/10.1080/10635150701701083>
- Dépraz, A., Hausser, J., & Pfenninger, M. (2009) A species delimitation approach in the *Trochulus sericeus/hispidus* complex reveals two cryptic species within a sharp contact zone. *BMC Ecology and Evolution*, 9, 171. <https://doi.org/10.1186/1471-2148-9-171>
- DeSalle, R., Egan, M.G., & Siddall, M. (2005). The unholy trinity: taxonomy, species delimitation and DNA barcoding. *Philosophical Transactions of the Royal Society B: Biological Sciences*, 360(1462), 1905–1916. <https://doi.org/10.1098/rstb.2005.1722>
- Duda, M., Kruckenhauser, L., Sattmann, H., Harl, J., Jaksch, K., & Haring, E. (2014). Differentiation in the *Trochulus hispidus* complex and related taxa (Pulmonata: Hygromiidae): Morphology, ecology and their relation to phylogeography. *Journal of Molluscan Studies*, 80, 371–387. <https://doi.org/10.1093/mollus/eyu023>

- Fišer, C., Robinson, C.T., & Malard, F. (2018). Cryptic species as a window into the paradigm shift of the species concept. *Molecular Ecology*, 27(3): 613–635. <https://doi.org/10.1111/mec.14486>
- Fortunato, H. Mollusks: Tools in Environmental and Climate Research (2015). *American Malacological Bulletin* 33(2), 310–324. <https://doi.org/10.4003/006.033.0208>
- Funk, W.C., Caminer, M., & Ron, S.R. (2011). High levels of cryptic species diversity uncovered in Amazonian frogs. *Proceedings of the Royal Society B: Biological Sciences*, 279(1734), 1806–1814. <https://doi.org/10.1098/rspb.2011.1653>
- Gemmell, R.M., Trewick, S.A., Crampton, J.S., Vaux, F., Hills, S.F.K., Daly, E.E., Marshall, B.A., Beu, A.G., & Morgan-Richards, M. (2018). Genetic structure and shell shape variation within a rocky shore whelk suggest both diverging and constraining selection with gene flow, *Biological Journal of the Linnean Society* 2 (4), 827–843, <https://doi.org/10.1093/biolinnean/bly142>
- Goodfriend, G.A. (1986). Variation in land-snail shell form and size and its causes: A review. *Systematic Zoology* 35(2), 204–223.
- Graf, A., Akçar, N., Ivy-Ochs, S., Strasky, S., Kubik, P. W., Christl, M., Burkhard, M., Wieler, R., & Schlüchter, C. (2015). Multiple advances of Alpine glaciers into the Jura Mountains in the Northwestern Switzerland. *Swiss Journal of Geosciences*, 108(2-3), 225–238. <https://doi.org/10.1007/s00015-015-0195-y>
- Hebert, P.D.N., Penton, E.H., Burns, J.M., Janzen, D.H., & Hallwachs, W. (2004). Ten species in one: DNA barcoding reveals cryptic species in the neotropical skipper butterfly *Astrartes fuligator*. *Proceedings of the National Academy of Sciences*, 101(41), 14812–14817. <https://doi.org/10.1073/pnas.0406166101>
- Hofman, S., Cameron, R.A.D., Proćków, M., Sîrbu, I., Osikowski, A., Jaszczyńska, A., Sokół, M., & Falniowski, A. (2022). Two new pseudocryptic species in the medium-sized common European land snails, *Fruticicola* Held, 1838; as a result of phylogeographic analysis of *Fruticicola fruticum* (O. F. Müller, 1774) (Gastropoda: Helicoidea: Camaenidae). *Molecular Phylogenetics and Evolution* 168. <https://doi.org/10.1016/j.ympev.2022.107402>
- Horsáková, V., Líznarová, E., Razkin, O., Nekola, J. C., & Horsák, M. (2022). Deciphering “cryptic” nature of European rock-dwelling *Pyramidula* snails (Gastropoda: Stylommatophora), *Contributions to Zoology* (published online of print 2022). <https://doi.org/10.1163/18759866-bja10032>
- Horsáková, V., Nekola, J.C., & Horsák, M. (2019). When is a “cryptic” species not a cryptic species: A consideration from the Holarctic micro-landsnail genus *Euconulus* (Gastropoda:

Stylommatophora). *Molecular Phylogenetics and Evolution*.
<https://doi.org/10.1016/j.ympev.2018.12.004>

International Union for Conservation of Nature, IUCN (2022). Accessed on 2022-06-24 at
<https://www.iucn.org/>

Jochum, A., Prieto, C.E., Kampschulte, M., Martels, G., Ruthensteiner, B., Vrabec, M., Dörge, D.D., Winter, de, A.J (2019). Re-evaluation of *Zospeum schaufussi* von Frauenfeld, 1862 and *Z. suarezi* Gittenberger, 1980, including the description of two new Iberian species using Computer Tomography (CT) (Eupulmonata, Ellobioidea, Carychiidae). *ZooKeys* 835, 65–86.
<https://doi.org/10.3897/zookeys.835.33231>

Johnson, S.B., Warén, A., Tunnicliffe, V., Dover, C.V., Wheat, C.G., Schultz, T.F., & Vrijenhoek, R.C. (2014). Molecular taxonomy and naming of five cryptic species of *Alviniconcha* snails (Gastropoda: Abyssochrysoidea) from hydrothermal vents. *Systematics and Biodiversity*, 13(3), 278–295. <https://doi.org/10.1080/14772000.2014.970673>

Jörger, K.M. & Schrödl, M. How to describe a cryptic species? Practical challenges of molecular taxonomy. *Frontiers in Zoology* 10, 59. <https://doi.org/10.1186/1742-9994-10-59>

Khan, B.M. & Liu, Y. (2019) Marine Mollusks: Food with Benefits: Marine mollusks. *Comprehensive Reviews in Food Science and Food Safety* 18, 548–564.
<https://doi.org/10.1111/1541-4337.12429>

Kruckenhauser, L., Duda, M., Bartel, D., Sattmann, H., Harl, J., Kirchner, S., & Haring, E., (2014). Paraphyly and budding speciation in the hairy snail (Pulmonata, Hygromiidae). *Zoologica Scripta* 43, 273–288. <https://doi.org/10.1111/zsc.12046>

Lindberg, D.R. (2001). Molluscs. *Encyclopedia of Biodiversity* (2), 373–383.
<https://doi.org/10.1016/B978-0-12-384719-5.00096-4>

Luchtel, D.L., Martin, A.W., Deyrup-Olsen, I., & Boer, H.H. (1997). Gastropoda: Pulmonata. In: F. W. Harrison & A. J. Kohn (Eds.) *Microscopic Anatomy of Invertebrates* (vol 6B, pp. 459–718). Mollusca II, Wiley-Liss, Inc., New York.

Maloof, A.C., Porter, S.M., Moore, J.L., Dudas, F.O., Bowring, S.A., Higgins, J.A., Fike, D.A., & Eddy, M.P. (2010). The earliest Cambrian record of animals and ocean geochemical change. *Geological Society of America Bulletin*, 122 (11–12), 1731–1774.
<https://doi.org/10.1130/b30346.1>

MolluscaBase eds. (2022). MolluscaBase. Accessed on 2022-07-07 at
<https://www.molluscabase.org>

- Mora, C., Tittensor, D.P., Adl, S., Simpson, A.G.B., & Worm, B. (2011). How Many Species Are There on Earth and in the Ocean? *PLoS Biology*, 9(8), e1001127. <https://doi.org/10.1371/journal.pbio.1001127>
- Padial, J.M., Miralles, A., De la Riva, I., & Vences, M. (2010). The integrative future of taxonomy. *Frontiers in Zoology* 7:16. <https://doi.org/10.1186/1742-9994-7-16>
- Pearce, T.A. (2008). When a Snail Dies in the Forest, how Long will the Shell Persist? Effect of Dissolution and Micro-bioerosion. *American Malacological Bulletin*, 26(1-2), 111–117. <https://doi.org/10.4003/006.026.0211>
- Pfenninger, M. & Schwenk, K. (2007). Cryptic animal species are homogeneously distributed among taxa and biogeographical regions. *BioMed Central Evolutionary Biology* 7, 121.
- Proćków, M. (2009). The genus *Trochulus* Chemnitz, 1786 (Gastropoda: Pulmonata: Hygromiidae) – a taxonomic revision. *Folia Malacologica*, 17, 101–176. <https://doi.org/10.2478/v10125-009-0013-0>
- Proćków, M., Kuźnik-Kowalska, E., & Mackiewicz, P. (2017a). Phenotypic plasticity can explain evolution of sympatric polymorphism in the hairy snail *Trochulus hispidus* (Linnaeus, 1758). *Current zoology*, 63(4), 389–402. <https://doi.org/10.1093/cz/zow082>
- Proćków, M., Kuźnik-Kowalska, E., & Mackiewicz, P. (2017b). The influence of climate on shell variation in *Trochulus striolatus* (C. Pfeiffer, 1828) (Gastropoda: Hygromiidae) and its implications for subspecies taxonomy. *Annales Zoologici*, 67, 199–220. <https://doi.org/10.3161/00034541an.z2017.67.2.002>
- Proćków, M., Kuźnik-Kowalska, E., Pieńkowska, J.R., Żeromska, A., & Mackiewicz, P. (2021). Speciation in sympatric species of land snails from the genus *Trochulus* (Gastropoda, Hygromiidae). *Zoologica Scripta* 50, 16–42. <https://doi.org/10.1111/zsc.12458>
- Proćków, M., Strzała, T., Kuźnik-Kowalska, E., & Mackiewicz, P. (2014). Morphological similarity and molecular divergence of *Trochulus striolatus* and *T. montanus*, and their relationship to sympatric congeners (Gastropoda: Pulmonata: Hygromiidae). *Systematics and Biodiversity*, 12, 366–384. <https://doi.org/10.1080/14772000.2014.925986>
- Purchon, R.D. (1977). The biology of the Mollusca (2nd ed.). Volume 57. Pergamon Press. <https://doi.org/10.1016/C2009-0-00735-1>
- Sites, J.W. Jr & Marshall, J.C. (2003). Delimiting species: a renaissance issue in systematics biology. *Trends in Ecology & Evolution* 18, 462–470. [https://doi.org/10.1016/S0169-5347\(03\)00184-8](https://doi.org/10.1016/S0169-5347(03)00184-8)

Struck, T.H., Feder, J.L., Bendiksbj, M., Birkeland, S., Cerca, J., Gusarov, V.I., Kistenich, S., Larsson, K.H., Liow, L.H., Nowak, M.D., Stedje, B., Bachmann, L., & Dimitrov, D. (2018). Finding Evolutionary Processes Hidden in Cryptic Species. *Trends in Ecology & Evolution*. 33(3), 153–163. <https://doi.org/10.1016/j.tree.2017.11.007>

Trontelj, P. & Fišer, C. (2009). Perspectives: Cryptic species diversity should not be trivialised, *Systematics and Biodiversity*, 7(1), 1–3, <https://doi.org/10.1017/S1477200008002909>

Vermeij, G.J. (1993). A natural history of shells. Princeton University Press. Princeton, USA. 216 pp.

Weigand, A.M., Jochum, A., Slapnik, R., Schnitzler, J., Zarza, E., & Klussmann-Kolb, A. (2013). Evolution of microgastropods (Ellobioidea, Carychiidae): Integrating taxonomic, phylogenetic and evolutionary hypotheses. *BMC Evolutionary Biology*, 13(1), 18. <https://doi.org/10.1186/1471-2148-13-18>